LUND UNIVERSITY

Modelling of transport processes involved in service life prediction of concrete: important principles

Johannesson, Björn

1998

LUND UNIVERSITY
LUND INSTITUTE OF TECHNOLOGY
Division of Building Materials

MODELLING OF TRANSPORT PROCESSES INVOLVED IN SERVICE LIFE PREDICTION OF CONCRETE

IMPORTANT PRINCIPLES

Björn Johannesson

Report TVBM - 3083 Licentiate Thesis
Lund 1998

ISRN: LUTVDG/TVBM–98/3083–SE(1-227)
ISSN: 0348-7911 TVBM

Lund Institute of Technology
Division of Building Materials
Box 118
SE-221 00 Lund, Sweden

Telephone: +46-46-2224052
Telefax: +46-46-2224427
WWW: http://www.ldc.lu.se/lthbml

Preface

This work has been carried out at the Division of Building Materials at the Lund Institute of Technology and has been financed by the Swedish Foundation for Concrete Research (Stiftelsen Svensk Betongforskning) and the Swedish Council for Building Research (Byggforskningsrådet, BFR). The research project was initiated by my supervisor, prof. Göran Fagerlund, whom I wish to thank for his support.

I would like to thank dr. Manouchehr Hassanzadeh and the rest of the staff at the Division of Building Materials for their help and support during the process.

A special thanks to Ebbe Lundgren, phil. lic., (Division of Mechanics, Lund) for sharing his knowledge in the field of mixture theories, and to dr. Christer Nilsson (Division of Structural Mechanics, Lund), for reading parts of the manuscript and making many valuable comments and corrections.

QUOTATIONS

From pp. 92-93 of *Six Lectures on Modern Natural Philosophy:* VI. Method and Taste in Natural Philosophy. Berlin: Springer-Verlag, 1966.

> The hard facts of classical mechanics taught to undergraduates today are, in their present forms, creations of James and John Bernoulli, Euler, Lagrange, and Cauchy, men who never touched a piece of apparatus; their only researches that have been discarded and forgotten are those where they tried to fit theory to experimental data. They did not disregard experiment; the parts of their work that are immortal lie in domains where experience, experimental or more common, was at hand, already partly understood through various special theories, and they abstracted and organized it and them. To warn scientists today not to disregard experiment is like preaching against atheism in church or communism among congressmen. It is cheap rabble-rousing. The danger is all the other way. Such a mass of experimental data on everything pours out of organized research that the young theorist needs some insulation against its disrupting, disorganizing effect. Poincaré said, "The science must order; science is made out of facts as a house is made out of stones, but an accumulation of facts is no more science than a heap of stones, a house."
>
> *Clifford Truesdell*

From p. 35 of *Six Lectures on Modern Natural Philosophy:* III. Thermodynamics of visco-elasticity. Berlin: Springer-Verlag, 1966.

> There is nothing that can be said by mathematical symbols and relations which cannot also be said by words. The converse, however, is false. Much that can be and is said by words cannot successfully be put into equations, because it is nonsense.
>
> *Clifford Truesdell*

Notations

Notations and symbols are explained in the text where they first appear; a list of main notations is given below.

General notations

a	Arbitrary constituent (subscript)
dv	Element of volume
$d\mathbf{s}$	Outward-drawn normal
div	Divergence operator
grad	Gradient operator
tr	Trace operator
Γ_a	Arbitrary property of the ath constituent
Γ	Mass-weighted sum of the ath constituents
$\dot{\Gamma}$	Derivative of Γ following the motion of the mixture
$\Gamma_a^{'}$	Material derivative following the ath constituent
$\Gamma_a^{''}$	Material (second) derivative following the ath constituent
$\Gamma_{\mathbf{I}}$	Inner part of Γ
Γ^{T}	Transpose
$\partial\Gamma/\partial t$	Time derivative
∇	Gradient operator in Cartesian coordinates
$\nabla\cdot$	Divergence operator in Cartesian coordinates
$\cdot$	Scalar product
$\otimes$	Dyad product
$\times$	Cross product
$\Re$	Number of constituents (or their corresponding element volume)
$\partial\Re$	Boundary area

Notations used in the mixture theory

$\mathbf{D}_a$	Stretching tensor (1/s)	$\dot{\mathbf{x}}$	Velocity of the mixt. (m/s)
$\mathbf{E}_a$	Lagrangian strain tensor (-)	$\ddot{\mathbf{x}}$	Acceler. of the mixture (m/s^2)
$\mathbf{F}_a$	Deformation gradient (-)	c_a	Mass concentration (-)
$\mathbf{H}_a$	Displacement gradient (-)	$\hat{c}_a$	Chem. reaction rate (kg/m^3/s)
$\mathbf{I}$	Identity matrix	r_a	Ext. heat supply (J/kg/s)
$\mathbf{K}_a$	Chemical potential (J/kg)	t	Time (s)
$\mathbf{L}_a$	Velocity gradient (1/s)	$\partial/\partial t$	Spatial time derivative (1/s)
$\hat{\mathbf{M}}_a$	Skew-sym. stress (N/m^2)	r_a	Local energy supply (J/kg/s)
$\mathbf{T}_a$	Stress tensor (N/m^2)	ε_a	Internal energy (J/kg)
$\mathbf{T}_\mathbf{I}$	Inner stress tensor (N/m^2)	$\varepsilon_\mathbf{I}$	Inner internal energy (J/kg)
$\mathbf{X}_a$	Material coordinates (m)	$\hat{\varepsilon}_a$	Local energy supply (J/kg/s)
$\mathbf{b}_a$	Body force (kgm^2/s)	ζ	Gibbs free energy (J/kg)
$\mathbf{e}_a$	Linear strain tensor (-)	η_a	Entropy (J/kg/K)
$\mathbf{h}_a$	Entropy flux (J/m^2/s/K)	θ_a	Temperature (K)
$\hat{\mathbf{p}}_a$	Momentum supply (N/m^3)	μ_a	Chemical potential (J/kg)
$\mathbf{q}_a$	Heat flux (J/m^2/s)	π_a	Partial hydr. pressure (N/m^2)
$\mathbf{q}_\mathbf{I}$	Inner heat flux (J/m^2/s)	ρ	Density of the mixt. (kg/m^3)
$\mathbf{u}_a$	Diffusion velocity (m/s)	ρ_a	Mass density (kg/m^3)
$\mathbf{w}_a$	Displacement (m)	ψ_a	Helmholz free energy (J/kg)
$\mathbf{x}$	Place (m)	$\psi_\mathbf{I}$	Free energy of the mixt. (J/kg)
$\mathbf{x}'_a$	Velocity (m/s)	$\mathcal{X}_a$	Motion (-)
$\mathbf{x}''_a$	Acceleration (m/s^2)	Θ	Positive-valued function (K)

Notations used in the finite element approach

$\mathbf{B}$	Derivative of shape func.	W	Weight func. in time dom.
$\mathbf{C}$	Damping matrix	h	Element length (1D)
$\mathbf{D}_\phi$	Constitutive matrix	h_{ch}	Charact. element length (3D)
$\mathbf{D}_0\mu_a$	Constitutive matrix	t_n	Time level
$\mathbf{K}$	Stiffness matrix	v	Weight func. in spatial dom.
$\tilde{\mathbf{K}}$	Convection matrix	α_{opt}	Opt. Petrov-Galerkin
$\mathbf{N}$	Shape function	β	Time integration param.
$\mathbf{a}$	Nodal parameter	γ	Time integration param.
$\dot{\mathbf{a}}$	Rate of change of param.	δ	Dirac function
$\mathbf{c}$	Arbitrary matrix	π_a	Hydrostatic pressure
$\mathbf{f}$	Load and bound. vector	τ	Normalized time
$\mathbf{n}$	Outward-drawn normal	$\bar{\tau}_a$	Deviatoric stress
$\mathbf{q}_a$	'Flow' vector	ϕ_a	Arbitrary potential
J	Flux	$\tilde{\phi}_i$	Nodal param.
$\hat{N}_n$	Shape func. in time	∇	Gradient operator
Pe	Peclet number	$\nabla\cdot$	Divergence operator
Pe^e	Element Peclet number	Δt	Time step
S	Boundary surface	Θ	Time integration param.
V	Element volume		

Notations introduced in Sections 6 and 8

C_{ijkl}	Tot. compl. (m^2/N)	e_{ij}	Tot. strain (-)
C^e_{ijkl}	Elast. compl. (m^2/N)	$\dot{e}_{ij}$	Global strain rate (1/s)
$\dot{C}^e_{ijkl}$	Rate of change ($m^2/N/s$)	$e^{c_l}_{ij}$	'Moisture' strain (-)
C^f_{ijkl}	Fr. compl. (m^2/N)	e^{θ}_{ij}	'Thermal' strain (-)
C^{*f}_{ijkl}	Local fr. compl. (m^2/N)	$e^{c_{ice}}_{ij}$	'Ice' strain (-)
$C^{c_{ice}}_{ijkl}$	'Ice' compl. (m^2/N)	$e_{\alpha\alpha}$	Local tot. strain (-)
J_α	Compliance (m^2/N)	$e^{*f}_{\alpha\alpha}$	Local fr. strain (-)
L_α	Equivalent length (m)	$\dot{e}^{*f}_{\alpha\alpha}$	Loc. strain rate (1/s)
N	'Slope' (N/m^3)	$\dot{e}^{f}_{ij}$	Global fr. strain rate (1/s)
Q	Reaction quotient (-)	$\hat{m}_{Fe}$	Corrosion rate ($kg/m^3/s$)
Q^{anode}	Reaction quotient at an. (-)	w^*_α	Crack opening (m)
$Q^{cathode}$	Reaction quotient at cat. (-)	$w^{*s}_{\alpha\beta}$	Shear disp. in crack (m)
T_{km}	Tot. stress (N/m^2)	$w^*_{\max}$	Prev. max. crack def. (m)
$\dot{T}_{km}$	Tot. stress rate ($N/m^2/s$)	α	Crack No. 1, loc. direction
$T^*_{\alpha\alpha}$	Loc. norm. stress (N/m^2)	β	Crack No. 2, loc. direction
$\dot{T}^*_{\alpha\alpha}$	Loc. stress rate ($N/m^2/s$)	δ_{ij}	Kronecker delta (-)
$T^*_{\alpha\beta}$	Local tot. sh. stress (N/m^2)	$\Delta_r\zeta$	React. energy (J/mol/K)
$\dot{T}^*_{\alpha\beta}$	Loc. stress rate ($N/m^2/s$)	$\Delta_{r0}\zeta$	Ref. energy (J/mol/K)
U	Cell potential (V)	$*$	Loc. coordinate syst.
U_0	Stand. electr. potential (V)	Δ_{ref}	Deviation from ref.
U^{force}	Electromotive force (V)	$\mathbf{e}$	Electric intensity (V/m)
U^{anode}	Anode potential (V)	$\mathbf{j}$	Current density (amp/m^2)
$U^{cathode}$	Cathode potential (V)		
a_{ij}	Transformation tensor (-)		

Material parameters

C	Heat capacity (J/kg/K)	k_{caco}	Mole weight relation (-)
D	Diff. coeff. in bulk (m^2/s)	$k_{dist.}$	Distribution func. (-)
D_c	Diffusion param., Cl^- (kg/s/m)	k_{Fe}	Rate constant (kg/m^3/s/K)
$D_{co}^{(g)}$	Diffusion param., CO_2 (kg/s/m)	k_{oh1}	Mole weight relation (-)
$D_{co\theta}^{(g)}$	Diffusion param.,. CO_2 (kg/s/m)	k_{oh2}	Mole weight relation (-)
$D_{co}^{(aq)}$	Diffusion param., CO_2 (kg/s/m)	k_s	Electrical conduct. (ohm/m)
D_{ion}	Diffusion (general) (kg/s/m)	m	Weighting param. (-)
D_{ionE}	Ionic mobility (kg/s/m/V)	v	Valence number (-)
D_o	Diffusion param., Oxy. (kg/s/m)	f_t	Unaxial tens. strength (N/m^2)
D_{oh}	Diffusion param., OH^- (kg/s/m)	$\alpha_{c_{ice}}$	'Ice' exp. (-)
D_v	Diffusion param., vap. (kg/s/m)	α_{c_l}	'Moisture' exp. (-)
$D_{v\theta}$	Diffusion param., vap. (kg/s/m/K)	α_θ	'Thermal' exp. (1/K)
E_s	Elastic moduli (N/m^2)	β_{bulk}	Damping (kg/m^3/s)
F	Faraday's const. (C/mol)	β_{ls}	Damping (kg/m^3/s)
G_F	Fracture energy (Nm/m^2)	$\gamma_{c_{ice}}$	Lame moduli (m^2/N)
G_s	Slip modulus (N/m^2)	γ_f	Unloading parameter (-)
G_{12}	Rate constant (kg^2/J/m^3/s)	λ	Heat conductivity (J/K/s/m)
K_1	Thermal property (J/m^3/K)	λ^f	Characteristic length (m)
L_{12}	Latent heat (J/kg)	μ_l	Viscosity (kg/s/m)
R	Gas constant (J/mol/K)	v_s	Poisson's ratio (-)
R_o	Equilibrium constant (-)	$\kappa_{c_{ice}}$	Lame moduli (m^2/N)
R_1	Rate constant (kg/m^3/K)		

Subscripts for the constituents

a	Arbitrary constituent
$bulk$	'Bulk' water
c	'Free' dissoved chloride ions
$caco$	Solid calcium carbonate
$cahos$	Solid calcium hydroxide
co	Carbon dioxide
cs	'Bound' chloride ions
l	Liquid water
o	Oxygen
oh	'Free' dissolved hydroxide ions
s	Solid matrix (concrete)
v	Water-vapor
$vic.$	'Vicinal' water

Abbreviations

BET	Brunauer, Emmett and Teller theory
C-S-H	Calcium Silicate Hydrate 'gel'
FEM	Finite Element Method
FDM	Finite Difference Method
OPC	Ordinary Portland Cement
REV	Representative Element Volume
SEM	Scanning Electrode Microscope
SHE	Standard Hygrogen Electrode

Contents

1. Introduction

Degradation processes such as frost attack and steel corrosion in cement-based porous materials cause the society considerably costs yearly. Therefore it is of interest to find a methodology to predict the performance of a structure in advance. Such a methodology is supposed to be used in order to avoid expensive repairing and also as a guideline when choosing materials and when designing constructions.

Today, constructions are indeed designed with powerful computer tools where deformations and stresses may be calculated with acceptable accuracy for both static loads and more complex dynamic load cases. A wide range of experimentally verified complex constitutive behaviors in terms of stresses and strains for different materials are implemented in such computer programs. These programs are used to design structures by civil engineers every day. It is the author's opinion that the reason such material models are gaining great popularity is due to the use of a stringent theory in which the material assumptions have a clear and physical meaning. The usefulness of such material models in designing structures is obvious. In fact, modern models dealing with, for example, material and geometrical non-linearities, elasticity and plasticity are based on over a hundred years of research.

The service life of a structure is, however, not determined solely by its resistance to maximum possible static and dynamic load cases in its initial virgin state. Instead, degradation of the bulk material and the material surfaces caused by environmentally induced effects such as reinforcement corrosion, deicing salt scaling, chemical attack, etc., determine the service life. This means that the

change of the material properties with time must be searched for in order to evaluate the expected deterioration and service life of a structure. By studying the mechanism of, for example, reinforcement corrosion and freezing and thawing of porous materials, one might eventually find physically relevant material parameters describing the degradation phenomenon of interest. If these mechanisms could be understood and hence modeled, the change of the mechanical properties with time may be predicted. Besides, in order to make this prediction, the external environmental properties and their variations must be known.

Processes such as carbonization, chloride penetration causing reinforcement corrosion, development of cracks due to freezing and thawing of pore water, leaching of hydroxide ions, vapor and capillary suction flows, and development of global crack patterns due to mechanical loadings and creep are all phenomena of great interest in the field of durability of cementitious materials. In fact, many of the separate deterioration processes will accelerate or slow down each other when they act on a structure simultaneously. It is to the coupling between different deterioration processes that this licentiate thesis is addressed. By 'durability' is mainly meant service life with regard to such properties as determine the structural stability, i.e. strength, reinforcement corrosion, stiffness, etc. Hence, aesthetic damage, wear etc. are not considered.

Since the topic is naturally very complex, the work is focused on a discussion (in terms of equations) of the main degradation processes and their couplings. This discussion is supposed to improve the possibilities to search for physically adequate material constants and parameters to be used in a model dealing with durability predictions of porous materials.

As the problem of estimating the durability of structures is complex, a physically stringent model describing degradation phenomena is necessarily extensive. Hence, the governing equation system reflecting such behaviors ought to be complex too, even if the problem is simplified.

Since important properties such as bearing capacity and maximum allowable deflections may be introduced as threshold values indicating the condition of a considered structure, it seems natural to use the concept of stress and deformation for estimating the service life of inorganic material structures with regard to structural stability. However, the determination of the stress and deformation state is very much a question of the presence and variation of the environmental conditions in terms of, for example, temperature, moisture, carbon dioxide and deleterious substances such as chloride ions, because these factors determine the 'inner climate' in the structure and thus the degradation rate and extent.

The main focus in this licentiate thesis is a description of the environmentally introduced action of diffusing and chemically reactive (e.g. carbonation and chemical-physical adsorption-desorption) matter in the pore solution and in the air-filled space in the pore system of the material. The governing equations describing the variation of concentrations of different substances and temperature within the material will then be used in a coupled description of the stress-deformation state using the so-called smeared crack approach.

The proposed material model, describing deterioration of cement-based materials, will without doubt be revised in the future. The use of physically stringent assumptions to describe degradation phenomena of mechanical properties is, however, believed to be a fruitful way of developing significant experimental setups; hence realistic simulations in the field of durability may be performed. The present work is a step in this direction.

The mixture theory, defined in the field of continuum mechanics, is an axiomatic structured theory which accounts for actions among multiple phase systems in terms of balance laws. A simple interpretation of this theory will be used as an important base when it comes to establishing the governing equations for the constituents, and for local interactions, and for the mixture as whole. As the suggested equation system for the diffusing-chemical reacting matter presented in this work is compiled on the basis of the mixture theory, it will be outlined in Section 2. The stress-strain description of the solid will, however, be treated with a somewhat more classical fracture mechanic theory.

The main important findings about the physical behavior in terms of chemical reaction, adsorption-desorption and motion of vapor and liquid water in the pore system of a porous material are discussed in Section 4. Other constituents introduced are chlorides, carbon dioxide, oxygen, hydroxide ions and calcium hydroxide. In this Section, equations describing the motion of these constituents and their interactions with each other and with the pore wall will be presented. These equations were obtained by using constitutive relations together with the balance laws proposed within the mixture theory.

In order to compare the pros and cons of different kinds of constitutive relations used in the framework of mixture theory, three types of models are outlined in general terms in Section 3. This is done to show that there are numerous ways of describing the problem that are physically correct and possible.

In Section 6 the initiation and propagation stage of corrosion of reinforcement bars embedded in cement based materials is dealt with. In this context, the constituents introduced in Section 4 will be analyzed further. It will be shown that

ions present in the pore solution will respond in a different way than considering pure diffusion only.

Damage induced by freezing and thawing is one of the most important causes of degradation of brittle inorganic materials in constructions in cold climates. Therefore, some important mechanisms describing the formation of ice crystals in the pore system are discussed in Section 7. A brief discussion of the type of constitutive relations which may be used to describe the ice growth in the pore system is performed.

A few remarks on how to introduce environmentally induced strains into a mechanical model are provided in Section 8. The environmentally imposed conditions of the material are given by the equations presented in Sections 4 to 7. These conditions are used to constitute the stresses in the solid material. The important softening behavior, valid for brittle materials, is involved in the presented model. The problem of changing the mechanical material properties in the so-called softening zones is recognized and discussed.

It certainly is of interest to solve the equations of the type presented, and compare them with the measured global response of a real structure or exposed specimen. For that purpose some of the basic methods of solving transient problems within the framework of finite elements will be outlined in Section 9.

It is concluded that a physically stringent model dealing with service life predictions becomes very complex. A large number of constituents that participate in the degradation mechanism must be described. However, when searching for a stringent physical model the important detailed individual processes must be analyzed systematically. Such an approach is believed to increase the possibility to perform the experiments needed for an application and verification of the model. The meanings of all the material constants and parameters introduced are carefully defined by the constitutive relations and the governing equation systems to be presented. Therefore, this licentiate thesis may serve as a springboard when it comes to improving the knowledge of degradation mechanisms in cement-based porous materials. It must be noted that this thesis mainly considers the material itself, including cast in reinforcement. It does not explicitly consider the structural stability of the entire structure. Such considerations may, however, be addressed using the smeared crack model outlined in Section 8.

2. Basic concepts of the theory of mixtures

To be able to describe the complicated process of how different constituents are transported in a porous medium such as concrete, one must make sure that all the introduced physical quantities satisfy the balance laws. The starting point will therefore be a description of a mixture theory, based on the methods and principles of modern continuum mechanics, which include postulates for the balance of mass, balance of momentum, balance of energy (first axiom of thermodynamics) and the entropy inequality (second axiom of thermodynamics).

Mixture theories include the statement of balance of the physical quantities for both the individual constituents and the mixture as a whole. In terms of modelling a physical behavior, the balance laws have no meaning unless they are supplemented with a set of constitutive relations, which of course must be confirmed by experimental evidence.

The mixture theory to be presented follows the concept described by Bowen, compare [1]. Other similar approaches may be studied in for example [2], [3], [4] and [5]. It should be observed, however, that no general agreement exists on how to formulate these theories. It is worth mentioning that the classical diffusion theories and porous media transport theories can be obtained as approximations of the general mixture theories.

A large number of mixture theories are strongly influenced by the so-called metaphysical principles as defined by Truesdell, compare [2]:

1. *All properties of the mixture must be mathematical consequences of properties of the constituent.*

2. *So as to describe the motion of a constituent, we may in imagination isolate it from the rest of the mixture, provided we allow properly for actions of the other constituents upon it.*

3. *The motion of the mixture is governed by the same equations as is a single body.*

The first metaphysical principle roughly asserts that the whole is no more than the sum of its parts. The second principle states that one may add terms accounting for interactions among the constituents when postulating balance equations for a single constituent in a mixture, provided that the other constituents present are allowed to be affected by this interaction. The third principle declares that a summation of the postulated balance equations for the individual constituents

should be equal to the balance equations for a single body, i.e. the balance equations for the mixture as a whole.

2.1. Kinematics and definitions

The *spatial position,* or the *place* $\mathbf{x}$, of a particle labeled X_a is given by a function $\mathcal{X}_a$ called the *deformation function* or the *motion*. The motion is defined as

$$\mathbf{x} = \mathcal{X}_a(\mathbf{X}_a, t) \tag{2.1}$$

where $\mathbf{X}_a$ is the *material coordinates* of the particle X_a of the ath body or *constituent* in its fixed reference configuration. At time t the *spatial position* $\mathbf{x}$ will be occupied by the particle X_a labeled with is corresponding material coordinates $\mathbf{X}_a$. Assuming that an inverse to the deformation functions, i.e. $\mathcal{X}^{-1}_{a=1,...,\Re}$, exists for all continuous bodies 1, ..., $\Re$ the motion of the ath constituent could be described as

$$\mathbf{X}_a = \mathcal{X}_a^{-1}(\mathbf{x}, t) \tag{2.2}$$

The *velocity* and *acceleration* of the particle X_a at time t are defined by

$$\mathbf{x}'_a = \partial \mathcal{X}_a(\mathbf{X}_a, t)/\partial t \tag{2.3}$$

$$\mathbf{x}''_a = \partial^2 \mathcal{X}_a(\mathbf{X}_a, t)/\partial t^2 \tag{2.4}$$

respectively. That is, the velocity and the acceleration are regarded as functions of the particle X_a having the material coordinates $\mathbf{X}_a$ and the time t. This is the so-called *material description*. Hence the prime affixed to a symbol with a subscript a will denote the *material derivative* following the motion of the ath constituent.

Given (2.2), the velocity and acceleration of $\mathbf{X}_a$ can be regarded as given by functions of $(\mathbf{x}, t)$, i.e.

$$\mathbf{x}'_a = \mathbf{x}'_a(\mathbf{x}, t) \tag{2.5}$$

$$\mathbf{x}''_a = \mathbf{x}''_a(\mathbf{x}, t) \tag{2.6}$$

The *velocity gradient* for the ath constituent at $(\mathbf{x}, t)$ is defined by

$$\mathbf{L}_a = \operatorname{grad} \mathbf{x}'_a(\mathbf{x}, t); \quad L_{(a)ij} = \frac{\partial x'_{(a)i}}{\partial x_j} \tag{2.7}$$

The velocity gradient can be decomposed as

$$\mathbf{L}_a = \mathbf{D}_a + \mathbf{W}_a \tag{2.8}$$

where $\mathbf{D}_a$ is the *symmetric* part of $\mathbf{L}_a$ defined by

$$\mathbf{D}_a = \frac{1}{2}\left(\mathbf{L}_a + \mathbf{L}_a^{\mathrm{T}}\right) \tag{2.9}$$

and $\mathbf{W}_a$ the *skew-symmetric* defined by

$$\mathbf{W}_a = \frac{1}{2}\left(\mathbf{L}_a - \mathbf{L}_a^{\mathrm{T}}\right) \tag{2.10}$$

Here $\mathbf{D}_a$ is called the *rate of strain* tensor or *stretching* tensor and $\mathbf{W}_a$ is called the *spin* tensor.

For a mixture, the $\Re$ bodies $1, ..., \Re$ are allowed to occupy common portions of physical space. Then each spatial position $\mathbf{x}$ in the mixture is occupied by $\Re$ particles, one from each constituent. Each constituent is assigned a density. The *mass density* for the ath constituent is denoted ρ_a. The density is a function of $(\mathbf{x}, t)$, i.e.

$$\rho_a = \rho_a(\mathbf{x}, t) \tag{2.11}$$

The density of the mixture at $\mathbf{x}$ and time t is defined by

$$\rho = \rho(\mathbf{x}, t) = \sum_{a=1}^{\Re} \rho_a(\mathbf{x}, t) \tag{2.12}$$

The *mass concentration* of the ath constituent at $(\mathbf{x}, t)$ is

$$c_a = c_a(\mathbf{x}, t) = \rho_a/\rho \tag{2.13}$$

Following (2.12) and (2.13), the mass concentrations are related by

$$\sum_{a=1}^{\Re} c_a = 1 \tag{2.14}$$

The *mean velocity,* or simply the *velocity of the mixture,* at $(\mathbf{x}, t)$ is the mass-weighted average of the constituent velocities defined by

$$\dot{\mathbf{x}} = \dot{\mathbf{x}}(\mathbf{x}, t) = \frac{1}{\rho}\sum_{a=1}^{\Re} \rho_a \mathbf{x}'_a(\mathbf{x}, t) \tag{2.15}$$

The *diffusion velocity* for the ath constituent at $(\mathbf{x}, t)$ is defined by

$$\mathbf{u}_a = \mathbf{u}_a(\mathbf{x}, t) = \mathbf{x}'_a(\mathbf{x}, t) - \dot{\mathbf{x}}(\mathbf{x}, t) \tag{2.16}$$

The diffusion velocity $\mathbf{u}_a$ is the velocity for the ath constituent related to the mixture. It follows from (2.15), (2.16), and (2.12) that

$$\sum_{a=1}^{\Re} \rho_a \mathbf{u}_a = \mathbf{0} \tag{2.17}$$

The velocity gradient for the mixture at $(\mathbf{x}, t)$ is

$$\mathbf{L} = \operatorname{grad} \dot{\mathbf{x}}\,(\mathbf{x}, t)\,; \qquad L_{ij} = \frac{\partial \dot{x}_i}{\partial x_j} \tag{2.18}$$

The relation between $\mathbf{L}$ and $\mathbf{L}_a$ is obtained by considering the identity

$$\operatorname{grad}\,(\rho_a \mathbf{u}_a) = \mathbf{u}_a \otimes \operatorname{grad} \rho_a + \rho_a \operatorname{grad} \mathbf{u}_a \tag{2.19}$$

where $\otimes$ denotes the dyad product. From (2.17), it follows that

$$\operatorname{grad} \sum_{a=1}^{\Re} \rho_a \mathbf{u}_a = \mathbf{0} \tag{2.20}$$

which together with (2.19) give the relation

$$\sum_{a=1}^{\Re} \mathbf{u}_a \otimes \operatorname{grad} \rho_a = \sum_{a=1}^{\Re} \rho_a \operatorname{grad} \mathbf{u}_a \tag{2.21}$$

In addition, the expression

$$\rho \mathbf{L} = \sum_{a=1}^{\Re} \rho_a \mathbf{L} = \sum_{a=1}^{\Re} \rho_a \operatorname{grad} \dot{\mathbf{x}} = \sum_{a=1}^{\Re} \rho_a \operatorname{grad}\,(\mathbf{x}'_a - \mathbf{u}_a) \tag{2.22}$$

must be considered, in which (2.12) and (2.16) are used. The definition (2.7) together with the expressions (2.21) and (2.22) give the relation between $\mathbf{L}$ and $\mathbf{L}_a$ as

$$\rho \mathbf{L} = \sum_{a=1}^{\Re} (\rho_a \mathbf{L}_a + \mathbf{u}_a \otimes \operatorname{grad} \rho_a) \tag{2.23}$$

Any time-dependent vector fields, and in fact any time-dependent scalar, vector, or tensor field Γ_a associated with the ath constituent, can be regarded either as a function $\Gamma_a\,(\mathbf{X}_a, t)$ of the *particle* X_a (having the fixed *material* coordinates $\mathbf{X}_a$) and the *time* t, or as a function $\Gamma_a\,(\mathbf{x}, t)$ of the *place* $\mathbf{x}$ and the *time* t, provided that a definite motion $\mathbf{x} = \mathcal{X}_a\,(\mathbf{X}_a, t)$ is given. Again, the prime affixed

to a symbol with a subscript a will denote the *material derivative* following the motion of the ath constituent. The material time derivative of Γ_a is defined by

$$\Gamma'_a = \frac{\partial \Gamma}{\partial t}\left[\mathcal{X}_a\left(\mathbf{X}_a, t\right), t\right]; \quad \mathbf{X}_a = const. \tag{2.24}$$

If the inverse to the deformation function $\mathcal{X}_a$ exists, the arbitrary function Γ_a can be expressed by functions of $(\mathbf{x}, t)$. The definition (2.24) and the chain rule for partial differentiation together produce

$$\Gamma'_a = \frac{\partial \Gamma}{\partial t}\left(\mathbf{x}, t\right) + \left[\text{grad } \Gamma\left(\mathbf{x}, t\right)\right] \mathbf{x}'_a\left(\mathbf{x}, t\right) \tag{2.25}$$

which is the relation between the material derivative Γ'_a and the spatial derivative $\partial\Gamma/\partial t$.

The derivative of Γ following the motion defined by the mixture, that is $\dot{\mathbf{x}}$, is denoted by $\dot{\Gamma}$ and is defined, in the same manner, by

$$\dot{\Gamma} = \frac{\partial \Gamma}{\partial t}\left(\mathbf{x}, t\right) + \left[\text{grad } \Gamma\left(\mathbf{x}, t\right)\right] \dot{\mathbf{x}}\left(\mathbf{x}, t\right) \tag{2.26}$$

For example, the material time derivative of the mass density ρ'_a can be related to the spatial time derivative $\partial\rho_a/\partial t$ by identifying Γ as ρ_a to yield

$$\rho'_a = \frac{\partial \rho_a}{\partial t} + \text{grad } \left(\rho_a\right) \cdot \mathbf{x}'_a \tag{2.27}$$

It follows directly from (2.16), (2.25), and (2.26) that

$$\Gamma'_a - \dot{\Gamma} = \left(\text{grad } \Gamma\right) \mathbf{u}_a \tag{2.28}$$

The deformation gradients for the ath constituent is defined by

$$\mathbf{F}_a = \text{GRAD } \mathcal{X}_a\left(\mathbf{X}_a, t\right); \qquad F_{(a)ik} = \frac{\partial x_i}{\partial X_{(a)k}} \tag{2.29}$$

where GRAD denote the gradient with respect to the material coordinates $\mathbf{X}_a$. Note that $\mathbf{F}_a^{-1}$ only exists if $\det \mathbf{F}_a \neq 0$, which is the case because of the assumed invertibility of $\mathcal{X}_a$. The linear transformation inverse to $\mathbf{F}_a$ is

$$\mathbf{F}_a^{-1} = \text{grad } \mathcal{X}_a^{-1}\left(\mathbf{x}, t\right); \qquad F^{-1}_{(a)kj} = \frac{\partial X_{(a)k}}{\partial x_j} \tag{2.30}$$

In accordance with (2.29) and (2.30) it is concluded that

$$\mathbf{F}_a\mathbf{F}_a^{-1} = \mathbf{F}_a^{-1}\mathbf{F}_a = \mathbf{I}; \qquad \frac{\partial x_i \partial X_{(a)k}}{\partial X_{(a)k}\partial x_j} = \delta_{ij} \tag{2.31}$$

Using the chain rule together with the definition of the velocity gradient as

$$L_{(a)ij} = \frac{\partial x'_{(a)i}}{\partial x_j} = \frac{\partial x'_{(a)i}}{\partial X_{(a)k}}\frac{\partial X_{(a)k}}{\partial x_j} \tag{2.32}$$

and noting that $\mathbf{X}_a$ is independent of the time t, it follows that

$$L_{(a)ij} = \left(\frac{\partial x_{(a)i}}{\partial X_{(a)k}}\right)' \frac{\partial X_{(a)k}}{\partial x_j} = F'_{(a)ik}F^{-1}_{(a)kj} \tag{2.33}$$

i.e.

$$\mathbf{L}_a = \mathbf{F}'_a\mathbf{F}_a^{-1} \tag{2.34}$$

which is the relation between the velocity gradient and the deformation gradient for the ath constituent.

For certain problems it is convenient to introduce the vector $\mathbf{w}_a$ denoting the *displacement* of particle X_a of the ath body from its place $\mathbf{X}_a$ in the reference configuration to its place $\mathbf{x} = \mathcal{X}_a(\mathbf{X}_a)$ in its deformed state:

$$\mathbf{w}_a(\mathbf{X}_a) = \mathcal{X}_a(\mathbf{X}_a) - \mathbf{X}_a \tag{2.35}$$

i.e.

$$\mathbf{w}_a(\mathbf{X}_a) = \mathbf{x}(\mathbf{X}_a) - \mathbf{X}_a \tag{2.36}$$

Differentiation yields

$$dx_i\left(X_{(a)}\right) = \frac{\partial x_i}{\partial X_{(a)j}}dX_{(a)j} = \left(\delta_{ij} + \frac{\partial w_{(a)i}}{\partial X_{(a)j}}\right)dX_{(a)j} \tag{2.37}$$

that is

$$\frac{\partial x_i}{\partial X_{(a)j}} = \delta_{ij} + \frac{\partial w_{(a)i}}{\partial X_{(a)j}} \tag{2.38}$$

The *displacement gradient* $\mathbf{H}_a$ is also introduced as

$$\mathbf{H}_a = \text{GRAD } \mathbf{w}_a; \qquad H_{(a)ij} = \frac{\partial w_{(a)i}}{\partial X_{(a)j}} \tag{2.39}$$

This definition together with (2.38) and (2.29) give the relation between the deformation gradient $\mathbf{F}_a$ and the displacement gradient $\mathbf{H}_a$ as

$$\mathbf{F}_a = \mathbf{I} + \mathbf{H}_a \tag{2.40}$$

One of the strain measures is the Lagrangian strain defined as

$$\mathbf{E}_a = \frac{1}{2}\left(\mathbf{F}_a^{\mathrm{T}}\mathbf{F}_a - \mathbf{I}\right) \tag{2.41}$$

which may be expressed in terms of the displacement gradient $\mathbf{H}_a$ as

$$\begin{aligned} \mathbf{E}_a &= \frac{1}{2}\left(\mathbf{F}_a^{\mathrm{T}}\mathbf{F}_a - \mathbf{I}\right) \\ &= \frac{1}{2}\left(\left(\mathbf{I} + \mathbf{H}_a\right)^{\mathrm{T}}\left(\mathbf{I} + \mathbf{H}_a\right) - \mathbf{I}\right) \\ &= \frac{1}{2}\left(\mathbf{H}_a + \mathbf{H}_a^{\mathrm{T}}\right) + \frac{1}{2}\mathbf{H}_a^{\mathrm{T}}\mathbf{H}_a \end{aligned} \tag{2.42}$$

where (2.40) was used. The Lagrangian strain measure has the benefit of giving zero contribution of strains during rigid body rotation. However, the linear strain measure

$$\mathbf{e}_a = \frac{1}{2}\left(\mathbf{H}_a + \mathbf{H}_a^{\mathrm{T}}\right) \tag{2.43}$$

is often adopted.

2.2. Balance of mass

The balance of mass for a mixture consists of two parts: The first is the balance of mass for each constituent, and the second the balance of mass for the mixture as a whole.

Associated with each constituent is a quantity called its *mass supply,* denoted $\hat{c}_a$. The fact that mass can be exchanged among the constituents, for example due to chemical reactions must be considered to guarantee mass balance for the individual constituents.

If $\Re$ is a fixed spatial volume and $\partial\Re$ is the boundary area of the volume $\Re$, the axiom of balance for the ath constituent is

$$\frac{\partial}{\partial t}\int_{\Re} \rho_a \, dv = -\oint_{\partial\Re} \rho_a \mathbf{x}_a' \cdot d\mathbf{s} + \int_{\Re} \hat{c}_a \, dv \tag{2.44}$$

where dv is the element of volume and $d\mathbf{s}$ the outward-drawn normal vector element of area. The rate of change of the mass density in a fixed volume must be balanced by the mass density flow through the boundary of the considered volume plus the production of mass due to supply from the other constituents present in the volume $\Re$.

The axiom of balance of mass for the mixture is

$$\frac{\partial}{\partial t}\int_{\Re}\rho\,dv = -\oint_{\partial\Re}\rho\dot{\mathbf{x}}\cdot d\mathbf{s} \tag{2.45}$$

It follows from (2.12), (2.15), (2.44), and (2.45) that

$$\sum_{a=1}^{\Re}\int_{\Re}\hat{c}_a\,dv = 0 \tag{2.46}$$

Thus, balance of mass for the mixture is equal to the requirement that there be no net production of mass in $\Re$.

If the divergence theorem, that is

$$\oint_{\partial\Re}\rho_a\mathbf{x}'_a\cdot d\mathbf{s} = \int_{\Re}\operatorname{div}(\rho_a\mathbf{x}'_a)\,dv \tag{2.47}$$

is used to convert the surface integral in (2.44) to a volume integral, the alternative form of (2.44) becomes

$$\int_{\Re}\left[\frac{\partial\rho_a}{\partial t} + \operatorname{div}(\rho_a\mathbf{x}'_a) - \hat{c}_a\right]\,dv = 0 \tag{2.48}$$

Assuming that (2.48) is valid for all parts of the volume $\Re$, the local form of balance of mass for the ath constituent is

$$\frac{\partial\rho_a}{\partial t} + \operatorname{div}(\rho_a\mathbf{x}'_a) = \hat{c}_a \tag{2.49}$$

When the same argument is applied to (2.45) and (2.46), it is necessary that the following relations, in the local form, hold for the mixture

$$\frac{\partial\rho}{\partial t} + \operatorname{div}(\rho\dot{\mathbf{x}}) = 0 \tag{2.50}$$

$$\sum_{a=1}^{\Re}\hat{c}_a = 0 \tag{2.51}$$

In the following it will be explained how the mass balance equations can be rewritten in terms of mass concentrations c_a instead of mass density ρ_a. By using (2.16), the mass balance for the ath constituent (2.49) can be rewritten as

$$\frac{\partial \rho_a}{\partial t} + \operatorname{div}(\rho_a \dot{\mathbf{x}}) = -\operatorname{div}(\rho_a \mathbf{u}_a) + \hat{c}_a \tag{2.52}$$

In accordance with (2.13), the first term on the left-hand side of (2.52) is

$$\frac{\partial \rho_a}{\partial t} = \frac{\partial (c_a \rho)}{\partial t} = c_a \frac{\partial \rho}{\partial t} + \rho \frac{\partial c_a}{\partial t} \tag{2.53}$$

where the rule of differentiating a product is used. The second term on the left-hand side of (2.52) is rewritten by use of (2.13) as

$$\operatorname{div}(\rho_a \dot{\mathbf{x}}) = \operatorname{div}(c_a \rho \dot{\mathbf{x}}) = c_a \operatorname{div}(\rho \dot{\mathbf{x}}) + \rho \dot{\mathbf{x}} \cdot \operatorname{grad} c_a \tag{2.54}$$

If (2.53) and (2.54) are inserted into (2.52),

$$c_a \left[\frac{\partial \rho}{\partial t} + \operatorname{div}(\rho \dot{\mathbf{x}}) \right] + \rho \frac{\partial c_a}{\partial t} + \rho \dot{\mathbf{x}} \cdot \operatorname{grad} c_a = -\operatorname{div}(\rho_a \mathbf{u}_a) + \hat{c}_a \tag{2.55}$$

is yielded. The terms in brackets in (2.55) cancels due to the axiom of mass balance for the mixture (2.50). This means that (2.55) can be written as

$$\rho \dot{c}_a = -\operatorname{div}(\rho_a \mathbf{u}_a) + \hat{c}_a \tag{2.56}$$

where $\dot{c}_a$ is the mass concentration following the motion defined by $\dot{\mathbf{x}}$, i.e.

$$\dot{c}_a = \frac{\partial c_a}{\partial t} + \dot{\mathbf{x}} \cdot \operatorname{grad} c_a \tag{2.57}$$

The equation (2.56) holds for all constituents.

By using the identity

$$\operatorname{div}(\rho_a \mathbf{x}'_a) = \rho_a \operatorname{div} \mathbf{x}'_a + \mathbf{x}'_a \cdot \operatorname{grad} \rho_a \tag{2.58}$$

together with the definition (2.25), with $\Gamma'_a = \rho'_a$, an alternative version of (2.49) is obtained as

$$\rho'_a + \rho_a \operatorname{div} \mathbf{x}'_a = \hat{c}_a \tag{2.59}$$

In the same manner,

$$\dot{\rho} + \rho \operatorname{div} \dot{\mathbf{x}} = 0 \tag{2.60}$$

is obtained, which is an alternative version of (2.50).

2.3. Balance of momentum

The axiom of balance of momentum involves statements about the *linear* and *angular* momentum of the constituents, as well as of the mixture. In this presentation, however, the linear momentum for the individual constituents and the mixture will be discussed, since the angular momentum only will be used to show that the stress tensor and the inner part of the stress tensor for the mixture are symmetric.

If $\Re$ is a fixed spatial volume and $\partial\Re$ is the boundary area of the volume $\Re$, the linear momentum for the ath constituent is given as

$$\begin{aligned}\frac{\partial}{\partial t}\int_{\Re}\rho_a\mathbf{x}'_a\,dv &= -\oint_{\partial\Re}\rho_a\mathbf{x}'_a\,(\mathbf{x}'_a\cdot d\mathbf{s})+\oint_{\partial\Re}\mathbf{T}_a d\mathbf{s} \\ &\quad+\int_{\Re}\left(\rho_a\mathbf{b}_a+\hat{\mathbf{p}}_a+\hat{c}_a\mathbf{x}'_a\right)\,dv\end{aligned} \tag{2.61}$$

where $\mathbf{T}_a$ is the *partial stress tensor* for the ath constituent, $\hat{\mathbf{p}}_a$ the *momentum supply*, and $\mathbf{b}_a$ the *external body force density*.

The relation (2.61) generalizes Euler's *first law,* which states that the *total force acting on a body* $\Re$ *is equal to the rate of change of the body's linear momentum.*

However, if a mixture is considered the constituents will interact and produce local forces (making a contribution to the total force of the ath constituent), that is the term $\int_{\Re}(\hat{\mathbf{p}}_a+\hat{c}_a\mathbf{x}'_a)\,dv$, representing a locally produced force on the ath constituent resulting from the presence of other constituents in $\Re$.

The first term on the right-hand side of (2.61) represents the loss of momentum through the boundary area of $\Re$, and the second term on the right-hand side represents the contact force on the ath constituent of $\Re$, resulting from the contact with *all* of the constituents outside $\Re$.

If the properties on the boundary surface $\partial\Re$ are converted to volume integrals with the help of the divergence theorem as

$$\oint_{\partial\Re}\rho_a\mathbf{x}'_a\,(\mathbf{x}'_a\cdot d\mathbf{s})=\int_{\Re}\mathrm{div}(\rho_a\mathbf{x}'_a\otimes\mathbf{x}'_a) \tag{2.62}$$

$$\oint_{\partial\Re}\mathbf{T}_a d\mathbf{s}=\int_{\Re}\mathrm{div}\mathbf{T}_a\,dv \tag{2.63}$$

the balance of linear momentum for the ath constituent could also be written as

$$\int_{\Re}\frac{\partial\left(\rho_a\mathbf{x}'_a\right)}{\partial t}\,dv=\int_{\Re}\left[-\mathrm{div}(\rho_a\mathbf{x}'_a\otimes\mathbf{x}'_a)+\mathrm{div}\mathbf{T}_a+\rho_a\mathbf{b}_a+\hat{\mathbf{p}}_a+\hat{c}_a\mathbf{x}'_a\right]\,dv \tag{2.64}$$

Assuming that (2.64) holds for all parts of the volume $\Re$, the local form of balance of linear momentum for the ath constituent is

$$\frac{\partial\left(\rho_a \mathbf{x}_a'\right)}{\partial t} = -\operatorname{div}\left(\rho_a \mathbf{x}_a' \otimes \mathbf{x}_a'\right) + div\, \mathbf{T}_a + \rho_a \mathbf{b}_a + \hat{\mathbf{p}}_a + \hat{c}_a \mathbf{x}_a' \tag{2.65}$$

If the rule of differentiating a product and (2.25) are used, the term on the left-hand side of (2.65) can be rewritten as

$$\frac{\partial\left(\rho_a \mathbf{x}_a'\right)}{\partial t} = \mathbf{x}_a' \frac{\partial \rho_a}{\partial t} + \rho_a \frac{\partial \mathbf{x}_a'}{\partial t} = \mathbf{x}_a' \frac{\partial \rho_a}{\partial t} + \rho_a \mathbf{x}_a'' - \rho_a \left[\operatorname{grad} \mathbf{x}_a'\right] \mathbf{x}_a' \tag{2.66}$$

The term $\operatorname{div}\left(\rho_a \mathbf{x}_a' \otimes \mathbf{x}_a'\right)$ in (2.65) can be rewritten as

$$\operatorname{div}\left(\rho_a \mathbf{x}_a' \otimes \mathbf{x}_a'\right) = \mathbf{x}_a'\, div\, \left(\rho_a \mathbf{x}_a'\right) + \rho_a \left[\operatorname{grad} \mathbf{x}_a'\right] \mathbf{x}_a' \tag{2.67}$$

If (2.66) and (2.67) are used, the local version of the linear momentum for the ath constituent, i.e. equation (2.65) becomes

$$\rho_a \mathbf{x}_a'' + \mathbf{x}_a' \left[\frac{\partial \rho_a}{\partial t} + \operatorname{div}\left(\rho_a \mathbf{x}_a'\right) - \hat{c}_a\right] = \operatorname{div} \mathbf{T}_a + \rho_a \mathbf{b}_a + \hat{\mathbf{p}}_a \tag{2.68}$$

where the terms in brackets cancels due to (2.49), i.e. the linear momentum for the ath constituent in local form can be written as

$$\rho_a \mathbf{x}_a'' = \operatorname{div} \mathbf{T}_a + \rho_a \mathbf{b}_a + \hat{\mathbf{p}}_a \tag{2.69}$$

The arguments applied to the ath constituent in receiving the local balance of momentum (2.69), are also applicable to the whole mixture, now ignoring the term $\int_{\Re}\left(\hat{\mathbf{p}}_a + \hat{c}_a \mathbf{x}_a'\right) dv$, since it describes the interaction *among* the constituents.

The local form of balance of linear momentum for the mixture is the postulate

$$\rho \ddot{\mathbf{x}} = \operatorname{div} \mathbf{T} + \rho \mathbf{b} \tag{2.70}$$

and the balance of angular momentum for the mixture is the postulate

$$\rho\, \dot{\overline{\mathbf{x} \times \dot{\mathbf{x}}}} = \operatorname{div}\left(\mathbf{x} \times \mathbf{T}\right) + \rho \mathbf{x} \times \mathbf{b} \tag{2.71}$$

One important consequence of (2.70) and (2.71) is

$$\mathbf{T} = \mathbf{T}^{\mathrm{T}} \tag{2.72}$$

Just as (2.46) is a consequence of the fact that constituents require balance of mass to be compatible with the mass balance of the mixture, a similar condition must be imposed for the momentum balance equation. The following discussion focuses on deriving this consequence for the balance of momentum.

The external body force density for the whole mixture is defined by

$$\mathbf{b} = \frac{1}{\rho} \sum_{a=1}^{\Re} \rho_a \mathbf{b}_a \tag{2.73}$$

which is an average value of the individual constituent's mass density. The *inner part of the stress tensor* for the mixture is defined by

$$\mathbf{T_I} = \sum_{a=1}^{\Re} \mathbf{T}_a \tag{2.74}$$

while the stress tensor for the mixture is defined by

$$\mathbf{T} = \mathbf{T_I} - \sum_{a=1}^{\Re} \rho_a \mathbf{u}_a \otimes \mathbf{u}_a \tag{2.75}$$

Due to the symmetry of $\mathbf{T}$ and $\sum_{a=1}^{\Re} \rho_a \mathbf{u}_a \otimes \mathbf{u}_a$, the important consequence $\mathbf{T_I} = \mathbf{T_I}^{\mathrm{T}}$ is observed. In general, however, $\mathbf{T}_a$ is not symmetric. Hence, one may introduce the property $\hat{\mathbf{M}}_a$ as

$$\hat{\mathbf{M}}_a = \mathbf{T}_a - \mathbf{T}_a^{\mathrm{T}} \tag{2.76}$$

where $\hat{\mathbf{M}}_a$ is a skew-symmetric linear transformation. Since $\mathbf{T_I} = \mathbf{T_I}^{\mathrm{T}}$, it follows that

$$\sum_{a=1}^{\Re} \hat{\mathbf{M}}_a = \mathbf{0} \tag{2.77}$$

The summation of the momentum equation (2.69) may now be expressed as

$$\sum_{a=1}^{\Re} \rho_a \mathbf{x}_a'' = \operatorname{div} \mathbf{T_I} + \rho \mathbf{b} + \sum_{a=1}^{\Re} \hat{\mathbf{p}}_a \tag{2.78}$$

where the definitions (2.73), (2.74), and (2.75) are used.

A property $\Gamma_a(\mathbf{x}, t)$, $a = 1, ..., \Re$ is considered for the ath constituent as well as the fact that $\Gamma(\mathbf{x}, t)$ is a mass-weighted sum defined by

$$\Gamma(\mathbf{x}, t) = \frac{1}{\rho} \sum_{a=1}^{\Re} \rho_a \Gamma_a(\mathbf{x}, t) = \sum_{a=1}^{\Re} c_a \Gamma_a(\mathbf{x}, t) \tag{2.79}$$

where (2.13) is used. Differentiation of the property Γ as

$$\dot{\Gamma}\left(\mathbf{x},t\right)=\sum_{a=1}^{\Re}\overset{\cdot}{\overline{\left(c_a\Gamma_a\right)}}=\sum_{a=1}^{\Re}\left(c_a\dot{\Gamma}_a+\dot{c}_a\Gamma_a\right) \tag{2.80}$$

and, furthermore, if the expression (2.80) is multiplied by ρ and (2.28), (2.56), and (2.13) are used,

$$\begin{aligned}\rho\dot{\Gamma}\left(\mathbf{x},t\right) &= \rho\sum_{a=1}^{\Re}\left(c_a\dot{\Gamma}_a+\dot{c}_a\Gamma_a\right)= \\ &\sum_{a=1}^{\Re}\left(\rho_a\Gamma_a'-\rho_a\left(\text{grad }\Gamma_a\right)\mathbf{u}_a-\Gamma_a\text{div}\left(\rho_a\mathbf{u}_a\right)+\hat{c}_a\Gamma_a\right)\end{aligned} \tag{2.81}$$

are yielded. Since the following identity holds

$$\text{div }\left(\rho_a\Gamma_a\mathbf{u}_a\right)=\rho_a\left(\text{grad }\Gamma_a\right)\mathbf{u}_a+\Gamma_a\text{div}\left(\rho_a\mathbf{u}_a\right) \tag{2.82}$$

the equation for $\rho\dot{\Gamma}\left(\mathbf{x},t\right)$ becomes

$$\rho\dot{\Gamma}=\sum_{a=1}^{\Re}\left(\rho_a\Gamma_a'-\text{div}\left(\rho_a\Gamma_a\mathbf{u}_a\right)+\hat{c}_a\Gamma_a\right) \tag{2.83}$$

By identifying the properties $\dot{\Gamma}=\ddot{\mathbf{x}}$, $\Gamma_a=\mathbf{x}_a'$ and $\Gamma_a'=\mathbf{x}_a''$ the equation (2.83) can be rewritten as

$$\rho\ddot{\mathbf{x}}=\sum_{a=1}^{\Re}\left(\rho_a\mathbf{x}_a''-\text{div}\left(\rho_a\mathbf{x}_a'\otimes\mathbf{u}_a\right)+\hat{c}_a\mathbf{x}_a'\right) \tag{2.84}$$

Following (2.16), the equation (2.84) can be written as

$$\begin{aligned}\rho\ddot{\mathbf{x}} &= \sum_{a=1}^{\Re}\left(\rho_a\mathbf{x}_a''\right)-\text{div}\sum_{a=1}^{\Re}\left(\rho_a\mathbf{u}_a\otimes\mathbf{u}_a\right)-\text{div}\sum_{a=1}^{\Re}\left(\rho_a\mathbf{u}_a\right)\otimes\dot{\mathbf{x}} \\ &+\sum_{a=1}^{\Re}\left(\hat{c}_a\mathbf{u}_a\right)+\sum_{a=1}^{\Re}\left(\hat{c}_a\right)\dot{\mathbf{x}}\end{aligned} \tag{2.85}$$

Due to (2.17) and (2.51), the expression (2.84) becomes

$$\rho\ddot{\mathbf{x}}=\sum_{a=1}^{\Re}\left(\rho_a\mathbf{x}_a''-\text{div}\left(\rho_a\mathbf{u}_a\otimes\mathbf{u}_a\right)+\hat{c}_a\mathbf{u}_a\right) \tag{2.86}$$

The term $\sum_{a=1}^{\Re}(\rho_a \mathbf{x}_a'')$ is solved in (2.86), and the result is inserted into (2.78), this yields

$$\rho\ddot{\mathbf{x}} = \operatorname{div}\left(\left(\mathbf{T_I} - \sum_{a=1}^{\Re}\rho_a \mathbf{u}_a \otimes \mathbf{u}_a\right)\right) + \rho\mathbf{b} + \sum_{a=1}^{\Re}(\hat{c}_a\mathbf{u}_a + \hat{\mathbf{p}}_a) \tag{2.87}$$

If the definition of the inner part of the stress tensor is used, (2.87) becomes

$$\rho\ddot{\mathbf{x}} = \operatorname{div}\mathbf{T} + \rho\mathbf{b} + \sum_{a=1}^{\Re}(\hat{c}_a\mathbf{u}_a + \hat{\mathbf{p}}_a) \tag{2.88}$$

Due to the balance of momentum of the mixture (2.70) and to (2.88), the following relation must hold

$$\sum_{a=1}^{\Re}(\hat{c}_a\mathbf{u}_a + \hat{\mathbf{p}}_a) = \mathbf{0} \tag{2.89}$$

2.4. Balance of energy

The balance of energy, or the first axiom of thermodynamics, involves two statements (like the balance of mass and momentum); one for the mixture and one for the constituents. According to Truesdell and Toupin, the axiom of balance of energy for the ath constituent in a fixed volume $\Re$ is

$$\begin{aligned}\frac{\partial}{\partial t}\int_{\Re}\rho_a\left(\varepsilon_a + \tfrac{1}{2}x_a'^2\right)dv \;=\; & -\oint_{\partial\Re}\rho_a\left(\varepsilon_a + \tfrac{1}{2}x_a'^2\right)\mathbf{x}_a'\cdot d\mathbf{s} \\ & + \oint_{\partial\Re}\left(\mathbf{T}_a^{\mathrm{T}}\mathbf{x}_a' - \mathbf{q}_a\right)\cdot d\mathbf{s} \\ & + \int_{\Re}\left[\rho_a r_a + \rho_a\mathbf{x}_a'\cdot\mathbf{b}_a + \mathbf{x}_a'\cdot\hat{\mathbf{p}}_a + \hat{\varepsilon}_a\right]dv \\ & + \int_{\Re}\hat{c}_a\left[\varepsilon_a + \tfrac{1}{2}x_a'^2\right]\,dv\end{aligned} \tag{2.90}$$

where $x_a'^2 = \mathbf{x}_a'\cdot\mathbf{x}_a'$. The *internal energy density* for the ath constituent is denoted ε_a. $\mathbf{q}_a$ is the *heat flux* vector for the ath constituent, r_a the *external heat supply* to the ath constituent, and $\hat{\varepsilon}_a$ the local interaction for energy to the ath constituent called the *energy supply*. The term $\rho_a\frac{1}{2}x_a'^2$ is the *kinetic energy density*.

If the divergence theorem on the first and second term on the left-hand side of (2.90) is used as

$$\oint_{\partial\Re}\rho_a\left(\varepsilon_a + \tfrac{1}{2}x_a'^2\right)\mathbf{x}_a'\cdot d\mathbf{s} = \int_{\Re}\operatorname{div}\left[\rho_a\left(\varepsilon_a + \tfrac{1}{2}x_a'^2\right)\mathbf{x}_a'\right]dv \tag{2.91}$$

$$\oint_{\partial\Re}\left(\mathbf{T}_a^{\mathrm{T}}\mathbf{x}_a' - \mathbf{q}_a\right)\cdot d\mathbf{s} = \int_{\Re}\operatorname{div}\left[\mathbf{T}_a^{\mathrm{T}}\mathbf{x}_a' - \mathbf{q}_a\right]dv \tag{2.92}$$

the local form of (2.90) becomes

$$\begin{aligned}\frac{\partial}{\partial t}\rho_a\left(\varepsilon_a + \tfrac{1}{2}x_a'^2\right) + \operatorname{div}\left[\rho_a\left(\varepsilon_a + \tfrac{1}{2}x_a'^2\right)\mathbf{x}_a'\right] &= \operatorname{div}\left[\mathbf{T}_a^{\mathrm{T}}\mathbf{x}_a' - \mathbf{q}_a\right] \\ &\quad +\rho_a r_a + \rho_a\mathbf{x}_a'\cdot\mathbf{b}_a + \hat{\varepsilon}_a \\ &\quad +\mathbf{x}_a'\cdot\hat{\mathbf{p}}_a + \hat{c}_a\left(\varepsilon_a + \tfrac{1}{2}x_a'^2\right)\end{aligned} \tag{2.93}$$

The following identities for the terms on the left-hand side of (2.93) establish that

$$\frac{\partial}{\partial t}\rho_a\left(\varepsilon_a + \tfrac{1}{2}x_a'^2\right) = \left(\varepsilon_a + \tfrac{1}{2}x_a'^2\right)\frac{\partial\rho_a}{\partial t} + \rho_a\frac{\partial}{\partial t}\left(\varepsilon_a + \tfrac{1}{2}x_a'^2\right) \tag{2.94}$$

$$\operatorname{div}\left[\rho_a\left(\varepsilon_a + \tfrac{1}{2}x_a'^2\right)\mathbf{x}_a'\right] = \left(\varepsilon_a + \tfrac{1}{2}x_a'^2\right)\operatorname{div}\left[\rho_a\mathbf{x}_a'\right] + \operatorname{grad}\left(\varepsilon_a + \tfrac{1}{2}x_a'^2\right)\cdot\rho_a\mathbf{x}_a' \tag{2.95}$$

The equation (2.25) should also be considered with $\Gamma_a = \left(\varepsilon_a + \frac{1}{2}x_a'^2\right)$, i.e.

$$\overline{\left(\varepsilon_a + \tfrac{1}{2}x_a'^2\right)}' = \frac{\partial}{\partial t}\left(\varepsilon_a + \tfrac{1}{2}x_a'^2\right) + \operatorname{grad}\left(\varepsilon_a + \tfrac{1}{2}x_a'^2\right)\cdot\mathbf{x}_a' \tag{2.96}$$

If one multiplies (2.96) with ρ_a and combines it with (2.95), the result is

$$\begin{aligned}\operatorname{div}\left[\rho_a\left(\varepsilon_a + \tfrac{1}{2}x_a'^2\right)\mathbf{x}_a'\right] &= \left(\varepsilon_a + \tfrac{1}{2}x_a'^2\right)\operatorname{div}\left[\rho_a\mathbf{x}_a'\right] \\ &\quad +\rho_a\overline{\left(\varepsilon_a + \tfrac{1}{2}x_a'^2\right)}' - \rho_a\frac{\partial}{\partial t}\left(\varepsilon_a + \tfrac{1}{2}x_a'^2\right)\end{aligned} \tag{2.97}$$

Furthermore, by writing the mass balance (2.49) as

$$\left(\varepsilon_a + \tfrac{1}{2}x_a'^2\right)\frac{\partial\rho_a}{\partial t} + \left(\varepsilon_a + \tfrac{1}{2}x_a'^2\right)\operatorname{div}\left(\rho_a\mathbf{x}_a'\right) - \left(\varepsilon_a + \tfrac{1}{2}x_a'^2\right)\hat{c}_a = 0 \tag{2.98}$$

and combining it with (2.97),

$$\begin{aligned}0 &= \left(\varepsilon_a + \tfrac{1}{2}x_a'^2\right)\frac{\partial\rho_a}{\partial t} + \rho_a\frac{\partial}{\partial t}\left(\varepsilon_a + \tfrac{1}{2}x_a'^2\right) + \operatorname{div}\left[\rho_a\left(\varepsilon_a + \tfrac{1}{2}x_a'^2\right)\mathbf{x}_a'\right] \\ &\quad -\rho_a\overline{\left(\varepsilon_a + \tfrac{1}{2}x_a'^2\right)}' - \left(\varepsilon_a + \tfrac{1}{2}x_a'^2\right)\hat{c}_a\end{aligned} \tag{2.99}$$

is achieved. If one uses (2.94) to rewrite (2.99) as

$$\begin{aligned}\frac{\partial}{\partial t}\rho_a\left(\varepsilon_a + \tfrac{1}{2}x_a'^2\right) &= -\operatorname{div}\left[\rho_a\left(\varepsilon_a + \tfrac{1}{2}x_a'^2\right)\mathbf{x}_a'\right] \\ &\quad +\rho_a\overline{\left(\varepsilon_a + \tfrac{1}{2}x_a'^2\right)}' + \left(\varepsilon_a + \tfrac{1}{2}x_a'^2\right)\hat{c}_a\end{aligned} \tag{2.100}$$

it becomes possible to write (2.93) as

$$\rho_a \left(\overline{\varepsilon_a + \tfrac{1}{2}x_a'^2}\right)' = \operatorname{div}\left(\mathbf{T}_a^{\mathrm{T}}\mathbf{x}_a' - \mathbf{q}_a\right) + \rho_a r_a + \rho_a \mathbf{x}_a' \cdot \mathbf{b}_a + \hat{\varepsilon}_a + \mathbf{x}_a' \cdot \hat{\mathbf{p}}_a \tag{2.101}$$

Since the following identities holds,

$$\left(\overline{\tfrac{1}{2}x_a'^2}\right)' = \mathbf{x}_a' \cdot \mathbf{x}_a'' \tag{2.102}$$

$$\operatorname{div}\left(\mathbf{T}_a^{\mathrm{T}}\mathbf{x}_a'\right) = \mathbf{x}_a' \cdot \operatorname{div}\mathbf{T}_a + \mathbf{T}_a^{\mathrm{T}} \cdot \operatorname{grad}\mathbf{x}_a' = \mathbf{x}_a' \cdot \operatorname{div}\mathbf{T}_a + \operatorname{tr}\mathbf{T}_a^{\mathrm{T}}\mathbf{L}_a \tag{2.103}$$

where $\mathbf{L}_a$ is the velocity gradient defined by (2.7) and tr the trace operation, the equation (2.101) can be written in yet another form:

$$\begin{aligned} \rho_a \varepsilon_a' &= \operatorname{tr}\mathbf{T}_a^{\mathrm{T}}\mathbf{L}_a - \operatorname{div}\mathbf{q}_a + \rho_a r_a + \hat{\varepsilon}_a \\ &\quad - \mathbf{x}_a' \cdot (\rho_a \mathbf{x}_a'' - \operatorname{div}\mathbf{T}_a - \rho_a \mathbf{b}_a - \hat{\mathbf{p}}_a) \end{aligned} \tag{2.104}$$

Following (2.69), equation (2.104) can be written as

$$\rho_a \varepsilon_a' = \operatorname{tr}\mathbf{T}_a^{\mathrm{T}}\mathbf{L}_a - \operatorname{div}\mathbf{q}_a + \rho_a r_a + \hat{\varepsilon}_a \tag{2.105}$$

It should be noted that information about the mass balance as well as the momentum balance for the constituents is used in order to reach (2.105).

The local energy equation for the mixture can be written in the form

$$\rho \left(\overline{\varepsilon + \tfrac{1}{2}\dot{x}^2}\right)^{\cdot} = \operatorname{div}\left(\mathbf{T}\dot{\mathbf{x}} - \mathbf{q}\right) + \rho r + \sum_{a=1}^{\Re} \left(\rho_a \mathbf{x}_a' \cdot \mathbf{b}_a\right) \tag{2.106}$$

Except for the last term, the equation (2.106) is identical to the usual energy equation for single materials. When there is no diffusion, i.e. $\mathbf{u}_a$ is zero for all constituents, the last term in (2.106) becomes $\dot{\mathbf{x}} \sum_{a=1}^{\Re} \rho_a \mathbf{b}_a = \rho \dot{\mathbf{x}} \cdot \mathbf{b}$, where (2.73) is used. This is the usual form of the rate of work of the external body force density.

The *external heat supply density* for the mixture is defined by

$$r = \frac{1}{\rho} \sum_{a=1}^{\Re} \rho_a r_a \tag{2.107}$$

The *inner part of the internal energy density* for the mixture is defined by

$$\varepsilon_{\mathbf{I}} = \frac{1}{\rho} \sum_{a=1}^{\Re} \rho_a \varepsilon_a \tag{2.108}$$

and the *internal energy density* for the mixture is defined by

$$\varepsilon = \varepsilon_{\mathbf{I}} + \frac{1}{2\rho}\sum_{a=1}^{\Re}\rho_a u_a^2 \tag{2.109}$$

The *inner part of the heat flux vector* for the mixture is defined by

$$\mathbf{q}_{\mathbf{I}} = \sum_{a=1}^{\Re}\left(\mathbf{q}_a - \mathbf{T}_a^{\mathrm{T}}\mathbf{u}_a + \rho_a\varepsilon_a\mathbf{u}_a\right) \tag{2.110}$$

and the *heat flux vector* for the mixture is defined by

$$\mathbf{q} = \mathbf{q}_{\mathbf{I}} + \tfrac{1}{2}\sum_{a=1}^{\Re}\rho_a u_a^2\mathbf{u}_a \tag{2.111}$$

Another quantity $\mathbf{k}$, which is related to the heat flux, will also be introduced:

$$\begin{aligned}\mathbf{k} &= \sum_{a=1}^{\Re}\left(\mathbf{q}_a + \rho_a\varepsilon_a\mathbf{u}_a\right) = \mathbf{q}_{\mathbf{I}} + \sum_{a=1}^{\Re}\mathbf{T}_a^{\mathrm{T}}\mathbf{u}_a \\ &= \mathbf{q} - \sum_{a=1}^{\Re}\rho_a\left(-\mathbf{T}_a^{\mathrm{T}}/\rho_a + \tfrac{1}{2}u_a^2\mathbf{I}\right)\mathbf{u}_a\end{aligned} \tag{2.112}$$

where the definitions (2.110) and (2.111) is used.

The following identities are valid for the terms in (2.106):

$$\rho\,\dot{\left(\varepsilon + \tfrac{1}{2}\dot{x}^2\right)} = \rho\dot{\varepsilon} + \rho\left(\dot{\tfrac{1}{2}\dot{\mathbf{x}}\cdot\dot{\mathbf{x}}}\right) = \rho\dot{\varepsilon} + \rho\dot{\mathbf{x}}\cdot\ddot{\mathbf{x}} \tag{2.113}$$

$$\sum_{a=1}^{\Re}\left(\rho_a\mathbf{x}_a'\cdot\mathbf{b}_a\right) = \sum_{a=1}^{\Re}\left(\rho_a\left(\dot{\mathbf{x}}+\mathbf{u}_a\right)\cdot\mathbf{b}_a\right) = \sum_{a=1}^{\Re}\left(\rho_a\mathbf{b}_a\right)\cdot\dot{\mathbf{x}} + \sum_{a=1}^{\Re}\rho_a\mathbf{u}_a\cdot\mathbf{b}_a \tag{2.114}$$

where equation (2.16) is used. Following (2.73), the expression (2.114) can be written as

$$\sum_{a=1}^{\Re}\left(\rho_a\mathbf{x}_a'\cdot\mathbf{b}_a\right) = \rho\mathbf{b}\cdot\dot{\mathbf{x}} + \sum_{a=1}^{\Re}\rho_a\mathbf{u}_a\cdot\mathbf{b}_a \tag{2.115}$$

and the term $\operatorname{div}(\mathbf{T}\dot{\mathbf{x}})$ in (2.106) can be identified as

$$\operatorname{div}\left(\mathbf{T}\dot{\mathbf{x}}\right) = \dot{\mathbf{x}}\cdot\operatorname{div}\mathbf{T} + \operatorname{tr}\mathbf{T}\mathbf{L} \tag{2.116}$$

where $\mathbf{L}$ is the velocity gradient for the mixture defined in (2.18). If the identities (2.113), (2.115), and (2.116) are used, the equation (2.106) can be written as

$$\rho\dot{\varepsilon} = \mathrm{tr}\mathbf{T}\mathbf{L} - \mathrm{div}\,\mathbf{q} + \rho r + \sum_{a=1}^{\Re} (\rho_a \mathbf{u}_a \cdot \mathbf{b}_a) - \dot{\mathbf{x}} \cdot (\rho\ddot{\mathbf{x}} - \mathrm{div}\,\mathbf{T} - \rho\mathbf{b}) \tag{2.117}$$

Because of (2.70) the equation (2.117) is reduced to

$$\rho\dot{\varepsilon} = \mathrm{tr}\mathbf{T}\mathbf{L} - \mathrm{div}\,\mathbf{q} + \rho r + \sum_{a=1}^{\Re} (\rho_a \mathbf{u}_a \cdot \mathbf{b}_a) \tag{2.118}$$

Next, the equation (2.117) will be written in terms of the inner part of the internal energy density. Consider the equation (2.109), written as

$$\rho\dot{\varepsilon} = \rho\dot{\varepsilon}_{\mathbf{I}} + \rho \sum_{a=1}^{\Re} \tfrac{1}{2} \left(\overline{\dot{c_a u_a^2}} \right) \tag{2.119}$$

where (2.13) is used.

By identifying $\Gamma_a = \frac{1}{2}u_a^2$ and hence observing that $\Gamma = \sum_{a=1}^{\Re} c_a \frac{1}{2} u_a^2$, it becomes possible to use the equation (2.83) to write the second term on the right-hand side of (2.119) as

$$\rho \sum_{a=1}^{\Re} \tfrac{1}{2} \left(\overline{\dot{c_a u_a^2}} \right) = \sum_{a=1}^{\Re} \left(\rho_a \tfrac{1}{2} \left(\overline{u_a^2} \right)' - \mathrm{div}\,(\rho_a \tfrac{1}{2} u_a^2 \mathbf{u}_a) + \hat{c}_a \tfrac{1}{2} u_a^2 \right) \tag{2.120}$$

Note that

$$\left(\overline{u_a^2} \right)' = \left(\overline{\mathbf{u}_a \cdot \mathbf{u}_a} \right)' = 2\mathbf{u}_a \cdot \mathbf{u}_a' \tag{2.121}$$

i.e.

$$\rho \sum_{a=1}^{\Re} \tfrac{1}{2} \left(\overline{\dot{c_a u_a^2}} \right) = \sum_{a=1}^{\Re} \left(\rho_a \mathbf{u}_a \cdot \mathbf{u}_a' - \mathrm{div}\,(\rho_a \tfrac{1}{2} u_a^2 \mathbf{u}_a) + \hat{c}_a \tfrac{1}{2} u_a^2 \right) \tag{2.122}$$

The term $\sum_{a=1}^{\Re} \rho_a \mathbf{u}_a \cdot \mathbf{u}_a'$ can further be written as

$$\sum_{a=1}^{\Re} \rho_a \mathbf{u}_a \cdot \mathbf{u}_a' = \sum_{a=1}^{\Re} \rho_a \mathbf{u}_a \cdot \left(\mathbf{x}_a'' - \left(\overline{\dot{\mathbf{x}}} \right)' \right) \tag{2.123}$$

where (2.16) is used. Following (2.28) with $\Gamma_a' = \left(\overline{\dot{\mathbf{x}}} \right)'$, (2.123) can also be written as

$$\sum_{a=1}^{\Re} \rho_a \mathbf{u}_a \cdot \mathbf{u}_a' = \sum_{a=1}^{\Re} \rho_a \mathbf{u}_a \cdot (\mathbf{x}_a'' - \ddot{\mathbf{x}} - \mathbf{L}\mathbf{u}_a) \tag{2.124}$$

where $\mathbf{L} = \operatorname{grad} \dot{\mathbf{x}}$. The term $\sum_{a=1}^{\Re} \rho_a \mathbf{u}_a \cdot (\mathbf{L}\mathbf{u}_a)$ in (2.124) can be identified as

$$\sum_{a=1}^{\Re} \rho_a \mathbf{u}_a \cdot (\mathbf{L}\mathbf{u}_a) = \sum_{a=1}^{\Re} \rho_{(a)} u_{(a)j} L_{jk} u_{(a)k} = \operatorname{tr} \sum_{a=1}^{\Re} \rho_a \mathbf{L} (\mathbf{u}_a \otimes \mathbf{u}_a) \tag{2.125}$$

We can also conclude from (2.125), (2.124), and (2.122) that

$$\begin{aligned} \rho \sum_{a=1}^{\Re} \tfrac{1}{2} \left(\overset{\cdot}{\overline{c_a u_a^2}} \right) &= \sum_{a=1}^{\Re} \rho_a \mathbf{u}_a \cdot \mathbf{x}_a'' - \sum_{a=1}^{\Re} (\rho_a \mathbf{u}_a) \cdot \ddot{\mathbf{x}} \\ &\quad - \operatorname{tr} \sum_{a=1}^{\Re} \rho_a \mathbf{L} (\mathbf{u}_a \otimes \mathbf{u}_a) - \operatorname{div} \sum_{a=1}^{\Re} (\rho_a \tfrac{1}{2} u_a^2 \mathbf{u}_a) + \sum_{a=1}^{\Re} \hat{c}_a \tfrac{1}{2} u_a^2 \end{aligned} \tag{2.126}$$

It should be noted that the term $\sum_{a=1}^{\Re} (\rho_a \mathbf{u}_a) \cdot \ddot{\mathbf{x}}$ cancels due to (2.17). If (2.118) is written as

$$\begin{aligned} \rho \dot{\varepsilon}_{\mathbf{I}} + \rho \sum_{a=1}^{\Re} \tfrac{1}{2} \left(\overset{\cdot}{\overline{c_a u_a^2}} \right) &= \operatorname{tr} \left(\mathbf{T}_{\mathbf{I}} - \sum_{a=1}^{\Re} \rho_a \mathbf{u}_a \otimes \mathbf{u}_a \right) \mathbf{L} \\ &\quad - \operatorname{div} \left(\mathbf{q}_{\mathbf{I}} + \tfrac{1}{2} \sum_{a=1}^{\Re} \rho_a u_a^2 \mathbf{u}_a \right) + \rho r + \sum_{a=1}^{\Re} (\rho_a \mathbf{u}_a \cdot \mathbf{b}_a) \end{aligned} \tag{2.127}$$

where (2.119), (2.75), and (2.111) are used, and (2.126) and (2.127) are combined,

$$\rho \dot{\varepsilon}_{\mathbf{I}} = \operatorname{tr} \mathbf{T}_{\mathbf{I}} \mathbf{L} - \operatorname{div} \mathbf{q}_{\mathbf{I}} + \rho r - \sum_{a=1}^{\Re} \mathbf{u}_a \cdot (\rho_a \mathbf{x}_a'' - \rho_a \mathbf{b}_a) - \sum_{a=1}^{\Re} \hat{c}_a \tfrac{1}{2} u_a^2 \tag{2.128}$$

is produced. The quantity $\operatorname{tr} \sum_{a=1}^{\Re} \mathbf{T}_a^{\mathrm{T}} \mathbf{L}_a$ should be considered next. By using (2.16), (2.18), and (2.74), it follows that

$$\begin{aligned} \operatorname{tr} \sum_{a=1}^{\Re} \mathbf{T}_a^{\mathrm{T}} \mathbf{L}_a &= \operatorname{tr} \sum_{a=1}^{\Re} \mathbf{T}_a^{\mathrm{T}} \operatorname{grad} \mathbf{x}_a' = \operatorname{tr} \sum_{a=1}^{\Re} \mathbf{T}_a^{\mathrm{T}} \operatorname{grad} (\mathbf{u}_a + \dot{\mathbf{x}}) \\ &= \operatorname{tr} \sum_{a=1}^{\Re} \mathbf{T}_a^{\mathrm{T}} \operatorname{grad} \mathbf{u}_a + \operatorname{tr} \sum_{a=1}^{\Re} \mathbf{T}_a^{\mathrm{T}} \mathbf{L} \\ &= \operatorname{tr} \sum_{a=1}^{\Re} \mathbf{T}_a^{\mathrm{T}} \operatorname{grad} \mathbf{u}_a + \operatorname{tr} \mathbf{T}_{\mathbf{I}} \mathbf{L} \end{aligned} \tag{2.129}$$

In addition, the term $\operatorname{tr} \sum_{a=1}^{\Re} \mathbf{T}_a^{\mathrm{T}} \operatorname{grad} \mathbf{u}_a$ can be written with the identity

$$\operatorname{tr} \sum_{a=1}^{\Re} \mathbf{T}_a^{\mathrm{T}} \operatorname{grad} \mathbf{u}_a = \operatorname{div} \sum_{a=1}^{\Re} \mathbf{T}_a^{\mathrm{T}} \mathbf{u}_a - \sum_{a=1}^{\Re} \mathbf{u}_a \cdot \operatorname{div} \mathbf{T}_a \tag{2.130}$$

i.e. (2.129) can be written

$$\mathrm{tr}\sum_{a=1}^{\Re}\mathbf{T}_a^{\mathrm{T}}\mathbf{L}_a = \mathrm{div}\sum_{a=1}^{\Re}\mathbf{T}_a^{\mathrm{T}}\mathbf{u}_a - \sum_{a=1}^{\Re}\mathbf{u}_a\cdot\mathrm{div}\,\mathbf{T}_a + \mathrm{tr}\mathbf{T}_{\mathbf{I}}\mathbf{L} \tag{2.131}$$

The equation (2.128) and (2.131) combined yield

$$\begin{aligned}\rho\dot{\varepsilon}_{\mathbf{I}} &= \mathrm{tr}\sum_{a=1}^{\Re}\mathbf{T}_a^{\mathrm{T}}\mathbf{L}_a - \mathrm{div}\,\mathbf{q}_{\mathbf{I}} - \mathrm{div}\sum_{a=1}^{\Re}\mathbf{T}_a^{\mathrm{T}}\mathbf{u}_a + \rho r - \sum_{a=1}^{\Re}\hat{c}_a\tfrac{1}{2}u_a^2 \\ &\quad - \sum_{a=1}^{\Re}\mathbf{u}_a\cdot(\rho_a\mathbf{x}_a'' - \rho_a\mathbf{b}_a - \mathrm{div}\,\mathbf{T}_a)\end{aligned} \tag{2.132}$$

Following (2.69), i.e. the momentum balance equation for the ath constituent, and the definition of $\mathbf{k}$, i.e. (2.112), (2.132) can be expressed as

$$\rho\dot{\varepsilon}_{\mathbf{I}} = \mathrm{tr}\sum_{a=1}^{\Re}\mathbf{T}_a^{\mathrm{T}}\mathbf{L}_a - \mathrm{div}\,\mathbf{k} + \rho r - \sum_{a=1}^{\Re}\hat{c}_a\tfrac{1}{2}u_a^2 - \sum_{a=1}^{\Re}\mathbf{u}_a\cdot\hat{\mathbf{p}}_a \tag{2.133}$$

As was discussed in association with the other field equations, it must be ensured that the balance of energy for the constituents is consistent with the balance of energy for the mixture. In order to examine this consistency, the sum of the $\Re$ equations of (2.105) must be considered, i.e.

$$\sum_{a=1}^{\Re}\rho_a\varepsilon_a' = \sum_{a=1}^{\Re}\mathrm{tr}\mathbf{T}_a^{\mathrm{T}}\mathbf{L}_a - \sum_{a=1}^{\Re}\mathrm{div}\,\mathbf{q}_a + \rho r + \sum_{a=1}^{\Re}\hat{\varepsilon}_a \tag{2.134}$$

where (2.107) is used. By using (2.108) together with (2.79) and (2.83) with $\Gamma_a = \varepsilon_a$, the term $\sum_{a=1}^{\Re}\rho_a\varepsilon_a'$ can be written

$$\sum_{a=1}^{\Re}\rho_a\varepsilon_a' = \rho\dot{\varepsilon}_{\mathbf{I}} + \sum_{a=1}^{\Re}\mathrm{div}\,(\rho_a\varepsilon_a\mathbf{u}_a) - \sum_{a=1}^{\Re}\hat{c}_a\varepsilon_a \tag{2.135}$$

The equation (2.134) and (2.135) combined with the definition (2.112) produce

$$\rho\dot{\varepsilon}_{\mathbf{I}} = \sum_{a=1}^{\Re}\mathrm{tr}\mathbf{T}_a^{\mathrm{T}}\mathbf{L}_a - \sum_{a=1}^{\Re}\mathrm{div}\,\mathbf{k} + \rho r + \sum_{a=1}^{\Re}\hat{\varepsilon}_a + \sum_{a=1}^{\Re}\hat{c}_a\varepsilon_a \tag{2.136}$$

A comparison of (2.136) and (2.133) immediately validates the relation

$$\sum_{a=1}^{\Re}\left(\hat{c}_a\left(\tfrac{1}{2}u_a^2 + \varepsilon_a\right) + \mathbf{u}_a\cdot\hat{\mathbf{p}}_a + \hat{\varepsilon}_a\right) = 0 \tag{2.137}$$

The equation (2.137) can be compared with the requirements on the mass balance (2.51) and the momentum balance (2.89) for the mixture.

2.5. Second axiom of thermodynamics

In this section a discussion of different forms of the entropy inequality will be outlined. Various forms of the second axiom of thermodynamics have been proposed, in which each constituent is assigned a temperature θ_a. These theories will be considered here, but only with the purpose of reaching the approximative entropy inequality used for mixtures with a single temperature θ.

Each constituent is assigned an *entropy density* η_a. The entropy density for the mixture at $(\mathbf{x}, t)$ is defined by

$$\eta = \eta(\mathbf{x}, t) = \frac{1}{\rho} \sum_{a=1}^{\Re} \rho_a \eta_a(\mathbf{x}, t) \tag{2.138}$$

Each constituent is also assigned a temperature θ_a. These temperatures are assumed to be given by a positive-valued function Θ_a such that

$$\theta_a = \Theta_a(\mathbf{x}, t) \tag{2.139}$$

The second axiom of thermodynamics for the part of the mixture that occupies a fixed region $\Re$ at time t is postulated to be

$$\frac{\partial}{\partial t} \int_{\Re} \rho\eta \, dv \geq - \oint_{\partial\Re} \rho\eta \dot{\mathbf{x}} \cdot d\mathbf{s} - \oint_{\partial\Re} \sum_{a=1}^{\Re} (\mathbf{h}_a/\theta_a) \cdot d\mathbf{s} + \int_{\Re} \sum_{a=1}^{\Re} (\rho_a r_a/\theta_a) \, dv \tag{2.140}$$

where $\mathbf{h}_a$ is an *influx* vector for the ath constituent not yet related to the heat flux vector $\mathbf{q}_a$. The local form of the entropy inequality (2.140) can be obtained by considering the terms

$$\oint_{\partial\Re} \rho\eta \dot{\mathbf{x}} \cdot d\mathbf{s} = \int_{\Re} \operatorname{div}(\rho\eta \dot{\mathbf{x}}) \, dv \tag{2.141}$$

and

$$\oint_{\partial\Re} \sum_{a=1}^{\Re} (\mathbf{h}_a/\theta_a) \cdot d\mathbf{s} = \int_{\Re} \operatorname{div} \sum_{a=1}^{\Re} (\mathbf{h}_a/\theta_a) \, dv \tag{2.142}$$

which allows (2.140) to be written in the local form

$$\frac{\partial(\rho\eta)}{\partial t} \geq -\operatorname{div}(\rho\eta \dot{\mathbf{x}}) - \operatorname{div} \sum_{a=1}^{\Re} (\mathbf{h}_a/\theta_a) + \sum_{a=1}^{\Re} \rho_a r_a/\theta_a \tag{2.143}$$

If the identity

$$\operatorname{div}(\rho\eta\dot{\mathbf{x}}) = \eta \operatorname{div}(\rho\dot{\mathbf{x}}) + \rho\dot{\mathbf{x}}\cdot\operatorname{grad}(\eta) \tag{2.144}$$

and also

$$\frac{\partial(\rho\eta)}{\partial t} = \eta\frac{\partial\rho}{\partial t} + \rho\frac{\partial\eta}{\partial t} \tag{2.145}$$

are used, the local form (2.143) can further be expressed as

$$\eta\left(\frac{\partial\rho}{\partial t} + \operatorname{div}(\rho\dot{\mathbf{x}})\right) + \rho\frac{\partial\eta}{\partial t} \geq -\rho\dot{\mathbf{x}}\cdot\operatorname{grad}(\eta) - \operatorname{div}\sum_{a=1}^{\Re}(\mathbf{h}_a/\theta_a) + \sum_{a=1}^{\Re}\rho_a r_a/\theta_a \tag{2.146}$$

Note that the first term on the left-hand side cancels due to (2.50) and that

$$\dot{\eta} = \frac{\partial\eta}{\partial t} + \dot{\mathbf{x}}\cdot\operatorname{grad}(\eta) \tag{2.147}$$

where (2.26) is used. With (2.146), (2.50), and (2.147),

$$\rho\dot{\eta} \geq -\operatorname{div}\sum_{a=1}^{\Re}(\mathbf{h}_a/\theta_a) + \sum_{a=1}^{\Re}\rho_a r_a/\theta_a \tag{2.148}$$

is obtained. Another postulate for the second axiom of thermodynamics is the inequality

$$\begin{aligned}\frac{\partial}{\partial t}\int_{\Re}\rho\eta\,dv \;\geq\; &-\oint_{\partial\Re}\sum_{a=1}^{\Re}\rho_a\eta_a\mathbf{x}'_a\cdot d\mathbf{s} - \oint_{\partial\Re}\sum_{a=1}^{\Re}(\mathbf{q}_a/\theta_a)\cdot d\mathbf{s} \\ &+\int_{\Re}\sum_{a=1}^{\Re}(\rho_a r_a/\theta_a)\;dv\end{aligned} \tag{2.149}$$

Note that

$$\oint_{\partial\Re}\sum_{a=1}^{\Re}(\mathbf{q}_a/\theta_a)\cdot d\mathbf{s} = \int_{\Re}\operatorname{div}\sum_{a=1}^{\Re}(\mathbf{q}_a/\theta_a)\;dv \tag{2.150}$$

and that

$$\oint_{\partial\Re}\sum_{a=1}^{\Re}\rho_a\eta_a\mathbf{x}'_a\cdot d\mathbf{s} = \int_{\Re}\operatorname{div}\sum_{a=1}^{\Re}(\rho_a\eta_a\dot{\mathbf{x}})\;dv + \int_{\Re}\operatorname{div}\sum_{a=1}^{\Re}(\rho_a\eta_a\mathbf{u}_a)\;dv \tag{2.151}$$

where (2.16) is used. Furthermore, the first term on the right-hand side of (2.151) can be written as

$$\int_{\Re}\operatorname{div}(\rho\eta\dot{\mathbf{x}})\;dv = \int_{\Re}\eta\operatorname{div}(\rho\dot{\mathbf{x}})\;dv + \int_{\Re}\rho\dot{\mathbf{x}}\cdot\operatorname{grad}(\eta)\;dv \tag{2.152}$$

where $\sum_{a=1}^{\Re} \rho_a \eta_a = \rho\eta$, i.e. (2.138) is used. If (2.147) is multiplied by ρ and this expression is combined with (2.145),

$$\frac{\partial(\rho\eta)}{\partial t} = \rho\dot{\eta} - \rho\dot{\mathbf{x}}\cdot\mathrm{grad}(\eta) + \eta\frac{\partial\rho}{\partial t} \tag{2.153}$$

is yielded. The inequality (2.149) can now be expressed in the local form by considering (2.150), (2.151), (2.152), and (2.153) in order to obtain

$$\rho\dot{\eta} \geq -\eta\left(\frac{\partial\rho}{\partial t} + \mathrm{div}(\rho\dot{\mathbf{x}})\right) - \mathrm{div}\sum_{a=1}^{\Re}(\mathbf{q}_a/\theta_a + \rho_a\eta_a\mathbf{u}_a) + \sum_{a=1}^{\Re}(\rho_a r_a/\theta_a) \tag{2.154}$$

If (2.50) is used, (2.154) can be reduced to

$$\rho\dot{\eta} \geq -\mathrm{div}\sum_{a=1}^{\Re}(\mathbf{q}_a/\theta_a + \rho_a\eta_a\mathbf{u}_a) + \sum_{a=1}^{\Re}(\rho_a r_a/\theta_a) \tag{2.155}$$

If the local statement of the entropy inequalities (2.148) and (2.155) are compared it can be concluded that the influx vector $\mathbf{h}_a$ takes the form

$$\mathbf{h}_a = \mathbf{q}_a + \rho_a\theta_a\eta_a\mathbf{u}_a \tag{2.156}$$

if (2.148) and (2.155) are to be compatible.

If the equation (2.83) is used with $\Gamma_a = \eta_a$, the inequality (2.155) takes the form

$$\sum_{a=1}^{\Re}(\rho_a\eta_a' + \mathrm{div}(\mathbf{q}_a/\theta_a) - \rho_a r_a/\theta_a + \hat{c}_a\eta_a) \geq 0 \tag{2.157}$$

If (2.157) is written as

$$\sum_{a=1}^{\Re}\frac{1}{\theta_a}(\theta_a\rho_a\eta_a' + \theta_a\mathrm{div}(\mathbf{q}_a/\theta_a) - \rho_a r_a + \theta_a\hat{c}_a\eta_a) \geq 0 \tag{2.158}$$

and it is taken into consideration that

$$\mathrm{div}\mathbf{q}_a = \mathrm{div}(\mathbf{q}_a\theta_a/\theta_a) = \theta_a\mathrm{div}(\mathbf{q}_a/\theta_a) + \mathrm{grad}(\theta_a)\cdot\mathbf{q}_a/\theta_a \tag{2.159}$$

the following inequality is obtained:

$$\sum_{a=1}^{\Re}\frac{1}{\theta_a}(\theta_a\rho_a\eta_a' + \mathrm{div}\mathbf{q}_a - \mathrm{grad}(\theta_a)\cdot\mathbf{q}_a/\theta_a - \rho_a r_a + \theta_a\hat{c}_a\eta_a) \geq 0 \tag{2.160}$$

If the energy equation (2.105), i.e.

$$\rho_a r_a = \rho_a \varepsilon'_a - \mathrm{tr}\mathbf{T}_a^{\mathrm{T}}\mathbf{L}_a + \mathrm{div}\,\mathbf{q}_a - \hat{\varepsilon}_a \tag{2.161}$$

is substituted by (2.160) through the elimination of $\rho_a r_a$ the result is

$$\begin{aligned}\sum_{a=1}^{\Re}\frac{1}{\theta_a}(\rho_a\left(\theta_a\eta'_a - \varepsilon'_a\right) \;\geq\; &\sum_{a=1}^{\Re}\frac{1}{\theta_a}\left(-\mathrm{tr}\mathbf{T}_a^{\mathrm{T}}\mathbf{L}_a + \mathrm{grad}\left(\theta_a\right)\cdot\mathbf{q}_a/\theta_a\right) \\ &+\sum_{a=1}^{\Re}\frac{1}{\theta_a}\left(\mathbf{u}_a\cdot\hat{\mathbf{p}}_a + \hat{c}_a\left(\varepsilon_a - \theta_a\eta_a + \tfrac{1}{2}u_a^2\right) - \hat{e}_a\right)\end{aligned} \tag{2.162}$$

where

$$\hat{e}_a = \hat{\varepsilon}_a + \mathbf{u}_a\cdot\hat{\mathbf{p}}_a + \hat{c}_a\left(\varepsilon_a + \tfrac{1}{2}u_a^2\right) \tag{2.163}$$

It is often convenient to eliminate the internal energies ε_a, 1, ... , $\Re$, in favor of the Helmholtz free energy densities ψ_a defined by

$$\psi_a = \varepsilon_a - \eta_a\theta_a \tag{2.164}$$

If the definition (2.164) is used and

$$\psi'_a = \varepsilon'_a - \eta'_a\theta_a - \eta_a\theta'_a \tag{2.165}$$

is considered, (2.162) can be replaced by

$$\begin{aligned}\sum_{a=1}^{\Re}\frac{1}{\theta_a}(-\rho_a\left(\psi'_a + \eta_a\theta'_a\right) \;\geq\; &\sum_{a=1}^{\Re}\frac{1}{\theta_a}\left(-\mathrm{tr}\mathbf{T}_a^{\mathrm{T}}\mathbf{L}_a + \mathrm{grad}\left(\theta_a\right)\cdot\mathbf{q}_a/\theta_a\right) \\ &+\sum_{a=1}^{\Re}\frac{1}{\theta_a}\left(\mathbf{u}_a\cdot\hat{\mathbf{p}}_a + \hat{c}_a\left(\psi_a + \tfrac{1}{2}u_a^2\right) - \hat{e}_a\right)\end{aligned} \tag{2.166}$$

The inequality (2.166) will now be used to obtain an expression, in which it will be assumed that the mixture is exposed to the following constraints:

$$\theta = \Theta\left(\mathbf{x}, t\right) \tag{2.167}$$

and

$$\Theta_1 = \Theta_2 = ... = \Theta_{\Re} \tag{2.168}$$

where Θ is a positive-valued function. In other words, a single temperature θ is used for all constituents.

The expression (2.28) should be considered together with $\Gamma = \theta$, i.e.

$$\theta'_a = \dot{\theta} + \operatorname{grad}(\theta) \cdot \mathbf{u}_a \tag{2.169}$$

If (2.169) is used the term $\sum_{a=1}^{\Re} \rho_a \eta_a \theta'_a$ in (2.166) can be written as

$$\sum_{a=1}^{\Re} \rho_a \eta_a \theta'_a = \rho\eta\dot{\theta} + \sum_{a=1}^{\Re} \rho_a \eta_a \operatorname{grad}(\theta) \cdot \mathbf{u}_a \tag{2.170}$$

where $\rho\eta = \sum_{a=1}^{\Re} \rho_a \eta_a$. The equation (2.156) with the constraints in (2.168) becomes

$$\sum_{a=1}^{\Re} \mathbf{q}_a = \mathbf{h} - \sum_{a=1}^{\Re} \rho_a \theta \eta_a \mathbf{u}_a \tag{2.171}$$

where $\mathbf{h} = \sum_{a=1}^{\Re} \mathbf{h}_a$. If (2.171) is rewritten as

$$\sum_{a=1}^{\Re} \mathbf{q}_a \cdot \operatorname{grad}(\theta)/\theta = \mathbf{h} \cdot \operatorname{grad}(\theta)/\theta - \sum_{a=1}^{\Re} \rho_a \eta_a \operatorname{grad}(\theta) \cdot \mathbf{u}_a \tag{2.172}$$

the inequality (2.166) can with the help of (2.170) and (2.172) be expressed as

$$\begin{aligned} 0 \;\leq\; & -\sum_{a=1}^{\Re} \rho_a \psi'_a - \rho\eta\dot{\theta} + \sum_{a=1}^{\Re} \operatorname{tr}\mathbf{T}_a^{\mathrm{T}} \mathbf{L}_a - \mathbf{h} \cdot \operatorname{grad}(\theta)/\theta \\ & - \sum_{a=1}^{\Re} \mathbf{u}_a \cdot \hat{\mathbf{p}}_a - \sum_{a=1}^{\Re} \hat{c}_a \left(\psi_a + \tfrac{1}{2} u_a^2\right) \end{aligned} \tag{2.173}$$

where it should be noted that $\sum_{a=1}^{\Re} \hat{e}_a = 0$ due to (2.137) and the constraints in (2.168).

If (2.107) is used, the special case of (2.155) corresponding to (2.148) with the constraints in (2.168) is

$$\rho\dot{\eta} + \operatorname{div}(\mathbf{h}/\theta) - \rho r/\theta \geq 0 \tag{2.174}$$

where $\mathbf{h} = \sum_{a=1}^{\Re} \mathbf{h}_a$.

It is possible to express inequality (2.173) in several equivalent forms. One of them is

$$\begin{aligned} 0 \;\leq\; & -\rho\left(\dot{\psi}_{\mathbf{I}} + \eta\dot{\theta}\right) + \operatorname{tr}\mathbf{T}_a^{\mathrm{T}} \mathbf{L}_a - \sum_{a=1}^{\Re} \left(\mathbf{u}_a \cdot \hat{\mathbf{p}}_a + \hat{c}_a \tfrac{1}{2} u_a^2\right) \\ & - \mathbf{h} \cdot \operatorname{grad}(\theta)/\theta - \operatorname{div}\left(\sum_{a=1}^{\Re} \rho_a \psi_a \mathbf{u}_a\right) \end{aligned} \tag{2.175}$$

where (2.83) is used to write

$$\sum_{a=1}^{\Re}\left(\rho_a\psi_a' + \hat{c}_a\psi_a\right) = \rho\dot{\psi}_{\mathbf{I}} + \operatorname{div}\left(\sum_{a=1}^{\Re}\rho_a\psi_a\mathbf{u}_a\right) \tag{2.176}$$

and where $\psi_{\mathbf{I}}$ is defined as

$$\psi_{\mathbf{I}} = \frac{1}{\rho}\sum_{a=1}^{\Re}\rho_a\psi_a = \varepsilon_{\mathbf{I}} - \eta\theta \tag{2.177}$$

Yet another form of (2.173) is

$$\begin{aligned} 0 \;\leq\; & -\sum_{a=1}^{\Re}\overline{(\rho_a\psi_a)}' - \rho\eta\dot{\theta} - \operatorname{tr}\sum_{a=1}^{\Re}\rho_a\mathbf{K}_a\mathbf{L}_a - \mathbf{h}\cdot\operatorname{grad}(\theta)/\theta \\ & -\sum_{a=1}^{\Re}\left(\mathbf{u}_a\cdot\hat{\mathbf{p}}_a + \hat{c}_a\tfrac{1}{2}u_a^2\right) \end{aligned} \tag{2.178}$$

where $\mathbf{K}_a$ is the chemical potential for general mixtures defined as

$$\mathbf{K}_a = \psi_a\mathbf{I} - \mathbf{T}_a^{\mathrm{T}}/\rho_a \tag{2.179}$$

and where

$$\sum_{a=1}^{\Re}\rho_a\mathbf{K}_a = \rho\psi_{\mathbf{I}}\mathbf{I} - \mathbf{T}_{\mathbf{I}} \tag{2.180}$$

which is a generalization of the classical formula in thermochemistry often written as $\sum_{a=1}^{\Re} c_a\mu_a = \zeta$, where ζ is the Gibbs free energy density for the mixture and μ_a the chemical potential. Note the difference between $\mathbf{K}_a$, which is the chemical potential for general mixtures, and μ_a, which is the chemical potential used in classical thermochemistry. If $\mathbf{K}_a = \mu_a\mathbf{I}$ the stress tensor is given by $\mathbf{T}_a = -\pi_a\mathbf{I}$, where π_a is the partial hydrostatical pressure for the ath constituent. During this condition the chemical potential defined in general mixture theories is reduced to the chemical potential used in classical thermochemistry.

It can be noted that the energy equation for the mixture (2.133), with the single temperature constraint imposed, can be formulated in terms of the introduced thermodynamic potentials η_a, ψ_a and $\mathbf{K}_a$ as

$$\rho\theta\dot{\eta} + \operatorname{div}\mathbf{h} + \sum_{a=1}^{\Re}\mathbf{u}_a\cdot\hat{\mathbf{p}}_a + \sum_{a=1}^{\Re}\hat{c}_a\tfrac{1}{2}u_a^2 - \rho r$$

$$
\begin{aligned}
&= -\sum_{a=1}^{\Re} \overline{(\rho_a \psi_a)}' - \rho\eta\dot{\theta} - \operatorname{tr} \sum_{a=1}^{\Re} \rho_a \mathbf{K}_a \mathbf{L}_a \qquad (2.181)\\
&= -\sum_{a=1}^{\Re} (\rho_a \psi_a' + \hat{c}_a \psi_a) - \rho\eta\dot{\theta} + \operatorname{tr} \sum_{a=1}^{\Re} \mathbf{T}_a^{\mathrm{T}} \mathbf{L}_a
\end{aligned}
$$

Compare [1] for a complete derivation of this form of the energy equation.

2.6. Summary of the general balance equations of a mixture

The balance equations for a mixture rest on the postulate that the local balance of mass, linear and angular momentum, and the energy of the constituents is given by similar relations to those for a single body continuum, but in this case representing the actions from the other constituents by supply terms. This is the second metaphysical principle given by Truesdell. As discussed in the previous sections, the postulated local equations for the constituents takes the form:

$$
\begin{aligned}
\frac{\partial \rho_a}{\partial t} &= -\operatorname{div}(\rho_a \mathbf{x}_a') + \hat{c}_a && (2.182)\\
\rho_a \mathbf{x}_a'' &= \operatorname{div} \mathbf{T}_a + \rho_a \mathbf{b}_a + \hat{\mathbf{p}}_a && (2.183)\\
\hat{\mathbf{M}}_a &= \mathbf{T}_a - \mathbf{T}_a^{\mathrm{T}} && (2.184)\\
\rho_a \varepsilon_a' &= \operatorname{tr} \mathbf{T}_a^{\mathrm{T}} \mathbf{L}_a - \operatorname{div} \mathbf{q}_a + \rho_a r_a + \hat{\varepsilon}_a && (2.185)
\end{aligned}
$$

Following the third metaphysical principle, it is required that a summation of the balance equations for the constituents should result in the balance equation for a single body continuum. The conclusion from such summations of the constituents is

$$
\begin{aligned}
0 &= \sum_{a=1}^{\Re} \hat{c}_a && (2.186)\\
\mathbf{0} &= \sum_{a=1}^{\Re} (\hat{c}_a \mathbf{u}_a + \hat{\mathbf{p}}_a) && (2.187)\\
\mathbf{0} &= \sum_{a=1}^{\Re} \hat{\mathbf{M}}_a && (2.188)\\
0 &= \sum_{a=1}^{\Re} \left(\hat{c}_a \left(\tfrac{1}{2} u_a^2 + \varepsilon_a \right) + \mathbf{u}_a \cdot \hat{\mathbf{p}}_a + \hat{\varepsilon}_a \right) && (2.189)
\end{aligned}
$$

In addition, the following identifications for the mixture quantities $\mathbf{b}$, $\mathbf{T}$, ε, $\mathbf{q}$ and r must be done:

$$\mathbf{b} = \frac{1}{\rho}\sum_{a=1}^{\Re}\rho_a\mathbf{b}_a \tag{2.190}$$

$$\mathbf{T} = \sum_{a=1}^{\Re}\left(\mathbf{T}_a - \rho_a\mathbf{u}_a\otimes\mathbf{u}_a\right) \tag{2.191}$$

$$\varepsilon = \frac{1}{\rho}\sum_{a=1}^{\Re}\left(\rho_a\varepsilon_a + \tfrac{1}{2}\rho_a u_a^2\right) \tag{2.192}$$

$$\mathbf{q} = \sum_{a=1}^{\Re}\left(\mathbf{q}_a - \mathbf{T}_a^{\mathrm{T}}\mathbf{u}_a + \rho_a\varepsilon_a\mathbf{u}_a + \tfrac{1}{2}\rho_a u_a^2\mathbf{u}_a\right) \tag{2.193}$$

$$r = \frac{1}{\rho}\sum_{a=1}^{\Re}\rho_a r_a \tag{2.194}$$

The restrictions (2.186)-(2.189) and the definitions (2.190)-(2.194) are direct consequences of the assumed principles. Compare previous Sections. Therefore the imposed restrictions and relations must be accepted and fulfilled in the mixture theory.

An obvious and direct way to postulate a local form of the second law of thermodynamics for the constituents is not available. One of the discussed entropy inequalities was, however, the restricted single temperature inequality for the mixture

$$\rho\dot{\eta} \geq -\mathrm{div}\sum_{a=1}^{\Re}\left(\mathbf{q}_a/\theta + \rho_a\eta_a\mathbf{u}_a\right) + \sum_{a=1}^{\Re}\left(\rho_a r_a/\theta\right) \tag{2.195}$$

where the entropy density for the constituents, i.e. η_a, is related to the entropy density for the mixture as a whole η by the definition

$$\eta = \frac{1}{\rho}\sum_{a=1}^{\Re}\rho_a\eta_a\left(\mathbf{x},t\right) \tag{2.196}$$

and where the entropy flux $\mathbf{h}$ is the term

$$\mathbf{h} = \sum_{a=1}^{\Re}\left(\mathbf{q}_a/\theta + \rho_a\eta_a\mathbf{u}_a\right) \tag{2.197}$$

One of the reasons that entropy inequalities should not be postulated for the constituents is that the inequality mainly plays the rule of imposing restrictions on

Table 2.1: Introduced physical properties for a mixture as a whole.

Property	Property name	Number of unknowns	Note
ρ	*Mass density*	1	*Const. indep.*
$\dot{\mathbf{x}}$	*Velocity of mix.*	3	*Const. indep.*
$\mathbf{T}$	*Stress tensor*	9	(9) *Const. dep.*
$\mathbf{b}$	*Body force*	3	-
ε	*Internal energy*	1	(1) *Const. dep.*
$\mathbf{q}$	*Heat flux*	3	(3) *Const. dep.*
r	*Ext. heat supply*	1	-
η	*Entropy*	1	(1) *Const. dep.*
θ	*Temperature*	1	*Const. indep.*
		Σ 23	Σ 14

the thermodynamical process studied and does not function as a direct governing equation. Furthermore, it seems difficult to use the third metaphysical principle due to the fact that the second law of thermodynamics is an inequality.

2.7. A few remarks on constitutive theory

In previous Sections the basic balance principles within the mixture theory were discussed. These equations are, however, not enough to yield a complete determination of, for example, the stress and motion. It is also necessary to define the mechanical behavior of the material in question by means of a relation between the stress and the motion. Such a relation is called a constitutive relation. A constitutive relation should be confirmed by experimental evidence. The relations can be established by a number of methods leading to the specification of dependent and independent physical quantities. In this Section the constitutive dependent and independent variables will be specified. Furthermore, a brief discussion of how these different variables can be combined and still satisfy the so-called invariant principle will be presented.

Powerful theorems based on the representation theory, which determines the most general relations between dependent and independent physical quantities, may be used to facilitate the process of measuring relevant material constants and parameters. That is, the choice of constitutive relations is not arbitrary, since they must satisfy the objectivity principle (frame invariance principle) and

requirements on material symmetry.

The introduced physical quantities for the mixture are listed in Table 2.1. The properties ρ, $\dot{\mathbf{x}}$, and θ are chosen to be the constitutive independent variables. Hence, the fourteen introduced constitutive dependent variables can only be functions of ρ, $\dot{\mathbf{x}}$, and θ and their corresponding gradients and time derivatives. However, the motion $\dot{\mathbf{x}}$ is not a reference frame independent property and can therefore not be included to describe a material function f relating, for example, the stress and motion.

It should be observed that the physical quantities ψ (Helmholtz free energy density) and $\mathbf{K}$ (the chemical potential) do not arise among the unknown properties listed in Table 2.1, since these quantities are given explicitly from the definition (2.164) and the linear transformation (2.179).

A constitutive function describing the physical (constitutive dependent) properties $\mathbf{T}$, ε, $\mathbf{q}$ and η is chosen as

$$(\mathbf{T}, \varepsilon, \mathbf{q}, \eta) = f\left(\rho, \mathrm{grad}\rho, \mathbf{D}, \theta, \mathrm{grad}\theta, H_k\right) \tag{2.198}$$

where $\mathbf{D}$ is the symmetrical part of the velocity gradient. The scalar quantity H_k in (2.198) represents a so-called internal variable (or hidden variable). This quantity may be used to justify the choice of constitutive relations. In fact, the introduction of internal variables is one of the corner stones in the theory of plasticity.

The constitutive function described in (2.198) is a so-called constitutive function of (i) a differential type. It should be observed, however, that such functions alternatively can be chosen to be of (ii) rate type or of (iii) integral type.

The equations describing the balance principles for the mixture are nine in all. Compare Table 2.2, where one of them is an inequality. The number of unknowns is therefore $23 - 9 = 14$, which is the sum of the constitutive dependent properties. That is, fourteen equations in the format illustrated in (2.198) must be introduced for the mixture when all of the properties $\mathbf{T}$, ε, $\mathbf{q}$, and η are of interest. All introduced assumptions must satisfy the principle of material frame indifference and the second axiom of thermodynamics. This makes the number of relevant assumptions somewhat restricted.

When a number of constituents are introduced with different physical properties in the model, special terms must also be introduced in order to describe the interacting thermodynamic forces among the different constituents. In that a summation of the postulated balance principles for the individual constituent is made, the classical balance equations for the mixture should be retained. Com-

Table 2.2: Introduced balance equations for the mixture as a whole.

Balance equations for the mixture	Nr. of equations	Equation
Mass balance	1	(2.50)
Momentum balance	3	(2.70)
Symmetry of stress tensor; $\mathbf{T} = \mathbf{T}^{\mathrm{T}}$	3	(2.72)
Energy balance	1	(2.106)
Second axiom of therm. dyn.	1	(2.173) *(Inequality)*
	Σ 9	

Table 2.3: Introduced physical properties accounting for local interaction.

Property	Property name	Number of unknowns	Note	Comp. Eq.
$\hat{c}_a$	*Local int., mass supply*	$1\Re$	*Const. dep.*	(2.51)
$\hat{\mathbf{p}}_a$	*Local int., momentum supply*	$3\Re$	*Const. dep.*	(2.89)
$\hat{\varepsilon}_a$	*Local int., energy supply*	$1\Re$	*Const. dep.*	(2.137)
		$\Sigma 5\Re$		

pare previous Sections. The introduced local interactions in the mixture theory are all constitutive dependent properties, compare Table 2.3. This means that the function f which relates the constitutive dependent and independent properties for a constituent, denoted a, will be more complex than for the same relation for the mixture. The constitutive function for a constituent in a mixture must be of the following general format:

$$(\mathbf{T}_a, \varepsilon_a, \mathbf{q}_a, \eta_a, \hat{c}_a, \hat{\mathbf{p}}_a, \hat{\varepsilon}_a) = f\left(\rho_a, \mathrm{grad}\rho_a, \mathbf{D}_a, \theta_a, \mathrm{grad}\theta_a, \mathbf{u}_a, H_{ak}\right) \tag{2.199}$$

It can be shown that the diffusion velocity $\mathbf{u}_a$, i.e. the velocity related to the velocity of the mixture, is unaffected by the choice of coordinate system and can therefore be used to describe the constitutive behavior of the quantities on the left-hand side of (2.199).

Indeed, it is important to be aware of the structure that the constitutive equations must take on to satisfy the postulated axiom, i.e. the format illustrated in (2.198) and (2.199). The representation theory, however, makes it possible to go one step further, i.e. a format where a determined number of scalar functions α_i (material functions) are defined, which are functions of the invariants in the problem. This means that the complete structure of how dependent and independent

variables are connected through the material functions α_i is known beforehand. Unfortunately, these general concepts become very complex, especially when interacting constituents are considered. However, intuitively proposed constitutive relations can be rejected if they do not fit into the structure given from the representation theory. Moreover, it is possible to use a systematic process when identifying significant material functions in experiments. It should also be noted that many of the generated material functions α_i can be assumed to be zero, simply by considering the nature of the physical process of interest.

For example, the stress tensor can be assumed to be given by an isotropic function $\mathbf{f}$ of the symmetric part of the velocity gradient only, i.e. $\mathbf{T} = \mathbf{f}(\mathbf{D})$. In this special case, it follows from the representation theory that the constitutive relation for the stress tensor must take the following general form:

$$\mathbf{T} = \alpha_1 \mathbf{I} + \alpha_2 \mathbf{D} + \alpha_3 \mathbf{D}^2 \tag{2.200}$$

where the material parameters α_1, α_2, and α_3 can be functions of the invariant measures, that is, $\mathrm{tr}\mathbf{D}$, $\mathrm{tr}\mathbf{D}^2$ and $\mathrm{tr}\mathbf{D}^3$. The linear viscous fluid assumption is obtained by setting $\alpha_1 = -\pi + \lambda \mathrm{tr}\mathbf{D}$, $\alpha_2 = 2\mu$, and $\alpha_3 = 0$, where λ and μ are material constants and where π is the hydrostatic pressure. The following relation for the stress tensor is obtained:

$$\mathbf{T} = -\pi \mathbf{I} + \lambda (\mathrm{tr}\mathbf{D}) \mathbf{I} + 2\mu \mathbf{D} \tag{2.201}$$

When coupled equations with different constituents are considered, the complexity of the problem grows dramatically, since the material functions α_i are dependent not only on separate physical invariants but on combinations of different invariants.

In the following, examples of models, based on simple interpretations of the mixture and constitutive theories, will be outlined. In Section 4, a more detailed model dealing with mass and heat transfer in porous materials will be presented. These problems are believed to be a key issue when studying deterioration phenomena of cement-based materials. The description of the stresses in the material caused by the environment will not, however, follow the general concept of the mixture theory but rather be described with a classical fracture-mechanical formulation.

3. Constitutive models: Three different approaches

In this section, basic structures of different models describing the same physical problem will be outlined. More detailed constitutive behavior will be discussed in Section 4.

The first approach concerns an example of a constitutive model, where the mass balance equations for the constituents and the energy equation will be used together with constitutive relations. The second example is an approach, which starts from the equation describing the balance of linear momentum, in which the stress tensors and the momentum supplies for the constituents are constituted. The mass balance equations are then used to calculate the concentration fields without introducing any extra constitutive relations. The third example concerns a mixture of constituting either the stress tensors or the mass diffusion velocities for different constituents.

The energy balance equation is treated in the same way in the three different approaches.

The problem at hand is the coupled transport of water, vapor and dissolved chloride ions in concrete. The effect of mechanical load is not considered in the following three examples. The constituents of interest are the solid concrete phase denoted s, the liquid phase l, the vapor phase v, and the chloride ion phase c.

3.1. Example - A quasi-static approach

This first approach will be referred to as the *quasi-static* approach, as it represents a transient process where the diffusion velocities for the constituents are described with constitutive relations. The primary unknowns are the mass densities, the velocities and internal mass supplies for constituents and temperature, internal energy, as well as the heat flux for the whole mixture. The unknown quantities are

$$\begin{matrix} \rho_s(\mathbf{x},t) \\ \rho_l(\mathbf{x},t) \\ \rho_v(\mathbf{x},t) \\ \rho_c(\mathbf{x},t) \end{matrix} ; \quad \begin{matrix} \mathbf{x}'_s(\mathbf{x},t) = 0 \\ \mathbf{x}'_l(\mathbf{x},t) \\ \mathbf{x}'_v(\mathbf{x},t) \\ \mathbf{x}'_c(\mathbf{x},t) \end{matrix} ; \quad \begin{matrix} \hat{c}_s(\mathbf{x},t) \\ \hat{c}_l(\mathbf{x},t) \\ \hat{c}_v(\mathbf{x},t) \\ \hat{c}_c(\mathbf{x},t) \end{matrix} ; \quad \theta(\mathbf{x},t) ; \varepsilon(\mathbf{x},t) ; \mathbf{q}(\mathbf{x},t) \tag{3.1}$$

where the subscript s, l, v, and c represent the solid (concrete), liquid, vapor, and chloride ion phases respectively. The solid is assumed to be non-deformable, i.e. $\mathbf{x}'_s(\mathbf{x},t) = 0$.

The following quantities

$$\begin{matrix} c_s\,(\mathbf{x},t) \\ c_l\,(\mathbf{x},t) \\ c_v\,(\mathbf{x},t) \\ c_c\,(\mathbf{x},t) \end{matrix} \; ; \; \begin{matrix} \mathbf{u}_s\,(\mathbf{x},t) \\ \mathbf{u}_l\,(\mathbf{x},t) \\ \mathbf{u}_v\,(\mathbf{x},t) \\ \mathbf{u}_c\,(\mathbf{x},t) \end{matrix} \; ; \; \dot{\mathbf{x}}\,(\mathbf{x},t) \; ; \; \rho\,(\mathbf{x},t) \tag{3.2}$$

can be calculated directly from the quantities listed in (3.1). The mass density for the mixture is given by (2.12) as

$$\rho\,(\mathbf{x},t) = \rho_s + \rho_l + \rho_v + \rho_c \tag{3.3}$$

The mean velocity or the velocity of the mixture is, following (2.15) given by

$$\dot{\mathbf{x}} = \dot{\mathbf{x}}\,(\mathbf{x},t) = \frac{1}{\rho}\left(\rho_l \mathbf{x}'_l + \rho_v \mathbf{x}'_v + \rho_c \mathbf{x}'_v\right) \tag{3.4}$$

The concentrations for the individual constituents, as defined in (2.13), are

$$c_s = \frac{\rho_s}{\rho}; \quad c_l = \frac{\rho_l}{\rho}; \quad c_v = \frac{\rho_v}{\rho}; \quad c_c = \frac{\rho_c}{\rho} \tag{3.5}$$

and the diffusion velocities (2.16) are

$$\begin{aligned} \mathbf{u}_s &= -\dot{\mathbf{x}} \\ \mathbf{u}_l &= \mathbf{x}'_l - \dot{\mathbf{x}} \\ \mathbf{u}_v &= \mathbf{x}'_v - \dot{\mathbf{x}} \\ \mathbf{u}_c &= \mathbf{x}'_v - \dot{\mathbf{x}} \end{aligned} \tag{3.6}$$

The system contains fourteen primary unknown quantities, i.e. the quantities listed in (3.1), but there are five balance laws only, which means that nine constitutive relations must be formulated using this approach. The mass balance expressed in terms of mass concentration for the solid phase s is given by (2.56) and (3.6) as

$$\rho\left(\frac{\partial c_s}{\partial t} + \dot{\mathbf{x}}\cdot\operatorname{grad} c_s\right) = \operatorname{div}\left(c_s \rho \dot{\mathbf{x}}\right) + \hat{c}_s \tag{3.7}$$

The mass balance for the liquid phase l is given by (2.56) as

$$\rho\left(\frac{\partial c_l}{\partial t} + \dot{\mathbf{x}}\cdot\operatorname{grad} c_l\right) = -\operatorname{div}\left(c_l \rho \mathbf{u}_l\right) + \hat{c}_l \tag{3.8}$$

The mass balance for the vapor phase v is by the same argument given as

$$\rho\left(\frac{\partial c_v}{\partial t}+\dot{\mathbf{x}}\cdot\operatorname{grad} c_v\right)=-\operatorname{div}\left(c_v\rho\mathbf{u}_v\right)+\hat{c}_v \tag{3.9}$$

The mass balance for the chloride ion phase c is

$$\rho\left(\frac{\partial c_c}{\partial t}+\dot{\mathbf{x}}\cdot\operatorname{grad} c_c\right)=-\operatorname{div}\left(c_c\rho\mathbf{u}_c\right)+\hat{c}_c \tag{3.10}$$

The internal mass supply $\hat{c}_a$ for the constituents are constitutive dependent properties, which will be described as functions of physical quantities defined in the model together with two constants describing the *porosity* n ($\mathrm{m}^3/\mathrm{m}^3$) and the *specific surface area* a (m^2/kg) of the solid material s in question. The assumption that mass exchange will only take place between the vapor phase and the liquid phase, and between the solid phase and the chloride ion phase will be introduced. Then, the equation (2.51) can be formulated as

$$\hat{c}_s+\hat{c}_c=0 \tag{3.11}$$

and

$$\hat{c}_v+\hat{c}_l=0 \tag{3.12}$$

The mass exchange rate between the chloride ion phase and the solid phase is now introduced in a general fashion as a function f, i.e.

$$\hat{c}_c=f\left(c_c,\, c_s,\, c_l,\, \theta,\, n,\, a\right) \tag{3.13}$$

where it should be noted that c_c, c_s, c_l and θ are quantities given by the model and that the porosity n and the specific surface area a are constants. A more detailed description and explanation of the choice of the function f in (3.13) will be performed in Section 4.6. The mass exchange rate between the vapor phase and the liquid phase is assumed to be described with the following general function:

$$\hat{c}_v=f\left(c_v\,, c_l\,,\, \theta,\, n,\, a\right) \tag{3.14}$$

The diffusion velocities for the constituents must be described with constitutive relations using the proposed strategy in this section. The following relation is assumed to hold for the constituents. The (mass) diffusion velocity for the liquid phase is described in general terms as

$$\rho_l\mathbf{u}_l=\mathbf{f}\left(\operatorname{grad} c_l,\, \operatorname{grad}\theta,\, \mathbf{u}_l,\, c_l,\, n,\, a\right) \tag{3.15}$$

The (mass) diffusion velocity for the vapor phase is assumed to be expressed by

$$\rho_v \mathbf{u}_v = \mathbf{f}\,(\,\mathrm{grad}\,c_v,\ \mathrm{grad}\,\theta,\ c_l,\ \theta,\ n,\ a) \tag{3.16}$$

and the (mass) diffusion velocity for the vapor phase by

$$\rho_c \mathbf{u}_c = \mathbf{f}(\,\mathrm{grad}\,c_c,\ \mathrm{grad}\,\theta,\ c_l,\ \theta,\ n,\ a) \tag{3.17}$$

Three properties still have to be determined: the temperature θ, the internal energy density ε, and the heat flux vector $\mathbf{q}$ for the mixture as a whole. At first, it will be assumed that the system is free from external heat supply, i.e. that

$$r = 0 \tag{3.18}$$

and that the term $\mathbf{TL}$ is a small quantity, i.e. that

$$\mathbf{TL} = 0 \tag{3.19}$$

where $\mathbf{T}$ is the stress tensor and $\mathbf{L}$ is the velocity gradient of the mixture. From a physics perspective, the assumption (3.19) means that the stress does not affect the rate of change of the internal energy. With the assumptions (3.18) and (3.19), the energy balance equation (2.118) becomes

$$\rho(\frac{\partial \varepsilon}{\partial t} + \dot{\mathbf{x}}\cdot\mathrm{grad}\,\varepsilon) = \mathrm{div}\,\mathbf{q} \tag{3.20}$$

where $\dot{\mathbf{x}}$ is, again, the mean velocity of the mixture. The constitutive relation for the internal energy density is expressed by a function of temperature only, namely as

$$\varepsilon = f\,(\theta) \tag{3.21}$$

During operations that include phase change problems, the function (3.21) will be a discontinuous function. The heat flux vector $\mathbf{q}$ is constituted with a function of the gradient of the temperature, i.e.

$$\mathbf{q} = \mathbf{f}\,(\,\mathrm{grad}\,\theta) \tag{3.22}$$

The equation system is now closed, the fourteen quantities listed in (3.1) are supplemented with five balance equations, one for the balance of energy for the whole mixture (3.20) and four mass balance equations for the individual constituents (3.7-3.10). The remaining necessary nine equations are the constitutive

relations (3.11-3.14), (3.15-3.17), and (3.21-3.22). It should also be noted that the constitutive relations are given by functions of variables defined in the model.

The diffusion velocities are constituted in the model described in this section. There is thus no point in introducing constitutive relations for the stress tensors for the individual constituents in order to compute the velocities, as it is assumed that it is possible to describe these properties explicitly by constitutive relations. One may, however, use an equation of state, for example the assumption of an *ideal* and *perfect fluid*, i.e. $\pi_a = R\rho_a\theta/M_a$, where R is the *universal gas constant*, and M_a the mole weight, to compute the partial pressures π_a. This will, of course, still not give any extra information, which can be used to constitute the diffusion velocities or the internal energy, since the partial pressures are given by functions of already introduced properties, in this example ρ_a and θ_a. This calls for a more physical and realistic model which accounts for and satisfies all three balance laws, i.e. the balances of momentum, mass and energy. This approach will be outlined in the next Section.

To be able to solve the equation system, *boundary conditions* and *initial conditions* must be imposed. In the quasi-static approach discussed in this Section, either the *natural boundary condition*, that is the description of the mass-flow at a boundary surface, e.g. $\rho_l\mathbf{u}_l$, $\rho_v\mathbf{u}_v$ and $\rho_c\mathbf{u}_c$, or an *essential boundary*, that is the description of the variable itself, e.g. c_l, c_v, and c_c can be given. For the simple version of the energy equation adopted here, the natural boundary condition is the heat flux vector $\mathbf{q}$ and the essential boundary condition is the temperature θ.

With types of problems associated with mass transport in porous materials, it is perhaps most realistic to impose essential boundary conditions, since they can be measured directly. When the capillary suction phenomena are studied, it may, however, be some advantages to use the natural boundary condition to evaluate measurements. Nonetheless, in order to capture realistic conditions at the boundary surface, it is sometimes necessary to have information both about the essential and natural boundary conditions, e.g. when considering *convection* phenomena *at* the boundary surface. This type of boundary conditions are called *mixed boundary conditions*. As the description and treatment of the boundary conditions play a very important part in the global solution behavior of the problem considered, a more detailed discussion on the subject will be presented in Section 4.

When it comes to solving the governing equation system, it should be observed that some numerical difficulties arise from the fact that *convective terms* are present, e.g. $\dot{\mathbf{x}}\cdot\text{grad}\, c_l$, in (3.8). Different numerical solution strategies to overcome

the difficulties will be treated in Section 9.4.

Indeed, it is possible to compute for the mass concentration fields without constitute the mass diffusion velocities. This method will be discussed in the next Section.

3.2. Example - A dynamic approach

The second approach differs from the first one on one important point: Here the diffusion velocities are computed instead of constituted by making constitutive assumptions for the stress tensors $\mathbf{T}_a$ and momentum supplies $\hat{\mathbf{p}}_a$ for the individual constituents.

The main reason why this method is included as a possible solution to the problem is to show that there are various ways to describe the phenomenon of mass transfer which satisfies the balance principles and from this standpoint get a wider perspective of the problem. Already at this point, it is important, to remember that the discussed approach will not be used to its full extent. It is assumed, however, that many interesting points can be drawn from an investigation where all balance laws are considered, as this represents a more stringent theory than the quasi-static one. It is also believed that an investigation of this approach can be used to improve the assumptions in the simple method presented in Section 3.1. Some examples will be discussed in the following sections.

The approach treated in this section will require more constitutive relations than the quasi-static approach discussed in Section 3.1, but not necessarily more material constants or parameters. This is not surprising, since the proposed dynamic approach is a more detailed and stringent physical method as it is based on all three balance equations for the individual constituents. This is not a claim, however, that this approach in is all parts superior to the quasi-static approach.

The following primary unknown physical properties are to be solved for

$$\begin{matrix} \mathbf{T}_s\left(\mathbf{x},t\right) \\ \mathbf{T}_l\left(\mathbf{x},t\right) \\ \mathbf{T}_v\left(\mathbf{x},t\right) \\ \mathbf{T}_c\left(\mathbf{x},t\right) \end{matrix} ; \begin{matrix} \hat{\mathbf{p}}_s\left(\mathbf{x},t\right) \\ \hat{\mathbf{p}}_l\left(\mathbf{x},t\right) \\ \hat{\mathbf{p}}_v\left(\mathbf{x},t\right) \\ \hat{\mathbf{p}}_c\left(\mathbf{x},t\right) \end{matrix} ; \begin{matrix} \rho_s\left(\mathbf{x},t\right) \\ \rho_l\left(\mathbf{x},t\right) \\ \rho_v\left(\mathbf{x},t\right) \\ \rho_c\left(\mathbf{x},t\right) \end{matrix} ; \begin{matrix} \mathbf{x}'_s\left(\mathbf{x},t\right)=0 \\ \mathbf{x}'_l\left(\mathbf{x},t\right) \\ \mathbf{x}'_v\left(\mathbf{x},t\right) \\ \mathbf{x}'_c\left(\mathbf{x},t\right) \end{matrix} ; \begin{matrix} \hat{c}_s\left(\mathbf{x},t\right) \\ \hat{c}_l\left(\mathbf{x},t\right) \\ \hat{c}_v\left(\mathbf{x},t\right) \\ \hat{c}_c\left(\mathbf{x},t\right) \end{matrix} \tag{3.23}$$

and also for the quantities needed to predict the temperature field and heat flux for the whole mixture, that is $\theta\left(\mathbf{x},t\right)$, $\varepsilon\left(\mathbf{x},t\right)$, and $\mathbf{q}\left(\mathbf{x},t\right)$, which are all unknowns and must therefore be added to the list (3.23).

The total primary unknown quantities is therefore twenty-two. This is a large number of unknowns which, indeed, needs twenty-two equations to make the

equation system closed. Surprisingly enough, methods of solving the mass concentration fields of the liquid, vapor, chloride (and other quantities) in a *mixture* and in temperature fields are often claimed to be described with a slight modification of material constants. For example, this is true of the diffusion constant in the *Fick's second law* for *each* constituent in the mixture considered. When this slight modification is performed, however, it is important to consider the fact that there is no stringent theory or physical background in making these assumptions for a mixture. Theoretically, therefore, no physically correct conclusions can be drawn, neither from any experiments nor computer simulations.

The dynamic approach, which will be discussed in this Section, makes use of nine balance equations: one for the energy of the whole mixture, four balance equations for the mass, and four balance equations for the momentum of the individual constituents. Furthermore, three relations are introduced for the mixture concerning the mass supplies and the momentum supplies. These reduce the number of required constitutive relations to ten. This means that a minimum of ten material constants is required.

Without making any deviation from the generality of the mixture theory, it can nevertheless be concluded that several of the remaining material constants are not important (which should be confirmed by experiments), and that an acceptable number of unknown material constants can be dealt with. The physical theory would still be stringent and the constitutive relations can be used to evaluate the measurements. However, experiments performed in the area of interest indicate that the problem is complex and needs powerful physical hypotheses and experiments.

The quantities in (3.24) are given from the relations (3.3-3.6)

$$\begin{array}{ll} c_s(\mathbf{x},t) & \mathbf{u}_s(\mathbf{x},t) \\ c_l(\mathbf{x},t) & \mathbf{u}_l(\mathbf{x},t) \\ c_v(\mathbf{x},t) & \mathbf{u}_v(\mathbf{x},t) \\ c_c(\mathbf{x},t) & \mathbf{u}_c(\mathbf{x},t) \end{array} \qquad \dot{\mathbf{x}}(\mathbf{x},t) \qquad \rho(\mathbf{x},t) \tag{3.24}$$

This means that these quantities are available, since they are given directly as functions of the primary unknowns listed in (3.23).

The body forces in the momentum balance equation (2.69) for the constituents

are assumed to have negligible influence, i.e.

$$\begin{array}{c} \rho_s \mathbf{b}_s = \mathbf{0} \\ \rho_l \mathbf{b}_l = \mathbf{0} \\ \rho_v \mathbf{b}_v = \mathbf{0} \\ \rho_c \mathbf{b}_c = \mathbf{0} \end{array} \tag{3.25}$$

From (2.89) it is concluded that the following relation must be valid for the mixture in consideration:

$$\hat{c}_v \left(\mathbf{u}_v - \mathbf{u}_l\right) + \hat{c}_c \left(\mathbf{u}_c - \mathbf{u}_s\right) + \hat{\mathbf{p}}_s + \hat{\mathbf{p}}_l + \hat{\mathbf{p}}_v + \hat{\mathbf{p}}_c = \mathbf{0} \tag{3.26}$$

If $\hat{\mathbf{p}}_s$ is solved in (3.26) and the result inserted into the balance of momentum in (2.69) for the solid constituent,

$$\mathbf{0} = div\, \mathbf{T}_s - \hat{c}_v \left(\mathbf{u}_v - \mathbf{u}_l\right) - \hat{c}_c \left(\mathbf{u}_c - \mathbf{u}_s\right) - \hat{\mathbf{p}}_l - \hat{\mathbf{p}}_v - \hat{\mathbf{p}}_c \tag{3.27}$$

is obtained, where the approximation for the body force is used. It is also assumed that the solid constituent is non-deformable, i.e. $\mathbf{x}'_s(\mathbf{x}, t) = 0$. Based on the material derivative for $\mathbf{x}''_l(\mathbf{x}, t)$, i.e. $\mathbf{x}''_l(\mathbf{x}, t) = \partial \mathbf{x}'_l / \partial t + \mathbf{x}'_l \cdot \operatorname{grad} \mathbf{x}'_l$, the momentum balance for the liquid phase produces the following relation:

$$\rho_l \left(\frac{\partial \mathbf{x}'_l}{\partial t} + \mathbf{x}'_l \cdot \operatorname{grad} \mathbf{x}'_l \right) = \operatorname{div} \mathbf{T}_l + \hat{\mathbf{p}}_l \tag{3.28}$$

With the same arguments, the momentum balance for the vapor phase produces

$$\rho_v \left(\frac{\partial \mathbf{x}'_v}{\partial t} + \mathbf{x}'_v \cdot \operatorname{grad} \mathbf{x}'_v \right) = \operatorname{div} \mathbf{T}_v + \hat{\mathbf{p}}_v \tag{3.29}$$

Finally, for the chloride ion phase, the following expression for the momentum balance is obtained:

$$\rho_c \left(\frac{\partial \mathbf{x}'_c}{\partial t} + \mathbf{x}'_c \cdot \operatorname{grad} \mathbf{x}'_c \right) = \operatorname{div} \mathbf{T}_c + \hat{\mathbf{p}}_c \tag{3.30}$$

The solid is, in this example, for simplicity, assumed to be non-deformable. Thus an simple ideal fluid assumption for the stress tensor is adopted, i.e.

$$\left(T_s\right)_{ij} = -\pi_s \delta_{ij} \tag{3.31}$$

where the *Kronecker delta* δ_{ij} is equal to the *unit matrix* $\mathbf{I}$, i.e. δ_{ij} is equal to 1 if $i = j$ and to 0 if $j \neq i$. The hydrostatic pressure is denoted π_s.

The other constituents are assumed to obey the laws of a *linear newtonian fluid*.

$$(T_l)_{ij} = \mathbf{f}(\mathbf{D}_l, \theta, \rho_l) \tag{3.32}$$

Stoke's relation is $\lambda + 2/3\mu \geq 0$, which allows for the possibility that *volumetric viscosity* exists. In this formula, μ and λ are Lamé's moduli. In this work, however, it is assumed that the volumetric viscosity is small compared to the other material constants and the Stoke's relation reduces to $\lambda + 2/3\mu = 0$. In turn, it is possible to write the *linearized* constitutive relation for the stress tensor for the liquid phase (assuming a linear newtonian fluid) as a function of the symmetric part of the velocity gradient $\mathbf{L}_l$, i.e. $\mathbf{D}_l$, and the temperature θ for the whole mixture as

$$\mathbf{T}_l = 2\mu_l(\theta)\,\mathbf{D}_l - \frac{2}{3}\mu_l(\theta)\; tr\,\mathbf{D}_l - \mathbf{I}\pi_l(\theta, \rho_l) \tag{3.33}$$

or written with *indicial notation* as

$$(T_l)_{ij} = \mu_l(\theta)\left[\frac{\partial x'_{il}}{\partial x_j} + \frac{\partial x'_{jl}}{\partial x_i} - \delta_{ij}\frac{2}{3}\frac{\partial x'_{il}}{\partial x_i}\right] - \delta_{ij}\pi_l(\theta, \rho_l) \tag{3.34}$$

where μ_l is a material constant for the liquid phase called *viscosity,* which is assumed to be a function of temperature, i.e. $\mu_l(\theta)$.

It is reasonable to assume that the temperature gradient induces stresses which can be incorporated into the assumption (3.34). However, according to (3.34), such a constitutive relation must be of tensor format. One way of involving the temperature, considering isotropic functions only, is therefore to add a function of the type $\mathrm{grad}\theta \otimes \mathrm{grad}\theta \equiv \partial^2\theta/(\partial x_j \partial x_i)$ to the constitutive relation for the stresses. This approach is very complex, since derivatives of the third order will appear when the constitutive relation inserted into the momentum balance equation is considered.

The same problem will be faced at an attempt to incorporate stresses in the solid matrix caused by mass concentration gradients of c_l. For example, a function of the type $\partial^2 c_l/(\partial x_j \partial x_i)$ can be used as an additional term. Instead of using the approach discussed above, it is proposed that the temperature induced stresses can be dealt with together with the constitutive relations for the momentum supplies $\hat{\mathbf{p}}_a$. Furthermore, so-called internal variables may be used to describe the stresses induced by the environment.

The type of constitutive relations that exist for the liquid are also assumed to hold for the stress tensors for the vapor phase as well as the chloride ion phase. Hence, the stress tensor for the vapor is constituted as

$$\mathbf{T}_v = \mathbf{f}(\mathbf{D}_v, \theta, \pi_v) \tag{3.35}$$

and the stress tensor for the chloride ion phase as

$$\mathbf{T}_c = \mathbf{f}(\mathbf{D}_c, \theta, \pi_c) \tag{3.36}$$

where it should be noted that in all equations above, the *hydrostatic* pressures π_a are defined as positive when compressive.

Furthermore, the hydrostatic pressures must be incorporated into the physical model and computed for. In many applications, it is assumed that a relation between the density ρ_a and the pressure π_a exists, e.g. $\partial\rho_a/\partial t = 1/c^2\partial\pi_a/\partial t$, where c is the acoustic wave velocity. This makes it possible to solve the pressures and velocities with the balance of mass and momentum together with the constitutive relations. This exemplified relation has no physical significance in the problem dealt with here. Another relation must be found. It is clear, however, that the individual fluid constituents are under stress even if the fluid in question is at rest. For instance, the hydrostatic pressure for the vapor can be calculated using the perfect gas law, which relates the pressure π_v to the mass density of the vapor ρ_v and the temperature θ. The pressures should not, however, be confused with the momentum supply among the constituents which, simply speaking, accounts for the exchange of forces and energies between the phases.

At this point, the reason why liquid starts to propagate through a porous medium stands clear. It is not difficult to imagine that the liquid phase flow will assert a great deal of resistance throughout the pore system (In the case of capillary suction of liquid into a porous medium without any external pressure gradients, this example may not be fully adequate). In terms of the mixture theory, this means that the momentum supplies $\hat{\mathbf{p}}_a$ among the constituents play an important part, that is, there exists a certain loss (or supply) of momentum from one constituent to another.

The momentum supply for the solid $\hat{\mathbf{p}}_s$ will not be constituted, since it is eliminated between (3.26) and (3.27). When it comes to the momentum supplies, the other constituents must, however, be supplemented by constitutive relations.

The momentum supply for the liquid phase is assumed to be constituted by the following function:

$$\hat{\mathbf{p}}_l = \mathbf{f}\left(\operatorname{grad} c_l,\, \operatorname{grad}\theta,\, \mathbf{u}_l,\, c_l,\, n,\, a\right) \tag{3.37}$$

where n and a, again, are the porosity and specific surface area of the solid. The following constitutive relation for the vapor phase is assumed:

$$\hat{\mathbf{p}}_v = \mathbf{f}\left(\operatorname{grad} c_v,\, \operatorname{grad}\theta,\, \mathbf{u}_v,\, c_l,\, c_{v,}\, n,\, a\right) \tag{3.38}$$

The momentum supply for the chloride ion phase is assumed to be described by a function of the following properties:

$$\hat{\mathbf{p}}_c = \mathbf{f}\left(\operatorname{grad} c_c,\, \mathbf{u}_c,\, c_l,\; n,\, a\right) \tag{3.39}$$

The momentum supplies are, essentially, assumed to be given by functions of the diffusion velocity of the liquid phase, and by the mass concentrations of the individual constituents.

The mass balance equations for the considered constituents are given by the equations (3.7-3.10). The mass conservation of the solid constituent gives

$$\rho\left(\frac{\partial c_s}{\partial t} + \dot{\mathbf{x}}\cdot\operatorname{grad} c_s\right) = \operatorname{div}\left(c_s\rho\dot{\mathbf{x}}\right) + \hat{c}_s \tag{3.40}$$

The liquid phase must fulfill the following mass balance equation:

$$\rho\left(\frac{\partial c_l}{\partial t} + \dot{\mathbf{x}}\cdot\operatorname{grad} c_l\right) = -\operatorname{div}\left(c_l\rho\mathbf{u}_l\right) + \hat{c}_l \tag{3.41}$$

The mass conservation for the vapor is

$$\rho\left(\frac{\partial c_v}{\partial t} + \dot{\mathbf{x}}\cdot\operatorname{grad} c_v\right) = -\operatorname{div}\left(c_v\rho\mathbf{u}_v\right) + \hat{c}_v \tag{3.42}$$

and for the chloride ions, the mass balance is given by

$$\rho\left(\frac{\partial c_c}{\partial t} + \dot{\mathbf{x}}\cdot\operatorname{grad} c_c\right) = -\operatorname{div}\left(c_c\rho\mathbf{u}_c\right) + \hat{c}_c \tag{3.43}$$

The same constitutive relations used in the quasi-static approach, are again adopted for the mass supply terms. That is, for the chloride ion phase, the following relation is assumed:

$$\hat{c}_c = f\left(c_c,\, c_s,\, c_l,\, \theta\right) \tag{3.44}$$

For the vapor phase, the assumption is

$$\hat{c}_v = f\left(c_v\,, c_l\,,\, \theta\right) \tag{3.45}$$

Mass exchange is assumed to be restricted by the following two relations:

$$\hat{c}_s + \hat{c}_c = 0 \tag{3.46}$$

and

$$\hat{c}_v + \hat{c}_l = 0 \tag{3.47}$$

which means that mass is exchanged only between the chloride ion phase and the solid phase one the one hand, and between the vapor phase and the liquid phase on the other.

The energy equation for the mixture as a whole is proposed to be given by the already presented three equations, namely (3.20-3.22).

The equation system is now closed. The twenty-two unknown properties can be calculated using the nine balance laws (3.28-3.30), (3.40-3.43), and (3.20), together with the remaining thirteen constitutive relations (3.31-3.36), (3.37-3.39), and (3.44-3.47).

The main purpose of the method presented in this section is indeed to illustrate that there exists alternative formulations to the more classical approach presented in Section 3.1 and, furthermore, the ambition to show that knowledge of the method may be used to improve the assumptions in the quasi-static approach.

When it comes to making the choice of which way to go, it is, however, primarily a question of which method that makes it possible to perform adequate measurements in order to determine the introduced material constants or material parameters. A minor problem in this context is the solution strategies, since powerful numerical methods exist that makes it possible to solve the equation system discussed above with satisfying accuracy. If, for example, the constitutive relations behind the simple quasi-static approach are chosen as a basis for an evaluation of the measurements, it should, however, be clear that the mass density flows $\rho_a \mathbf{u}_a$ must be constituted in a way that takes the effect of forces interacting among the constituents into account, although there does not exist any deeper underlying physical theory that suggests such a consideration.

As this work, in extension, is aimed at finding relations, and hence models, describing deteriorating mechanisms in concrete and other porous materials due to interactions between external applied loads and stresses induced by the environment, the dynamic approach seems to be a more realistic platform to work from, even considering the possibilities of measuring the material constants introduced. The dynamic approach may for example, be a very useful approach when freeze-thaw damage, due to ice formation in the pore system is studied, as it in

all essential parts is a question of momentum supply (or loss) between the solid and the ice causing the damages. This phenomenon can hardly be investigated without introducing the balance of momentum equations for the constituents. That is, the concept of stress and strain rates must be considered. Unfortunately, there is no stringent argument to incorporate these concepts into the quasi-static approach which does not include the momentum equations for the constituents.

A strategy which involves to solving the dynamic equation system above, with a numerical method, will be outlined in Section 9. The main idea is to solve the velocities for the individual constituents with the momentum balance equations, together with the suggested constitutive relations. The boundary conditions in these equations will be the partial pressures (hydrostatic pressures) for the constituents. These pressures will, simply speaking, induce the constituent to move in the pore system. When the velocities are computed, these known quantities are used as input to the mass balance equations and their corresponding constitutive equations. The mass concentration fields can then be calculated by introducing boundary conditions for the mass concentrations and indeed without specifying any diffusion constants for the constituents, since the velocity of the different constituents are calculated by the momentum balance equations together with the constitutive relations for the stress tensor and the momentum supplies.

3.3. Example - A mixed approach

As discussed above, it seems reasonable to treat the liquid water phase as a newtonian liquid with a complementary force accounting for the liquid-solid interaction. This makes it possible to compute the diffusion velocity for the liquid water, rather than to constitute this property. However, as the vapor molecules and the chloride ions are in general in a weak concentration in the considered applications, it might be sufficient to constitute the mass diffusion velocities $\rho_a \mathbf{u}_a$ directly, and therefore not include the balance of momentum equation for these two constituents. As this method makes use of the momentum and the mass balance equation for the liquid phase, and only the mass balance equations for the vapor and the chlorides, it will be referred to as the mixed approach.

This method will be outlined in the same general manner as the two other approaches, i.e. the quasi-static and the dynamic approaches.

The primarily unknown properties in the mixed approach are assumed to be

$$\begin{matrix} \mathbf{T}_s\left(\mathbf{x},t\right) \\ \mathbf{T}_l\left(\mathbf{x},t\right) \end{matrix} ; \quad \begin{matrix} \hat{\mathbf{p}}_s\left(\mathbf{x},t\right) \\ \hat{\mathbf{p}}_l\left(\mathbf{x},t\right) \end{matrix} ; \quad \begin{matrix} \rho_s\left(\mathbf{x},t\right) \\ \rho_l\left(\mathbf{x},t\right) \\ \rho_v\left(\mathbf{x},t\right) \\ \rho_c\left(\mathbf{x},t\right) \end{matrix} \quad \begin{matrix} \mathbf{x}'_s\left(\mathbf{x},t\right)=\mathbf{0} \\ \mathbf{x}'_l\left(\mathbf{x},t\right) \\ \mathbf{x}'_v\left(\mathbf{x},t\right) \\ \mathbf{x}'_c\left(\mathbf{x},t\right) \end{matrix} ; \quad \begin{matrix} \hat{c}_s\left(\mathbf{x},t\right) \\ \hat{c}_l\left(\mathbf{x},t\right) \\ \hat{c}_v\left(\mathbf{x},t\right) \\ \hat{c}_c\left(\mathbf{x},t\right) \end{matrix} \tag{3.48}$$

and

$$\theta\left(\mathbf{x},t\right); \, \varepsilon\left(\mathbf{x},t\right); \, \mathbf{q}\left(\mathbf{x},t\right); \tag{3.49}$$

which makes the number of unknown quantities eighteen.

Again, the following properties are given from (3.3-3.6), which are functions of the unknowns in (3.48).

$$\begin{matrix} c_s\left(\mathbf{x},t\right) \\ c_l\left(\mathbf{x},t\right) \\ c_v\left(\mathbf{x},t\right) \\ c_c\left(\mathbf{x},t\right) \end{matrix} \quad \begin{matrix} \mathbf{u}_s\left(\mathbf{x},t\right) \\ \mathbf{u}_l\left(\mathbf{x},t\right) \\ \mathbf{u}_v\left(\mathbf{x},t\right) \\ \mathbf{u}_c\left(\mathbf{x},t\right) \end{matrix} \quad \dot{\mathbf{x}}\left(\mathbf{x},t\right); \quad \rho\left(\mathbf{x},t\right). \tag{3.50}$$

The body forces for the solid and the liquid are assumed to have negligible influence on the considered system, i.e.

$$\begin{matrix} \rho_s \mathbf{b}_s = \mathbf{0} \\ \rho_l \mathbf{b}_l = \mathbf{0} \end{matrix} \tag{3.51}$$

According to (2.89) and (3.48), the following relation must hold for the mixture:

$$\hat{c}_v\left(\mathbf{u}_v-\mathbf{u}_l\right)+\hat{c}_c\left(\mathbf{u}_c-\mathbf{u}_s\right)+\hat{\mathbf{p}}_s+\hat{\mathbf{p}}_l=\mathbf{0} \tag{3.52}$$

If $\hat{\mathbf{p}}_s$ is solved in (3.52), the result is inserted into the balance of momentum (2.69) for the solid constituent, and, finally, it is noted that the velocity of the solid phase is assumed to be negligibly small, i.e. $\mathbf{x}'_s\left(\mathbf{x},t\right)=\mathbf{0}$, one obtains

$$\mathbf{0}=\operatorname{div}\mathbf{T}_s-\hat{c}_v\left(\mathbf{u}_v-\mathbf{u}_l\right)-\hat{c}_c\left(\mathbf{u}_c-\mathbf{u}_s\right)-\hat{\mathbf{p}}_l \tag{3.53}$$

The momentum balance for the liquid phase is: (compare (3.28))

$$\rho_l\left(\frac{\partial \mathbf{x}'_l}{\partial t}+\mathbf{x}'_l\cdot\operatorname{grad}\mathbf{x}'_l\right)=\operatorname{div}\mathbf{T}_l+\hat{\mathbf{p}}_l \tag{3.54}$$

The stress tensor for the liquid phase is constituted in the same way as in the dynamic approach, compare Section 3.2. Therefore

$$(T_l)_{ij} = \mu_l(\theta)\left[\frac{\partial x'_{il}}{\partial x_j} + \frac{\partial x'_{jl}}{\partial x_i} - \delta_{ij}\frac{2}{3}\frac{\partial x'_{il}}{\partial x_i}\right] - \pi_l(\theta, \rho_l)\delta_{ij} \tag{3.55}$$

The momentum supply for the liquid phase is assumed to be constituted by the following function:

$$\hat{\mathbf{p}}_l = \mathbf{f}\left(\operatorname{grad} c_l,\, \operatorname{grad}\theta,\, \mathbf{u}_l,\, c_l,\, n,\, a\right) \tag{3.56}$$

The simple constitutive relation for the solid is again adopted, i.e.

$$(T_s)_{ij} = -\pi_s \delta_{ij} \tag{3.57}$$

The mass balance equations for the considered constituents are given by the equations (3.7-3.10). The conservation of mass of the solid, liquid, and vapor as well as the chloride ions' constituents is

$$\rho\left(\frac{\partial c_s}{\partial t} + \dot{\mathbf{x}}\cdot\operatorname{grad} c_s\right) = \operatorname{div}\left(c_s\rho\dot{\mathbf{x}}\right) + \hat{c}_s \tag{3.58}$$

$$\rho\left(\frac{\partial c_l}{\partial t} + \dot{\mathbf{x}}\cdot\operatorname{grad} c_l\right) = -\operatorname{div}\left(c_l\rho\mathbf{u}_l\right) + \hat{c}_l \tag{3.59}$$

$$\rho\left(\frac{\partial c_v}{\partial t} + \dot{\mathbf{x}}\cdot\operatorname{grad} c_v\right) = -\operatorname{div}\left(c_v\rho\mathbf{u}_v\right) + \hat{c}_v \tag{3.60}$$

$$\rho\left(\frac{\partial c_c}{\partial t} + \dot{\mathbf{x}}\cdot\operatorname{grad} c_c\right) = -\operatorname{div}\left(c_c\rho\mathbf{u}_c\right) + \hat{c}_c \tag{3.61}$$

The mass supply terms for the chloride ion phase and the vapor phase are, again, constituted as

$$\hat{c}_c = f\left(c_c,\, c_s,\, c_l,\, \theta,\, n,\, a\right) \tag{3.62}$$

$$\hat{c}_v = f\left(c_v\,, c_l\,,\, \theta,\, n,\, a\right) \tag{3.63}$$

and the following restrictions are assumed to hold:

$$\hat{c}_s + \hat{c}_c = 0 \tag{3.64}$$

$$\hat{c}_v + \hat{c}_l = 0 \tag{3.65}$$

where (2.51) is used.

The mass diffusion flows $\rho_v \mathbf{u}_v$ and $\rho_c \mathbf{u}_c$ are constituted by the following general functions:

$$\rho_v \mathbf{u}_v = \mathbf{f}\,(\,\mathrm{grad}\, c_v,\, \mathrm{grad}\,\theta,\, c_l,\, \theta,\, n,\, a) \tag{3.66}$$

$$\rho_c \mathbf{u}_c = \mathbf{f}(\,\mathrm{grad}\, c_c,\, \mathrm{grad}\,\theta,\, c_l,\, \theta,\, n,\, a) \tag{3.67}$$

Three properties remain to be constituted, namely the temperature θ, the internal energy density ε and the heat flux vector $\mathbf{q}$ for the mixture as a whole. The three relations leading to the standard heat conduction (with an additional term accounting for internal forced convection) are the balance of energy (3.20) and the two constitutive relations (3.21) and (3.22).

The introduced number of unknown quantities in this example, as listed in (3.48) and (3.49), are now supplemented with an equal number of balance equations and constitutive relations. The introduced momentum balance equations are (3.53) and (3.54). The mass balance equations for the constituents are (3.58), (3.59), (3.60), and (3.61). The energy balance is given by (3.20). The constitutive relations for the stress tensors are (3.55) and (3.57), and the momentum supply for the liquid water is the relation (3.56). The remaining relations are the four constitutive assumptions for the local interactions in terms of mass exchanges among the constituents, i.e. (3.62), (3.63), (3.64), and (3.65), the relations for the mass diffusion flows (3.66) and (3.67), and finally the relations for the thermal properties (3.21) and (3.22).

4. Mass transport phenomena in porous media

Usually, only global response at macro-scale is detected in experiments. Having this in mind, it may be advantageous to use a more detailed physical stringent theory and detailed constitutive description as a working hypothesis. The actual global response measured at the macro-scale is a consequence of different constituents interacting at the micro-scale, which could not be ignored. If a physical stringent description is searched for, such considerations can not be overlooked.

One may claim that a very simple engineering approach is sufficient to solve flow problems in the field of building materials. It should be noted, however, that classical models using types of equations based on Fick's second law must be supplemented with material parameters, such as the diffusion parameter D, which inevitably becomes extremely non-linear in order to capture the measured response in the laboratory. Some of these introduced non-linearities even seem unrealistic from a physical viewpoint. For example, the diffusion parameter for vapor must increase as the liquid water content increases in the pore system. This occurs at attempts to fit measured data using one state variable only and thus describing the action of vapor and liquid water as one single constituent.

Furthermore, it may be reasonable to use more detailed physical models as the classical non-linear models require computer analyses. They can not be solved in a simple manner. Therefore the alternative of building a more stringent physical model would provide a competitive candidate, since powerful computer algorithms are required in both cases.

The stringency of the assumptions behind the classical Fick's second law in the field of moisture mechanics in building materials, which treats vapor and liquid water as one constituent, fails if a dissolved agent such as chloride ions is added to the system. This is due to the fact that liquid water flow makes the motion description of the considered dissolved matter somewhat more complex.

In this work, it is proposed to be an advantage to use separate descriptions and hence different equations for the different constituents considered, i.e. vapor, liquid water and dissolved agents such as chloride ions. These equations will be supplemented with proper terms accounting for interactions between the different constituents in terms of chemical reactions (or physical bindings) and momentum supply. A similar approach has been proposed in, for example [6], where steel corrosion in concrete structures is dealt with, and in [7], where the durability of cement-based materials used for the construction of radioactive waste containment barriers is studied.

4.1. Adsorption and capillary condensation at isothermal and steady state conditions

The fixation of water onto the pore walls is presumably caused by a phenomenon called *adsorption*. Adsorption is the fixation of vapor 'molecules', present in the pore space, onto a completely dry pore wall or to water molecules already adsorbed on the wall. One of the first to study adsorption of molecules on solid surfaces was Langmuir in 1918, who suggested that the surface consists of a certain number of sites, some of which are occupied by adsorbed vapor and some of which are free. The rate of evaporation is taken to be proportional to the amount of occupied sites and the rate of condensation proportional to the 'bare' surface and to the gas pressure of the vapor in the pore space. In other words, the description of the problem is obtained by considering the collision frequency together with a probability of adsorption and condensation.

By setting the condensation and evaporation rates to be equal, the so-called *Langmuir equilibrium adsorption isotherm* is obtained [8]. The Langmuir type of equilibrium isotherm is roughly characterized by a monotonic approach to a limiting adsorption, which should theoretically correspond to a complete monolayer. It does not, however, reflect the measured equilibrium isotherm for the most common building materials such as concrete.

It is generally believed that a multilayer formation of adsorbate is formed in certain materials such as cement-based materials. One model based on this assumption is the BET *equilibrium isotherm*. The basic assumption behind this method is that the Langmuir equation applies to each layer formed, with the added postulate that for the first layer, the energy of adsorption may have some special value, whereas for all succeeding layers, the energy of adsorption is equal to the energy of condensation of the liquid adsorbate. Furthermore, it is assumed that evaporation and condensation only can occur from or to the exposed surfaces [8]. The shape of the normal BET equilibrium isotherm somewhat reflects the behavior of the physical adsorption of vapor in porous materials. According to the BET theory, the adsorbed layer should be infinite when the surrounding vapor pressure is saturated. In reality, however, it reaches a certain limit corresponding to the limiting number of adsorbed layers. Normally, the BET equation is valid up to about 30% or 40% relative humidity.

When a number of adsorbed layers are formed at the pore surfaces, so that a liquid meniscus can be formed, another mechanism is also active, which makes the amount of adsorbed liquid grow under the condition that the relative vapor pressure in the pore space is high enough. This phenomenon is called *capillary*

condensation. The capillary condensation becomes significant when the relation between the vapor pressure π_v and the saturation pressure π_{vs} at a given temperature exceeds a certain level, usually between 25% and 45%, dependent on the type of adsorbate, [9], [10]. For water, it is about 45%.

The capillary condensation phenomenon is a consequence of liquid water present in the pores forming curved surfaces [11]. That is, if the adsorption of molecules forms layers at the surfaces due to a certain relative vapor pressure in the pores, a diffuse point will be reached, where the adsorbate starts to behave more or less like a 'normal' liquid (roughly, when a few molecule layers have been formed). This creates a curved boundary surface neighboring the vapor phase. This curvature is maintained by the balance between the surface tension (surface energy) and the hydrostatic pressure difference over the same surface. This pressure difference is often referred to as the *capillary pressure* π_{cap}.

One may claim that the only phenomenon of interest is the capillary condensation, since the outer climate of interest in the present type of application is almost always above 40% relative humidity. At that level, capillary condensation is usually more important than adsorption. It must be remembered, however, that moisture movement, and perhaps even the movement of dissolved ions, also takes place in the adsorbed layers. The thickness of this layer is, however, normally less then 15Å, a small value compared with the pore size, where a capillary condensation takes place at higher relative humidities. The main advantage of the theories behind the equilibrium sorption isotherms is, perhaps, that they make possible estimations of the pore distribution and porosity. In this sense, the description of the properties and behavior of the molecule layers is important, since these implicitly are a measure of the microstructure for example in terms of the pore distribution and the specific surface area. Moreover, the physical properties of the molecule layers near the solid surfaces may affect the overall behavior of the solid matrix, especially in terms of cement-based materials, which strive to incorporate liquid water into the chemically composed hydration products even a long time after they have been manufactured. Besides, the adsorbed water interacts with the very high value of the specific surface of the cement paste, and highly influences its mechanical properties such as strength and creep. The capillary condensed water also determines such properties as shrinkage and freezable water.

In order to show the kind of approximations that are incorporated in an estimate of the important material properties, namely pore distribution and pore sizes, a discussion of the underlying theory that leads to the so-called *Kelvin equation* will be performed. It is also believed, that this derivation may increase the

understanding of moisture mechanics in porous materials, at least at an initial stage, even if somewhat crude approximations are introduced.

A steady state and isothermal condition is the basic restriction imposed to derive the Kelvin equation. The following assumptions concerning the stress tensors for the liquid and vapor phases are introduced:

$$\mathbf{T}_l = -\pi_l \mathbf{I} \tag{4.1}$$

$$\mathbf{T}_v = -\pi_v \mathbf{I} \tag{4.2}$$

The capillary pressure is defined to be the difference of these pressures, e.g. compare [12].

$$\pi_{cap}\mathbf{I} = \pi_l \mathbf{I} - \pi_v \mathbf{I} \tag{4.3}$$

The existence of the capillary pressure π_{cap} is believed to be a consequence of a discontinuity in pressure across the interface separating two pure immiscible fluids, in this case vapor and liquid water. The magnitude of the pressure difference depends on the interfacial curvature, which in turn depends on the saturation.

The defined properties in Section 2.5 will now be used in order to establish simple expressions for the chemical potentials of the vapor and liquid, both in a state of rest, i.e. only the equilibrium conditions are considered. With the help of the chemical potentials, the capillary pressure π_{cap} can then be estimated.

The definition of the chemical potential for a single pure constituent such as vapor is the same as the chemical potential for a mixture. If the stress tensor is approximated according to (4.1), the expression for the chemical potential $\mathbf{K} = \mu\mathbf{I}$ is given by the following expression:

$$\mu = \psi + \pi\,(1/\rho) \tag{4.4}$$

Compare the definition (2.180). Helmholz free energy ψ of a pure constituent is defined as: (compare equation (2.164)).

$$\psi = \varepsilon - \eta\theta \tag{4.5}$$

The expressions for the chemical potential and the free energy are differentiated as

$$\dot{\mu} = \dot{\psi} + \dot{\pi}\,(1/\rho) + \pi\left(\dot{1/\rho}\right) \tag{4.6}$$

$$\dot{\psi} = \dot{\varepsilon} - \dot{\eta}\theta - \eta\dot{\theta} \tag{4.7}$$

Furthermore, the following *Gibbs relation* (de Groot and Mazur) for the mixture is assumed:

$$\theta\dot{\eta} = \dot{\varepsilon}_{\mathbf{I}} + \pi\left(\dot{1/\rho}\right) - \sum_{a=1}^{\Re} \mu_a \dot{c}_a \tag{4.8}$$

Under the very special condition $\sum_{a=1}^{\Re} \mu_a \dot{c}_a = 0$, i.e., the Gibbs relation for a pure constituent with no change in mass concentration, is simplified as

$$\theta\dot{\eta} = \dot{\varepsilon} + \pi\left(\dot{1/\rho}\right) \tag{4.9}$$

By combining (4.6), (4.7), and (4.9) the rate of change of the chemical potential for a pure constituent can be written as

$$\dot{\mu} = \dot{\theta}\eta - \dot{\pi}(1/\rho) \tag{4.10}$$

As the Kelvin equation claims to be valid during isothermal conditions only, i.e. $\dot{\theta} = 0$, expression (4.10) is reduced to

$$\dot{\mu}_v = -\dot{\pi}_v(1/\rho_v) \tag{4.11}$$

for the vapor phase, and

$$\dot{\mu}_l = -\dot{\pi}_l(1/\rho_l) \tag{4.12}$$

for the liquid phase.

Equation (4.12) is rewritten as

$$\mu_l = \mu_{l0} + \int_{\pi_{vs}}^{\pi_l} V_l d\pi \tag{4.13}$$

where μ_{l0} is the reference value of the chemical potential, taken at the point where the vapor pressure of the surrounding medium is saturated. This measure is denoted π_{vs} at a certain constant temperature θ. V_l in equation (4.13) is the specific volume of the liquid water phase, i.e. $V_l = 1/\check{\rho}_l$, where $\check{\rho}_l$ is the mass density concentration of liquid water. $\check{\rho}_l = 1000\,(\mathrm{kg/m^3})$, which should not be confused with the mass density ρ_l. Compare (2.11), (2.12), and (2.13). The difference between $\check{\rho}_l$ and ρ_l actually reveals that the equations to be derived only hold at micro-scale, that is, in a representative volume (REV), where the property $\check{\rho}_l$ can be defined.

By introducing the idealized assumption that the rate of change of the chemical potential for the liquid phase is linear with respect to a change of the hydrostatic

pressure π, and assuming further that the liquid water phase is incompressible in the range of pressures considered, i.e. $\check{\rho}_l = const.$, (4.13) can be written as

$$\mu_l = \mu_{l0} + V_l\,(\pi_l - \pi_{vs}) = \mu_{l0} + V_l\,(\pi_l - \pi_v) + V_l\,(\pi_v - \pi_{vs}) \tag{4.14}$$

If the perfect gas law, for the vapor phase is adopted, that is

$$\pi_v = \frac{R}{M_v}\rho_v\theta \tag{4.15}$$

where R is the *universal gas constant*, $R = 8.314\,(\mathrm{J/mol/K})$, and M_v is the mol mass, $M_v = 0.018\,(\mathrm{kg/mol})$, expression (4.11) is simplified to the following expression:

$$\mu_v = \mu_{v0} + \frac{R}{M_v}\theta\int_{\pi_{vs}}^{\pi_v}\frac{1}{\pi_v}d\pi = \mu_{v0} + \frac{R}{M_v}\theta\ln\left(\frac{\pi_v}{\pi_{vs}}\right) \tag{4.16}$$

where μ_{v0} is the reference value of the chemical potential for the vapor at the saturation pressure π_{vs} at the considered constant temperature θ.

The *Young-Laplace relation* suggests that it is possible to constitute the capillary pressure with help from the *surface tension* (or surface energy) γ_l (N/m) of liquid water, if it is assumed that the liquid water boundary has an axial symmetric shape. The Young-Laplace relation is

$$\pi_{cap} = \pi_l - \pi_v = \gamma_l\left(\frac{1}{\tilde{r}_{l1}} + \frac{1}{\tilde{r}_{l2}}\right) \tag{4.17}$$

where $\tilde{r}_{l1}$ and $\tilde{r}_{l2}$ are the curvature radii of the liquid boundary, facing the vapor phase in the two axial symmetric planes. The assumption (4.17) can be verified simply by considering the equilibrium of forces on an infinitesimal element of a curved liquid water-vapor interface and assuming that the surface tension γ_l is constant over the same element, compare [12]. Some values of the surface tension γ_l at different temperatures are shown in Table 4.1.

In [13] it is shown by experiments that the Young-Laplace relation holds for water down to a radius of 2nm for a circular cylindrical pore. However, the momentum supply on the liquid water-solid interface is assumed to have negligible influence on the capillary pressure π_{cap}, when the Young-Laplace relation is used. Therefore, the Kelvin equation (4.20) will suffer from the same drawback.

The equation (4.14) can be written as

$$\mu_l = \mu_{l0} + V_l\gamma_l\left(\frac{1}{\tilde{r}_{l1}} + \frac{1}{\tilde{r}_{l2}}\right) + V_l\,(\pi_v - \pi_{vs}) \tag{4.18}$$

Table 4.1: Surface tension of liquid water, [24].

Temp. (^{o}C)	Surface tension, γ_l (N/m)	Density of bulk water $\breve{\rho}_l$ (kg/m^3)
0	0.0756	999.8395
5	0.0749	999.9638
10	0.0742	999.6996
15	0.0735	999.0996
20	0.0728	998.2041
25	0.0720	997.0449
30	0.0712	995.6473
50	0.0679	988.0363
70	0.0644	977.7696

where (4.17) is used

By a local equilibrium between the vapor and the liquid water interface, the chemical potentials fulfill the relation $\mu_l = \mu_v$. If this relation is used together with (4.16) and (4.18)

$$\frac{R}{M_v}\theta \ln\left(\frac{\pi_v}{\pi_{vs}}\right) = V_l\gamma_l\left(\frac{1}{\tilde{r}_{l1}} + \frac{1}{\tilde{r}_{l2}}\right) + V_l\left(\pi_v - \pi_{vs}\right) \tag{4.19}$$

is obtained. At normal pressures and temperatures, the term $V_l\left(\pi_v - \pi_{vs}\right)$ is small compared to the others, e.g. compare [14]. Hence (4.19) can be written

$$\ln\left(\frac{\pi_v}{\pi_{vs}}\right) = \frac{M_v V_l \gamma_l}{R\theta}\left(\frac{1}{\tilde{r}_{l1}} + \frac{1}{\tilde{r}_{l2}}\right) \tag{4.20}$$

known as the Kelvin equation.

By using the Young-Laplace relation the capillary pressure, i.e. the pressure difference over the liquid-vapor interface, can be expressed as

$$\pi_{cap} = \frac{R\theta}{M_v V_l} \ln\left(\frac{\pi_v}{\pi_{vs}}\right) \tag{4.21}$$

which suggests that at an equilibrium, for example imposed by letting a porous material sample be conditioned by a certain relative vapor pressure at a sufficiently long time, all menisci in the material will have the same principal radii of curvature $\tilde{r}_l$ and the same capillary pressure π_{cap} independently of the actual mass concentration of liquid water in a representative material volume. In other

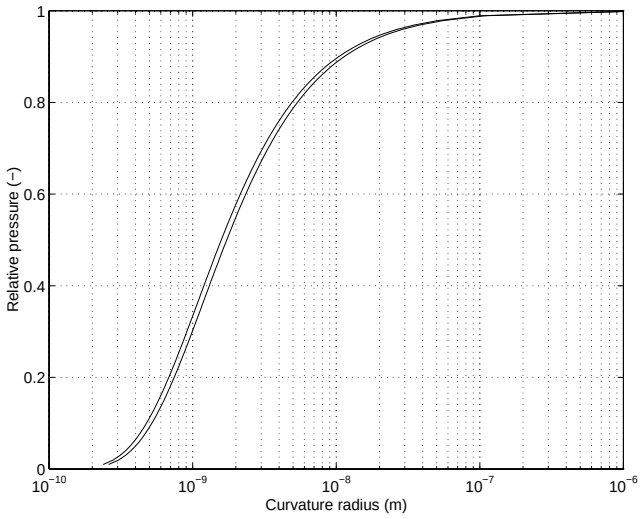

Figure 4.1: *Curvature radius of water at equilibrium with different relative pressures, equation (4.23).*

words, the capillary pressure π_{cap} at a certain temperature is solely determined by the outer relative pressure π_v/π_{vs}, once an equilibrium has been established.

By making additional approximations to the Kelvin equation, it is possible to get an idea of which pores will be drained at a certain externally applied capillary pressure π_{cap}. That is, what pore shapes that can maintain the curvatures $\tilde{r}_l$ and $\tilde{r}_2$ of the liquid interface given by the Kelvin equation (4.20).

The most elementary assumption is that the pore system only consists of interconnected cylinders with circular cross-sections of different radii r_p. The considered cylindrical pores must, furthermore, have a sufficiently large radii to ensure that the water in the pores behaves as a liquid, i.e. they must be able to produce a surface tension γ_l. Moreover, a relation between the interface curvature and the pore radii of the cylindrical needles must be found. This last relation can be found by making an assumption of the contact angle ϕ_{lp} between the liquid water (present in the cylindrical needles) and the inner envelope surface of the considered pore. By a truly geometrical consideration, the relation

$$\tilde{r}_{l1} = \tilde{r}_{l2} = -r_p \cos\left(\phi_{lp}\right) \tag{4.22}$$

is found, where the minus sign in (4.22) is incorporated to distinguish a convex curvature from a concave one.

The next classical assumption is the assertion that the liquid water present in the pore system is *wetting* the pore walls. The terms *wetting* and *nonwetting* tend to be defined in terms of desired effect. Usually, however, wetting means that the contact angle ϕ_{lp} between a liquid and a solid is zero or so close to zero that the liquid spreads over the solid easily. Nonwetting means that the angle ϕ_{lp} is greater than 90^o, and the liquid hence tends to ball up and run off the surface easily [8].

If a wetting liquid like water is assumed in concrete, i.e. $\phi_{lp} = 0$, the Kelvin equation (4.20) and the relation (4.22) give

$$\ln\left(\frac{\pi_v}{\pi_{vs}}\right) = -\frac{2M_v V_l \gamma_l}{R\theta r_p} \tag{4.23}$$

Expression (4.23) will be referred to as the modified Kelvin equation based on the many questionable assumptions discussed in this Section. Despite these assumptions this is one of the fundamental relations in surface chemistry, e.g. compare [8].

The different equilibrium conditions between the relative pressure π_v/π_{vs} and the curvature radius r_p are shown in Figure 4.1, where equation (4.23) is used.

Measurements performed in [15] show that the Kelvin equation predicts the same values of equilibrium on sandstones, in terms of externally applied pressures (obtained by using a pressure plate extractor) and liquid water contents, as the method of conditioning samples in different relative pressures (relative humidities). The method of applying an external pressure to a sample, compare [15] for details, is advantageous when studying high water contents corresponding to high relative vapor pressures, i.e. relative pressures near unity, as these conditions are impossible to obtain in a climate chamber at atmospheric pressure, compare Figure 4.2.

Equation (4.23) suggests that equally sized pores will be drained at different constant temperatures θ when the relative pressure is constant. Thus, the equilibrium isotherm, i.e. the relation between relative pressures and the liquid water content in a porous sample, corresponds to lower liquid water contents (at an equilibrium) in the whole range of relative pressures if the temperature increases.

It is very important to note that no information about the flow properties for vapor or liquid water could be estimated with the Kelvin equation, since only the equilibrium conditions are considered. Furthermore, it is possible to measure the equilibrium isotherms for porous materials directly without introducing any assumptions. Compare the principal shape of an equilibrium isotherm in Figure

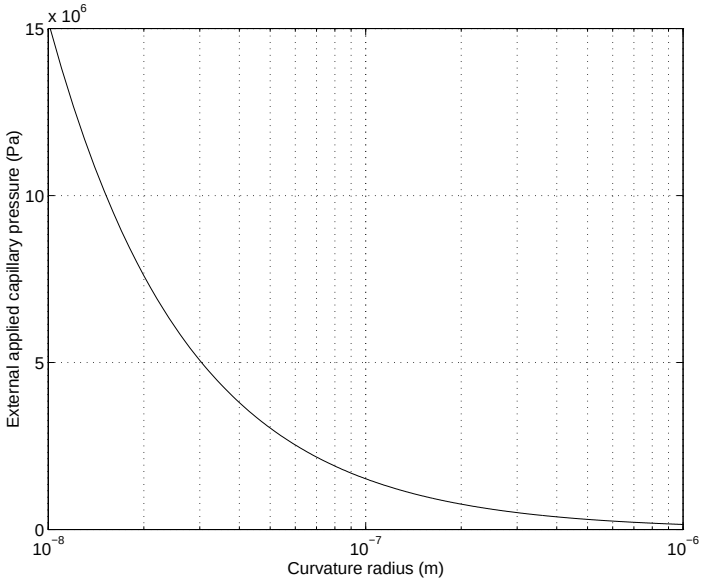

Figure 4.2: *Capillary pressure as a function of curvature radius of water present in a pore system, equation (4.21).*

4.4. Still, the Kelvin equation is very important when it comes to predicting the pore distribution, which indirectly is a measure of the flow properties for vapor and liquid water in the pore system.

4.2. Diffusion and fixation of vapor in porous media

In the field of moisture mechanics in building materials, the approach of splitting the moisture flow into a vapor flow and liquid flow together with a description of the mass exchange between these phases has, surprisingly, gained little interest. This is due to the fact that it is believed to be a to complicated process to measured and described with constitutive equations. Instead, methods, where the total flow of vapor and liquid is treated as one constituent are frequently proposed, e.g. compare [16].

One main drawback of such an assumption is the fact that the physical behavior of vapor and liquid are very different, especially when considering non-isothermal flow conditions. Even under isothermal conditions, extremely strong non-linearities will appear in Fick's second law, especially when trying to incorpo-

rate the *capillary suction* phenomena into the models also. The capillary suction phenomena is discussed in Section 4.3. The state variable used in these traditional models can be the *relative pressure* or the mass concentration of liquid. The mass flows are constituted by functions of these corresponding gradients.

The one-phase flow models are furthermore constrained by a given relation between the relative humidity (in the pore system) and the mass concentration of liquid at the same material point, since only one equation is used to describe the action of the system. In order to tackle this problem the *equilibrium isotherm curves* for the material in question are used. These show a measured relation between the *outer* relative humidity (in the surroundings) and the mass concentration of water *within* the porous material at *equilibrium* — see Section 4.1.

Another drawback is the fact that the mass concentration of liquid water due to hysteresis in the equilibrium isotherm can not be interpreted as a state variable having a given relation with the relative vapor pressure. Hence, when using the traditional approaches, the mass concentration of liquid water is not only a function of the relative pressure, but also of the manner in which equilibrium has been reached. For concrete, this hysteresis is considerable at relative humidities above 50% — compare Figure 4.4. Problems related to this kind of hysteresis are often treated by introducing so-called scanning curves. The scanning curves describe the relation between the liquid water concentration and the relative vapor pressure at points located in the gap between the absorption and desorption isotherms. Later, a method will be proposed, at which the transient process to reach equilibrium is studied. Such an approach makes it possible to treat the hysteresis phenomenon in a more explicit manner. Furthermore, the effect of temperatures changing the equilibrium conditions can be considered in the same explicit manner.

For example, an initially dry thin plate of concrete will gain about 35-65 (kg/m^3) liquid water when stored at room temperature and at 75% relative pressure during a sufficiently long time, i.e. until equilibrium is reached. Having in mind that all this water, which approximately corresponds to 15-25% of the total available pore space, has been supplied through the boundaries of the thin specimen as vapor, it is not surprising that measurements performed by means of gammametry [17] roughly indicate that the time to reach equilibrium between the outer relative humidity and the saturation degree just beneath the boundary surface of a cement mortar sample takes about 300-500 hours or more.

If the equilibrium between the vapor and the mass concentration in any material point is not established instantaneously, considerable errors will be induced

when the equilibrium isotherm is used as a state function in the constitutive model. In fact, not even the mass balance equations will be satisfied.

When more constituents e.g. chloride ions, hydroxide ions, and carbon dioxide, are added as is the subject of this work, the significance of a stringent model based on physics becomes even more important than dealing with vapor and liquid phases only. A simple example will serve as a justification of the above.

By considering, again, a concrete sample gaining liquid water in its pores from vapor supplied through the boundary surfaces only, the question arises whether or not the liquid water phase present in the pore system, which at least initially has been built up by vapor from the surroundings, is at rest or if it is subject to motion induced by some physical driving force. Suppose, for example, that the liquid phase is always at rest, i.e. it has no motion in relation to the solid matrix. Suppose, too, that the vapor 'molecules' slowly spread throughout the pore system (or get stucked at the pore walls) in order to level out a non-equilibrium condition imposed by a change of relative pressure in the surroundings. Under such conditions, the mass transport of chloride ions will presumably be limited to 'diffusion' in the capillary condensated and adsorbed water only.

On the other hand, if the liquid water phase built up can have a motion relatively the solid matrix induced by some potential, e.g. a mass concentration gradient (not yet considering the capillary suction induced by applying liquid water at the boundary surface), it is very likely that the dissolved chlorides will be forced to follow the motion imposed by the liquid water phase.

In order to find a realistic model based on physics for mass transfer and fixation of vapor, which makes it possible to incorporate mass transfer and fixation of chloride ions and other constituents present in the liquid water phase in a reasonable way it will be assumed that a non-equilibrium situation between vapor and the neighboring liquid-gas interface exists. This implies an exchange of mass between the two phases whenever a transient process is considered. This approach has been suggested by [17] for transient wetting of mortar by vapor.

Consequently, the microscopic thermodynamic state on the local vapor-liquid interfaces may differ more or less from the properties in bulk. This results in a microscopic vapor diffusion. It is assumed that such phenomena may occur during transient condensation in media such as mortar and concrete containing pore size magnitude orders. It has been pointed out, however, that the vapor-liquid equilibrium on the interface separating the two phases should be reached instantaneously [18], leaving the possibility that a significant portion of the equilibration time in a porous medium is caused by microscopic vapor diffusion into

small pores. Measurements performed in [17] clearly show that non-equilibrium situations exist, and it is concluded that this phenomenon is due to microscopic diffusion and evaporation in porous media with various orders of magnitudes of pore sizes such as mortar and concrete. Figure 4.3 shows how the distribution of liquid water in a sample of initially dry mortar changes with time as moist air (relative humidity 90%) flows across one exposed face. These results led to speculations that the vapor and liquid phases of water in the small pores of the mortar had yet not reached a state of local equilibrium [17].

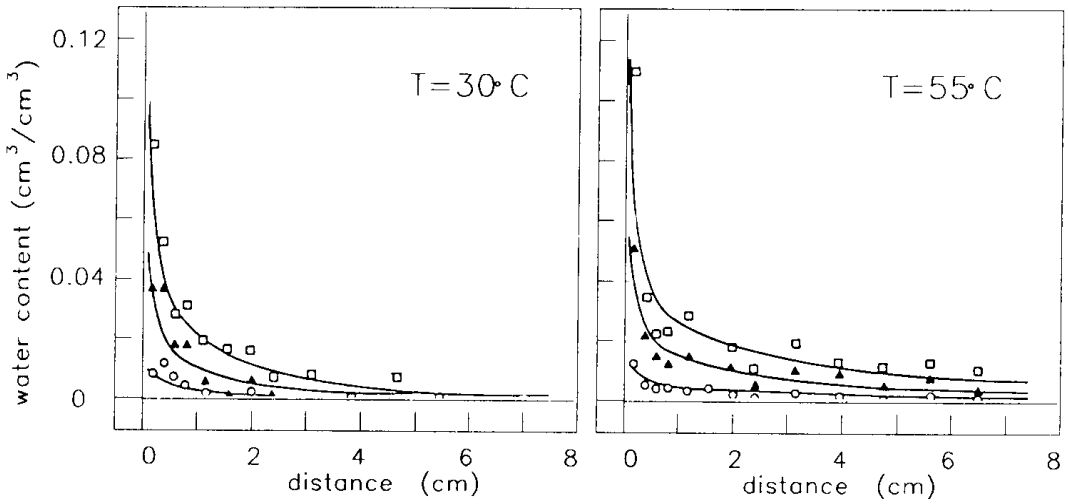

Figure 4.3: *Initially dry mortar specimens exposed to moist air (relative humidity 90% at two different temperatures). Experimemental profiles: circle 20 hours of exposure, triangles 100 hours and squares 300 hours [17].*

Figure 4.3 shows that the test performed at 55 ^{o}C give significantly higher water contents at the different times 20 hours, 100 hours and 300 hours, when the mortar is exposed to a constant outer relative humidity of 90%, compared to the test at 30 ^{o}C. The modified Kelvin equation (4.23) suggests, however, that an equilibrium at high temperatures should contain less water than an equilibrium at a lower temperature at the same relative pressure. The most interesting conclusion that can be drawn from the results presented in Figure 4.3 is, perhaps, the fact that the water content steadily increases near the boundary surface. This clearly shows that the time allowed for a substance to reach equilibrium is significant. Therefore, the transient process occurring *before* the equilibrium is reached between the

relative pressure and the water content within the material must be dealt with. This phenomenon will be treated by considering the transient exchange of mass between the vapor phase and the liquid phase in every material point. This is carried out by introducing a constitutive relation in an explicit manner. It is important to note that the traditional methods of solving the mass concentration fields at different times, using a non-linear Fick's second law, can not capture the behavior shown in Figure 4.3. This is due to the assumed equilibrium relation between the relative pressure and the water content.

The Kelvin equation does not include any assumptions about the thermodynamic state of vapor and vicinal liquid water when they are fixated in small pores due to a transient micro diffusion. This indicates that the study of curved liquid surfaces with a certain surface energy, which assures that the bulk liquid and the vapor have the same chemical potential at equilibrium, is not sufficient to explain the equilibration of a sample exposed to vapor inhibition.

The equilibrium adsorption-desorption isotherms for concrete $w/c = 0.48$ is shown in Figure 4.4. The lower curve are the equilibrium conditions obtained by wetting an initially dry specimen and the upper curve are the measured equilibrium conditions obtained by drying an initially saturated specimen of the same type.

The mass transfer without local equilibrium suggests that combinations of the vapor content and liquid content at a certain material point may deviate from the equilibrium curves of the type shown in Figure 4.4 whenever a non-equilibrium situation is considered. It seems reasonable to assume that the rate of phase change, presumably caused by microscopic vapor diffusion towards small pores during isothermal conditions, is dependent on the extent, to which the real water content deviates from the equilibrium water content given from the proper sorption isotherm.

In order to illustrate a model of diffusion and fixation of vapor in porous media, which captures the most important phenomena, a short presentation of the governing balance equations and the constitutive relations, in one dimension only, will be discussed.

The mass balance equation for the vapor phase can, according to (2.56) and (2.57) be written, in one dimension as

$$\rho \frac{\partial c_v}{\partial t} = -\frac{\partial (\rho_v u_{xv})}{\partial x} - \rho \dot{x}_x \frac{\partial c_v}{\partial x} + \hat{c}_v \tag{4.24}$$

where the velocity of the mixture in the x-direction $\dot{x}_x$ (m/s) is given by (2.15). The exchange of mass of vapor molecules, i.e. the mass supply term is denoted

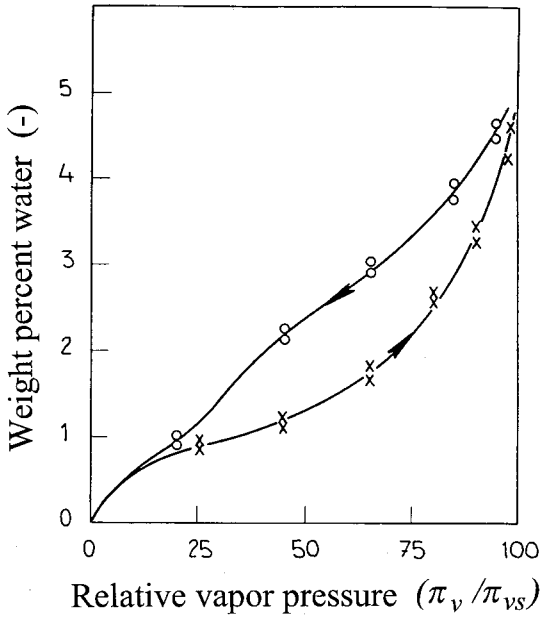

Figure 4.4: *Eqilibrium isotherm at room temperature, concrete w/c = 0.48 [14].*

$\hat{c}_v$ (kg/s/m^3). The density for the vapor is denoted ρ_v (kg/m^3), u_{xv} (m/s) is the diffusion velocity in the x-direction, ρ (kg/m) is the density of the mixture, and c_v (-) is the mass concentration of vapor. Compare the definitions in section 2.

In addition, it will be assumed that the exchange of mass occurs between the vapor phase and the liquid water phase only, that is

$$\hat{c}_v = -\hat{c}_l \tag{4.25}$$

where (2.51) is used. Consequently, no chemical reactions between the solid and the water in the pores will be considered, i.e. chemical hydration reactions will not be included.

The mass balance for the liquid water phase is according to (2.56) and (2.57) given as

$$\rho\frac{\partial c_l}{\partial t} = -\frac{\partial(\rho_l u_{xl})}{\partial x} - \rho\dot{x}_x\frac{\partial c_l}{\partial x} - \hat{c}_v \tag{4.26}$$

where (4.25) is used.

The following constitutive relation is assumed as a working hypothesis for the mass diffusion flow of vapor $\rho_v u_{xv}$

$$\rho_v u_{xv} = -D_v(c_l,\theta,n)\frac{\partial c_v}{\partial x} - D_{v\theta}(c_l,n)\frac{\partial\theta}{\partial x} \tag{4.27}$$

where c_l, θ, and n are the mass concentration of liquid water, temperature and porosity respectively, and where D_v and $D_{v\theta}$ are material parameters. The same type of constitutive relation for the mass diffusion flow $\rho_v u_{xv}$ has been proposed in for example [19]. It should be noted that it is possible to use alternative methods where the diffusion velocity u_{xa} and the mass density ρ_a for an arbitrary constituent denoted a may be computed for separately. Compare the discussion in section 3.2.

It is possible that also the pore size distribution will affect the mass diffusion flow. It can therefore be included as a property describing the diffusion parameter D_v in equation (4.27).

Already at this point it is worth mentioning that the mass diffusion flow constituted in (4.27) and (4.28) is the combined effect of two separate independent physical properties, i.e. the diffusion velocity u_a and the mass concentration density ρ_a.

The diffusion parameter D_v in (4.27) is assumed to be a function of the mass concentration density of the liquid water c_l, the temperature θ, and the porosity of the material. Table 4.2 shows that the dependency on temperature for the

Table 4.2: Diffusion constants for vapor in air, [24].

Temperature (^{o}C)	Diffusion coefficient, D (m^2/s)
0	$22.2 \cdot 10^{-6}$
5	$22.9 \cdot 10^{-6}$
10	$23.6 \cdot 10^{-6}$
15	$24.3 \cdot 10^{-6}$
20	$25.0 \cdot 10^{-6}$

mass gradient diffusion of vapor in bulk air is weak. The temperature is, however, assumed to affect the equilibrium condition between vapor and fixated liquid water, i.e. the sorption isotherms. Furthermore, the temperature will affect the adsorption and desorption *speeds* to reach these different equilibrium isotherms. Therefore, the temperature plays a very important role when it comes to the global response.

The second term in (4.27) represents the so-called *Soret effect*, which suggests that there exists a significant driving force inducing a mass density flow of vapor from high to low temperature regions.

The mass diffusion flow for the liquid water $\rho_l u_{xl}$ is the assumption

$$\rho_l u_{xl} = -\tilde{D}_l(c_l, n)\frac{\partial c_l}{\partial x} \tag{4.28}$$

where c_l is the mass concentration of liquid water and n denotes the porosity. The diffusion parameter for the liquid water is denoted $\tilde{D}_l$ to distinguish it from a more general case, where also the capillary suction is considered.

The relation (4.28) suggests that a motion of the liquid water in the porous material may occur during vapor uptake or drying. This phenomenon may be of importance if the diffusing vapor contributes to building up liquid water islands, which may eventually become connected creating a slow flow of liquid water.

Even if the numerical values of the diffusion velocities u_{xl} are small compared to the values of u_{xv}, still very dramatic changes of the mass concentrations may be induced since the mass density ρ_v is, typically, of the size $10^{-4}-10^{-5}\rho_l$. Due to this fact, it may be advantageous not to separate the vapor and liquid water flow but rather treat them like one single flow potential as is done in most applications in the field, e.g. compare [20]. However, when constituents such as chloride ions, hydroxide ions, and carbon dioxide are considered, which appear dissolved in the liquid water in the pores of the materials, a separate description — correct from a

physical viewpoint — of the mass diffusion velocity of the liquid water is crucial. This is due to the fact that the motion of the liquid water will effect the behavior of the dissolved matter in the pore solution.

The rate of exchange between the two phases is described in general terms with a state function as

$$\hat{c}_v = f_{vl}(c_v, c_l, \theta, n, a) \tag{4.29}$$

where a denotes the specific surface area. Figure 4.5 shows a principal hypothetical shape of the function (4.29) under isothermal non-equilibrium and equilibrium conditions, where the principal findings in [17] are utilized. When the function $\hat{c}_v$ gives the value zero, the sorption isotherm is recovered for the actual temperature considered. Other combinations of c_v and c_l, which values give $\hat{c}_v \neq 0$, represent a transient process. When non-isothermal conditions are considered, the function $\hat{c}_v$, illustrated in Figure 4.5, will exhibit different shapes for different temperatures, i.e. the rate of exchange for mass as well as the equilibrium conditions will be different at different temperatures.

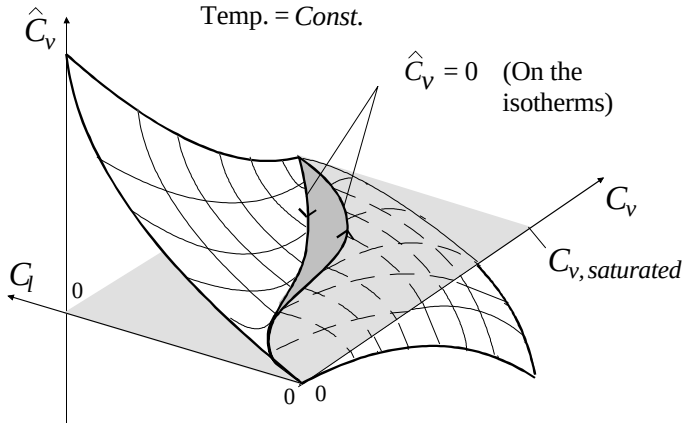

Figure 4.5: *Schematic illustration of the assumed mass exchange rate between vapor and liquid water.*

The values of the function $\hat{c}_v$ in the gap between the absorption and desorption isotherms (in the c_v-c_l plane); — compare Figure 4.5 — must be specified. By introducing realistic assumptions for the mass exchange rate in the gap between the absorption and desorption isotherms, the hysteresis phenomenon, as discussed earlier, might be taken into account in the model.

From (4.24) and the assumptions (4.27) and (4.29), the governing equation for the vapor phase becomes

$$\rho\frac{\partial c_v}{\partial t} = D_v(c_l,\theta,n)\frac{\partial^2 c_v}{\partial x^2} + D_{v\theta}\frac{\partial^2\theta}{\partial x^2} - \rho\dot{x}\frac{\partial c_v}{\partial x} + f_{vl}(c_v,c_l,\theta,n,a);\ \text{in}\, V \tag{4.30}$$

with the boundary conditions

$$c_v(0,t) = h_v(0,t);\ \text{on}\ \partial V \tag{4.31}$$

$$\text{or}\ \rho_v u_{xv}(0,t) = g_{xv}(0,t);\ \text{on}\ \partial V \tag{4.32}$$

where h_v or/and g_{xv} are known values at the boundary ∂V at the time level t. Note that the temperature field and the mass concentration field of liquid water must be known from other equations, since the equation (4.30) can not be solved without this information.

From from the mass balance equation (4.26), the condition (4.25), and the assumption (4.28), the governing equation for the liquid water phase becomes

$$\rho\frac{\partial c_l}{\partial t} = \tilde{D}_l(c_l,n)\frac{\partial^2 c_l}{\partial x^2} - \rho\dot{x}_x\frac{\partial c_l}{\partial x} - f_{vl}(c_v,c_l,\theta,n,a);\ \text{in}\, V \tag{4.33}$$

As it is assumed that liquid water can not enter or leave a body when only diffusion and fixation of vapor are considered, the boundary conditions for the liquid water phase must be represented by the formula

$$\rho_l u_{xl}(0,t) = 0;\ \text{on}\ \partial V \tag{4.34}$$

In discussions about capillary suction or external water pressure, the boundary condition (4.34) has no relevance.

The combined action of diffusion, fixation of vapor and capillary suction together with the boundary conditions are treated in Section 4.4.

It should be observed that the equations for liquid (4.33) and vapor (4.30) are coupled. This is due to the material parameter D_v's dependence on the mass concentration of liquid water and also due to the present source/sink term f_{vl}, which is dependent on both the mass concentration of liquid water and the mass concentration of vapor. Furthermore, the velocity of the mixture $\dot{x}_x$ and the temperature θ may be interpreted as coupling terms.

The diffusion parameter $\tilde{D}_l$ arises from the fact that initially discontinuous liquid water islands at any material point may turn into a continuous system of

liquid as the vapor condensation keeps building up the amount of liquid in the pore system. Based on the evaluation of the experiments performed in [17], it can be suggested that the mass diffusion flow induced by a concentration gradient of the liquid water phase is very small compared to the flow of vapor in a porous body with various pore magnitudes existing together. In other words, for materials such as concrete and mortar, $\tilde{D}_l$ is very small compared to other terms in the equation system, when capillary suction induced by presence of liquid water at a boundary surface is not considered.

In Section 4.3, an alternative way to that in equation (4.33) of dealing with the motion of the liquid water phase will be discussed. This method suggests that a dynamic viscous description is a more stringent assumption seen from a physical viewpoint than the mass diffusion flow description dependent on the concentration gradient used above, since the capillary suction phenomenon is supposed to be a completely different phenomenon, contributing to the motion of the liquid water phase, than liquid motion occurring while the porous material is exposed to vapor (or to drying caused by evaporation).

One important point in this context is that when the material constants and parameters D_v, $D_{v\theta}$, f_{vl} and $\tilde{D}_l$ are searched for in order to arrange and evaluate measurements, this hypothesis should be used as a foundation. However, these constants and parameters are, of course, not 'true' physical quantities, but rather a consequence of the choice of constitutive relations used as the hypothetical base for evaluating and arranging measurements. If the other type of hypothesis (to be discussed in the next Section) is used as a foundation instead, one should search for the viscosity and interaction forces among the constituents in order to be able to describe the motion of capillary sucked water. Hence, one will end up with other types of equations describing the same phenomenon, but with completely different material parameters and experiments to confirm the constitutive relations introduced.

Having this in mind, it is obvious that it is advantageous to choose constitutive relations which offer the possibility to experimentally confirm (or reject) the hypothesis. However, as the mass transport phenomena at the micro-scale reflect important actions, such as physical and chemical bindings, the situation is more complex. Indeed, the constitutive relations presented in this Section must be considered as valid on the micro-scale only. They could hardly be confirmed or rejected by measurements at the micro-scale because such measurements is very difficult to perform. Therefore the only possibility is to 'fit' the material parameters that are required to the global response measured in the laboratory.

The proposed way to treat the transient wetting or drying of porous materials by vapor, discussed in this Section, has many advantages compared to the classical single-phase, non-linear Fick's second law combined with an additional state function between the vapor content and the liquid water content. First of all, the physical interpretation is clear, since no flow potential accounting for the combined effect of vapor and liquid water on the flow is used. A very strong intuitively based argument is that the vapor mass diffusion flow should decrease when the liquid content increases as the cross section of vapor diffusion decreases. Using one single flow potential, the effect is reverse, i.e. the diffusion parameter D must increase when the liquid water increases in order to capture the measured response.

The two-phase model suggests that the vapor diffusion parameter is not necessarily given by a function of the vapor content itself as assumed in most of the classical theories in the area. The apparent increase of the mass diffusion flow $\rho_v u_{xv}$ may instead be a consequence of the transient incorporation of vapor molecules into the confined pores in the material, and also due to significant motion of the liquid water within the pore system.

The use of a, in a physical sense, meaningful description of the boundary conditions becomes very important as all mass transfer problems treated here are boundary value problems. No problems in interpreting the significance of the boundary conditions using the proposed approach will, however, occur since liquid water at the surface of the body may only be built up by vapor condensation or decreased by evaporation. The only situation which will contribute to a mass flow of liquid water into the body through the boundary is capillary suction. This occurs when liquid water (at normal pressure or at a pressure above that of the atmosphere) is applied to the boundary surface. This situation will be discussed and incorporated in the proposed model in Sections 4.3 and 4.4.

Some numerical difficulties occur when it comes to solving the suggested equation system, i.e. the equations (4.30) and (4.33), not present in the classical models since very small time steps must be used in order to follow the solution path. This is not due to the dependency of the diffusion parameters on the liquid content, or to any critical time steps introduced, but to the fact that the evaporation - condensation process takes place on a completely different time scale than the diffusion process does. The numerical treatment of this problem is discussed further in Section 9.

The problem of describing the vapor fixation and diffusion becomes complex when concretes or mortars are considered at early age, since the chemical reaction

rate of the hydration then becomes important. This complication will, however, not be discussed in this work.

4.3. Transient capillary suction flow

Capillary suction phenomena are a consequence of liquid water in the pore space having a lower free energy (or chemical potential) than the outer liquid water in its normal reference state. A flow of liquid water will therefore level out the free energy difference. The lower free energy of liquid pore-water compared to the outer liquid is a consequence of the curved liquid-vapor interface between liquid and vapor, and also due to the free energy conditions of completely dry solid surfaces.

Measurements on mass concentration distribution of liquid water, at different times from an initial exposure to external water show that a more or less distinct front is formed, which proceeds through the porous material, e.g. compare [21] and [15]. This phenomenon is experimentally verified for thin pieces of material such as aerated concrete and sandstone [21]. For more dense materials such as cement mortars, it is difficult to use the most widespread methods of non-destructive moisture measurements. Therefore, a simple gravimetric method is often adopted, which, of course, contains no information of the water distribution profiles at different times from exposure.

Traditional models to evaluate measurements of transient capillary suction flow often include a modification of Fick's second law as a working hypothesis. In this the diffusion parameter (or transport coefficient) becomes strongly dependent on the driving potential used. The gradient-dependent mass diffusion flow, i.e. the constitutive relation for $\rho_l \mathbf{u}_l$, becomes strongly non-linear for all potentials, compare [22]. The potential in such models is for example the capillary suction pressure π_{cap}, determined by equation (4.21), together with the assumption of a known state relation between the vapor pressure π_v and the mass concentration of liquid water ρ_l in every material point. This relation is the so-called sorption isotherm or moisture equilibrium curve discussed in previous Sections.

Other potentials frequently used are the relative vapor pressure π_v/π_{vs} or the mass concentration ρ_l, compare [22].

Some proposed models are believed to describe the combined action of liquid water motion, capillary suction, vapor fixation and diffusion of vapor by using only one differential equation, in which the unknown variable must be able to characterize the essential boundary conditions in terms of concentrations of liq-

uid water and vapor when using simple equations of the type Fick's second law. An additional problem related to the boundary conditions is the fact that some materials, such as aerated concrete and some sandstones, show an increase of the mass concentration close to the boundary when exposed to liquid water. Compare the measurements performed by [21]. This phenomenon may be a consequence of liquid water flow into more or less confined pores, making the capillary *active porosity* gradually increase with time [23].

However, the capillary suction phenomenon is hardly a problem which is in accordance with the basic assumptions behind Fick's second law, i.e. gradient dependent mass concentration flows (with negligible inertia). The very strong non-linearities of the transport coefficient, which must be introduced when trying to make curve fittings with the help of the Fick's second law type equation to consider also capillary suction, explicitly give an indication that the basic assumptions behind this approach can be improved.

Mass transfer of many different types of molecules or ions at low concentration without chemical reactions or temperature gradients most likely follows the overall behavior predicted by Fick's second law without introducing any extreme non-linearities in the constitutive relation for the mass diffusion flows. A liquid in motion, such as capillary-sucked water in a porous material, has very few physical property similarities with diffusing molecules and ions (independently of linear or non-linear gradient flow behavior). For this reason, two additional classical assumptions concerning liquids in motion seem attractive, namely that the assumption of a linear newtonian fluid can be used and the assumption that an interaction between the fluid medium and the solid can take place.

Simply speaking, a linear newtonian fluid will assert a deviatoric stress at a certain material point, which is proportional to the velocity gradient at the same point (and in the same direction). The material constant linking the linear relation between the deviatoric stress components and the velocity gradients is the viscosity μ. This assumption can be used to describe the velocity of the liquid water constituent in the porous material with the help of the momentum balance equation, e.g. compare (2.69). However, the motion of the liquid water will presumably be highly affected by the physical properties of the porous medium expressed, for example in terms of porosity and specific surface area. In the theory of mixtures, such an interacting 'force' among the constituents appears in the momentum balance equation as the momentum sink/source term $\hat{\mathbf{p}}_a$, which is a constitutive dependent property.

By following classical assumptions of the interacting force between a moving

Table 4.3: Viscosity of water, [24].

Temp. (^{o}C)	Viscosity, μ_l (kg/s/m)
0	0.0756
5	0.0749
10	0.0742
15	0.0735
20	0.0728
25	0.0720
30	0.0712
50	0.0679
70	0.0644

fluid and a neighboring solid phase at rest, the momentum supply might, typically, be a function of the velocity of the fluid relative to the solid. This assumption introduces yet another material constant describing the exchange rate of momentum between the liquid and the solid.

By introducing the assumptions of a newtonian fluid and a momentum interaction $\hat{p}_{xl}$ proportional to the diffusion velocity u_{xl}, the equation describing the motion of the liquid water phase can be written using the momentum balance equation (2.69) in a one-dimensional case as

$$\rho_l \frac{\partial x'_{xl}}{\partial t} = \frac{\partial}{\partial x}\left(\frac{4}{3}\mu_l \frac{\partial x'_{xl}}{\partial x} - \pi_l\right) - \beta_{ls} u_{xl};\ \text{in}\, V \tag{4.35}$$

$$-\pi_{xl}(0,t) + \tau_{xl}(0,t) = g_{xl}(0,t);\ \text{on}\ \partial V \tag{4.36}$$

$$\text{or}\ x'_{xl}(0,t) = h_{xl}(0,t);\ \text{on}\ \partial V \tag{4.37}$$

where μ_l (kg/s/m) is the viscosity of pure liquid water and β_{ls} (kg/s/m^3) is the constant describing the interaction between the liquid water and the solid pore walls. Values of the viscosity coefficients of pure liquid water at different temperatures are given in Table 4.3, from [24].

A more detailed description of the assumptions of a newtonian fluid is performed in Section 3.2. Note, however, the difference between the definitions of the velocity of the liquid water x'_{xl} and the diffusion velocity of liquid water u_{xl}, compare (2.15) and (2.16).

The natural boundary condition (4.36) is a description of the deviatoric stress plus the hydrostatic pressure in the liquid, i.e. a prescribed value of the term

$(-\pi_{xl} + \tau_{xl})$, which is equal to a known value denoted g_{xl}. This stress is directed normal to the boundary surface, and the essential boundary condition (4.37) is the description of a known value for the velocity of the liquid water constituent x'_{xl}, denoted h_{xl}.

Equation (4.35) contains three unknown physical quantities: the mass density ρ_l, the velocity of the liquid water x'_{xl}, and the hydrostatic pressure π_l (for a moment the difference between the velocities x'_{xl} and u_{xl} is ignored, compare Section 3.2 for details). Obviously, three equations are required to solve these quantities. Assuming, however, that the hydrostatic pressure gradients within the considered body in this test example are small, only one supplementary equation is needed. By using the mass balance equation with no mass supply, the sought equation is found without introducing any extra constitutive relations, hence without introducing any material constants. The mass balance (2.49) in a one-dimensional case without mass exchange between constituents becomes

$$\frac{\partial \rho_l}{\partial t} = -\rho_l \frac{\partial x'_{xl}}{\partial x} - x'_{xl} \frac{\partial \rho_l}{\partial x}; \text{ in } V \tag{4.38}$$

$$\rho_l(0,t) = h_l(0,t); \text{ on } \partial V \tag{4.39}$$

where h_l is a known value of the mass concentration just beneath the surface of the porous material, at a time when the body is exposed to liquid water, i.e. to a capillary suction situation (or hydrostatic pressure situation).

In (4.38), only the essential boundary condition (4.39) must be prescribed, i.e. the value of ρ_l at the boundary surface.

The two sets of equations, (4.35) and (4.38) close the equation system, since the velocity and the mass density are the only properties searched for in this example. It should be noted that the assumptions of a newtonian fluid and the momentum supply are introduced primarily in order to compute the velocities and not to compute the stress in the fluid considered. It should also be observed that the diffusion velocities and mass densities must be calculated for by solving (4.35) and (4.38) simultaneously.

The transient capillary suction problem can now be solved in a way that is alternative to the strongly non-linear Fick's second law by introducing proper physical boundary conditions.

Indeed, an equation for the liquid water phase has already been introduced in association with vapor fixation (equation (4.33)). In the next Section, a discussion is presented about how this equation can co-exist in the general case where also capillary suction occurs when liquid water is present at the boundary.

4.4. Simultaneous action of capillary suction and vapor diffusion

In this Section, the possibility of using one governing equation describing diffusion, adsorption and desorption of vapor will be discussed, and of using another equation simultaneously describe the capillary suction. These equations must describe the response under conditions, at which different parts of the boundary are exposed to vapor and liquid water in different locations and at the same time.

At the end of the Section, the advantages and disadvantages of such an approach will be analyzed.

Since capillary suction and absorption of liquid water due to vapor diffusion are two different physical phenomena, it seems reasonable to have two different, coupled equations describing such problems. It will be shown, however, that these two different equations can not be used simultaneously without introducing certain additional approximations.

In Section 4.2, two governing equations were discussed, one for the liquid water and another for describing the action of the vapor valid for the case where capillary suction is excluded. In Section 4.3, the action of the liquid water was discussed in situations of capillary suction only. This means that two independent equations are used to describe the liquid water constituent. When cases are considered, where a certain domain is subjected to both capillary suction and vapor at different locations of the boundary, it is obvious that the capillary suction can not be treated in a separate equation without assigning special properties to the capillary-sucked liquid water. Otherwise, one equation too many is introduced.

The capillary action is almost always incorporated in one single equation accounting both for vapor diffusion and capillary suction. This means that extremely non-linear diffusion parameters must be introduced in order to match Fick's second law to measured concentration profiles. These extreme non-linearities might be a consequence of using a model based on constitutive relations, which do not reflect the actual physical behavior during capillary suction, but are rather adjusted to fit measured data.

Indeed, the complexity of the model will increase when capillary action and vapor diffusion are separated and treated as different phenomena, using different equations for the two types of flow. It is, however, realized that a stringent description of the liquid water's action in porous materials is important, since nearly every deterioration process depends on the concentration and flow of liquid water. The most important issue is to obtain a realistic description of the entire mixture's velocity. In such a description, the capillary suction is a chief factor, since matter (i.e. chloride ions, hydroxide ions, etc.) dissolved into the liquid

water are also subjected to convection determined by the mean velocity. If a realistic value of the velocity of the mixture can be predicted, it will be possible to significantly improve the description of dissolved matter in the pore system.

In order to obtain an estimate of the mixture's velocity, causing convection, assumptions on the mobility of adsorbed and capillary condensed water, subjected to capillary suction, must be considered. It is supposed that capillary sucked water could hardly force already adsorbed and capillary-condensed water to obtain a significant motion in the direction of the flow of capillary-sucked water.

When Fick's second law is used to describe both capillary action and the effect of vapor diffusion in a single equation, the mass diffusion flow, i.e. $\rho_l \mathbf{u}_l(\mathbf{x},t)$, is forced to be the total flow of all liquid water present in each material point, since no special properties of adsorbed and capillary condensed water are introduced. This type of description supposedly gives erroneous predictions of the velocity of the mixture, and hence erroneous descriptions of the diffusing matter in the pore solution.

The difference in properties between adsorbed and capillary-condensed water and capillary water is quite obvious. One important issue is that capillary-sucked liquid water can easily occupy space which is not available for capillary-condensed water and vice versa.

Water supplied by capillary suction will be treated as a separate constituent and this liquid water will be referred to as bulk water although it is not completely 'free'. Adsorbed and capillary-condensed water will be referred to as vicinal water. The third constituent considered is the vapor phase. By making the distinction between bulk and vicinal water, it is possible to use a separate equation to model capillary suction. The consequences of such an approach will be discussed in the following paragraphs.

Using this approach, the following primary unknown physical properties are to be solved:

$$\mathbf{T}_{bulk}(\mathbf{x},t)\ ;\ \hat{\mathbf{p}}_{bulk}(\mathbf{x},t)\ ;\ \begin{matrix}\rho_v(\mathbf{x},t)\\ \rho_{bulk}(\mathbf{x},t)\\ \rho_{vic.}(\mathbf{x},t)\end{matrix}\ ;\ \begin{matrix}\mathbf{x}'_v(\mathbf{x},t)\\ \mathbf{x}'_{bulk}(\mathbf{x},t)\\ \mathbf{x}'_{vic.}(\mathbf{x},t)\end{matrix}\ ;\ \begin{matrix}\hat{c}_v(\mathbf{x},t)\\ \hat{c}_{bulk}(\mathbf{x},t)\\ \hat{c}_{vic}(\mathbf{x},t)\end{matrix} \tag{4.40}$$

The temperature field must also be analyzed, and the following unknown physical properties must be found:

$$\theta(\mathbf{x},t)\,;\ \varepsilon(\mathbf{x},t)\,;\ \mathbf{q}(\mathbf{x},t)\,; \tag{4.41}$$

In total, fourteen primary unknowns are introduced into the problem of non-isothermal combined vapor diffusion (including fixation-evaporation) and capillary suction. Hence, fourteen equations must be introduced. Five balance equations can be used, i.e. three mass balance equations, the momentum balance of the bulk water, and the energy balance of the whole mixture. That is, nine constitutive relations describing the physical behavior of the constituents must be introduced to make the equation system closed.

The mass exchange among the three constituents must fulfill (2.51), i.e.

$$\hat{c}_{bulk} + \hat{c}_{vic.} + \hat{c}_v = 0 \tag{4.42}$$

The mass exchange rate of the total liquid water is $\hat{c}_l = \hat{c}_{bulk} + \hat{c}_{vic.}$, hence

$$\hat{c}_l + \hat{c}_v = 0 \tag{4.43}$$

It will further be assumed that bulk and vicinal water exchange mass with the vapor phase only. The total consumption or production rate of vapor is constituted with the following general relation:

$$\hat{c}_v = f(c_v, c_l, \theta, n, a) \tag{4.44}$$

where $c_l = c_{bulk} + c_{vic}$.

That is, the exchange between vapor and liquid is assumed to be a function of the mass concentration of vapor c_v, the total liquid water mass concentration c_l, the temperature θ, the porosity n, and the specific surface area a.

In order to somewhat capture the evaporation and condensation phenomenon between curved surfaces of bulk and vicinal water, a distribution function $k_{dist.}$ is introduced as

$$\hat{c}_{bulk} = -k_{dist.}\hat{c}_v \tag{4.45}$$

and

$$\hat{c}_{vic.} = -\left(1 - k_{dist}\right)\hat{c}_v \tag{4.46}$$

where $0 \leq k_{dist} \leq 1$.

It is then obvious that (4.43) is fulfilled, since

$$k_{dist.} f(c_v, c_l, \theta, n, a) + \left(1 - k_{dist}\right) f(c_v, c_l, \theta, n, a) = -\hat{c}_v \tag{4.47}$$

If the distribution function k_{dist} is chosen as

$$k_{dist} = \frac{c_{bulk}}{c_{vic.} + c_{bulk}} = \frac{c_{bulk}}{c_l} \tag{4.48}$$

the function $k_{dist.}$ is zero when the mass concentration of bulk water c_{bulk} is zero. Hence the equation (4.29), which describes the rate of mass exchange between vicinal water and vapor is retained. At a certain material point when $c_{vic.}$ is very small compared to c_{bulk}, $k_{dist.}$ tends towards 1, that is, the exchange of mass between vapor and bulk water is dominant.

During drying processes after a period of capillary suction, the equations (4.44), (4.45), (4.46), and (4.48) predict that a major part of the bulk water must be evaporated before the mass concentration of vicinal water at the same point can decrease. The equations represent the effect of vicinal water being locked due to the presence of bulk water.

No exchange of mass between bulk and vicinal water is considered. This means that water supplied through capillary suction (i.e. bulk water) maintains its special properties independently of the current mass concentration of vicinal water. This is, of course, a rough approximation. Using different equations for capillary suction and diffusion (including adsorption-desorption processes) of vapor, which seems correct from a physical viewpoint, calls for separate properties of liquid water, i.e. bulk and vicinal water, however.

Using the constitutive relation, which describes vapor fixation (sink) and evaporation (source) for the vapor constituent, i.e. equation (4.44), mass balance (2.56), and the constitutive relation for the mass diffusion flow (4.27) gives the governing equation for the vapor as

$$\begin{aligned} \rho\frac{\partial c_v}{\partial t} &= D_v(c_l,\theta,n)\nabla^2 c_v - \rho\dot{\mathbf{x}}\cdot\nabla c_v + D_{v\theta}\nabla^2\theta \\ &\quad + f(c_v,c_l,\theta,n,a);\ \text{in}\, V \end{aligned} \tag{4.49}$$

where ∇^2 is the Laplace operator, i.e.

$$\nabla^2 \equiv \left(\frac{d^2}{dx_1^2} + \frac{d^2}{dx_2^2} + \frac{d^2}{dx_3^2}\right) \tag{4.50}$$

and

$$\nabla \equiv \left[\begin{array}{ccc} \frac{d}{dx_1} & \frac{d}{dx_2} & \frac{d}{dx_3} \end{array}\right] \tag{4.51}$$

is the gradient operator.

If a situation is considered, where no liquid water is present in a certain part of the boundary surface, denoted ∂V_v, the boundary conditions for the vapor phase are

$$c_v(\mathbf{x}_b,t) = h_v(\mathbf{x}_b,t);\ \text{on}\,\partial V_v \tag{4.52}$$

$$or\ \rho_v \mathbf{u}_v(\mathbf{x}_b, t) \cdot \mathbf{n} = g_{vn}(\mathbf{x}_b, t);\ \text{on}\, \partial V_v \tag{4.53}$$

where h_v in (4.52) and/or g_{vn} in (4.53) are known quantities of the concentration and the mass diffusion velocity respectively, at the part of the boundary exposed to vapor ∂V_v.

It is assumed that the vapor phase can not escape from the parts of the body exposed to liquid water, written in terms of the boundary condition for the vapor phase as

$$\rho_v \mathbf{u}_v(\mathbf{x}_b, t) \cdot \mathbf{n} = 0;\ \text{on}\ \partial V_l \tag{4.54}$$

where ∂V_l denotes a boundary part exposed to liquid water.

And the equation which describes the action of the vicinal water phase can be written as

$$\rho \frac{\partial c_{vic.}}{\partial t} = \tilde{D}_{vic.}(c_l, n) \nabla^2 c_{vic.} - \rho \dot{\mathbf{x}} \cdot \nabla c_{vic.} - (1 - k_{dist})\, f(c_v, c_l, \theta, n, a);\ \text{in}\, V \tag{4.55}$$

where the mass balance equation (2.56), the constitutive relation for the mass diffusion flow of the format (4.28), and the relation for the mass exchange (4.46) are used.

The corresponding boundary condition to solve for the mass concentration of the vicinal water phase in (4.55) is the assumption

$$\rho_{vic.} \mathbf{u}_{vic} \cdot \mathbf{n} = 0;\ \text{on}\ \partial V \tag{4.56}$$

This is the assumption that the vicinal water can not escape from the domain as liquid, under any circumstances. The mass concentration of vicinal water in the pore structure near the boundary surface can only be decreased once it has been converted into vapor (according to (4.44)), and has after that been evaporated (as vapor) through the boundary surface (this may not happen during exposure to liquid at the surface, compare equation (4.54)).

In a situation, in which the essential boundary condition is liquid water, i.e. when capillary suction take place, the proposed equation for the vapor phase is (4.49). The motion of the bulk water, however, which can be supplied by capillary action only, is supposed to be described as a viscous problem, i.e. equation (4.61).

The adopted constitutive relation for the stress tensor of the bulk water is

$$\mathbf{T}_{bulk} = \mu_{bulk}(\theta) \mathbf{D}_0 \tilde{\nabla} \mathbf{x}'_{bulk} - \pi_{bulk} \mathbf{I} \tag{4.57}$$

which is the assumption describing a linear newtonian fluid in a Cartesian coordinate system. The viscosity of the bulk water is denoted μ_{bulk}.

The divergence operator $\tilde{\nabla}$ is written down in (9.25). Compare Section 9.2, where π_{bulk} is the hydrostatic pressure of the bulk water. The so-called constitutive matrix for $\mu_{bulk}\mathbf{D}_0$ becomes

$$\mu_{bulk}(\theta)\mathbf{D}_0 = \mu_{bulk}(\theta)\begin{bmatrix} \frac{4}{3} & -\frac{2}{3} & -\frac{2}{3} & 0 & 0 & 0 \\ -\frac{2}{3} & \frac{4}{3} & -\frac{2}{3} & 0 & 0 & 0 \\ -\frac{2}{3} & -\frac{2}{3} & \frac{4}{3} & 0 & 0 & 0 \\ 0 & 0 & 0 & 1 & 0 & 0 \\ 0 & 0 & 0 & 0 & 1 & 0 \\ 0 & 0 & 0 & 0 & 0 & 1 \end{bmatrix} \tag{4.58}$$

Compare (9.27) in Section 9.2.

The momentum supply vector for the bulk water is constituted as a linear function of the diffusion velocity $\mathbf{u}_{bulk}$ as

$$\hat{\mathbf{p}}_{bulk} = -\beta_{bulk}(c_{vic})\mathbf{u}_{bulk} \tag{4.59}$$

where β_{bulk} is a material parameter, which is assumed to depend on the mass concentration of vicinal water c_{vic}.

The balance of momentum for the bulk liquid water is, according to (2.69),

$$\rho_{bulk}\frac{\partial \mathbf{x}'_{bulk}}{\partial t} = div\,\mathbf{T}_{bulk} + \hat{\mathbf{p}}_{bulk} \tag{4.60}$$

where the term $\mathbf{x}'_{bulk}\cdot\mathrm{grad}\mathbf{x}'_{bulk}$ is assumed to be small compared to the others and where also the body force $\rho_{bulk}\mathbf{b}_{bulk}$ is assumed to have negligible influence.

The equations (4.57), (4.59), and (4.60) produce

$$\rho_{bulk}\frac{\partial \mathbf{x}'_{bulk}}{\partial t} = \tilde{\nabla}^{\mathrm{T}}\mu_{bulk}\mathbf{D}_0\tilde{\nabla}\mathbf{x}'_{bulk} - \nabla\pi_{bulk} - \beta_{bulk}(c_{vic})\mathbf{u}_{bulk};\ \text{in}\,V \tag{4.61}$$

The boundary conditions to be described are

$$-\pi_{bulk}(\mathbf{x}_b, t) = g_{bulk}(\mathbf{x}_b, t);\ \text{on}\ \partial V_l \tag{4.62}$$

or

$$\mathbf{x}'_{bulk}(\mathbf{x}_b, t)\cdot\mathbf{n} = h_{bulk}(\mathbf{x}_b, t);\ \text{on}\ \partial V_l \tag{4.63}$$

where g_{bulk} and/or h_{bulk} are known quantities at the boundary ∂V_l of the stress component and the velocity respectively at the time t.

The velocity field of the bulk water, computed from (4.61), is used to compute the mass density distribution with the mass balance equation (2.49) by rewriting

the term $\mathrm{div}(\rho_a \mathbf{x}'_a)$ as $\mathrm{div}(\rho_a \mathbf{x}'_a) = \rho_a \mathrm{div}\mathbf{x}'_a + \mathbf{x}'_a \cdot \mathrm{grad}\rho_a$. The following equation is obtained by introducing the constitutive relation for $\hat{c}_{bulk}$, i.e. equation (4.45).

$$\begin{aligned} \frac{\partial \rho_{bulk}}{\partial t} &= -\rho_{bulk}\left(\nabla \cdot \mathbf{x}'_{bulk}\right) - \mathbf{x}'_{bulk} \cdot \nabla \rho_{bulk} \\ &\quad - (1 - k_{dist})\, f(c_v, c_l, \theta, n, a);\ \text{in}\, V \end{aligned} \tag{4.64}$$

where $(\nabla \cdot)$ is the divergence operator in a Cartesian coordinate system.

The essential boundary condition to be used in (4.61) is a description of the mass density ρ_{bulk}, which occupies the actual active porosity at the near surface ∂V_l, that is

$$\rho_{bulk}(\mathbf{x}_b, t) = j_{bulk}(\mathbf{x}_b, t);\ \text{on}\ \partial V_l \tag{4.65}$$

where j_{bulk} is a known value of ρ_{bulk} occupying the accessible porosity at the time level t.

The nine constitutive equations sought are given by (4.44), (4.45), and (4.46) which describe the mass exchange among the constituents. The mass diffusion flows for vapor and vicinal water are the assumptions (4.27) and (4.28). The velocity field of the bulk water is given from the constitutive relations (4.57) and (4.59). The two missing relations are the assumptions leading to the standard heat conduction equation, that is (3.21) and (3.22).

It is concluded that a more detailed study can be performed by assigning different properties to the liquid water, hence using a separate equation for the capillary action. The non-isothermal case can also be studied, since the vapor phase is highly effected. In other words, the equilibrium condition between vicinal water and vapor changes when the temperature is changed, and the temperature can be included in the description of the mass diffusion flow of vapor. Compare the assumption (4.27). The temperature effect on the capillary suction can, for example, be introduced by making the viscosity of water dependent on temperature.

It is also concluded that the drawback of using a separate equation describing capillary suction is that the liquid water must be separated into two different constituents with different properties. This may not be physically adequate for materials such as concrete.

4.5. General aspects of concrete deterioration caused by diffusion of ions and gases

Concrete deteriorates due to many different mechanisms. One the most important reinforcement corrosion induced by deleterious substances reaching the embedded

reinforcement bars. The external sources of deleterious materials can be, for example, chlorides from deicing salts, or sea water and carbon dioxide.

Though research attempts have been made to determine the threshold values. This was done in order to find out at which concentration of chlorides in concrete the reinforcement corrosion is induced, that is, at which point the passive condition close to the reinforcement turns into an active state [25], [26]. In order to predict when this threshold value is reached, the flow properties of the aggressive substances in the concrete, mainly chloride and CO_2, must be known.

Some of the most important phenomena governing the motion of dissolved matter in concrete are: (*i*) diffusion of the ions in the pore water (diffusion is the name given to a motion of molecules or ions in a weak concentration imposed by a concentration gradient), (*ii*) adsorption and desorption of matter onto the pore walls, and (*iii*) convection of the dissolved matter due to the motion of the mixture itself. The main part of the mixture is liquid water.

There are two main conditions to be considered:

1. *The initiation phase;* during which CO_2 and chloride penetrate the cover. The duration of this phase depends on the rate of penetration. For gases, the penetration rate is lower the higher the water content. This depends on the fact that gas transport in water is many magnitudes lower than gas transport in air. For chloride, the penetration rate increases with increased water content. Chloride can not move in air and it is doubtful whether it can move in adsorbed water.

2. *The corrosion phase;* during which the steel is dissolved. The corrosion rate depend on two factors: (*i*) the availability of oxygen, and (*ii*) the electrical resistance of the pure solution surrounding the bar. The availability of oxygen is reduced with increased water content. The electrical conduction is increased with increased water and chloride contents. Hence, there is a sort of 'optimum' water content where the corrosion rate is at a maximum.

A more detailed discussion of the corrosion phenomena in association with chloride penetration into concrete will be presented in Section 6.

The physical and chemical bindings of chlorides are important when considering the global action of chloride penetration into cement based materials. However, the binding capacity and the binding rate have been shown to be highly affected by the mass concentration of hydroxide ions in the pore solution and also by the chemical character of the binder. That is, in order to make a description

which is physically stringent, of the behavior of chlorides penetrating concrete, the behavior of the variation of hydroxide ion concentration in the domain of interest must be known.

The hydroxide ions, which appear naturally in the pore solution in cement-based materials have a neutralizing effect on reinforcement corrosion. These ions will, however, be subjected to a motion within the liquid water in the pore system. Measurements on the composition of the pore solution of concrete show, clearly, that hydroxide ions will be washed out to some extent when the concrete is stored in pure water. For example, an initial concentration of hydroxide ions of 0.5 (mol/l) near the surface of a sample may easily be decreased to a value 0.1, as a consequence of ions moving out towards the surrounding pure water, e.g. compare [27]. Such a behavior will surely affect the binding capacity of chlorides in concrete.

Interaction between diffusing hydroxide ions moving outwards and chloride ions moving inwards has also been reported, compare [28].

The transport of carbon dioxide CO_2 is somewhat different from the transport of other material in the pore system, since it significantly changes the pore structure. Hence, the conditions controlling the diffusion and binding of chlorides will be changed too. Carbon dioxide reacts chemically with the calcium hydroxide $Ca(OH)_2$ or other hydration products in the cement, and hence change the structure of the solid. This presumably changes the mobility of other substances such as chloride and hydroxide ions. The phenomenon referred to as carbonation is discussed in more detail in Section 4.7.

The motion of carbon dioxide is dominant within the air-filled space in the pore system. This is the reason why corrosion is found to be greater in average liquid water contents.

An approximate value about 0.6 of the ratio $[Cl^-]/[OH^-]$ to trigger corrosion of reinforcement bars in aqueous solutions has been reported, compare [25]. When the reinforcement bars are embedded in a cement-based material it is, however, not only the ratio $[Cl^-]/[OH^-]$ in the pore solution which will determine the risk of corrosion. Also the character of the cementitious material in contact with the steel and the liquid water content near the steel is crucial for assessment of a passive condition.

Research has been devoted to developing dense concretes by using mineral additives such as silica fume and fly ash with low cement-to-binder ratios in order to minimize the penetration of CO_2 and chloride. Concretes containing such additives are more difficult to cast, which might cause defects in the concrete

cover. Besides, they will have less protecting hydroxide ions in the pore solution due to reactions between the additives and the portland cement in the concrete. Therefore, the chloride-induced corrosion can be induced at a lower chloride concentration at the reinforcement bar than in ordinary concrete.

A realistic description of liquid water flow and vapor diffusion, fixation and desorption is important, since these phenomena affect the overall behavior of chloride and hydroxide ions, carbon dioxide and oxygen. Hence, the transport of gases and ions is intimately coupled with the transport and fixation of water in the pore system. The transport of 'aggressive agents' and of water must therefore be studied together.

It is also important to note that measurements performed on chloride ingress found in concrete exposed at field stations differ significantly from measurements performed under more controlled conditions in laboratory tests. The main difference is that a slower ingress of chloride is almost always observed in the field measurements [26]. This may be due to many different things, such as temperature effects and clogging of the pore system caused by chemical reactions between different components in the seawater and concrete not considered in controlled laboratory tests during comparable chloride exposure in terms of concentration.

4.6. Chloride penetration and binding

Below, a simplified picture of the constitutive relations involved in chloride penetration into cement-based materials is presented. In fact, the proposed way of modelling the problem only claims to be valid during ideal conditions, despite the fact that numerous factors are introduced which supposed affect the action of chlorides.

The mass diffusion velocity, represented as a one-dimensional case, is constituted with a concentration gradient assumption as

$$\rho_c u_{xc} = -D_c(c_l, \theta, n)\frac{\partial c_c}{\partial x} \tag{4.66}$$

where the diffusion parameter D_c is assumed to be a function of the mass concentration of liquid water c_l in the porous material, the temperature θ and the porosity n. Indeed, the possibility to include also a dependency of the pore size distribution on D_c appears attractive. This phenomenon is, however, not included in the assumption (4.66).

Typical values of diffusion constants for ions in bulk water at 25 ^{o}C are $D_c^l = 2.03 \cdot 10^{-9}\,(\mathrm{m}^2/\mathrm{s})$ for Cl^-, $D_{oh}^l = 5.30 \cdot 10^{-9}\,(\mathrm{m}^2/\mathrm{s})$ for OH^-, and $D_{na}^l = 1.33 \cdot$

10^{-9} (m^2/s) for Na^+, e.g. compare [29]. These values are supposed to be heavily reduced for diffusion in porous materials due to the tortuosity effect caused by the pore system.

The mass diffusion velocity $\rho_c u_{xc}$ constituted in (4.66) may also be a function of an electrical field induced by the corrosion process, since the considered diffusing material is electrically charged. This effect is very important when the action of different ions in the pore solution during corrosion in its propagation stage is studied.

The binding rate, $\hat{c}_c$, of the free chloride ions in the pore solution is assumed to be given by a function of the concentration of the free chloride ions c_c, the amount of physically bound chloride mass density ρ_{cs} (denoted ρ_{cs}, since the bound chlorides are assumed to get stuck on the solid pore walls and contribute to a small weight change of the mass density of the solid phase), the mass concentration of hydroxide ions c_{oh}, the temperature θ, the porosity n and the specific surface area a, i.e.

$$\hat{c}_c = f_c(c_c, \rho_{cs}, c_{oh}, \theta, n, a) \tag{4.67}$$

The binding of chlorides onto the pore walls and the release of bound chlorides are assumed to be a consequence of two different phenomena: an adsorption/desorption and a micro-diffusion into and out of gel pores. The chlorides may also react chemically with the cement hydration products and form for example Friedel's salt. The numerical value of the reaction rate $\hat{c}_c$ might be both positive and negative.

It is assumed that the mass exchange of chlorides only occurs between free chlorides in the pore solution and chlorides bound physically or chemically at the solid surfaces. The equation (2.51) gives

$$\hat{c}_c = -\hat{c}_{cs} \tag{4.68}$$

where $\hat{c}_{cs}$ is the reaction rate for the immobilized chloride ions.

It may be tempting to a priori assume that the equilibrium between the free mass concentration of chlorides and the mass concentration of adsorbed (bound) chlorides is established instantaneously, i.e. that a local equilibrium is immediately established according to the non-linear equilibrium sorption isotherm $c_c = k c_{cs}^n$, where k and n are constants. Indeed, simple analytical solutions based on Fick's second law exist to this problem under the condition that the boundary concentration in terms of prescribed free mass concentration is constant, compare for example [30]. The assumption of instantaneous binding used in Fick's second

law will lead to the conclusion that the 'true' diffusion parameter D_c, compare (4.66), will be very much reduced compared to the so-called effective diffusion parameter D_{eff}. This decreased value is often also referred to as the apparent diffusion parameter. Under the condition that $n = 1$, the equation to be solved is of standard format, that is, $\partial c_c/\partial t = D_c/(k+1)\partial^2 c_c/\partial x^2$, where $D_c/(k+1) = D_{\text{eff}}$. Naturally, the overall penetration depth of chloride will be diminished due to binding.

When situations are studied, where the boundary conditions in terms of free mass concentration of chlorides change with time, as in the important problem of chloride ingress in constructions exposed to deicing salts or in the splash zone of a bridge column, the use of the above-mentioned instantaneous equilibrium with the chloride-sorption isotherm gives erroneous results. This is mainly due to the assumptions about a perfect instantaneous equilibrium with reversible conditions. Field measurements on deicing salt exposed to concrete specimens [31] clearly indicate that binding of chlorides in concrete is not a perfectly reversible process, as the instantaneous equilibrium binding isotherm suggests. Due to this fact, the description (4.67) is suggested, which in essence describes a so-called second-order reversible system, e.g. compare [30].

Experiments performed in [32] also show the importance of dealing with the binding and the boundary conditions in a stringent way. Table 4.4 shows mass concentration profiles in OPC paste, with $w/c = 0.5$ exposed to a 5 wt% sodium chloride concentration. The Table4.4 shows the concentration of total chloride, free chloride in pore solution, and of hydroxide ion concentration in pore solution at three different exposure times [32].

Extrapolation of the free chloride concentration to the depth equal to zero corresponds fairly well to the storage concentration (855 mmol/l). However, the extrapolation of the total chloride concentration (i.e. bound plus free chloride) to the depth equal to zero shows a significant increase in time. After six months, the approximate extrapolated value of total chloride at the surface is 16 mg per g cement and at twelve and twenty-two months, the approximate concentrations at the surface become 18 and 25 mg per g cement respectively. This indicates that the binding of chloride is a transient process, which does not reach equilibrium instantaneously. The same conclusion can be drawn from Figure 4.6.

The same type of transient binding is observed during moisture uptake, at which a significant time of equilibration is supposed to be caused by microscopic vapor diffusion towards gel pores, compare [17] and Figure 4.3. A phenomenon of this type might also be the cause of the transient type of binding of chloride ions.

Table 4.4: Data for specimens of OPC paste, w/c = 0.5, stored in NaCl solution of 855 mol/l, [32].

Time (months)	Depth (mm)	Total chloride (mg per g cement)	Free chloride (mmol/l)	pH
6	10	11.3	225	13.35
	20	7.1	51	13.51
	30	5.3	33	13.54
	40	3.7	14	13.58
12	10	13.0	230	13.24
	20	11.9	125	13.37
	30	9.0	35	13.53
	40	8.3	30	13.56
24	10	21.0	623	13.04
	20	16.7	484	13.24
	30	13.9	323	13.40
	40	12.1	235	13.47

Table 4.4 also shows the effect of hydroxide ions being leached out into the surrounding storage solution. The somewhat low outflow of hydroxide is due to the fact that a storage solution with a volume of only 1 l was used. This solution rapidly reached the pH value 12.5 and was therefore replaced weekly.

A second set of OPC paste specimens was exposed to a weekly wet/dry cycle, in which a 100ml salt solution was applied to the surface and allowed to dry for three or four days by evaporation to the air, compare [32]. Directly after this, 100ml of pure liquid water was applied to the surface and left to evaporate. The result in terms of total and free chloride concentration profiles and hydroxide ion profiles for three different times are shown in Table 4.5 [32]. It is clear that the free chloride concentration profiles become significantly higher than in the experiment with constant exposure shown in Table 4.4. This is probably due to the higher boundary concentration of chloride caused by the evaporation of water from the storage solution. Table 4.5 also shows that the outflow of chloride during the exposure of pure water affects the global ingress of chloride to a very little extent. Furthermore, it is noted that the total chloride concentration profiles are only slightly higher after six and twelve months' exposure compared to the profiles presented in Table 4.4 for the same times.

The third method of exposure, used in [32], consisted of drying the samples for

Table 4.5: Data for specimens of OPC paste, w/c = 0.5 exposed to weekly chloride solution - pure water cycles [32].

Time (months)	Depth (mm)	Total chloride (mg per g cement)	Free chloride (mmol/l)	pH
6	10	12.6	650	13.46
	20	7.9	145	13.58
	30	5.6	85	13.61
	40	4.8	48	13.61
12	10	16.6	900	13.45
	20	16.0	580	13.51
	30	10.4	280	13.59
	40	8.7	140	13.61
24	10	32.6	2196	13.28
	20	24.7	1478	13.51
	30	21.3	1368	13.58
	40	19.8	1094	13.58

one week at 35^{o}C, after which 1 l of 5 wt% sodium chloride solution was applied and then exposed and maintained for three weeks. The remaining solution was then siphoned off and the cycle repeated. The results from this experiment are shown in Table 4.6. The overall chloride ingress is seen to be higher in this experiment compared to the results presented in Table 4.5. One reason for this is presumably the capillary suction of saline water after the drying periods. The drying may also affect the concentration of free chloride in the pore solution, which in turn may accelerate both the chloride diffusion and the chloride binding.

It is observed that the concentrations of free chloride at the surface, shown in Table 4.6, widely exceed the concentration of the outer storage solution, i.e. 855 mmol/l. This can be a consequence of the drying process contributing to a gradual increase in the free chloride concentration. However, it is pointed out in [32] that the pore liquid expression device used to separate the pore solution from the sample with a pressure as high as 350 MPa may cause loosely bound chlorides to be released, which in turn may result in an overestimation of the level of free chloride [33]. An alternative method is to leach the chloride.

From the general behavior shown in Tables 4.4, 4.5, and 4.6, it is concluded that a powerful model accounting for the diffusion of chlorides in pore solution, non-equilibrium binding (transient binding due to micro-diffusion into gel pores),

Table 4.6: Data for specimens of OPC paste w/c = 0.5 exposed to monthy cyclic exposure to NaCl-solution and drying [32].

Time (months)	Depth (mm)	Total chloride (mg per g cement)	Free chloride (mmol/l)	pH
6	10	17.9	750	13.32
	20	11.5	430	13.56
	30	9.2	310	13.61
	40	7.0	280	13.58
12	10	21.9	1080	13.22
	20	18.4	840	13.39
	30	15.4	635	13.48
	40	12.8	530	13.57
24	10	35.9	2306	12.81
	20	35.1	2267	13.03
	30	32.4	2261	13.23
	40	30.3	2215	13.34

and the convection of chlorides due to capillary suction must be considered in order to capture the most important processes involved in chloride penetration into porous materials with a wide range of pore sizes.

Figure 4.6 from [34] shows, among other things, that the constant boundary conditions do not influence the penetration profiles in the way described by Fick's second law — with an incorporation of linear or non-linear equilibrium binding isotherms. In fact, the global response of the chloride ingress for various water-to-cement ratios (w/c) is very insensitive to the boundary concentrations, presumably due to the dominating physical action of the chloride binding.

According to Figure 4.6, it seems that the boundary concentration of total chloride at the surface of the samples is not constant with time. This is most dominant for concrete with $w/c = 0.47$ and $w/c = 0.73$ stored in 150 g/l NaCl solution. The same conclusion is drawn in [35].

The observation that the concentration of total chloride at the specimen surface increases with time (when exposed to a constant outer chloride concentration, Table 4.4, Figure 4.6) means that the use of a linear or non-linear equilibrium binding isotherm will give erroneous predictions of the evolution in time of the mass concentration in the domain. Again, the use of the proposed second-order reversible system to describe the action of chloride binding seems attractive.

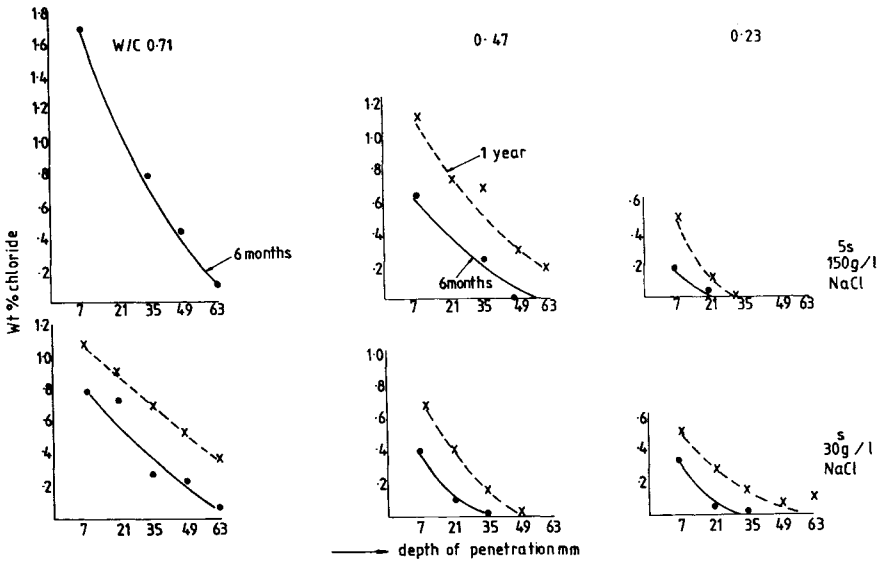

Figure 4.6: *Quantity of total chloride found in hardened cement pastes at various water-to-cement ratios and at various depths after exposure during six and twelve months to chloride solutions of 150 g/l and 30 g/l, [34].*

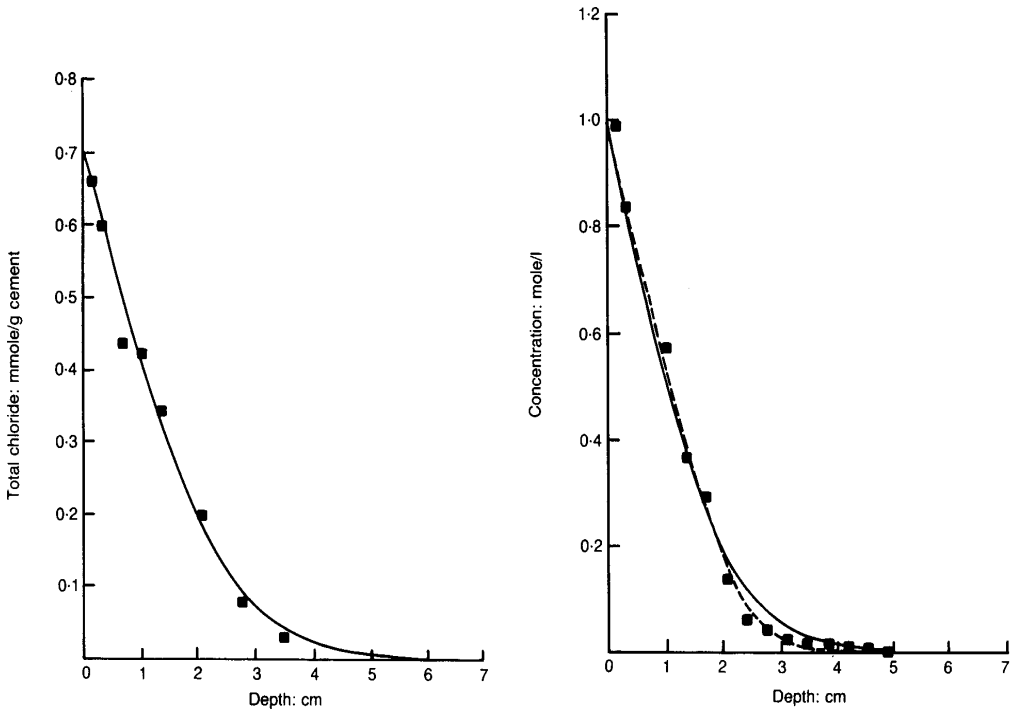

Figure 4.7: *Total chloride ion profile (left) and free chloride concentration in the pore solution (right) [28].*

It should be observed, however, that leaching of hydroxide ions from the pore solution to the storage solution changes the condition of the chloride binding. This makes it difficult to describe the cause of chloride binding, since different physical phenomena interact even under somewhat ideal conditions in laboratory measurements. Some aspects of the action of hydroxide and its effects on chloride binding will be discussed in Section 4.8.

Indeed, the shape of the total chloride concentration profile obtained after a certain time of exposure, seems to follow the solution behavior of Fick's second law including an equilibrium chloride binding isotherm, see Figure 4.7. Therefore, it may be tempting to use a curve to fit the result to Fick's second law to evaluate the diffusion constant, or the effective diffusion constant, and then extrapolate the result to obtain a prediction of the evolution of the total chloride profile in time. But as the binding seems to be a truly transient process, e.g. compare

Figure 4.6 and Table 4.4, such an extrapolation will give unacceptable, erroneous predictions.

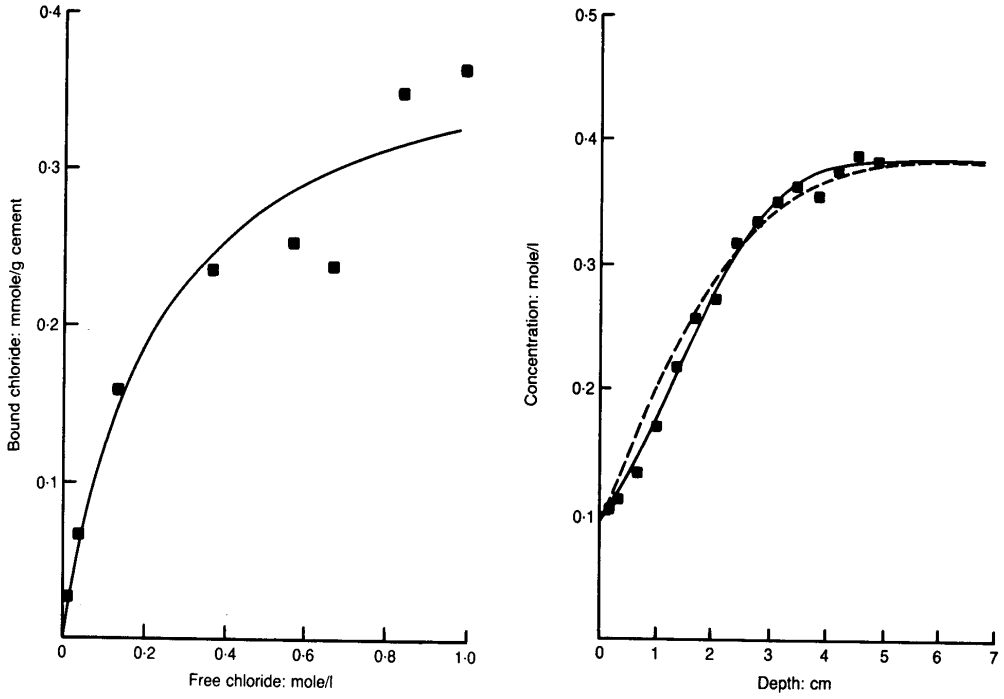

Figure 4.8: *Relation between free and bound chloride (left) at a certain time of exposure. Hydroxide ion concentration profile in pore solution (right) [28].*

Figure 4.7 and 4.8 show results in terms of the profile of total and free chloride concentrations and hydroxide concentration for an OPC paste specimen with $w/c = 0.5$ and exposed to 5 liters of 1 (mol/l) sodium-chloride solution saturated with calcium hydroxide [28]. The hydroxide ion concentration in this mixture was estimated to be 0.09 (mol/l) [28]. The profiles were measured after a period of 100 days. The relation between the bound and the free chloride after 100 days is shown in Figure 4.8 (left). This relation can be used as an adsorption isotherm (non-linear binding equilibrium isotherm). That is, when the reaction rate is described the binding equilibrium isotherm should be obtained as a special case, i.e. the net mass exchange between free and bound chloride is zero in this special situation. This means that the measurements presented in Figure 4.8 (left) must be verified to be a real equilibrium condition. Indeed, this might not be the case,

i.e. the measurement presented in Figure 4.8 (left) might give different results at different exposure times.

By using the two constitutive relations (4.66) and (4.67) together with the mass balance equation (2.56), i.e.

$$\rho\frac{\partial c_c}{\partial t} = -div\,(\rho_c u_{xc}) - \rho\dot{x}_x \cdot grad\, c_c + \hat{c}_c \tag{4.69}$$

the following equation describing the reversible binding and diffusion of the chloride ions will be obtained:

$$\rho\frac{\partial c_c}{\partial t} = D_c(c_l,\theta,n)\frac{\partial^2 c_c}{\partial x^2} - \rho\dot{x}_x\frac{\partial c_c}{\partial x} - f_c(c_c,\rho_{cs},c_{oh},\theta,n,a);\ \text{in}\, V \tag{4.70}$$

The essential boundary condition at the boundary surface ∂V is given at any time t as

$$c_c(0,t) = h_c(0,t);\ \text{on}\ \partial V \qquad (\text{if}\ c_v(0,t) = 0;\ \text{on}\ \partial V) \tag{4.71}$$

where h_c represents a known value of the outer boundary condition in terms of mass concentration of dissolved chloride at different times t. Note that this boundary condition is only used when the same boundary surface is exposed to liquid water (containing dissolved chlorides). This condition is denoted $c_v(0,t) = 0; \text{on}\ \partial V$.

The natural boundary, i.e. a description of the mass diffusion flow through the boundary is, under the same conditions, described as

$$\rho_c u_{xc}(0,t) = g_{xc}(0,t);\ \text{on}\ \partial V \qquad (\text{if}\ c_v(0,t) = 0;\ \text{on}\ \partial V) \tag{4.72}$$

where g_{xc} is a known value of the mass flow through the boundary at the time t. This type of boundary condition is, however, seldom used to solve chloride penetration problems.

When the boundary is exposed to water vapor only, the natural boundary condition for the chloride ions is assumed to obey the following relation:

$$\rho_c u_{xc}(0,t) = 0;\ \text{on}\ \partial V \qquad (\text{if}\ c_l(0,t) = 0;\ \text{on}\ \partial V) \tag{4.73}$$

which means that no chloride ions can pass through the boundary during the exposure to vapor.

The field equation for the mass density distribution of bound chlorides in the domain V is simply given by the mass balance equation (2.49). It is assumed that

the velocity of the bound chloride x'_{xcs} is zero, and the relation (4.68) is used. This gives

$$\frac{\partial \rho_{cs}}{\partial t} = f_c(c_c, \rho_{cs}, c_{oh}, \theta, n, a); \text{ in } V \tag{4.74}$$

It should be noted that no boundary conditions are used in the equation to describe the mass concentration of bound chlorides.

The equations (4.70) and (4.74) are together with the proper boundary conditions supposed to capture the main physical phenomenon observed in the measurements presented in Tables 4.4, 4.5, and 4.6. The important convection of chlorides due to the velocity of the mixture $\dot{x}_x$ is also discussed in [36].

4.7. Carbonation and carbon dioxide flow

Carbonation of cement-based materials, i.e. the chemical reaction of calcium hydroxide and calcium silicate hydrate with carbon dioxide, which results in the formation of calcium carbonate and water, is one of the processes, which take place in the concrete pores and may limit the service life of reinforced concrete structures. There are two main important consequences of carbonation: (*i*) the drop of pH, i.e. the drop in hydroxide concentration in the pore solution, which destroys the passive condition of the reinforcement bars, and (*ii*) the change of the effective permeability due to volume changes and micro-cracking caused by the chemical reactions. The permeability change can be an increase, for instance in concrete which contains blast furnace slag or fly ash, or a decrease as in OPC concrete [37]. Measurements on carbonation of different kinds of concretes can, for example, be found in [38].

The final result of the several steps, through which the calcium carbonate is formed, can simply be described by the following reaction, which is assumed to be irreversible:

$$\mathrm{CO_2(aq)} + \mathrm{Ca^{2+}(aq)} + 2\mathrm{OH^-(aq)} \longrightarrow \mathrm{CaCO_3(s)} + \mathrm{H_2O} \tag{4.75}$$

The dissolution of carbon dioxide in its gaseous phase is simply described as

$$\mathrm{CO_2(g)} \rightleftharpoons \mathrm{CO_2(aq)} \tag{4.76}$$

and the dissolution of calcium hydroxide, as

$$\mathrm{Ca(OH)_2(s)^*} \longrightarrow \mathrm{Ca^{2+}(aq)} + 2\mathrm{OH^-(aq)} \tag{4.77}$$

where the symbol $(s)^*$ is introduced to stress that the $Ca(OH)_2$ is arranged in a crystalline structure. This structure is assumed to be intimately intergrown with the C-S-H, the more or less amorphous calcium silicate hydrate formed during hydration of C_3S and C_2S. The formed C-S-H also has a variable stoichiometry, which makes the kinetics of the dissolution reaction (4.77) difficult to constitute, since the process most likely becomes diffusion-controlled at the microscopic level. The amount $Ca(OH)_2(s)^*$ is about 30 weight-% of the fully hydrated OPC. In blended cements like fly ash cement or slag cement, the amount of $Ca(OH)_2$ is considerably lower. It should be observed that also C-S-H itself becomes carbonated. It is assumed that this reaction takes place in a similar way as the carbonation of $Ca(OH)_2$. That is, C-S-H can be described as C-S-H = $3CaO{\cdot}SiO_2{\cdot}3H_2O$ = $3Ca(OH)_2$ + SiO_2. The carbonation of C-S-H probably occurs at a somewhat slower rate than the carbonation of 'pure' $Ca(OH)_2$. The solubility properties of the C-S-H can be studied in for example [39].

Actually, the dissolved CO_2 will form carbonic acid $H_2CO_3(aq)$ together with water. H_2CO_3 will further be dissolved into $2H^+$ and CO_3^{2-} ions. Hence, the reaction (4.75) can also be expressed as

$$Ca^{2+}(aq) + CO_3^{2-}(aq) \longrightarrow CaCO_3(s) \tag{4.78}$$

The calcium carbonate formed has a very low solubility and will therefore contribute to a clogging of the pore system. However, the volume expansion involved in the reaction (4.75) and (4.78) will cause micro cracks. Due to carbonation it is thus difficult to predict the change of transport properties for gases such as $CO_2(g)$ and $O_2(g)$. The compressive and tensile strength of OPC is markedly increased due to carbonation [37]. This effect does not, however, give any explicit information about the changes of the transport properties.

The formation of calcium carbonate requires a diffusion of carbon dioxide from the atmosphere into the pores of the concrete, and an addition of liquid water to the calcium dioxide to form carbonic acid $H_2CO_3(aq)$, equation (4.75) and (4.78), the carbonation will be largely ruled out if the pore system is filled with water, since that will hinders the diffusion of carbon dioxide in its gaseous phase, or if the pore system is completely dry. It is, however, quite normal that the pores in a concrete surface are only partly filled with water, thus making both diffusion of carbon dioxide in its gaseous phase and formation of carbonic acid possible.

The decrease of pH due to carbonization in the pore solution depends on the relation between the dissolution rate of the solid calcium hydroxide in (4.77) and the consumption rate of OH^- in the carbonization process (4.75). However,

when the solid calcium hydroxide at and near the pore walls is consumed, the dissolution process becomes more and more 'diffusion-controlled'. As a result, the dissolution rate of calcium hydroxide gradually becomes slower. Therefore, a high concentration of hydroxide ions in the pore solution can not be maintained when carbonation takes place.

The depth of carbonation is often measured with a phenolphthalein indicator, measuring the depth to the color change. Such tests only reveal the level, where the pH value falls below nine. Pore expression measurements in terms of hydroxide ion concentration in the pore solution is a better method, since it makes it possible to measure the total pH profile, compare Figure 4.8. The decrease of hydroxide ion content is an indirect method to measure carbonation. SEM by backscatter electron imaging, however, enables the study of the formed $CaCO_3$. Such measurements show that a dense rim, consisting largely of $CaCO_3$ is formed at the surface. Within this zone, CH is largely absent and C-S-H, including that formed in situ from the alite or belite, is in varying degrees decalcified. The carbonated surface layers are about 50-100 μm thick, [37].

In order to capture the most important basic factors governing the carbonation of cement-based materials, the mass diffusion flow behavior of the gas carbon dioxide, and the reaction rate forming calcium carbonate in the liquid water of the pore system must be described.

The mass diffusion flow of the gaseous carbon dioxide in the air-filled space of the pore system is assumed to be described as

$$\rho_{co}^{(g)} u_{xco}^{(g)} = -D_{co}^{(g)}(c_l, n)\frac{\partial c_{co}^{(g)}}{\partial x} - D_{co\theta}^{(g)}\frac{\partial \theta}{\partial x} \tag{4.79}$$

where the diffusion parameter $D_{co}^{(g)}$ is strongly dependent on the liquid water concentration c_l and the porosity n, and where $c_{co}^{(g)}$ denotes the mass concentration of carbon dioxide in its gaseous phase. The second term represents the so-called Soret effect caused by temperature gradients. It should be observed that the porosity n may be significantly changed during the carbonation. Furthermore, it is possible that also the pore size distribution will affect the mass diffusion flow. It can therefore be included as a property describing the diffusion parameter $D_{co}^{(g)}$ in equation (4.79).

The assumed constitutive behavior of the mass diffusion flow of dissolved carbon dioxide in the liquid phase in the pore system is

$$\rho_{co}^{(aq)} u_{xco}^{(aq)} = -D_{co}^{(aq)}(c_l, n)\frac{\partial c_{co}^{(aq)}}{\partial x} \tag{4.80}$$

where $c_{co}^{(aq)}$ denotes the mass concentration of dissolved carbon dioxide.

The reaction (4.76) will, most likely, reach equilibrium instantaneously at a thin layer between the gaseous and the liquid phase, that is, a given relation of the mass concentration of gaseous and dissolved carbon dioxide could be assumed — $c_{co}^{(aq)} = R_{co}c_{co}^{(g)}$. However, the reason for introducing the concentration $c_{co}^{(aq)}$ is to be able to describe the kinetics of the carbonization reaction (4.75). This reaction is assumed to be diffusion-controlled, since the dissolved carbon dioxide must find its way through the pore system (in micro-scale) and form $CaCO_3$(s) at a location, where the reaction is favorable, presumably at surfaces, where calcium hydroxide and calcium silicate hydrate are located. In order to capture the important time scale for this diffusion-controlled reaction, it will be assumed that the constitutive relation for the process of forming reactive, dissolved carbon dioxide must be introduced.

According to the reactions (4.76) and (4.75), and to the conservation of mass during the reaction, i.e. (2.51), it is clear that the net change of the carbon dioxide is zero. This is written as

$$\hat{c}_{co}^{(g)} + \hat{c}_{co}^{(aq)} + \hat{c}_{caco}^{(s)} k_{caco} = 0 \tag{4.81}$$

where the constant k_{caco} simply relates the mole weights of CO_2 and $CaCO_3$ during the reaction (4.75).

The kinetics of the reaction (4.75) will be constituted in a general function as

$$\hat{c}_{caco}^{(s)} = f\left(c_{co}^{(aq)}, c_{oh}, \rho_{caco}^{(s)}, c_l, \theta, a\right) \tag{4.82}$$

where c_{oh} is the mass concentration of hydroxide ions in the pore solution, c_l is the mass concentration of liquid water, $\rho_{caco}^{(s)}$ is the mass density concentration of formed $CaCO_3$(s), θ denotes the temperature and a is the specific surface area of the solid matrix. When the simple equation (4.75) is used to describe the formation of $CaCO_3$, it is natural to assume that the reaction rate forming $CaCO_3$ depends on the mass concentration of dissolved hydroxide ions, CO_2, and also on the amount of $CaCO_3$ already formed. It is noted, however, that the specific surface area a may change significantly during carbonation.

The change of mass due to the dissolution of gaseous carbon dioxide is described as

$$\hat{c}_{co}^{(g)} = f\left(c_{co}^{(g)}, c_{co}^{(aq)}, c_l, \theta, a\right) \tag{4.83}$$

Hence, the expression for $\hat{c}_{co}^{(aq)}$ is given from (4.81), (4.82), and (4.83).

The mass balance equation (2.56) in a one-dimension case for the gaseous carbon dioxide becomes

$$\rho\frac{\partial c_{co}^{(g)}}{\partial t} = -\frac{\partial(\rho_{co}^{(g)}u_{xco}^{(g)})}{\partial x} - \rho\dot{x}_x\cdot\frac{\partial c_{co}^{(g)}}{\partial x} + \hat{c}_{co}^{(g)} \tag{4.84}$$

The constitutive relation (4.79) together with (4.84) yields

$$\rho\frac{\partial c_{co}^{(g)}}{\partial t} = D_{co}^{(g)}(c_l,n)\frac{\partial^2 c_{co}^{(g)}}{\partial x^2} - \rho\dot{x}_x\frac{\partial c_{co}^{(g)}}{\partial x} + D_{co\theta}^{(g)}\frac{\partial^2\theta}{\partial x^2} + \hat{c}_{co}^{(g)};\ \text{in}\, V \tag{4.85}$$

The boundary conditions used in (4.85) depend on the outer climate. If the outer condition is a vapor phase, written as $c_l(0,t) = 0;$ on ∂V, the outer concentration of carbon dioxide $c_{co}^{(g)}$ or the mass diffusion flow $\rho_{co}^{(g)}u_{xco}^{(g)}$ of carbon dioxide through the boundary is described with the known values $h_{co}^{(g)}$ or $g_{xco}^{(g)}$ at the time t respectively, that is

$$c_{co}^{(g)}(0,t) = h_{co}^{(g)}(0,t);\ \text{on}\ \partial V \qquad (\text{if}\ c_l(0,t) = 0;\ \text{on}\ \partial V) \tag{4.86}$$

or

$$\rho_{co}^{(g)}u_{xco}^{(g)}(0,t) = g_{xco}^{(g)}(0,t);\ \text{on}\ \partial V \qquad (\text{if}\ c_l(0,t) = 0;\ \text{on}\ \partial V) \tag{4.87}$$

If the boundary consists of liquid water, denoted by $c_v(0,t) = 0;$ on ∂V, the mass diffusion flow of the gaseous phase carbon dioxide through the boundary is assumed to be negligibly small, i.e.

$$\rho_{co}^{(g)}u_{xco}^{(g)}(0,t) = 0;\ \text{on}\ \partial V \qquad (\text{if}\ c_v(0,t) = 0;\ \text{on}\ \partial V) \tag{4.88}$$

The governing equation in a one-dimensional case for the dissolved carbon dioxide $c_{co}^{(aq)}$ is given by the mass balance equation (2.56), i.e.

$$\rho\frac{\partial c_{co}^{(aq)}}{\partial t} = -\frac{\partial(\rho_{co}^{(aq)}u_{xco}^{(aq)})}{\partial x} - \rho\dot{x}_x\frac{\partial c_{co}^{(aq)}}{\partial x} + \hat{c}_{co}^{(aq)};\ \text{in}\, V \tag{4.89}$$

and the assumptions (4.80) and (4.81) by

$$\rho\frac{\partial c_{co}^{(aq)}}{\partial t} = D_{co}^{(aq)}(c_l,n)\frac{\partial^2 c_{co}^{(aq)}}{\partial x^2} - \rho\dot{x}_x\frac{\partial c_{co}^{(aq)}}{\partial x} - \hat{c}_{co}^{(g)} - \hat{c}_{caco}^{(s)}k_{caco};\ \text{in}\, V \tag{4.90}$$

where the term: $-\hat{c}_{co}^{(g)} - \hat{c}_{caco}^{(s)}k_{caco}$ denotes the net rate of consumption or production of dissolved carbon dioxide.

The boundary conditions in (4.85) are described by the known values $h_{co}^{(aq)}$ and $g_{xco}^{(aq)}$ at the time t respectively, during situations when liquid water is exposed at the surface. Hence

$$c_{co}^{(aq)}(0,t) = h_{co}^{(aq)}(0,t); \text{ on } \partial V \qquad (\text{if } c_v(0,t) = 0; \text{ on } \partial V) \tag{4.91}$$

or

$$\rho_{co}^{(aq)} u_{xco}^{(aq)}(0,t) = g_{xco}^{(aq)}(0,t); \text{ on } \partial V \qquad (\text{if } c_v(0,t) = 0; \text{ on } \partial V) \tag{4.92}$$

In situations with water vapor at the boundary, denoted by $c_l(0,t) = 0$; on ∂V, the mass diffusion flow through the boundary of dissolved carbon dioxide present in the pore solution is assumed to be negligibly small, i.e.

$$\rho_{co}^{(aq)} u_{xco}^{(aq)}(0,t) = 0; \text{ on } \partial V \qquad (\text{if } c_l(0,t) = 0; \text{ on } \partial V) \tag{4.93}$$

The overall penetration of carbon dioxide is slowed down due to the tortuosity of the pore system. Furthermore, the water content affects the penetration. These two phenomena are modelled by making the diffusion parameters $D_{co}^{(g)}$ and $D_{co}^{(aq)}$ dependent on the mass concentration of liquid water c_l and the porosity n, compare the equations (4.79) and (4.80).

The initial mass concentration of solid calcium hydroxide $Ca(OH)_2(s)$ in the concrete, which is assumed to be the only *solid* material participating in the carbonization process is, of course, different for various kinds of binders and concrete mixtures.

In [40] and [41], similar assumptions are introduced for the mass supply term $\hat{c}_{co}$. They describe, however, the rate of calcium carbonate formed by the relation of concentrations of carbon dioxide and calcium hydroxide, and by a function dependent on the relative humidity and the temperature in the material.

To make things easy it will further be assumed that calcium ions, hydroxide ions, and dissolved carbon dioxide form calcium carbonate without significantly affecting the liquid water concentration c_l and the concentration of vapor c_v. That is, the equation for determining c_l ((4.55) and (4.61), (4.64)) and c_v (4.49) is assumed not to be significantly affected by the production of liquid water due to the carbonation, compare (4.75).

The solid $CaCO_3(s)$ formed in the carbonation process is assumed to have zero velocity, i.e: $\rho_{caco} x'_{xcaco} = 0$. The mass balance equation (2.49), and the constitutive relation (4.82), which describe the production of $CaCO_3(s)$, therefore give

$$\frac{\partial \rho_{caco}^{(s)}}{\partial t} = \hat{c}_{caco}^{(s)}; \text{ in } V \tag{4.94}$$

The mass density of calcium hydroxide, which belongs to the solid matrix, i.e. $Ca(OH)_2(s)$, is decreased at the same rate as carbon dioxide is consumed, compare the reaction (4.75). The overall changes in the mass concentration of solid calcium hydroxide is not, however, determined solely by the carbonization. It is assumed that a irreversible dissolute reaction exists between the solid calcium hydroxide and the hydroxide ions in the pore solution. This reaction strives to reach equilibrium whenever the concentrations of $Ca(OH)_2(s)$ and/or the concentration of OH^- in the pore solution are changed, independently of the concentration of $CO_2(aq)$ in the pore system.

The reaction kinetics and the equilibrium condition for the dissolute reaction (4.77) will be discussed together with the behavior of the hydroxide ions in the pore solution; see Section 4.8.

4.8. Hydroxide mobility and changes in the mass concentration of solid calcium hydroxide

It is a well-known fact that hydroxide ions, which appear naturally in a pore solution (at an initial concentration of approximately 0.4 (mol OH^-)/l) in cement-based materials, will be leached out to some extent if a sample is stored in pure water. This phenomenon is presumably caused by dissolution and global diffusion in the pore system of the cement based material.

It is reasonable to assume that the initial equilibrium condition between solid calcium hydroxide and dissolved hydroxide ions in the pore solution will be disturbed when a leach of hydroxide ions into a surrounding storage solution occurs. However, the buffer concentration of solid calcium hydroxide is in general high for most cement-based materials. Besides, also C-S-H can be decomposed and thus add to the buffering capacity. The dissolution process will, however, probably be diffusion-controlled once the solid calcium hydroxide located close to the pore walls has been consumed. Measurements performed show that the production rate of hydroxide ions due to dissolution can not compensate for the loss of the same ions due to 'global' diffusion. This means that the global response is a decrease of hydroxide ions in the pore solution.

When the same leaching process is considered in the presence of chloride ions it becomes clear that the equilibrium condition between solid calcium hydroxide and dissolved hydroxide ions may be affected, since the hydroxide ions and chloride ions probably compete for free adsorption sites on the pore walls. Experiments show that a low concentration of hydroxide ions, i.e. a low pH, increases the

capability of chloride binding [42].

Experiments performed in [28] show that the concentration of hydroxide ions in the pore solution decreases when a sample is stored in a NaCl solution saturated with $Ca(OH)_2$, in which the hydroxide ion concentration is estimated to be 0.09 (mole OH^-/l). This is believed to be a consequence of two different phenomena: (i) when chloride ions penetrate the pore system, the initial equilibrium condition of the pore solution and the pore walls may change. This contributes to a momentary increase of dissolved hydroxide ions and, (ii) a diffusion of dissolved hydroxide ions towards the outer storage solution. Diffusion of hydroxide ions towards the outer storage solution takes place due to the fact that the concentration of hydroxide ions in the outer solution is (approximately 0.09 (mole OH^-/l)) considerably lower than the concentration in the pore solution (approximately 0.4 (mole OH^-/l)). In fact, it is difficult to distinguish the diffusion process, i.e. the leach, from the effect of changes in the equilibrium condition between solid calcium hydroxide and hydroxide ions in the pore solution with or without the presence of chloride ions.

However, the mass flow and the equilibrium conditions for the dissolved hydroxide ions with respect to other constituents is crucial when durability problems of cement based materials are considered. The hydroxide ions are involved in the corrosion process, the carbonation process and in the chloride penetration process. In the last process, hydroxides affect the binding capacity of chloride.

As for all other considered ions moving in the liquid pore water, a gradient-dependent mass flow will be assumed as

$$\rho_{oh} u_{xoh} = -D_{oh}(c_l, n) \frac{\partial c_{oh}}{\partial x} \tag{4.95}$$

where the diffusion parameter D_{oh} strongly depends on the liquid water mass concentration c_l and the porosity n.

The constituents of interest, which participate in the reactions (see (4.75) and (4.77)) contribute to a change in the mass concentration of dissolved hydroxide c_{oh}, are carbon dioxide and the solid calcium hydroxide. The mass conservation of the chemical reactions in terms of dissolved hydroxide must fulfill (2.51), that is

$$\hat{c}_{caco} k_{oh1} + \hat{c}_{caohs} k_{oh2} + \hat{c}_{oh} = 0 \tag{4.96}$$

where k_{oh1} and k_{oh2} are constants relating the mole weights of $CaCO_3$(s) and OH^-(aq) in the reaction (4.75), and the mole weights of $Ca(OH)_2$(s) and OH^-(aq) in (4.77).

The rate of reaction (4.77) and its equilibrium condition is expressed as a function of the relation between the available mass concentrations of hydroxide ions in the pore solution c_{oh} and the solid calcium hydroxide ρ_{caohs}, and between the liquid water mass concentration c_l, the mass density concentration of bound chlorides ρ_{cs}, the temperature θ, and the specific surface area a, i.e.

$$\hat{c}_{caohs} = f(c_{oh}, \rho_{caohs}, c_l, \rho_{cs}, \theta, a) \tag{4.97}$$

By using the mass balance equation (2.56) in a one-dimensional case, i.e.

$$\rho \frac{\partial c_{oh}}{\partial t} = -\frac{\partial(\rho_{oh} u_{xoh})}{\partial x} - \rho \dot{x}_x \frac{\partial c_{oh}}{\partial x} + \hat{c}_{oh} \tag{4.98}$$

together with the constitutive relations (4.95), (4.97), and (4.82),

$$\rho \frac{\partial c_{oh}}{\partial t} = D_{oh}(c_l, n) \frac{\partial^2 c_{oh}}{\partial x^2} - \rho \dot{x} \frac{\partial c_{oh}}{\partial x} - \hat{c}_{caco} k_{oh1} - \hat{c}_{caohs} k_{oh2} - \hat{m}_{oh}; \text{ in } V \tag{4.99}$$

is obtained, where the term $\hat{m}_{oh}$ has been included to represent an external source or sink. The source is due to the production of OH^- at the cathode areas during corrosion and, the sink is due to the consumption of OH^- at anode areas. Compare the corrosion reactions (6.2) and (6.3) below. Before the corrosion process is initiated, the term $\hat{m}_{oh}$ is zero both at the anode and cathode.

The boundary conditions used in (4.99) depend on the outer conditions, i.e. the boundary conditions, in terms of liquid water and vapor. If the outer condition is a liquid water phase, written as $c_v(0,t) = 0$; on ∂V, the outer concentration of carbon dioxide c_{oh} or the mass diffusion flow $\rho_{oh} u_{xoh}$ through the boundary is described by the known values h_{co} or g_{xco} at the time t, respectively. That is

$$c_{oh}(0,t) = h_{oh}(0,t); \text{ on } \partial V \qquad (\text{if } c_v(0,t) = 0; \text{ on } \partial V) \tag{4.100}$$

or

$$\rho_{oh} u_{xoh}(0,t) = g_{xoh}(0,t); \text{ on } \partial V \qquad (\text{if } c_v(0,t) = 0; \text{ on } \partial V) \tag{4.101}$$

When the boundary consists of vapor, denoted by $c_l(0,t) = 0$; on ∂V, the mass diffusion flow of the hydroxide ions through the boundary is assumed to be negligible small, i.e.

$$\rho_{oh} u_{xoh}(0,t) = 0; \text{ on } \partial V \qquad (\text{if } c_l(0,t) = 0; \text{ on } \partial V) \tag{4.102}$$

If the velocity of the solid calcium hydroxide is assumed to be zero, i.e. $x'_{xcs} = 0$, the mass balance equation (2.49) and (4.97) give

$$\frac{\partial \rho_{caohs}}{\partial t} = \hat{c}_{caohs};\ in\, V \tag{4.103}$$

Another approach for modelling the leaching of calcium hydroxide from cement pastes can be studied in for example [43].

4.9. Oxygen mobility

The mobility of oxygen in porous materials is, of course, of great interest when dealing with corrosion of embedded reinforcement bars in concrete. The water content is, again, an important factor, since it reduces the motion of oxygen in its gaseous phase within the air-filled space in the pore system.

Oxygen permeability has been reported in terms of diffusion coefficients based on Fick's law for concretes with different water to cement ratios and at different degrees of saturation [44], [25].

In [25], it was found that the 'effective' diffusion coefficient for Slite Portland cement concrete, $w/c = 0.42$, at the temperature 20 (^{o}C) (specimen age 6-12 months) was $\tilde{D}_{\text{eff}} \approx 8 \cdot 10^{-8}$ (m^2/s), $\tilde{D}_{\text{eff}} \approx 1.7 \cdot 10^{-8}$ (m^2/s) and $\tilde{D}_{\text{eff}} \approx 0.3 \cdot 10^{-8}$ (m^2/s) for specimens equilibrated at 0, 50 and 80% relative humidity respectively. For completely saturated samples, the value obtained was $\tilde{D}_{\text{eff}} \approx 0.03 \cdot 10^{-8}$ (m^2/s). The fact that the diffusion coefficient for oxygen is decreased at increased liquid water content may be a consequence of water clogging the pores. Oxygen has a low solubility in water and its mobility is limited by the comparatively high density of the water. The conditions in air are different. The concentration can be high and the diffusion coefficient can be $10^4 - 10^5$ times greater than in liquid water [25]. The diffusion coefficient for oxygen in air at normal atmospheric pressure and at the temperature 0 (^{o}C) is $1780 \cdot 10^{-8}$ (m^2/s), see Table 5.8.

The 'effective' diffusion coefficients based on Fick's law in [25] were also found to depend on the water-to-cement ratio of the concrete mix, and on the composition of the binder.

As for the other gaseous constituents discussed, i.e. carbon dioxide and water-vapor, the labyrinth effect (caused by the pore system and the presence of liquid water in the pore system) for the diffusion becomes very important also. Hence, the description of the action of the liquid water phase has a major part in the mass transfer problem treated in connection with durability considerations.

The mass density flow of oxygen in its gaseous phase in the air-filled space of the pore system is constituted as

$$\rho_o^{(g)} u_{xo}^{(g)} = -D_o(c_l, n) \frac{\partial c_o^{(g)}}{\partial x} \tag{4.104}$$

where the diffusion parameter D_o is assumed to be strongly dependent on the liquid water mass concentration c_l and the porosity n.

It is assumed that oxygen does not participate in any chemical reaction but the simple dissolution reaction

$$\mathrm{O_2(g)} \rightleftharpoons \mathrm{O_2(aq)} \tag{4.105}$$

According to (2.51), the mass conservation during the chemical dissolution reaction (4.105) must fulfil

$$\hat{c}_o^{(g)} + \hat{c}_o^{(aq)} = 0 \tag{4.106}$$

The assumption of instantaneously reached equilibrium is introduced for the reaction (4.105). Therefore, the mass concentration of oxygen $c_o^{(g)}$ in its gaseous and in its dissolute state $c_o^{(aq)}$ can be related to each other explicitly as

$$c_o^{(aq)} = R_o c_o^{(g)} \tag{4.107}$$

where R_o is a constant describing the relation between the mass concentration of dissolved oxygen and oxygen in its gaseous phase.

According to (2.56), the mass balance for oxygen is

$$\rho \frac{\partial c_o^{(g)}}{\partial t} = -\frac{\partial (\rho_o^{(g)} u_{xo}^{(g)})}{\partial x} - \rho \dot{x}_x \frac{\partial c_o^{(g)}}{\partial x} + \hat{c}_o^{(g)} \tag{4.108}$$

By combining the constitutive relation (4.104) and the mass balance (4.108)

$$\rho \frac{\partial c_o^{(g)}}{\partial t} = D_o(c_l, n) \frac{\partial^2 c_o^{(g)}}{\partial x^2} - \rho \dot{x}_x \frac{\partial c_o^{(g)}}{\partial x} + \hat{c}_o^{(g)}; \text{ in } V \tag{4.109}$$

is obtained. If the somewhat crude assumption is introduced, that the velocity in relation to the velocity of the mixture is zero, i.e. $u_{xo}^{(aq)} \approx 0$, the corresponding mass balance equation for the dissolved oxygen is

$$\rho \frac{\partial c_o^{(aq)}}{\partial t} = -\rho \dot{x}_x \frac{\partial c_o^{(aq)}}{\partial x} + \hat{c}_o^{(aq)} - \hat{m}_o^{(aq)} \tag{4.110}$$

where the equation (2.56) for the one-dimensional case is used. It should be noted that the transport of dissolved oxygen only is due to convection, which is described by the first term on the right-hand side of (4.110). The term $\hat{m}_o^{(aq)}$ represents an external point sink due to the consumption of oxygen at the cathode, compare equation (6.2), and at the anode, compare equation (6.5). The term $\hat{m}_o^{(aq)}$ is valid only in the propagation stage of corrosion. Otherwise, the sink term $\hat{m}_o^{(aq)}$ is equal to zero. The consumption rate of oxygen is assumed to be directly linked to the production of Fe^{2+}. This production is constituted in (6.27).

If the four equations (4.106), (4.107), (4.109), and (4.110) are combined, the equation describing the behavior of the oxygen in its gaseous phase in the air-filled pore space can be written as

$$\rho \frac{\partial c_o^{(g)}}{\partial t} = \frac{D_o(c_l, n)}{(1 + R_o)} \frac{\partial^2 c_o^{(g)}}{\partial x^2} - \rho \dot{x}_x \frac{\partial c_o^{(g)}}{\partial x} - \frac{\hat{m}_o^{(aq)}}{(1 + R_o)}; \text{ in } V \tag{4.111}$$

where is should be noted that the diffusion parameter for oxygen in its gaseous phase, $D_o(c_l, n)$, is scaled with the factor $1/(1 + R_o)$ due to the dissolution of oxygen. By solving the mass concentration field $c_o^{(g)}(x, t)$ with (4.111), together with the proper boundary conditions, the mass concentration field $c_o^{(aq)}(x, t)$ can be calculated simply by using equation (4.107). This is due to the assumption of an instantaneously reached equilibrium for the reaction (4.105), leading to the relation (4.107). Furthermore, the proposed equations describing the transport of oxygen in concrete assume that dissolved oxygen is convected with the velocity of the mixture $\dot{x}_x$. This velocity is mainly determined from the equation that describes the capillary suction of liquid water.

As for the other constituents considered, the boundary conditions to be used in (4.111) is dependent on outer conditions in terms of liquid water and water-vapor.

If the outer condition is a water-vapor phase written as $c_l(0, t) = 0$; on ∂V, the outer concentration of the gas oxygen $c_o^{(g)}$ or the mass diffusion flow $\rho_o^{(g)} u_{xo}^{(g)}$ through the boundary can be described by the known values $h_o^{(g)}$ and $g_{xo}^{(g)}$ respectively, i.e.

$$c_o^{(g)}(0, t) = h_o^{(g)}(0, t); \text{ on } \partial V \qquad (\text{if } c_l(0, t) = 0; \text{ on } \partial V) \tag{4.112}$$

or

$$\rho_o^{(g)} u_{xo}^{(g)}(0, t) = g_{xo}^{(g)}(0, t); \text{ on } \partial V \qquad (\text{if } c_l(0, t) = 0; \text{ on } \partial V) \tag{4.113}$$

In other words, $h_o^{(g)}$ describes the known mass concentration of oxygen in the surrounding (air) environment at different times t, and $g_{xo}^{(g)}$ describes a known

mass concentration flow through the boundary (This condition is, however, seldom used in the type of problem considered).

When the boundary consists of liquid water, denoted by $c_v(0,t) = 0$; on ∂V, the mass diffusion flow of the gaseous oxygen through the boundary is assumed to be negligibly small, i.e.

$$\rho_o^{(g)} u_{xo}^{(g)}(0,t) = 0; \text{ on } \partial V \qquad (\text{if } c_v(0,t) = 0; \text{ on } \partial V) \tag{4.114}$$

In fact, problems related to the boundary conditions for the mass concentration of dissolved oxygen are observed when the simplified equation (4.107) is used. That is, no explicit information can be introduced for the boundary condition in terms of a known value of an outer mass concentration of dissolved oxygen (in situations when liquid water containing dissolved oxygen is present at the boundary). Instead, the relation (4.107) has to be used in order to convert the known value of the mass concentration of dissolved oxygen at the boundary to a mass concentration in terms of gaseous oxygen. This value should be used to solve equation (4.111). To avoid this drawback two separate but coupled differential equations must be introduced, one for the gaseous phase and another for the dissolved phase. This method was used when the behavior of carbon dioxide was described.

The diffusion of oxygen is supposed to be of importance only when reinforcement corrosion in its propagation stage is considered. This will be discussed in Section 6. It should be observed, however, that rust may be produced at the steel bar surfaces in concrete without any presence of oxygen.

5. Summary of the equation system for the diffusing matter in the pore system

Here a summary is made of the proposed equations to describe the mass exchange among the constituent, i.e. the reaction kinetics, and the mass transport of different constituents in porous cement-based materials. The constituents considered are all of interest when studying deterioration phenomena such as chloride-induced corrosion, carbonation, and also temperature- and moisture-induced strains. In fact, the model discussed in Sections 4.2 to 4.9 includes a total of thirty-seven unknown quantities. The following thirty-two unknown mass density fields, velocity fields and mass supply terms are considered:

$$\begin{array}{lll} \rho_c\,(x,t) & x'_{xc}\,(x,t) & \hat{c}_c\,(x,t) \\ \rho_{cs}\,(x,t) & x'_{xcs}\,(x,t)=0 & \hat{c}_{cs}\,(x,t) \\ \rho_v\,(x,t) & x'_{xv}\,(x,t) & \hat{c}_v\,(x,t) \\ \rho_{vic.}\,(x,t) & x'_{xvic.}\,(x,t) & \hat{c}_{vic.}\,(x,t) \\ \rho_{bulk}\,(x,t) & x'_{xbulk}\,(x,t) & \hat{c}_{bulk}\,(x,t) \\ \rho_{co}^{(g)}\,(x,t) & x'^{(g)}_{xco}\,(x,t) & \hat{c}_{co}^{(g)}\,(x,t) \\ \rho_{co}^{(aq)}\,(x,t) \quad ; & x'^{(aq)}_{xco}\,(x,t) \quad ; & \hat{c}_{co}^{(aq)}\,(x,t) \\ \rho_{caco}\,(x,t) & x'_{xcaco}\,(x,t)=0 & \hat{c}_{caco}\,(x,t) \\ \rho_{oh}\,(x,t) & x'_{xoh}\,(x,t) & \hat{c}_{oh}\,(x,t) \\ \rho_{caohs}\,(x,t) & x'_{xcaohs}\,(x,t)=0 & \hat{c}_{caohs}\,(x,t) \\ \rho_o^{(g)}\,(x,t) & x'^{(g)}_{xo}\,(x,t) & \hat{c}_o^{(g)}\,(x,t) \\ \rho_o^{(aq)}\,(x,t) & x'^{(aq)}_{xo}\,(x,t)=0 & \hat{c}_o^{(aq)}\,(x,t) \end{array} \tag{5.1}$$

In addition the two unknown quantities

$$T_{xbulk}\,(x,t)\,; \qquad \hat{p}_{xbulk}\,(x,t) \tag{5.2}$$

and the three thermal properties

$$\theta\,(x,t)\,; \qquad \varepsilon\,(x,t)\,; \qquad q_x\,(x,t) \tag{5.3}$$

are considered. Obviously, thirty-seven equations are needed to make the system closed. In essence twelve mass balance equations, one momentum balance equation, and one energy balance equation are introduced. The remaining twenty-three equations are constitutive relations.

From the mixture theory, the following physical quantities

$$c_a\,(x,t)\,; \quad u_{xa}\,(x,t)\,; \quad \dot{x}_x\,(x,t)\,; \quad \rho\,(x,t) \tag{5.4}$$

may be considered as functions of the unknown properties in (5.1), (5.2), and (5.3).

The mass density for the mixture is given by (2.12) as

$$\rho = \rho\left(x,t\right) = \sum_{a=1}^{R} \rho_a\left(x,t\right) \tag{5.5}$$

The mean velocity or the velocity of the mixture in a one-dimensional case is, according to (2.15), given by

$$\dot{x}_x = \dot{x}_x\left(x,t\right) = \frac{1}{\rho}\sum_{a=1}^{R} \rho_a x'_{xa} \tag{5.6}$$

The concentrations for the individual constituents, as defined in (2.13), are

$$c_a = c_a\left(x,t\right) = \rho_a/\rho$$

and the diffusion velocities for the individual constituents, as defined in (2.16), are

$$u_{xa} = u_{xa}\left(x,t\right) = x'_{xa}\left(x,t\right) - \dot{x}_x\left(x,t\right) \tag{5.7}$$

Hence, the constitutive relations can be introduced using both the quantities in (5.1), (5.2), and (5.3), and the quantities in (5.4), since they are direct functions of each other.

The eleven introduced assumptions for the mass diffusion flows are listed in Table 5.1. Three of the introduced constituents are restricted to having zero velocities. The diffusion velocity for the dissolved oxygen, i.e. the velocity in relation to the velocity of the mixture, is assumed to be zero.

The introduced relations dealing with mass exchanges (or chemical reactions) among the constituents are summarized in Table 5.2. It should be noted that the reaction kinetics involved in the problem must be described as functions of for example the mass concentration of the individual constituents and the temperature. These relations are not explicitly given. Of course, material constants and parameters will be introduced when the rate of the reactions is constituted.

The equations involved to reach the one-dimensional standard transient heat conduction equation are shown in Table 5.3. In Section 7, a more detailed study of the energy equation is presented. This description is used to model latent heat effects involved in phase change problems, e.g. in the transformation of water to ice or vice versa.

Table 5.1: Seven constitutive equations for mass diffusion flows.

Mass flow	Equation	Remarks
$\rho_c u_{xc}$	(4.66)	
$\rho_{cs} u_{xcs}$	-	*Velocity assumed to be zero, i.e.* $x'_{xcs} = 0$
$\rho_v u_{xv}$	(4.27)	
$\rho_{vic.} u_{xvic.}$	*comp.* (4.28)	
$\rho_{co}^{(g)} u_{xco}^{(g)}$	(4.79)	
$\rho_{co}^{(aq)} u_{xco}^{(aq)}$	(4.80)	
$\rho_{caco} u_{xcaco}$	-	*Velocity assumed to be zero, i.e.* $x'_{xcaco} = 0$
$\rho_{oh} u_{xoh}$	(4.95)	
$\rho_{caohs} u_{xcaohs}$	-	*Velocity assumed to be zero, i.e.* $x'_{xcaohs} = 0$
$\rho_o^{(g)} u_{xo}^{(g)}$	(4.104)	
$\rho_o^{(aq)} u_{xo}^{(aq)}$	-	*Diffusion velocity assumed:* $u_{xo}^{(aq)} = 0$

Table 5.2: Twelve constitutive equations for chemical reactions.

Chem. react.	Equation	Remarks
$\hat{c}_c$	(4.67)	*Adsorption-desorption*
$\hat{c}_{cs}$	(4.68) *i.e.,* $\hat{c}_{cs} = -\hat{c}_c$	*Adsorption-desorption*
$\hat{c}_v$	(4.29)	*Adsorption-desorption*
$\hat{c}_{vic.}$	(4.46) *i.e.,* $\hat{c}_{vic.} = -(1 - k_{dist})\,\hat{c}_v$	$\hat{c}_v$ *distributed by* k_{dist}
$\hat{c}_{bulk}$	(4.45) *i.e.,* $\hat{c}_{bulk} = -k_{dist}\hat{c}_v$	$\hat{c}_v$ *distributed by* k_{dist}
$\hat{c}_{co}^{(g)}$	(4.83)	*Diff. contr. chem. react.*
$\hat{c}_{co}^{(aq)}$	(4.81) *i.e.,* $\hat{c}_{co}^{(aq)} = -\hat{c}_{co}^{(g)} - \hat{c}_{caco}k_{co}$	*Diff. contr. chem. react.*
$\hat{c}_{caco}^{(s)}$	(4.82)	*Diff. contr. chem. react.*
$\hat{c}_{oh}$	(4.96) *i.e.,* $\hat{c}_{oh} = -\hat{c}_{caohs}k_{oh2} - \hat{c}_{caco}k_{oh1}$	*Diff. contr. chem. react.*
$\hat{c}_{caohs}$	(4.97)	*Diff. contr. chem. react.*
$\hat{c}_o^{(g)}$	*Not explicitly described due to Eq.* (4.107)	*Inst. reached equilibrium*
$\hat{c}_o^{(aq)}$	(4.106) i.e., $\hat{c}_o^{(aq)} = -\hat{c}_o^{(g)}$	*Inst. reached equilibrium*

Table 5.3: Three equations used to compute for the temperature.

Quan.	Equation	Remarks
ε	(3.20)	*Energy balance;* $\rho\frac{\partial \varepsilon}{\partial t} = \frac{\partial q_x}{\partial x} - \dot{x}_x \cdot \frac{\partial \varepsilon}{\partial x}$
θ	*comp.* (3.21)	*Const. rel.;* $\theta = C(c_l, n, a)\varepsilon$
q_x	*comp.* (3.22)	*Const. rel.;* $q_x = -\lambda(c_l, n, a)\frac{\partial \theta}{\partial x}$

Table 5.4: Three equations involved in the capillary suction equation.

Quan.	Equation	Remarks
T_{xbulk}	(4.57)	*Const. relation;* $T_{xbulk} = \mu_{bulk}(\theta)\frac{4}{3}\frac{\partial x'_{xbulk}}{\partial x} - \pi_{bulk}(\theta, \rho_l)$
$\hat{p}_{xbulk}$	(4.59)	*Const. relation;* $\hat{p}_{xbulk} = \gamma_{bulk} u_{xbulk}$
x'_{xbulk}	(4.60)	*Balance of momentum;* $\rho_{bulk}\frac{\partial x'_{xbulk}}{\partial t} = \frac{\partial T_{xbulk}}{\partial x} + \hat{p}_{xbulk}$

Table 5.5: Twelve mass balance equations.

Quan.	Equation	Remarks
c_c	(4.69)	*Free chlorides in pore water*
ρ_{cs}	(4.74)	*Described with the mass density, bound chlorides*
c_v	(4.24)	*Mass concentration of vapor*
$c_{vic.}$	*comp.* (4.26)	*Adsorbed and capillary-condensed water*
ρ_{bulk}	(4.64)	*Described with the mass density, capillary water*
$c_{co}^{(g)}$	(4.84)	*Carbone dioxide, gaseous phase*
$c_{co}^{(aq)}$	(4.89)	*Carbone dioxide, aqueous phase*
ρ_{caco}	(4.94)	*Solid,* $CaCO_3$(s), *described with the mass density*
c_{oh}	(4.98)	*Dissolved hydroxide ions*
ρ_{caohs}	(4.103)	*Described with the mass density, solid calcium hyd.*
$c_o^{(g)}$	(4.108)	*Instantaneously reached equilibrium, gaseous oxygen*
$c_o^{(aq)}$	(4.110)	*Elim. of* $c_o^{(aq)}$ *due to the assump.* $c_o^{(aq)} = R_o c_o^{(g)}$

The equations, which give the one-dimensional velocity field of 'bulk' water supplied by capillary action are listed in Table 5.4. Constitutive relations are introduced both for the stress tensor T_{xbulk} and the momentum supply $\hat{p}_{xbulk}$.

In Table 5.5, the equations related to mass balance for the constituents are listed. It should be observed that an instantaneous reaction isotherm is involved in the description of the mass exchange between the dissolved and the gaseous phase of oxygen. This results in the elimination of one mass balance equation, compare Section 4.9. The mass diffusion flow of both the dissolved and the gaseous carbon dioxides is, however, described, with constitutive relations.

The governing equations for the twelve introduced constituents are shown in Table 5.6. By solving these coupled equations, the mean velocity of the mixture can be estimated through the computing of the individual mass diffusion velocities. That is, a so-called staggered solution procedure can be adopted in order to compute the coupling in terms of the mean velocity of the mixture and the

Table 5.6: Twelve governed equations for the constituents.

Quantity	Equation
c_c	(4.70)
ρ_{cs}	(4.74)
c_v	(4.49)
$c_{vic.}$	(4.55)
ρ_{bulk}	(4.64) and (4.61)
$c_{co}^{(g)}$	(4.85)
$c_{co}^{(aq)}$	(4.90)
ρ_{caco}	(4.94)
c_{oh}	(4.99)
ρ_{caohs}	(4.103)
$c_o^{(g)}$	(4.111)
$c_o^{(aq)}$	(4.107)

dependencies of material parameters on introduced properties such as the water mass concentration and temperature.

To solve the equations listed in Table 5.6, the boundary conditions for the individual constituents must be introduced. These boundary conditions are assumed to depend on the moisture state at the boundary surfaces. Compare the discussion in Sections 4.2 to 4.9.

The introduced material parameters are shown in Table 5.9. It is supposed that the constants describing the reaction kinetics are the most difficult parameters to identify among all the material parameters introduced.

The various diffusion parameters D introduced are assumed to be given from the corresponding diffusion constants in pure water (or in air for the gases) at a given temperature. Six diffusion parameters of this kind are introduced into the model. The values of the diffusion constants (in a pure medium, i.e. liquid water or air) can then be scaled by a tortuosity factor determined by the porosity, the specific surface area, and the concentration of liquid water in order to estimate the effective mass flow behavior in the material of interest. The different diffusion constants determined from experiments in for example pure water do not deviate very much from each other. The tortuosity factor for different ions diffusing in a pore system with liquid water present can also be scaled with the same factors, since all dissolved diffusing constituents are exposed to the same geometrical labyrinth effects. The same approach can be used for the diffusion of gases in

Table 5.7: Diffusion coefficients in water at 298 K, [29].

Ion	Diffusion coefficient, D (m^2/s)
Cl^-	$2.03 \cdot 10^{-9}$
OH^-	$5.30 \cdot 10^{-9}$
Na^+	$1.33 \cdot 10^{-9}$
K^+	$1.96 \cdot 10^{-9}$

Table 5.8: Diffusion of gases in air at normal atmospheric pressure [24].

Gas or vapor	Temp. (^{o}C)	Diffusion coefficient, D (m^2/s)	Observer
CO_2	0.0	$13.9 \cdot 10^{-6}$	*Mean of various*
O_2	0.0	$17.8 \cdot 10^{-6}$	*Obermayer*
Water, vapor	8.0	$23.9 \cdot 10^{-6}$	*Guglielmo*

air-filled spaces in the pore system. It should be observed that this approach is only significant when describing the reaction kinetics with separate constitutive relations, since the diffusing matter considered is not inert with respect to the pore walls.

Some values of diffusion coefficients for matter dissolved in water are given in Table 5.7, e.g. compare [29]. Values for diffusion coefficients of gases in air of normal pressure are given in Table 5.8, e.g. compare [24].

Indeed, global response determined by experiments on real porous materials shows that the action of different diffusing constituents is very different. This may, however, be a consequence of attraction or repulsion effects between the dry or wet solid pore walls and the diffusing substance. This means that the problem is not solely a diffusion problem but rather a problem involving chemical effects and surface effects.

The attraction and repulsion forces between different diffusing components and the inner surfaces of a porous cement-based material are supposed to be very different in nature for different diffusing components. Therefore, the constitutive relations for the mass exchanges of the format illustrated in Table 5.2 describe the main underlying physical reason for the different global responses for different diffusing constituents.

The reaction kinetics between solid surfaces and diffusing matter may, however, not be constituted with standard arguments. The reactions on a micro-scale (i.e. a adsorption-desorption phenomenon or purely chemical reactions) become

Table 5.9: Material parameters used in the twelve governed equations. Note that no explicit description has been intoduced for the reaction kinetics.

Param.	Used in equation	Note
$D_c(c_l, \theta, n)$	(4.70)	*Diff. param.*
$\hat{c}_c = f_c(c_c, \rho_{cs}, c_{oh}, \theta, n, a)$	(4.70), (4.74)	*Reac. kinetics*
$D_v(c_l, \theta, n)$	(4.49)	*Diff. param.*
$D_{v\theta}^{(g)}$	(4.49)	*Soret eff.*
$\tilde{D}_{vic.}(c_l, n)$	(4.55)	*(Diff. param.)*
$k_{dist.}$	(4.55), (4.64)	*(Reac. kinetics)*
$\hat{c}_v = f(c_v, c_l, \theta, n, a)$	(4.49), (4.55), (4.64)	*Reac. kinetics*
$\beta_{bulk}(c_{vic})$	(4.61)	*Damping*
$\mu_{bulk}(\theta)$	(4.61)	*Viscosity*
$D_{co}^{(g)}(c_l, n)$	(4.85)	*Diff. param.*
$D_{co\theta}^{(g)}$	(4.85)	*Soret eff.*
$D_{co}^{(aq)}(c_l, n)$	(4.90)	*Diff. param.*
$\hat{c}_{caohs} = f(c_{oh}, \rho_{caohs}, c_l, c_{cs}, \theta, a)$	(4.99), (4.103)	*Reac. kinetics*
$D_{oh}(c_l, n)$	(4.99)	*Diff. param.*
$\hat{c}_{caco}^{(s)} = f\left(c_{co}^{(aq)}, c_{oh}, c_l, \theta, a\right)$	(4.90), (4.94), (4.99)	*Reac. kinetics*
$\hat{c}_{co}^{(g)} = f\left(c_{co}^{(g)}, c_{co}^{(aq)}, c_l, \theta, a\right)$	(4.85), (4.90)	*Reac. kinetics*
$D_o(c_l, n)$	(4.111)	*Diff. param.*
R_o	(4.111)	*(Reac. kinetics)*
$C(c_l, n, a)$	(3.21)	*Heat cap.*
$\lambda(c_l, n, a)$	(3.22)	*Conductivity*

diffusion-controlled due to consumption (or production) of accessible components located near the reactants in the pore solution. The background for introducing reaction kinetics to the water-vapor phase is the micro-diffusion into smaller pores, which are not easily penetrated by the vapor. This phenomenon may be the explanation to the measured response for moisture uptake, e.g. compare Figure 4.3.

By using the proposed strategy of separating the constitutive relations for the mass exchange effect (reaction kinetics) between diffusing matter and the solid, and the constitutive relations for the mass diffusion velocities (which are based on a scaling of the diffusion constants for a component moving in a pure medium), the problem more or less becomes a question of finding proper expressions to describe the reaction kinetics (or surface attraction or repulsion kinetics).

In order to show how the different introduced constituents and their governing equations can be used as a base for the analysis of the reinforcement corrosion problem, a separate discussion is presented in Section 6.

In Section 7, the problem of introducing yet another constituent is discussed. The constituent of interest is the ice formed in the pore system at low temperatures. It will be shown that the complexity of the system considered increases dramatically when one tries to introduce stringent physically based assumptions for the formation and melting of ice within the porous material. Nevertheless, damage caused by the freezing and thawing of concrete is of great interest when considering the durability of concrete structures in cold climate.

It is realized that a model for physical degradation like carbonation, reinforcement corrosion, and frost damage based on threshold values in terms of the mass concentration (at a certain location) of, for example, chloride ions is not sufficient. It will be claimed that the governing equations in Table 5.6 must be introduced into a description of a stress-strain relation of the solid. Compare the discussion in Section 8. Not until a realistic description of the environmentally induced stresses and strains in the considered structure is added to the strains induced by the normal load on the structure is obtained, a threshold value in terms of bearing capacity or maximum allowable deflections of the given structure may serve as a limit of service life.

Finally, it should be observed that the *outer* climate variations, i.e. the boundary conditions, must be known in order to solve the proposed equation system for the diffusing and chemically reacting constituents. The boundary conditions (and their variations) to be described are: (*i*) the mass concentration of vapor, (*ii*) the mass concentration of the gaseous carbon dioxide, (*iii*) the mass concentration of

oxygen in the air, (*iv*) a situation with liquid water on the outer surface, with the water concentration corresponding to saturation in the porous material, (*v*) the mass concentration of dissolved chloride, (*vi*) a concentration of dissolved hydroxide ions (zero at normal conditions), (*vii*) the dissolved carbon dioxide, and (*viii*) the temperature. In cases where capillary suction is considered, i.e. when liquid water is present at the boundary, a hydrostatic pressure must also be included as a boundary condition. Furthermore, the initial conditions *within* the material must be specified. The initial conditions should be given for all properties discussed above but also for (*i*) the mass concentration of bound chlorides (initially zero), (*ii*) the concentration of solid calcium carbonate (initially zero), (*iii*) the solid calcium hydroxide concentration, and (*iv*) the concentration of vicinal water.

6. The initiation and propagation stage of corrosion

In order to estimate under which conditions the corrosion of embedded reinforcement will be triggered, the action of the corrosion cell in its propagation stage is of interest. The equations describing the action of the constituents in the corrosion initiation problem, i.e. chloride ions, hydroxide ions, carbon dioxide and oxygen, have been dealt with in previous Sections. Here, a brief discussion on the mechanism of steel corrosion is presented. Factors that may control an initiation of such a process will are also discussed. Furthermore, conditions which may control the propagation stage of corrosion are touched upon, since it is believed that an initiated corrosion process may cease if the conditions required to maintain the corrosion are not fulfilled. For example, the availability of oxygen consumed in the corrosion is related to the amount of oxygen supplied by diffusion and convection from external sources, i.e. from the outer surface, and is thus of great importance. The conditions might be such that they are ideal for the initiation of corrosion, while the conditions to maintain a propagation are not. This is only one reason why the problem of estimating the damage caused by corrosion, and so establish physically stringent durability models of reinforced concrete structures, is very grave.

A key issue is in fact the initiation of corrosion in areas with imperfections such as cracks in the protecting surrounding concrete. In this report only homogeneous uncracked concrete will be discussed, for simplicity reasons.

The oxidation reaction in the corrosion process involves the dissolution of iron in the pore water near the steel, written as

$$\mathrm{Fe(s)} \longrightarrow \mathrm{Fe^{2+}(aq)} + 2e^- \quad \text{(at the anode)} \tag{6.1}$$

where e^- denotes an electron. This reaction may only occur if the depassivation of the steel has been induced by for example the presence of chloride ions in the pore solution at a sufficiently high concentration (presumably caused by breaking the oxide film on the steel surface) or/and a decrease in the basicity. By this is meant a situation when a threshold value for initiation of corrosion is reached (not considering imperfections such as cracks). The reaction (6.1) makes the steel negatively charged.

The electron liberated in the anodic area moves through the steel towards a neighboring cathodic area and creates an electric current flowing from the anode to the cathode area. Incoming electrons from the steel bar at the cathodic area

form hydroxide ions in the presence of water. The oxygen reduction reaction is

$$O_2(aq) + 2H_2O + 4e^- \longrightarrow 4OH^-(aq) \quad \text{(at the cathode)} \tag{6.2}$$

Apparently, the rate of the induced reaction (6.2) is very much determined by the concentration of the hydroxide ions in the pore solution near the steel. A relatively high concentration of hydroxide ions near the steel decreases the reaction rate significantly compared to a case where the hydroxide ion concentration is low. Furthermore, the amount of dissolved oxygen is important at attempts to estimate the reaction rate in (6.2). Thus it must be estimated as closely as possible. On the other hand, it is very likely that the electrons find their way to a cathodic area, where the conditions are favorable for a formation of hydroxide ions, i.e. an area with sufficient amounts of oxygen and water. As discussed before, the main reasons for a decreased value of the hydroxide ion concentration are supposed to be carbonization and the leaching of hydroxide ions from the pore solution to the surrounding pure water.

The location of the developed anodic and cathodic areas is much a question of imperfections at the steel surface and in the concrete near the steel bar. In cases with well embedded bars and no cracks or other defects in the cover, it is believed that tiny narrow pits are formed at the steel surface. These soon become uniformly distributed, forming a large anodic area with neighboring cathodic regions.

The hydroxide ions that are liberated in the cathode area are balanced by a reaction in the anodic region, to form ferrous hydroxide, i.e.

$$Fe^{2+}(aq) + 2OH^-(aq) \longrightarrow 2Fe(OH)_2(s) \quad \text{(anode)} \tag{6.3}$$

Since the hydroxide ions liberated at the cathode can be transferred through the electrolyte, in this case the pore solution, the flow properties of the hydroxide ions in the pore solution near or at interface between the concrete and the steel are of importance. However, since high concentrations of hydroxide ions initially appear naturally in the pore solution of cement-based materials, the supply of these ions may not necessarily be transferred from cathodic to anodic regions. In fact, all ions present in the pore solution are involved in assuring that the process is electrically balanced. During situations with significantly high concentrations of chloride ions near the anodic and cathodic areas, the reaction (6.1) may be accelerated due to the flow of negatively charged ions towards the anode.

The total cell reaction, i.e. the result of the reactions (6.1), (6.2), and (6.3), is

$$2Fe + 2H_2O + O_2 \longrightarrow 4Fe(OH)_2 \quad \text{(cell)} \tag{6.4}$$

The ferrous hydroxide will, furthermore, react with available dissolved oxygen or oxygen in its gaseous phase to form hydrated red rust $Fe(OH)_3$:

$$4Fe(OH)_2(s) + O_2(aq \text{ or } g) + 2H_2O \longrightarrow 4Fe(OH)_3(s) \quad \text{(anode)} \tag{6.5}$$

where, again, the availability of oxygen and liquid water are important for the reaction rate.

Of course, the presented reactions give a simplified picture of the essential electro-chemical reaction. For example, other compounds may form, such as $FeSO_4$ and black rust Fe_3O_4; $3Fe+8OH^- \longrightarrow Fe_3O_4+8e^-+4H_2O$, which may be corrosion products if the availability of oxygen is restricted. Black rust, i.e. a thickening of the oxide film, is not as liable to cause the cracking of concrete, since the volume of black rust is twice as large as that of steel, compared to red rust which is four times as large [6]. The damages caused by the formation of rust in embedded steel bars in situations when the availability of oxygen is restricted are, however, far from negligible. Actually, the embedded steel bars might be completely dissolved under such conditions, especially when chloride ions are present from external sources.

Oxygen is consumed both in the cathodic and the anodic areas, compare (6.2) and (6.5). This makes the availability of oxygen one of the important factors in the control of the corrosion process (when the production of, for example, black rust is not considered). The supply of water is not, however, believed to control the process directly. The mass concentration of liquid water will, however, surely affect the mobility of oxygen and chloride ions from the external outer surface. Furthermore, the degree of water saturation will radically affect the electrical resistivity of the concrete [6].

In physical chemistry, the *reaction molar Gibbs energy* $\Delta_r\zeta$ is often assumed to be related to the composition of the reaction mixture, in this case for the reactions (6.1) and (6.2) as

$$\Delta_r\zeta = \Delta_{r0}\zeta + R\theta \ln Q \tag{6.6}$$

where $\Delta_{r0}\zeta$ is the standard (reference) reaction molar Gibbs energy of a certain reaction, and Q is the *reaction quotient* in terms of *activities,* for the individual constituents which in general depend on the composition. The absolute temperature is denoted θ and the gas constant R (given as 8.314 (J/mol/K)).

The cell potentials U_0, denoting the standard electrode potential, and U (in

volts) can be written in terms of the reaction molar Gibbs energies as

$$U_0 = \frac{\Delta_{r0}\zeta}{v\mathrm{F}}; \quad \text{and} \quad U = \frac{\Delta_r\zeta}{v\mathrm{F}} \tag{6.7}$$

where v is the valence number for the substance that passes into the solution, also equal to the number of electrons involved in the reaction studied, and F is Faraday's constant, 96485 (C/mol), a measure of the charge per mole of electrons.

Following (6.6) and (6.7), the *Nernst equation* is obtained as

$$U = U_0 + \frac{R\theta}{vF}\ln Q \tag{6.8}$$

That is, the corrosion cell potential related to a standard potential U_0 is the Gibbs energy of the reaction expressed as a potential in volts.

By making the rough approximation that the reaction quotient Q may be determined solely in terms of molar concentrations for the constituents reacting in the cathode and anode areas, i.e. considering the activity of the constituents to be equal to their molar concentrations, the term Q can be expressed for the anode reaction (6.1) as

$$Q^{anode}(\mathbf{x}_{anode}, t) = [\mathrm{Fe}^{2+}] \,/\, [\mathrm{Fe}] \quad \text{(at the anode)} \tag{6.9}$$

where $[\mathrm{Fe}^{2+}]$ is the molarity, i.e. the concentration of Fe^{2+} in moles per liter of electrolyte (pore water) at the spatial position $\mathbf{x}_{anode}$ and at the time t. This definition of concentration is different from the concentration denoted c_a discussed in previous sections. They are easily related to each other through the use of the mass concentration of the solvent, i.e. the concentration of liquid water c_l in the pores of the porous medium.

The activity of a pure solid or liquid is by definition equal to 1, that is $[\mathrm{Fe}] = 1$. This represents the activity of a Fe molecule in the steel bar.

The reaction quotient Q for the cathode reaction (6.2) is determined by the same approximations, that is

$$Q^{cathode}(\mathbf{x}_{cathode}, t) = [\mathrm{O}_2]\ [\mathrm{H_2O}]^2 /\ [\mathrm{OH}^-]^4 \quad \text{(at the cathode)} \tag{6.10}$$

where the activity for the pure liquid water is defined as $[\mathrm{H_2O}] = 1$.

The *standard hydrogen electrode* (SHE) is used as the defined zero potential U_0, i.e. the reaction $2\mathrm{H}^+ + 2\mathrm{e}^- = \mathrm{H}_2$. The measured standard potential for the anode

Table 6.1: Standard electrode potentials at 298 K, [29].

Reduction half-reaction	U_0 (V)
$Fe^{2+} + 2e^- \longrightarrow Fe$	-0.44
$Fe^{3+} + 3e^- \longrightarrow Fe$	-0.04
$Fe^{3+} + e^- \longrightarrow Fe^{2+}$	$+0.77$
$2H^+ + 2e^- \longrightarrow H_2$	± 0, *by definition*
$O_2 + 2H_2O + 4e^- \longrightarrow 4OH^-$	$+0.40$

reaction (6.1) is $U_0^{anode} = -0.44$ (V), e.g. compare [29]. The valence number is $v^{anode} = 2$. Then the anodic potential becomes (in volts)

$$U^{anode}(\mathbf{x}_{anode}, t) = -0.44 + 4.3 \cdot 10^{-5}\theta \ln\left([Fe^{2+}]\right) \tag{6.11}$$

It should be noted that a molar concentration of $[Fe^{2+}] = 1$ (mole per liter of pore water) corresponds to the measured standard potential, i.e. $U^{anode} = U_0^{anode}$ for this special case.

The measured standard potential for the cathode reaction (6.2) is $U_0^{cathode} = +0.40$ (V), e.g. compare [29] and Table 6.1. The valence number is $v^{cathode} = 4$. Then, the cathodic potential can be written as

$$U^{cathode}(\mathbf{x}_{cathode}, t) = 0.40 + 4.3 \cdot 10^{-5}\theta \ln\left([O_2] \,/\, [OH^-]^4\right) \tag{6.12}$$

The *electromotive force* $U^{force} = U^{cathode} - U^{anode}$ is simply the difference between the two potentials in (6.11) and (6.12).

It should be observed that the estimation of $U^{cathode}$ and U^{anode}, using the equations discussed, are only significant under extreme, ideal conditions. In fact, these potentials will be very much reduced by polarization phenomena. This is discussed at the end of this section.

In order to predict how the ions in the pores of the porous medium are affected by a current induced by the corrosion cell, the field equation describing a conductive media is of interest. The subject will be outlined briefly as follows.

Due to the fact that the anode and cathode areas can be developed at locations along a steel bar in concrete, a one-dimensional representation of the problem is not sufficient. Therefore, a more general, three-dimensional presentation will be adopted.

The continuity equation for the *current density* $\mathbf{j}$ (amp/m^2) without any global current source can be written as

$$\mathrm{div}\mathbf{j} = 0 \tag{6.13}$$

where $\mathbf{j}$ is a vector quantity.

The *electric field intensity vector* $\mathbf{e}$ (V/m) is assumed to be related to the current density vector $\mathbf{j}$ as

$$\mathbf{j} = k_s(c_l, c_c, c_{oh})\mathbf{e} \tag{6.14}$$

where k_s (ohm/m) is the *electrical conductivity* of the solid matrix (e.g. concrete). This is assumed to be a function of the mass concentration of liquid water c_l in the pores of the solid and of the dissolved chloride ion concentration c_c and hydroxide concentration c_{oh} in the pore solution. This quantity is for concrete w/c ≈ 0.5 not 'infected' by chloride measured to be, $k_s = 40$ (ohm/m) at 100% saturation, $k_s = 90$ (ohm/m) at 80% saturation, $k_s = 400$ (ohm/m) at 60% saturation and $k_s = 90000$ (ohm/m) at 40% saturation by water [45]. The values depend very much on the type of binder, however.

In electric conduction field problems the electric field intensity is defined as

$$\mathbf{e} = -\text{grad}U \tag{6.15}$$

By combining (6.13), (6.14) and (6.15) the governing equation for the electrical potential field $U(\mathbf{x})$ becomes

$$-\text{div}(k_s(c_l, c_c, c_{oh})\,\text{grad}U) = 0; \quad \text{in}\, V \tag{6.16}$$

This equation needs boundary conditions in terms of prescribed potentials and/or prescribed current densities along boundary surfaces. In fact, the anodic and cathodic areas will be interpreted as boundary conditions expressed by the values of the potentials at the anode and cathode calculated by equations (6.11) and (6.12), in which also the effect of the polarization will be incorporated. It should be noted that the potential field calculated by (6.16) is zero within the whole domain of interest before the corrosion is initiated.

The prescribed boundary values to be used in equation (6.16) in terms of the potentials at the anode and cathode located at the spatial position $\mathbf{x}_{anode}$ and $\mathbf{x}_{cathode}$ respectively are written

$$U(\mathbf{x}_{anode}, t) = U^{anode}(\mathbf{x}_{anode}, t); \qquad \text{(when corrosion is initiated)} \tag{6.17}$$

and

$$U(\mathbf{x}_{cathode}, t) = U^{cathode}(\mathbf{x}_{cathode}, t); \qquad \text{(when corrosion is initiated)} \tag{6.18}$$

One difficulty consists in predicting at what locations the anodic and cathodic are formed when corrosion is initiated. It is, in fact, extremely important to predict the spatial positions of the anodic and cathodic areas correctly, since the gradient of the potential is assumed to cause a significant motion of ions in the pore solution. Motion of chloride ions in concrete due to an electrical field has been studied in [46]. In a situation where the anodic and cathodic areas are located far from each other, a smaller electric field intensity, relatively speaking, will develop than if the distance is short.

The electric boundary condition normal to the outer surface can be expressed as

$$\mathbf{j}(\mathbf{x},t)\mathbf{n} = \mathbf{0}; \quad \text{on } \partial V \quad (\text{if } c_l(x,t) = 0; \text{ on } \partial V) \tag{6.19}$$

under the condition that the surface of the porous medium is exposed to air (written as $c_l(x,t) = 0$; on ∂V). The vector $\mathbf{n}$ denotes the outward unit normal to the boundary surface ∂V. The condition

$$U(\mathbf{x},t) = 0; \quad \text{on } \partial V \quad (\text{if } c_v(x,t) = 0; \text{ on } \partial V) \tag{6.20}$$

can be used if the outer surface is submerged in liquid water [6] (written as $c_l(x,t) = 0$; on ∂V).

In order to derive an equation valid for ions exposed to an electric field and concentration gradients the mass density flow can in somewhat general terms be constituted as

$$\rho_{ion}\mathbf{u}_{ion} = f(\operatorname{grad} c_{ion},\ \operatorname{grad} U,\ c_{ion}) \tag{6.21}$$

Using the somewhat crude approximation that the mass density flow consists of one part described by a concentration gradient, and another described by a linear combination of the concentration c_{ion} and the gradient of the potential U, the following relation is obtained:

$$\rho_{ion}\mathbf{u}_{ion} = -D_{ion}(c_l, \theta,\ n,\ a)\operatorname{grad} c_{ion} + c_{ion}D_{ionE}(\theta,\ n,\ a)\operatorname{grad} U \tag{6.22}$$

where the mass concentration c_{ion} in the second term can be interpreted as a quantity representing activity. The constitutive assumption (6.22) will, however, be of the standard diffusion-convection format, when inserted into the mass balance equation.

For positively charged ions, the coefficient D_{ionE} is defined as a negative quantity, and for negatively charged ions, D_{ionE} is positive. Some measured ionic mobility values for ions dissolved in bulk liquid water are listed in Table 6.2.

Table 6.2: Ionic mobilities in water at 298 K, [29].

Ion	Ionic mobility ($m^2/s/V$)
K^+	$7.62 \cdot 10^{-8}$
Ca^{+2}	$6.17 \cdot 10^{-8}$
Na^+	$5.19 \cdot 10^{-8}$
Cl^{-1}	$7.91 \cdot 10^{-8}$
CO_3^{-2}	$7.46 \cdot 10^{-8}$
OH^-	$20.64 \cdot 10^{-8}$

Corresponding measured diffusion constants in bulk liquid water for the some ions are $D_c^l = 2.03 \cdot 10^{-9}\,(m^2/s)$, $D_{oh}^l = 5.30 \cdot 10^{-9}\ (m^2/s)$, and $D_{na}^l = 1.33 \cdot 10^{-9}\ (m^2/s)$, e.g. compare [29] and see Table 5.7.

By comparing the magnitude of the electromotive force with the concentration gradient force for a situation, where the cathodic and anodic areas are not located too far from each other, it is found that the motion induced by the corrosion cell in terms of the electromotive force acting on the ions in the electrolyte becomes dominant when the corrosion process is in its propagation stage.

The divergence operating on the second term in (6.22) gives

$$D_{ionE}\,\mathrm{div}(c_{ion}\mathbf{e}) = D_{ionE}\,c_{ion}\,\mathrm{div}\,(\mathbf{e}) + D_{ionE}\,\mathbf{e}\cdot\mathrm{grad}\,c_{ion} \tag{6.23}$$

where $\mathbf{e} = grad\,U$. Making the assumption that the term

$$D_{ionE}\,c_{ion}\,\mathrm{div}\,(\mathbf{e}) \approx 0 \tag{6.24}$$

is small compared to the others, the constitutive relation (6.22) and the approximation (6.24) inserted into the mass balance equation (2.56) becomes

$$\begin{aligned} \rho\frac{\partial c_{ion}}{\partial t} \;=\; & -\mathrm{div}\,\left(D_{ion}(c_l, \theta,\, n,\, a)\,\mathrm{grad}\,c_{ion}\right) - \\ & (\rho\dot{\mathbf{x}} + D_{ionE}(\theta,\, n,\, a)\,\mathrm{grad}\,U)\cdot\mathrm{grad}\,c_{ion} - \hat{c}_{ion} - \hat{m}_{ion};\ \ \mathrm{in}\,V \end{aligned} \tag{6.25}$$

where the dependencies upon the mass concentration of liquid water c_l, temperature θ, porosity n, and specific surface area a have been included as material parameters in the diffusion and ion mobility parameters.

The term omitted, i.e. $D_{ionE}c_{ion}\,\mathrm{div}(\mathbf{e})$ can, of course, be added to the equation (6.25). This term will be given as $-c_{ion}D_{ionE}(c_l, \theta,\, n,\, a)\,\mathrm{div}(\,\mathrm{grad}\,U)$, which in all essential parts means that the Laplace on the electrical potential field $U(\mathbf{x})$ is

introduced as a source/sink term in (6.25), with a material parameter identified as $k = c_{ion} D_{ionE}(c_l, \theta, n, a)$.

Equation (6.25) represents a situation with molecule diffusion and forced convection due to the mean velocity of the mixture $\dot{\mathbf{x}}$ and the driving force imposed by the electric field intensity $\mathbf{e}$ (i.e. grad$U$). Furthermore, the mass supply term $\hat{c}_{ion}$ is included, which describes the reversible binding of ions to the solid pore wall in the whole domain V. Constitutive relations for these quantities have been suggested in previous sections. The property $\hat{m}_{ion}$ denotes the source/sink term due only to the reactions at the anode and cathode. Therefore, it is also a constitutive-dependent property. This will be discussed at the end of this Section.

The constitutive relation for the quantity $\hat{c}_{ion}$ is more difficult to describe than the, somewhat, ideal case where there is only molecule diffusion and binding without any external applied electric field $\mathbf{e}$. This is due to ions getting stuck in cavities on the pore walls, located in the direction of the applied electrical field. Hence, the conditions that determine the removal rate of free diffusing molecules towards the solid pore walls, where they might get stuck, will be very different when motion induced by an external electromotive force is considered, acting in the whole domain of interest. This should be compared to the case where only molecule diffusion takes place.

Such complex phenomena must be considered when trying to estimate the diffusion parameter D_{ion} with the so-called *Einstein relation.* This relates the ion mobility D_{ionE} to the pure diffusion parameter D_{ion}, in cases where an electric field with the intensity $\mathbf{e}$ is applied to bulk liquid containing dissolved ions of low concentration. The Einstein relation can be written: $D_{ionE} = D_{ion} vF/(R\theta)$.

One crucial point when it comes to estimating the corrosion rate is the effect of electrode polarization. The values of electrode potentials are known to be significantly lowered when the electric current density $\mathbf{j}$ increases. Usually, the drop in the electromotive force U^{force} due to polarization is denoted η. The actual electromotive force is then written as $U^{force}_{pol} = U^{force} - \eta$. The physical source of polarization is believed to be of two kinds: *Activation polarization* η_a and *concentration polarization* η_p, i.e. $\eta = \eta_a + \eta_p$.

The concentration polarization is caused by a decrease of ion concentration near the electrode surface due to corrosion. As the ions are consumed by the corrosion process, the voltage is reduced and the current eventually becomes inhibited. In the field of electrochemistry, the approximation of the concentration profile near the electrode is often assumed to be linear across the so-called *Nernst diffusion layer,* which is typically 0.1 mm. However, as field equations in the

format shown in (6.25) can be used to describe the ion behavior within the whole domain of interest, no additional approximations for the region near the electrode are needed to describe the concentration field at different time levels. Nevertheless, some kind of special assumption as to the boundary conditions, in terms of the potential U at the electrodes, must be incorporated in order to capture the concentration polarization phenomenon.

Another problem related to concentration polarization is that Fe^{2+} dissolved into the pore liquid near the steel at a developed anode may form complexes with dissolved chloride ions present. Such complex formations of negative and positive ions of interest in the corrosion process complicates the picture when it comes to defining the concentrations of, for example, OH^-,Fe^{2+} and Cl^-. These are important variables when predicting the anode and cathode potentials with the equations (6.11) and (6.12). Yet another question which has to be answered is if chlorides in complexes with Fe^{2+} may contribute to a further acceleration of the corrosion process.

Activation polarization is a drop in the electrode potential due to changes of the current magnitude in the mechanism of ion transfer through the interface between the electrode itself and the surrounding bulk material, in this case the steel-concrete interface. The most primitive model of this interface is an *electrical double layer*. It consists of a thin sheet with positive charge towards the electrode surface and a sheet with negative charge towards the solution (or vice versa). By corrosion of reinforcement bars in concrete, it is assumed, however, that the concentration polarization prevails since the activation polarization has its source in a very thin surface layer, which builds up rapidly compared to the concentration polarization [6].

In order to close the equation system, constitutive relations must be introduced for the source/sink terms $\hat{m}_{ion}$ to describe the reaction rate of the ions, which participate at the cathode and anode areas. A condition for initiation of corrosion must also be specified.

Due to the low solubility of $Fe(OH)_2$ and $Fe(OH)_3$, which are formed at the anode (during situations when oxygen is available), one may suspect that the concentration of Fe^{2+} near the steel is kept at a rather low, constant level when the corrosion process is in its propagation phase. In turn, such an approximation means that the potential $U^{anode}(\mathbf{x}_{anode}, t)$ determined by equation (6.11) is also kept constant on condition that the temperature θ is also constant. Therefore, the reaction rate of Fe^{2+} at the cathode can be constituted as shown in equation (6.1), as a function of concentrations in the pore solution near the cathode area

of chloride ions, hydroxide ions and oxygen, and as a function of the amount of rust produced and the temperature. This can be described in general term as

$$\hat{m}_{Fe}(\mathbf{x}_{anode}, t) = f\left([\mathrm{OH}^-], [\mathrm{Cl}^-], [\mathrm{O}_2], [\mathrm{Fe(OH)}_3], \theta\right) \text{ (at active corr.)} \quad (6.26)$$

where the equation describing the action of the hydroxide ions, the chloride ions and the oxygen should be used to calculate the corresponding concentrations at the location where the anodic area has been developed, i.e. equations of the kind illustrated in (6.25). The concentration of $\mathrm{Fe(OH)_3}$ at the same spatial location is simply supposed to be calculated by the stoichiometric relations (6.1), (6.2), (6.3), and (6.4). Since no equation to describe the diffusion behavior of $\mathrm{Fe(OH)_3}$ has been introduced, it is suggested that the red rust that is formed in the anode area (and which stays there) contributes to a diffusion barrier for other substances. The reaction rate (6.26) is simply interpreted as a decrease of the reaction rate as the concentration of red rust at the cathode increases, while all other concentrations remain constant. In fact, such a behavior is similar to the polarization phenomenon. It should be observed that the concentrations in (6.26) are affected by a change in liquid water concentration c_l, since they are defined as mol per litre solute.

A possible linear combination of the quantities in (6.26) is the constitutive relation

$$\hat{m}_{Fe}(\mathbf{x}_{anode}, t) = k_{Fe} \frac{[\mathrm{Cl}^-]\,[\mathrm{O}_2]\;\theta}{[\mathrm{OH}^-]\,[\mathrm{Fe(OH)}_3]} \quad \text{(at active corrosion)} \quad (6.27)$$

where k_{Fe} is the rate constant for the reaction (6.1).

By using the stoichiometric relations (6.1), (6.2), (6.3), and (6.4), the source/sink terms in the anode and cathode areas $\hat{m}_o(\mathbf{x}_{anode}, t)$ (rate of consumption of oxygen), $\hat{m}_{oh}(\mathbf{x}_{anode}, t)$ (rate of consumption of hydroxide ions), and $\hat{m}_{redrust}(\mathbf{x}_{anode}, t)$ (rate of production of $\mathrm{Fe(OH)_3}$) can be calculated directly without any extra constitutive relations apart from (6.27). It should be noted, however, that the cathode potential $U^{cathode}(\mathbf{x}_{cathode}, t)$ is changed significantly due to the consumption of oxygen and hydroxide ions when the diffusion-convection process does not serve the cathode with negatively charged ions at the same rate as the consumption of these. This changes the movement of negatively charged ions towards the cathode caused by the electric field.

The conditions for onset of steel corrosion in bulk water solutions are often expressed by the concentration ratio $[\mathrm{Cl}^-]/[\mathrm{OH}^-]$. Experiments confirm that the approximative value of 0.6 is required to initiate corrosion in aquatic water

solutions, e.g. compare [25]. Here, it is suggested that the initiation criterion can be extended to include the availability of oxygen. Besides, the temperature is supposed to have an effect on the initiation. The new criteria would then be

$$\text{if} \quad k_{cl}^{anode} \frac{[\mathrm{Cl}^-]\ \theta}{[\mathrm{OH}^-]\, 293} + k_o^{anode} \frac{[\mathrm{Cl}^-]\,[\mathrm{O}_2]}{2.8 \cdot 10^{-8}} \geq 1 \ \text{(initiation at anode)} \tag{6.28}$$

where the solubility of oxygen in water at room temperature and at normal pressure is $2.8 \cdot 10^{-8}$ (mol/l). This should be compared to the amount of oxygen in air, which is in the magnitude of $8.8 \cdot 10^{-3}$ (mol/l).

By setting the constants to $k_{cl}^{anode} = 1.67$ and $k_o^{anode} = 0$, and the temperature to $\theta = 293\,\mathrm{K}$, the classical initiation criterion $[\mathrm{Cl}^-]/[\mathrm{OH}^-] \geq 0.6$, relevant for aqueous solutions only, is obtained.

Note that (6.28) is supposed to determine when and in which spatial position corrosion will be initiated. The constants k_{cl} and k_o will, presumably, depend on the porosity n, the specific area a, and the binder type of the concrete in question.

The location of the cathodic area in relation to the anode in the same cell is of interest when the magnitude of the electric field intensity $\mathbf{e}$ in the porous medium is considered. This in turn is important for the determination of the mass transfer of ions at the propagation stage. That is, an additional criterion must be specified for the location of the cathodic spatial position once the anode reaction has been initiated, e.g. when (6.27) is fulfilled. Such a criterion might typically be

$$k^{cathode} \frac{[\mathrm{O}_2]\ [\mathrm{H}_2\mathrm{O}]\, \theta}{[\mathrm{OH}^-]\, 293} \geq 1 \tag{6.29}$$

where $k^{cathode}$ is a material constant. Note that the assumed cathode reaction is (6.2). The criterion (6.29) only determines the spatial position along the steel bar where the cathodic reaction occurs once the relation (6.28) has been fulfilled. At this specific location, the source terms at the cathode, which describe the production of hydroxide ions, denoted $\hat{m}_{oh}(\mathbf{x}_{cathode}, t)$, can be calculated with the stoichiometric relations (6.1), (6.2), (6.3), and (6.4).

Another question to be addressed in this context is whether the anodic corrosion reaction resulting in the production of rust can proceed if the criteria for a cathodic reaction are not fulfilled within the domain of interest. In that hypothetical, case both (6.28) and (6.29) should be used simultaneously to determine the condition of triggered corrosion, since both the anodic and cathodic reactions must be active when also a closed electric circuit in the corrosion cell exists.

7. A few remarks on heat transfer and phase change problems

In this section, the classical heat conduction equation for a single temperature θ of the mixture will be derived using a simplified version of the energy balance equation (2.118) together with required constitutive relations. A more detailed description of the problem, involving the concepts of the free energy density ψ_a and the entropy η_a for the constituents in a mixture, will also given to show the difficulties involved in improving the assumptions.

In the so-called Stefan's problem, a modified version of the linear classical heat conduction equation is used to track the propagation of a freezing or melting front of a pure material undergoing a phase change. Essentially, six material parameters are used in this approach. However, the formation of ice in a porous material with a wide range of pore sizes filled, or partly filled, with a pore solution and containing different chemical components does not satisfy the basic assumptions introduced for solving the Stefan's problem. The important difference between the Stefan's problem and the freezing of liquid water in a porous medium will be discussed.

The most important phase change problem in the area of durability of porous building materials is probably the formation of ice in the pore system. Ice may cause damage such as internal micro-cracks and scaling of material surfaces. A problem of special interest, in this context, is the formation of ice in combination with deicing salts. This damage differs from the one which arises when a pore solution freezes without the presence of external salts.

To obtain the standard heat conduction equation, the internal energy ε must be constituted with the material constant C and the temperature θ, as

$$\varepsilon = C\theta \tag{7.1}$$

where C represents the specific heat capacity of the material considered.

The heat flux q_x in a one-dimensional case is constituted by a temperature gradient assumption and the material constant λ called the conductivity as

$$q_x = -\lambda \frac{\partial \theta}{\partial x} \tag{7.2}$$

The body force of all constituents $\mathbf{b}_a$, the influence of the term including the stress tensor and the velocity gradient for the mixture $\mathrm{tr}\mathbf{T}^{\mathrm{T}}\mathbf{L}$, and the external heat supply for the mixture r are all assumed to be negligibly small quantities

compared to the others in the energy balance equation (2.118). The simplified energy balance equation in one dimension becomes

$$\rho\frac{\partial\varepsilon}{\partial t}=-\frac{\partial q_x}{\partial x}-\rho\dot{x}_x\frac{\partial\varepsilon}{\partial x} \tag{7.3}$$

where ρ is the mass density of the mixture defined in (2.12) and $\dot{x}_x$ is the mean velocity of the mixture defined in (2.15).

If the constitutive relations (7.1) and (7.2) are introduced into the simplified energy balance equation (7.3),

$$\rho C\frac{\partial\theta}{\partial t}=\lambda\frac{\partial^2\theta}{\partial x^2}-\rho C\dot{x}_x\frac{\partial\theta}{\partial x} \tag{7.4}$$

is obtained. If the mean velocity $\dot{x}_x$ vanish, the equation (7.4) represents the standard heat conduction problem, which must be supplemented with boundary conditions in terms of temperature and/or a heat flux. Furthermore, the initial conditions must be specified.

In the Stefan's problem, the mean velocity of the mixture $\dot{x}_x$ vanish, and the material parameters C and λ are assumed to be functions of the temperature itself. Thus, the temperature field in a domain where a phase change occurs can be solved, and assure energy balance, with a non-linear version of (7.4). The governing equation in the Stefan's problem can be obtained by introducing the constitutive relation of a rate type for the internal energy as

$$\dot{\varepsilon}=C\left(\theta\right)\dot{\theta} \tag{7.5}$$

The heat flux is constituted as

$$q_x=-\lambda\left(\theta\right)\frac{\partial\theta}{\partial x} \tag{7.6}$$

Furthermore, the divergence of the heat flux can be expressed by

$$\frac{\partial q_x}{\partial x}=-\frac{\partial}{\partial x}\left(\lambda\left(\theta\right)\frac{\partial\theta}{\partial x}\right)=-\lambda\left(\theta\right)\left(\frac{\partial\theta}{\partial x}\right)^2-\lambda\left(\theta\right)\frac{\partial^2\theta}{\partial x^2} \tag{7.7}$$

It is assumed that

$$\left(\frac{\partial\theta}{\partial x}\right)^2\ll 1 \tag{7.8}$$

Table 7.1: Material constants for water and ice used in the Stefan's problem.

Constant	Value	Remarks
C_l	$1.762 \cdot 10^3$ (J/kg/K)	*Specific heat capacity, liquid water*
C_{ice}	$4.226 \cdot 10^3$ (J/kg/K)	*Specific heat capacity, ice*
λ_l	2.220 (J/s/m/K)	*Conductivity of liquid*
λ_{ice}	0.556 (J/s/m/K))	*Conductivity of ice*
L	$333.6 \cdot 10^3$ (J/kg)	*Latent heat of fusion*
θ_f	273.15 (K)	*Transition temperature*
$\Delta\theta_f$	$\sim 0.01 - 0.0001$ (K)	*Used to compute C_f from L*

With (7.5), (7.6), (7.8), and (7.3), the non-linear version of the standard heat equation becomes

$$\rho C(\theta)\frac{\partial\theta}{\partial t} = \lambda(\theta)\frac{\partial^2\theta}{\partial x^2} \tag{7.9}$$

if the velocity of the mixture $\dot{x}$ vanish.

Whenever the phase change temperature θ_f is reached, the material parameter $C(\theta)$ will exhibit a discontinuous jump. This is due to the latent heat effect L (J/kg), since the latent heat L is adsorbed or emitted during the phase change.

Integrating around the phase change temperature θ_f gives

$$L = \int_{\theta_f^-}^{\theta_f^+} C(\theta)d\theta \tag{7.10}$$

which is a material constant for pure materials undergoing a certain phase change. It is important that certain material parameters are known when the Stefan's problem is applied to liquid water and ice. These are the specific heat capacities of liquid water C_l and ice C_{ice}, and the 'specific' heat capacity during the phase change C_L. The C_L value represents the latent heat effect calculated from the material constant L together with an assumption of a small temperature interval, during which the phase change is supposed to occur. Furthermore, two different constant values of the conductivity λ are adopted, that is, the conductivity of liquid water λ_l and ice λ_{ice}. Compare the data for water and ice in Table 7.1.

Within the assumed phase change temperature interval, the conductivity λ is often assumed to be linear between the values λ_l and λ_{ice}. The change of the mass density of the mixture ρ is, however, normally incorporated into the C values. Besides, the pressure effects upon the formation of ice are ignored in the Stefan's problem.

By solving the non-linear equation (7.9) with the above-mentioned material parameters, a discontinuous freezing or melting front can be followed for all kinds of variation of the boundary conditions, simply by checking at which locations in the domain the temperature is below the specified temperature θ_f. Numerical methods solving the equation (7.9) have been proposed, e.g. compare [47].

However, an inherent problem when studying porous materials with a wide range of pore sizes is that not all of the liquid water present in the pore system is transformed from water to ice when a certain freezing temperature θ_f is reached, as assumed in the Stefan's problem. In order to use the energy balance concept to calculate the mass density of ice $\rho_{ice}(\mathbf{x}, t)$ formed in a porous material, modifications to the classical Stefan's problem must be introduced.

It is believed that liquid water present in different pore sizes in a saturated porous material will exhibit different freezing temperatures θ_f, i.e. a scatter of different latent heat effects at different temperatures must be overcome. The initial mass concentration of liquid water c_l, however, give no information as to how this liquid water is distributed among the different pore sizes in a representative material volume (REV). That is, some kind of geometrical consideration in addition to the porosity n and the specific surface area a must be introduced, and some relation must give the distribution of liquid water in this geometry.

By using for example the modified Kelvin equation (4.23) together with quantitative measurements or microscope studies the pore distribution curves can be evaluated. The pore distribution curves indicate of which pore size radii r_p the total porosity consists. The most simple distribution function of liquid water for such a geometry is the assumption that a given mass concentration of liquid water c_l occupies the smallest pores completely. In other words, if half of the porosity in a porous medium consists of pores smaller than a given value r_{p50} and the degree of saturation is 50%, all these pores are assumed to be completely filled with liquid and all the remaining pores, larger or equal to r_{p50} will be assumed to be completely dry. A simple way to improve this assumption is by distinguishing between adsorbed water molecules and liquid water stuck to the pore walls due to capillary condensation. That is, the adsorbed water can be assumed to be distributed among the different pore sizes in relation to its corresponding envelope-specific surface areas.

Furthermore, a function relating the freeze temperature θ_f to the different pore size radii r_p must be introduced in order to evaluate the function $C(\theta)$ for a specific material with a known pore size distribution. The latent heat L is, however, not a constant even when the fusion of ice in a normal condition is considered. Thus,

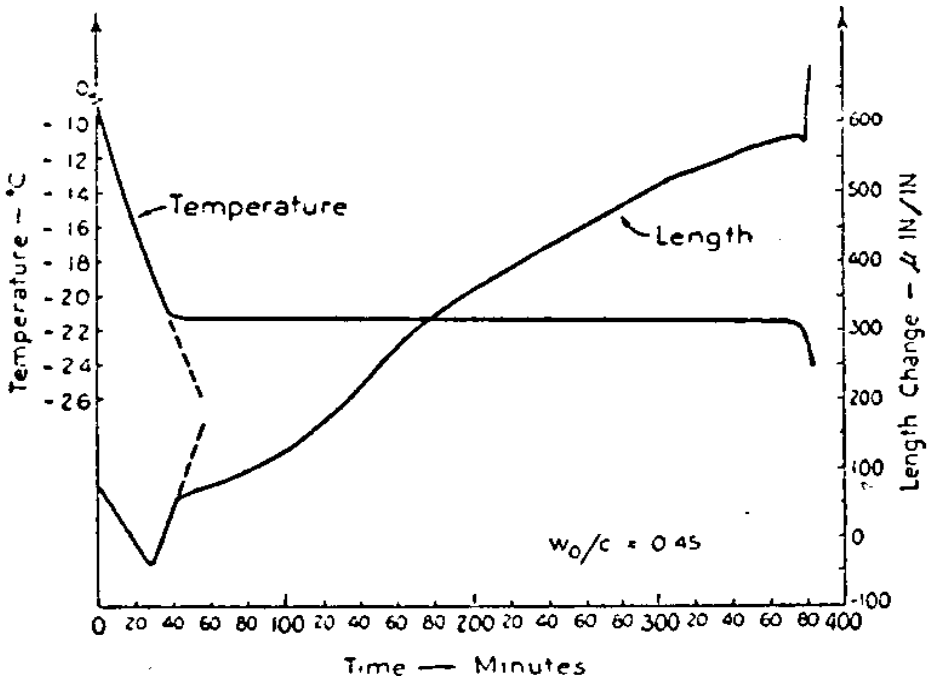

Figure 7.1: *Effect of holding temperature constant after freezing starts in a relatively dense paste, [50].*

supercooled or undercooled water will exhibit different latent heat L at different temperatures. At 273.15 (K), 263.15 (K), and 253.15 (K), the latent heat of fusion of ice is 333.6 (kJ/kg), 284.8 (kJ/kg), and 241.4 (kJ/kg) respectively [48].

There are many other important effects which must not be overlooked. One of them is that the liquid water (on a microscopic scale) present in the largest pores (having a certain known θ_f) will form ice when the ice formation is nucleated. This first ice formed is, however, believed to attract water from neighboring pores with smaller radii than that contained in the ice in its vapor and liquid phases. This phenomenon may significantly change the assumed distribution function of liquid water during the freezing process. The equation (7.9) together with assumptions of pore size distributions can not be used alone to calculate the mass density of ice $\rho_{ice}(\mathbf{x}, t)$. The effects of water from neighboring pores or from the surroundings being drawn towards ice islands created in the pore system is often referred to as cryogenic suction or cryosuction, e.g. compare [49]. Cryosuction is explained

by the difference in the free energy of ice at a certain temperature and unfrozen water at the same temperature.

Furthermore, if the attraction of water-vapor towards the ice islands in the pore system is significant, the amount of vapor to be converted to ice, i.e. the sublimation, might be of importance. The latent heat of fusion is approximately 12% of the latent heat of sublimation at 273.15 (K) and at atmospheric pressure.

It is noted that calorimeter measurements can not reveal the amount of ice formed in the pore system directly without making assumptions of the involved latent heat of fusion and sublimation at different temperatures and at different mass concentrations of water in the pore system. One problem to be considered is for example that the latent heat of fusion of capillary water is different from the latent heat of fusion of adsorbed and capillary-condensed water at a certain temperature. Furthermore, the latent heat of sublimation and the fusion can not be distinguished, since the calorimeter measures the total response in terms of heat output or heat input.

Since the ice grown from the vapor phase is very different in structure than ice grown from bulk water, the sublimation phenomenon may have important consequences in terms of micro-cracking of the solid material. Besides, as the growth of ice becomes diffusion-controlled, the time scale of vapor flow towards ice islands and the degree of external cooling rate become important. If, for example, the external cooling rate is fairly rapid, the diffusion-controlled sublimation is supposed to be small, and if the external cooling rate is slow, the ice growth due to sublimation (or, rather, damages caused by sublimation) might prevail, compare Figure 7.1.

In a situation, where the diffusion-controlled ice growth, i.e. the sublimation, is active, different ice crystals will be formed depending on the degree of super-cooling. The various ice crystals growing at different temperatures in a diffusion cloud chamber are: (*i*) hexagonal plates from 273.15 to 270 K, (*ii*) needles from 270 to 268 (K), (*iii*) prismatic columns from 268 to 265 K, (*iv*) hexagonal plates from 265 to 261 (K), (*v*) dendrites from 261 to 257 (K), (*vi*) hexagonal plates from 257 to 248 (K) [48]. The saturation pressure of the vapor involved in the sublimation has been shown not to affect the overall formation pattern of these different crystals. Temperature, it seems, is the main factor. Due to the different geometrical shape of these crystals, they might cause different kinds of damage to the solid. Dendrites and needles might be the most damaging products formed due to the needle-like shape of these crystals.

The thermomechanical problem of ice growth in concrete is often studied by

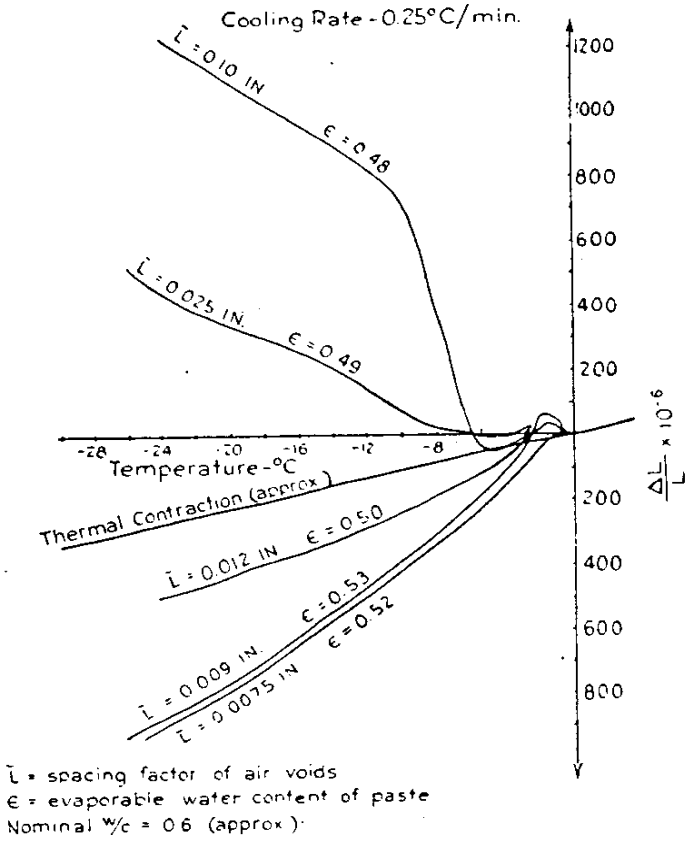

Figure 7.2: *Effect of entrained air and the spacing factor, [50].*

measuring the length changes due to a temperature depression and due to ice growth in the pore system, see Figures 7.1 and 7.2, [50]. In order to evaluate such measurements, the concept of stress and strain must be introduced. This subject is discussed in Section 8.

By combining the first and second axiom of thermodynamics, the thermomechanical coupling can be studied. Here, the free specific energy potential ψ_a and the entropy η_a are used as constitutive dependent properties. Indeed the thermodynamic properties ψ_a and η_a can be quite generally constituted, and therefore a more general energy equation than (7.4) can be obtained. This general equation is believed to be more adequate when phase change problems are studied, where factors other than temperature itself will affect the thermodynamic state variables

ε_a or ψ_a and η_a. Similar approaches have been proposed, e.g. compare [51], [52], and [53]. The Helmholz energy ψ and the entropy η are often introduced as well when studying thermomechanical coupling, e.g. compare [54].

For example, the mass concentration of dissolved chloride ions and pore water present in different pore sizes will be factors affecting the freezing temperature. Hence, the thermodynamic state variables ε_a, ψ_a and η_a will also be affected. The derivation of a more general equation than (7.9) is not straightforward, since such formulations often include so-called internal variables. Furthermore, problems associated with the fulfillment of the second axiom of thermodynamics must also be dealt with. However, it will be shown that it is possible to study freeze-thaw problems in porous materials using the concept of mixture theory. Here, two different strategies to obtain an equation dealing with heat conductivity and chemically reacting constituents will be presented. It will be shown that different thermodynamic laws can be defined due to the second axiom of thermodynamics. The definitions of the thermodynamic laws do not follow directly from the second axiom of thermodynamics, but rather from the combination of this axiom and the choice of constitutive relations.

Consider the second axiom of thermodynamics (2.173), as expressed in terms of the Helmholtz free energy ψ_a and the entropy η_a, i.e.

$$\begin{aligned} 0 \quad \leq \quad & -\sum_{a=1}^{\Re} \rho_a \psi_a' - \sum_{a=1}^{\Re} \rho_a \eta_a \dot{\theta} + \sum_{a=1}^{\Re} \mathrm{tr}\mathbf{T}_a^{\mathrm{T}} \mathbf{L}_a \\ & - \sum_{a=1}^{\Re} \left(\mathbf{q}_a + \rho_a \theta \eta_a \mathbf{u}_a \right) \cdot \mathrm{grad}\left(\theta\right) / \theta \\ & - \sum_{a=1}^{\Re} \mathbf{u}_a \cdot \hat{\mathbf{p}}_a - \sum_{a=1}^{\Re} \hat{c}_a \left(\psi_a + \tfrac{1}{2} u_a^2 \right) \end{aligned} \tag{7.11}$$

where the definitions (2.138) and (2.171) have been used.

Two examples will be studied, both based on the assumption that the Helmholz free energy depends only on the temperature and the mass density, that is

$$\psi_a = \psi_a \left(\theta, \rho_a \right) \tag{7.12}$$

At first, the partial hydrostatic pressures π_a will be defined with the help of the Helmholz free energy ψ_a described through (7.12). In order to define the pressure, consider the derivative of (7.12), i.e.

$$\rho_a \psi_a' = \rho_a \frac{\partial \psi_a}{\partial \theta} \theta' + \rho_a \frac{\partial \psi_a}{\partial \rho_a} \rho_a' \tag{7.13}$$

It should further be noted that $\operatorname{div}\mathbf{x}'_a = \operatorname{tr}(\operatorname{grad}\mathbf{x}'_a) = \operatorname{tr}\mathbf{L}_a$, which allows the mass balance (2.59) to be written

$$\rho'_a = -\rho_a \operatorname{tr}\mathbf{L}_a + \hat{c}_a \tag{7.14}$$

If (7.13) and (7.14) are combined

$$\rho_a \psi'_a = \rho_a \frac{\partial \psi_a}{\partial \theta}\theta' - \rho_a^2 \frac{\partial \psi_a}{\partial \rho_a} tr\,\mathbf{L}_a + \rho_a \frac{\partial \psi_a}{\partial \rho_a}\hat{c}_a \tag{7.15}$$

is yielded.

Only the terms in the second axiom of thermodynamics containing the term $\mathbf{L}_a$ will be considered at this stage. It is concluded that the first term and the third term in (7.11) together with (7.15) result in a validation of the following restriction:

$$\sum_{a=1}^{\Re} \operatorname{tr}\left(\rho_a^2 \frac{\partial \psi_a}{\partial \rho_a}\mathbf{I} + \mathbf{T}_a^{\mathrm{T}}\right)\mathbf{L}_a \geq 0 \tag{7.16}$$

Since $\mathbf{L}_a$ is arbitrary, it follows that the parenthesis in equation (7.16) must be equal to zero in order to satisfy the part of the inequality containing the velocity gradient term. This makes it possible to define the thermodynamic law for the stress tensor as

$$\mathbf{T}_a = -\rho_a^2 \frac{\partial \psi_a}{\partial \rho_a}\mathbf{I} \tag{7.17}$$

The stress tensor is described with the hydrostatic pressure only, i.e.

$$\mathbf{T}_a = -\pi_a \mathbf{I} \tag{7.18}$$

Following the thermodynamic law (7.17) as well as (7.18), the expression for the hydrostatic pressure can be written as

$$\pi_a = \rho_a^2 \frac{\partial \psi_a}{\partial \rho_a} \tag{7.19}$$

This means for example that the choice $\psi_a(\theta, \rho_a) = R\theta \ln \rho_a$ gives the expression $\pi_a = R\theta\rho_a$ which is the ideal gas law.

The following discussion will concern two constituents denoted 1 and 2. For simplicity, the following restrictions will be assumed:

$$\begin{matrix} \mathbf{x}'_1(\mathbf{x}, t) = \mathbf{0} \\ \mathbf{x}'_2(\mathbf{x}, t) = \mathbf{0} \end{matrix}; \tag{7.20}$$

This means that also the velocity of the mixture $\dot{\mathbf{x}}$ and the diffusion velocities $\mathbf{u}_a$ are restricted to be zero. That is, a problem with heat conduction and chemical reactions will be studied, in which the constituents have zero velocities and where the hydrostatic pressures for the constituents are defined by $\pi_1 = \rho_1^2 \partial\psi_1/\partial\rho_1$ and $\pi_2 = \rho_2^2 \partial\psi_2/\partial\rho_2$, i.e. by the equation (7.19).

The fifteen unknown properties in both the test problems for the heat conducting and reacting constituents 1 and 2 are:

$$\begin{matrix} \rho_1(\mathbf{x},t) \\ \rho_2(\mathbf{x},t) \end{matrix} ; \quad \theta(\mathbf{x},t) ; \quad \begin{matrix} \hat{c}_1(\mathbf{x},t) \\ \hat{c}_2(\mathbf{x},t) \end{matrix} ; \quad \begin{matrix} \eta_1(\mathbf{x},t) \\ \eta_2(\mathbf{x},t) \end{matrix} ; \quad \begin{matrix} \psi_1(\mathbf{x},t) \\ \psi_2(\mathbf{x},t) \end{matrix} ; \quad \begin{matrix} \mathbf{q}_1(\mathbf{x},t) \\ \mathbf{q}_2(\mathbf{x},t) \end{matrix} ; \tag{7.21}$$

where the independent variables are the mass densities ρ_1 and ρ_2 and the temperature θ. The rest of the properties listed in (7.21) are the constitutive variables. It should be noted that the heat fluxes $\mathbf{q}_1$ and $\mathbf{q}_2$ involves three unknown properties each.

Due to the assumptions in (7.20), the inequality (7.11) is simplified to

$$-\sum_{a=1}^{2} \rho_a \dot{\psi}_a - \rho\eta\dot{\theta} - \sum_{a=1}^{2} \mathbf{q}_a \cdot \operatorname{grad}(\theta)/\theta - \sum_{a=1}^{2} \hat{c}_a \psi_a \geq 0 \tag{7.22}$$

where $\psi_a' = \dot{\psi}_a$ and $\mathbf{h} = \mathbf{q}_1 + \mathbf{q}_2$ due to the restriction of zero velocities for the two considered constituents.

It is further assumed that the Helmholz free energy for the constituents 1 and 2 are given as functions of the temperature and the mass densities ρ_1 and ρ_2, i.e.

$$\begin{matrix} \psi_1 = \psi_1(\theta, \rho_1) \\ \psi_2 = \psi_2(\theta, \rho_2) \end{matrix} \tag{7.23}$$

The entropies for the constituents 1 and 2 are assumed to depend on the same quantities, i.e.

$$\begin{matrix} \eta_1 = \eta_1(\theta, \rho_1) \\ \eta_2 = \eta_2(\theta, \rho_2) \end{matrix} \tag{7.24}$$

The chemical reaction rate $\hat{c}_1$ is constituted as a function of the temperature θ and the mass density of the constituents.

$$\begin{matrix} \hat{c}_1 = f_1(\theta, \rho_1, \rho_2) \\ \hat{c}_2 = f_2(\theta, \rho_1, \rho_2) \end{matrix} \tag{7.25}$$

At last, the heat fluxes is constituted as

$$\begin{matrix} \mathbf{q}_1 = \mathbf{f}_1(\operatorname{grad}\theta) \\ \mathbf{q}_2 = \mathbf{f}_2(\operatorname{grad}\theta) \end{matrix} \tag{7.26}$$

The differentiation of ψ_1 and ψ_2, given from (7.23), yields

$$\dot{\psi}_1 = \frac{\partial \psi_1}{\partial \theta}\dot{\theta} + \frac{\partial \psi_1}{\partial \rho_1}\dot{\rho}_1 \tag{7.27}$$

$$\dot{\psi}_2 = \frac{\partial \psi_2}{\partial \theta}\dot{\theta} + \frac{\partial \psi_2}{\partial \rho_2}\dot{\rho}_2 \tag{7.28}$$

Equation (2.138) is

$$\rho\eta = \sum_{a=1}^{\Re} \rho_a \eta_a \tag{7.29}$$

If (7.27), (7.28), and (7.29) are introduced into the simplified inequality (7.22), the result is

$$-\sum_{a=1}^{2} \rho_a \left(\frac{\partial \psi_a}{\partial \theta}\dot{\theta} + \frac{\partial \psi_a}{\partial \rho_a}\dot{\rho}_a \right) - \sum_{a=1}^{2} \rho_a \eta_a \dot{\theta} - \sum_{a=1}^{2} \mathbf{q}_a \cdot \operatorname{grad}(\theta)/\theta - \sum_{a=1}^{2} \hat{c}_a \psi_a \geq 0 \tag{7.30}$$

The mass balance for constituents 1 and 2, compare (2.49), is broken down to

$$\dot{\rho}_1 = \hat{c}_1 \tag{7.31}$$

$$\dot{\rho}_2 = \hat{c}_2 \tag{7.32}$$

since $\partial \rho_a / \partial t = \dot{\rho}_a$ when $\mathbf{x}'_a$ and $\dot{\mathbf{x}}$ is equal to zero, e.g. compare (2.49), (2.25), and (2.26). The constraint on the mass balance equation (see (2.51)) is

$$\sum_{a=1}^{2} \hat{c}_a = 0 \tag{7.33}$$

If the mass balance equations (7.31), (7.32), and the constraint (7.33) are introduced into (7.30),

$$-\sum_{a=1}^{2} \rho_a \left(\frac{\partial \psi_a}{\partial \theta} + \eta_a \right) \dot{\theta} - \sum_{a=1}^{2} \left(\rho_a \frac{\partial \psi_a}{\partial \rho_a} + \psi_a \right) \dot{\rho}_a - \sum_{a=1}^{2} \mathbf{q}_a \cdot \operatorname{grad}(\theta)/\theta \geq 0 \tag{7.34}$$

is yielded. Since $\dot{\theta}$ is an arbitrary quantity, it seems natural to define the thermodynamic laws

$$\frac{\partial \psi_1}{\partial \theta} = -\eta_1; \tag{7.35}$$

$$\frac{\partial \psi_2}{\partial \theta} = -\eta_2; \tag{7.36}$$

which assure that the first terms in (7.34) fulfill the reduced inequality.

A so-called dissipation inequality is introduced for the second term in (7.33) by replacing $\dot{\rho}_1$ with $\hat{c}_1$ and also $\dot{\rho}_2$ with $\hat{c}_2$. In other words, the equations (7.31) and (7.32) are inserted into the second term in (7.34). This yields the dissipation inequality

$$\varphi_{chem.} = -\sum_{a=1}^{2} \left(\rho_a \frac{\partial \psi_a}{\partial \rho_a} + \psi_a \right) \hat{c}_a \geq 0 \tag{7.37}$$

This inequality is valid only when the velocity of both constituents is zero, i.e. when the relation $\dot{\rho}_a = \hat{c}_a$ holds for the constituents 1 and 2. The property $\varphi_{chem.}$ will be referred to as the chemical dissipation.

It can be established that the dissipation inequality (7.37) is positive by making a proper constitutive assumption for the rate of the chemical reaction, $\hat{c}_a$, involving rather than introducing thermodynamic definitions or laws.

To obtain a constitutive relation, which describes the reaction kinetics, (7.33) must be considered, which yields

$$\hat{c}_1 = -\hat{c}_2 \tag{7.38}$$

The chemical dissipation $\varphi_{chem.}$ for the constituents 1 and 2 then becomes

$$\varphi_{chem.} = -\sum_{a=1}^{2} \left(\rho_a \frac{\partial \psi_a}{\partial \rho_a} + \psi_a \right) \hat{c}_a = -\left(\rho_1 \frac{\partial \psi_1}{\partial \rho_1} + \psi_1 - \rho_2 \frac{\partial \psi_2}{\partial \rho_2} - \psi_2 \right) \hat{c}_1 \tag{7.39}$$

This makes the constitutive relation describing the chemical reaction rate $\hat{c}_a$ restricted. The following natural choice appears attractive:

$$\hat{c}_1 = \dot{\rho}_1 = -G_{12} \left(\rho_1 \frac{\partial \psi_1}{\partial \rho_1} + \psi_1 - \rho_2 \frac{\partial \psi_2}{\partial \rho_2} - \psi_2 \right) \tag{7.40}$$

where G_{12} is a positive scalar quantity denoting a material property, which describes the reaction kinetics. From (7.40) and (7.37) it is concluded that the chemical dissipation is always positive in this case, since $\varphi_{chem.}$ is a quadratic assumption. It is noted that the chemical reaction rate $\hat{c}_1$ is a function of the mass densities ρ_1 and ρ_2 and the temperature θ, compare (7.25). This is due to the fact that ψ_1 and ψ_2 depend on the same quantities, compare (7.23).

The so-called thermal dissipation is the last term in the reduced inequality (7.34), i.e.

$$\varphi_{therm.} = -\frac{\sum_{a=1}^{2} \mathbf{q}_a}{\theta} . \operatorname{grad} \theta \geq 0 \tag{7.41}$$

If an isotropic heat flux is assumed, the thermal dissipation can be assured to be a non-negative quantity by introducing the constitutive relations

$$\mathbf{q}_1 = -\tilde{\lambda}_1 \operatorname{grad}\theta \tag{7.42}$$
$$\mathbf{q}_2 = -\tilde{\lambda}_2 \operatorname{grad}\theta \tag{7.43}$$

which means that the dissipation is quadratic in $\operatorname{grad}\theta$. Both material constants $\tilde{\lambda}_1$ and $\tilde{\lambda}_2$ are restricted to be positive scalars. When studying anisotropic heat flux problems, i.e. using an assumption of the type $\mathbf{q}_a = -\mathbf{C}_{(\lambda)a} \operatorname{grad}\theta$, the thermal dissipation inequality, i.e. $\varphi_{therm.} \geq 0$, imposes the restriction that the conductivity tensor $\mathbf{C}_{(\lambda)a}$ must be positive definite.

From the introduced thermodynamic laws (7.35) and (7.36), the expression for the rate of change of the entropies $\dot{\eta}_a$ for the constituents 1 and 2 takes the form

$$\dot{\eta}_1 = -\frac{\partial^2 \psi_1}{\partial \theta^2}\dot{\theta} - \frac{\partial^2 \psi_1}{\partial \theta \partial \rho_1}\dot{\rho}_1 \tag{7.44}$$
$$\dot{\eta}_2 = -\frac{\partial^2 \psi_2}{\partial \theta^2}\dot{\theta} - \frac{\partial^2 \psi_2}{\partial \theta \partial \rho_2}\dot{\rho}_2 \tag{7.45}$$

where it is assumed that η_1 and η_2 depend on the same quantities as ψ_1 and ψ_2 do, compare (7.24).

In addition, the energy balance equation written in the form (2.181), i.e.

$$\rho\theta\dot{\eta} + \operatorname{div}\mathbf{h} + \sum_{a=1}^{\Re} \mathbf{u}_a \cdot \hat{\mathbf{p}}_a + \sum_{a=1}^{\Re} \hat{c}_a \tfrac{1}{2} u_a^2 - \rho r \tag{7.46}$$
$$= -\sum_{a=1}^{\Re} (\rho_a \psi_a' + \hat{c}_a \psi_a) - \rho\eta\dot{\theta} + \operatorname{tr} \sum_{a=1}^{\Re} \mathbf{T}_a^{\mathrm{T}} \mathbf{L}_a$$

should be considered. With the constraints in (7.20), the simplified version of the energy equation (7.46) is

$$\rho\theta\dot{\eta} + \operatorname{div} \sum_{a=1}^{2} \mathbf{q}_a + \sum_{a=1}^{2} \rho_a \dot{\psi}_a + \sum_{a=1}^{2} \hat{c}_a \psi_a + \rho\eta\dot{\theta} = 0 \tag{7.47}$$

It follows from (7.29) that

$$\eta = \frac{1}{\rho} \sum_{a=1}^{\Re} \rho_a \eta_a \tag{7.48}$$

By the differentiation of the quantity η as

$$\dot{\eta} = \frac{1}{\rho} \sum_{a=1}^{2} (\dot{\rho}_a \eta_a + \rho_a \dot{\eta}_a) \tag{7.49}$$

where it should be observed that $\rho = const.$ due to the simplified mass balance equations (7.31) and (7.32) and due to (7.33), i.e.

$$\sum_{a=1}^{2} \hat{c}_a = \dot{\rho}_1 + \dot{\rho}_2 = \dot{\rho} = 0 \tag{7.50}$$

where also the mass balance for the mixture (2.60) and the assumption $\dot{\mathbf{x}} = \mathbf{0}$ are used.

If the assumed expressions are introduced for $\dot{\eta}_a$ and $\dot{\psi}_a$, the energy equation (7.46) can be written as

$$\begin{aligned} 0 \;=\; & \theta \sum_{a=1}^{2} \left(\dot{\rho}_a \left(-\frac{\partial \psi_a}{\partial \theta} \right) + \rho_a \left(-\frac{\partial^2 \psi_a}{\partial \theta^2} \dot{\theta} - \frac{\partial^2 \psi_a}{\partial \theta \partial \rho_a} \dot{\rho}_a \right) \right) \\ & + \text{div} \sum_{a=1}^{2} \mathbf{q}_a + \sum_{a=1}^{2} \rho_a \left(\frac{\partial \psi_a}{\partial \theta} \dot{\theta} + \frac{\partial \psi_a}{\partial \rho_a} \dot{\rho}_a \right) \\ & + \sum_{a=1}^{2} \hat{c}_a \psi_a + \sum_{a=1}^{2} \rho_a \left(-\frac{\partial \psi_a}{\partial \theta} \right) \dot{\theta} \end{aligned} \tag{7.51}$$

where (7.49), (7.44), and (7.45) together with the thermodynamic laws (7.35) and (7.36) are used. If this expression is rearranged and $\hat{c}_1$ and $\hat{c}_2$ are replaced by $\dot{\rho}_1$ and $\dot{\rho}_2$, through the use of the mass balance equations, i.e. (7.31) and (7.32), the result is

$$\begin{aligned} 0 \;=\; & \theta \sum_{a=1}^{2} \left(\dot{\rho}_a \left(-\frac{\partial \psi_a}{\partial \theta} \right) + \rho_a \left(-\frac{\partial^2 \psi_a}{\partial \theta^2} \dot{\theta} - \frac{\partial^2 \psi_a}{\partial \theta \partial \rho_a} \dot{\rho}_a \right) \right) \\ & + \text{div} \sum_{a=1}^{2} \mathbf{q}_a + \sum_{a=1}^{2} \rho_a \frac{\partial \psi_a}{\partial \rho_a} \dot{\rho}_a + \sum_{a=1}^{2} \dot{\rho}_a \psi_a \end{aligned} \tag{7.52}$$

This expression can be referred to as a generalization of the standard heat conduction equation, e.g. compare (7.9).

If the Helmholz free energies ψ_1 and ψ_2 are specified in more detail by introducing constitutive relations containing the material constants C_1, C_2, K_1, K_2,

L_1 and L_2 as

$$\psi_1(\theta, \rho_1) = C_1\theta(1 - \ln\theta) + K_1\theta/\rho_1 + L_1 \tag{7.53}$$
$$\psi_2(\theta, \rho_2) = C_2\theta(1 - \ln\theta) + K_2\theta/\rho_2 + L_2 \tag{7.54}$$

where C_1 can be referred to as the heat capacity for the constituent denoted 1, K_1 represents a factor describing the dependency of the free energy on the composition of the mixture, i.e. the relation between the mass densities ρ_1 and ρ_2 during the chemical reaction or, equally, during the phase change. The material constant $L_{12} = L_1 - L_2$ represents the latent heat effect of the reaction studied.

The needed derivatives in the energy equation (7.52) can now be written down explicitly as

$$\frac{\partial\psi_1}{\partial\theta} = -C_1\ln\theta + K_1/\rho_1 \tag{7.55}$$

which is the expression for the entropy with an opposite sign of the constituent denoted 1. The second derivative of the Helmholz free energy with respect to the temperature is

$$\frac{\partial^2\psi_1}{\partial\theta^2} = -C_1/\theta \tag{7.56}$$

Furthermore

$$\frac{\partial\psi_1}{\partial\rho_1} = -K_1\theta/\rho_1^2 \tag{7.57}$$

is obtained, and finally

$$\frac{\partial^2\psi_1}{\partial\theta\partial\rho_1} = -K_1/\rho_1^2 \tag{7.58}$$

This term can be referred to as the thermochemical coupling. That is, the constitutive relations (7.53) and (7.54) explicitly result in a predicted coupling term, which will affect the temperature distribution in the mixture.

Insertion of these assumptions into the expression (7.52) yields

$$\begin{aligned} 0 = &\sum_{a=1}^{2}\dot{\rho}_a\left(C_a\ln\theta - \frac{K_a}{\rho_a}\right)\theta + \sum_{a=1}^{2}(\rho_a C_a)\,\dot{\theta} \\ &+ \sum_{a=1}^{2}\left(\frac{K_a}{\rho_a}\dot{\rho}_a\right)\theta + \operatorname{div}\sum_{a=1}^{2}\mathbf{q}_a \\ &+ \sum_{a=1}^{2}\left(-\frac{K_a}{\rho_a}\dot{\rho}_a\right)\theta + \sum_{a=1}^{2}\dot{\rho}_a\left(C_a\theta(1 - \ln\theta) + \frac{K_a}{\rho_a}\theta + L_a\right) \end{aligned} \tag{7.59}$$

Following (7.42) and (7.43), the total heat flux $\mathbf{q}$ becomes

$$\mathbf{q} = \sum_{a=1}^{2} \mathbf{q}_a = -\left(\tilde{\lambda}_1 + \tilde{\lambda}_2\right) \operatorname{grad} \theta \tag{7.60}$$

If (7.60) is inserted into (7.59) and it is noted that some of the terms are canceled out, the result is

$$\sum_{a=1}^{2} \rho_a C_a \dot{\theta} - \operatorname{div}\left(\tilde{\lambda}_1 + \tilde{\lambda}_2\right) \operatorname{grad} \theta + \sum_{a=1}^{2} \dot{\rho}_a \left(C_a \theta + L_a\right) = 0 \tag{7.61}$$

Furthermore, the total heat flux is assumed to be weighted with the mass densities ρ_1 and ρ_2 and with a material constant m as

$$\lambda_{tot} = \tilde{\lambda}_1 + \tilde{\lambda}_2 = \left(\frac{\rho_1}{\rho}\lambda_1^m + \frac{\rho_2}{\rho}\lambda_2^m\right)^{1/m} \tag{7.62}$$

where $-1 \leq m \leq 1$.

It should be noted again that $\rho_2 = \rho - \rho_1$, $\rho = const.$, and that $\dot{\rho}_2 = -\dot{\rho}_1$. The heat equation (7.61) can then be written as

$$\left(\rho C_2 + \rho_1 \left(C_1 - C_2\right)\right) \dot{\theta} - \operatorname{div}\left(\lambda_{tot}\right) \operatorname{grad} \theta + \left(C_1 - C_2\right) \dot{\rho}_1 \theta + L_{12} \dot{\rho}_1 = 0 \tag{7.63}$$

where $L_{12} = L_1 - L_2$, and where it should be observed that $\dot{\rho}_1$ must be given from a constitutive relation of the type suggested in (7.40). This restriction is imposed on the constitutive behavior due to the second axiom of thermodynamics. If the given relations for the Helmholz free energy for the constituents are inserted into (7.40), the result is the expression for the assumed reaction kinetics.

The fifteen unknown properties in (7.21) can now be solved by using (7.40) and (7.63). That is, the temperature field $\theta\left(\mathbf{x}, t\right)$ and the two mass concentration fields $\rho_1\left(\mathbf{x}, t\right)$ and $\rho_2\left(\mathbf{x}, t\right)$ can be calculated. Note that the used equations are the two mass balance equations (7.31) and (7.32), the energy balance equation (7.31), the two thermodynamic laws for the constituents relating the Helmholz free energy to its corresponding entropies (7.35) and (7.36), the constitutive relation for the reaction kinetics (7.40) together with the restriction (7.33), the two constitutive relations for the heat flux vectors (7.42) and (7.43) (in all six equations are thus involved to describe the heat fluxes for the two constituents), and finally the two constitutive relations for the Helmholz free energy (7.53) and (7.54). That is, the number of unknown properties equals the number of equations introduced.

In order to illustrate that alternative constitutive equations yield different thermodynamic definitions and hence governing equations, yet another method will be examined. The same restrictions and unknown properties will be studied as in the previous example, i.e.

$$\begin{matrix}\rho_1(\mathbf{x},t)\\ \rho_2(\mathbf{x},t)\end{matrix};\quad \theta(\mathbf{x},t);\quad \begin{matrix}\hat{c}_1(\mathbf{x},t)\\ \hat{c}_2(\mathbf{x},t)\end{matrix};\quad \begin{matrix}\eta_1(\mathbf{x},t)\\ \eta_2(\mathbf{x},t)\end{matrix};\quad \begin{matrix}\psi_1(\mathbf{x},t)\\ \psi_2(\mathbf{x},t)\end{matrix};\quad \begin{matrix}\mathbf{q}_1(\mathbf{x},t)\\ \mathbf{q}_2(\mathbf{x},t)\end{matrix};\qquad (7.64)$$

There is one main difference compared to the first example, namely the constitutive relation for the reaction kinetics. The following rate type of assumption will be introduced:

$$\begin{matrix}\hat{c}_1 = f_1\left(\dot{\theta}\right)\\ \hat{c}_2 = f_2\left(\dot{\theta}\right)\end{matrix} \qquad (7.65)$$

which can be compared with the constitutive relations used in the first example, see (7.21). The Helmholz free energy, the entropy and the heat flux are assumed to be dependent on the same quantities as in the first example, i.e. compare (7.23), (7.24) and (7.26).

The equations for $\hat{c}_1$ and $\hat{c}_2$ will be constituted as

$$\hat{c}_1 = R_1\dot{\theta} \qquad (7.66)$$

and

$$\hat{c}_2 = R_2\dot{\theta} \qquad (7.67)$$

where R_1 and R_2 are the rate constants for the chemical reaction. From (7.33) it follows that these constants must be related as

$$R_1 + R_2 = 0 \qquad (7.68)$$

where (7.33) is used. Consider, furthermore, the reduced second axiom of thermodynamics (7.34) together with the equations (7.66) and (7.67), i.e.

$$-\sum_{a=1}^{2}\rho_a\left(\frac{\partial\psi_a}{\partial\theta}+\eta_a+R_a\frac{\partial\psi_a}{\partial\rho_a}+\frac{R_a}{\rho_a}\psi_a\right)\dot{\theta}-\sum_{a=1}^{2}\mathbf{q}_a\cdot\operatorname{grad}(\theta)/\theta\geq 0 \qquad (7.69)$$

where the relation $\dot{\rho}_a = \hat{c}_a$ is used.

The thermal dissipation $\varphi_{therm.}$, compare (7.41), is proven to be a positive quantity due to the relations (7.42) and (7.43).

In this example, the assumed reaction kinetics, i.e. (7.66) and (7.67), makes it possible to introduce the following thermodynamic definitions relating the Helmholtz free energy and the entropy for the constituents since $\dot{\theta}$ is arbitrary:

$$\frac{\partial \psi_1}{\partial \theta} + R_1 \frac{\partial \psi_1}{\partial \rho_1} + \frac{R_1}{\rho_1} \psi_1 = -\eta_1 \tag{7.70}$$

and

$$\frac{\partial \psi_2}{\partial \theta} - R_1 \frac{\partial \psi_2}{\partial \rho_2} - \frac{R_1}{\rho_2} \psi_2 = -\eta_2 \tag{7.71}$$

where equation (7.68) is used. The equations (7.70) and (7.71) are sufficient to ascertain that (7.69) is true. It should be noted, however, that a more general condition can be obtained if the thermodynamic definitions for the entropies for the two constituents are not separated.

A differentiation of (7.70) yields

$$\begin{aligned} \dot{\eta}_1 \;=\; & -\frac{\partial^2 \psi_1}{\partial \theta^2} \dot{\theta} - \frac{\partial^2 \psi_1}{\partial \theta \partial \rho_1} \dot{\rho}_1 - R_1 \frac{\partial \psi_1}{\partial \rho_1 \partial \theta} \dot{\theta} \\ & - R_1 \frac{\partial^2 \psi_1}{\partial \rho_1^2} \dot{\rho}_1 + \frac{R_1}{\rho_1^2} \psi_1 - \frac{R_1}{\rho_1} \frac{\partial \psi_1}{\partial \theta} - \frac{R_1}{\rho_1} \frac{\partial \psi_1}{\partial \rho_1} \end{aligned} \tag{7.72}$$

and a differentiation of (7.71) yields

$$\begin{aligned} \dot{\eta}_2 \;=\; & -\frac{\partial^2 \psi_2}{\partial \theta^2} \dot{\theta} - \frac{\partial^2 \psi_2}{\partial \theta \partial \rho_2} \dot{\rho}_2 + R_1 \frac{\partial \psi_2}{\partial \rho_2 \partial \theta} \dot{\theta} \\ & + R_1 \frac{\partial^2 \psi_1}{\partial \rho_2^2} \dot{\rho}_2 - \frac{R_1}{\rho_2^2} \psi_2 + \frac{R_1}{\rho_2} \frac{\partial \psi_2}{\partial \theta} + \frac{R_1}{\rho_2} \frac{\partial \psi_2}{\partial \rho_2} \end{aligned} \tag{7.73}$$

Slightly different assumptions are introduced for $\psi_1(\theta, \rho_1)$ and $\psi_2(\theta, \rho_2)$ compared to the previous example, using

$$\psi_1(\theta, \rho_1) = C_1 \theta (1 - \ln \theta) + K_1 \rho_1 + L_{12} \tag{7.74}$$

$$\psi_2(\theta, \rho_2) = C_2 \theta (1 - \ln \theta) + K_2 \rho_2 \tag{7.75}$$

where C_1, C_2, K_1, K_2, and L_{12} are material constants. The derivatives of interest in the reduced energy equation (7.52) are

$$\frac{\partial \psi_1}{\partial \theta} = -C_1 \ln \theta \tag{7.76}$$

and

$$\frac{\partial^2 \psi_1}{\partial \theta^2} = -C_1/\theta \tag{7.77}$$

and finally

$$\frac{\partial \psi_1}{\partial \rho_1} = K_1 \tag{7.78}$$

The thermochemical coupling $\partial^2 \psi_1 / (\partial \theta \partial \rho_1)$ is ignored in this example, due to the structure of the constitutive relations for $\psi_1(\theta, \rho_1)$ and $\psi_2(\theta, \rho_2)$. The same type of derivatives are obtained for the constituent denoted 2. The rest of the derivatives for the constituents are equal to zero following the assumptions (7.74) and (7.75). Hence, the explicit expressions for $\dot{\eta}_1$ become

$$\begin{aligned} \dot{\eta}_1 &= \frac{C_1}{\theta}\dot{\theta} + \frac{R_1}{\rho_1^2}\left(C_1\theta\left(1-\ln\theta\right) + K_1\rho_1 + L_{12}\right) \\ &\quad + \frac{R_1 C_1}{\rho_1}\ln\theta - \frac{R_1}{\rho_1}K_1 \end{aligned} \tag{7.79}$$

For $\dot{\eta}_2$,

$$\begin{aligned} \dot{\eta}_2 &= \frac{C_2}{\theta}\dot{\theta} - \frac{R_1}{\rho_2^2}\left(C_2\theta\left(1-\ln\theta\right) + K_2\rho_2\right) \\ &\quad - \frac{R_1 C_2}{\rho_2}\ln\theta + \frac{R_1}{\rho_2}K_2 \end{aligned} \tag{7.80}$$

is obtained. The rate of change of the Helmholz free energy is

$$\dot{\psi}_1 = -\dot{\theta} C_1 \ln\theta + K_1 \dot{\rho}_1 \tag{7.81}$$

and

$$\dot{\psi}_2 = -\dot{\theta} C_2 \ln\theta + K_2 \dot{\rho}_2 \tag{7.82}$$

where (7.27), (7.76), and (7.78) is used.

To show that the problem is complex even though the constitutive assumptions are quite simple in structure, the terms needed in the energy equation will be written down. The reduced energy equation (7.47) together with (7.49) may be written as

$$\begin{aligned} 0 &= \theta \sum_{a=1}^{\Re} \dot{\rho}_a \eta_a + \theta \sum_{a=1}^{\Re} \left(\rho_a \dot{\eta}_a\right) + \operatorname{div} \sum_{a=1}^{\Re} \mathbf{q}_a \\ &\quad + \sum_{a=1}^{\Re} \rho_a \dot{\psi}_a + \sum_{a=1}^{\Re} \hat{c}_a \psi_a + \dot{\theta} \sum_{a=1}^{\Re} \rho_a \eta_a \end{aligned} \tag{7.83}$$

The first term in (7.83) is the expression

$$\begin{aligned}\theta\sum_{a=1}^{2}\dot{\rho}_a\eta_a &= \theta\dot{\rho}_1\left(-\frac{\partial\psi_1}{\partial\theta}-R_1\frac{\partial\psi_1}{\partial\rho_1}-\frac{R_1}{\rho_1}\psi_1\right)\\ &\quad+\theta\dot{\rho}_2\left(-\frac{\partial\psi_2}{\partial\theta}+R_1\frac{\partial\psi_2}{\partial\rho_2}+\frac{R_1}{\rho_2}\psi_2\right)\end{aligned}\tag{7.84}$$

i.e.

$$\begin{aligned}\theta\sum_{a=1}^{2}\dot{\rho}_a\eta_a &= \theta\dot{\rho}_1\left(C_1\ln\theta-R_1K_1\right)\\ &\quad+\theta\dot{\rho}_1\left(-\frac{R_1}{\rho_1}\left(C_1\theta\left(1-\ln\theta\right)+K_1\rho_1+L_{12}\right)\right)\\ &\quad+\theta\dot{\rho}_2\left(C_2\ln\theta+R_1K_2\right)\\ &\quad+\theta\dot{\rho}_2\left(\frac{R_1}{\rho_2}\left(C_2\theta\left(1-\ln\theta\right)+K_2\rho_2\right)\right)\end{aligned}\tag{7.85}$$

The second term is

$$\begin{aligned}\theta\sum_{a=1}^{2}\left(\rho_a\dot{\eta}_a\right) &= \theta\rho_1\left(\frac{C_1}{\theta}\dot{\theta}+\frac{R_1}{\rho_1^2}\left(C_1\theta\left(1-\ln\theta\right)+K_1\rho_1+L_{12}\right)\right)\\ &\quad+\theta\rho_1\left(\frac{R_1C_1}{\rho_1}\ln\theta-\frac{R_1}{\rho_1}K_1\right)\\ &\quad+\theta\rho_2\left(\frac{C_2}{\theta}\dot{\theta}-\frac{R_1}{\rho_2^2}\left(C_2\theta\left(1-\ln\theta\right)+K_2\rho_2\right)\right)\\ &\quad+\theta\rho_2\left(-\frac{R_1C_2}{\rho_2}\ln\theta+\frac{R_1}{\rho_2}K_2\right)\end{aligned}\tag{7.86}$$

The third term is given by the constitutive assumptions (7.42) and (7.43). The fourth term in (7.83) is

$$\sum_{a=1}^{2}\rho_a\dot{\psi}_a=\rho_1\left(-\dot{\theta}C_1\ln\theta+K_1\dot{\rho}_1\right)+\rho_2\left(-\dot{\theta}C_2\ln\theta+K_2\dot{\rho}_2\right)\tag{7.87}$$

The fifth term is

$$\begin{aligned}\sum_{a=1}^{2}\hat{c}_a\psi_a &= \sum_{a=1}^{\Re}\dot{\rho}_a\psi_a=\dot{\rho}_1\left(C_1\theta\left(1-\ln\theta\right)+K_1\rho_1+L_{12}\right)\\ &\quad+\dot{\rho}_2\left(C_2\theta\left(1-\ln\theta\right)+K_2\rho_2\right)\end{aligned}\tag{7.88}$$

and the last term is

$$\begin{aligned} \dot{\theta} \sum_{a=1}^{2} \rho_a \eta_a &= \dot{\theta}\rho_1 \left(-\frac{\partial \psi_1}{\partial \theta} - R_1 \frac{\partial \psi_1}{\partial \rho_1} - \frac{R_1}{\rho_1} \psi_1 \right) \\ &\quad + \dot{\theta}\rho_2 \left(-\frac{\partial \psi_2}{\partial \theta} + R_1 \frac{\partial \psi_2}{\partial \rho_2} + \frac{R_1}{\rho_2} \psi_2 \right) \end{aligned} \tag{7.89}$$

i.e.

$$\begin{aligned} \dot{\theta} \sum_{a=1}^{2} \rho_a \eta_a &= \dot{\theta}\rho_1 \left(C_1 \ln \theta - R_1 K_1 \right) \\ &\quad + \dot{\theta}\rho_1 \left(-\frac{R_1}{\rho_1} \left(C_1 \theta \left(1 - \ln \theta \right) + K_1 \rho_1 + L_{12} \right) \right) \\ &\quad + \dot{\theta}\rho_2 \left(C_2 \ln \theta + R_1 K_2 \right) \\ &\quad + \dot{\theta}\rho_2 \left(\frac{R_1}{\rho_2} \left(C_2 \theta \left(1 - \ln \theta \right) + K_2 \rho_2 \right) \right) \end{aligned} \tag{7.90}$$

Some of the terms in (7.85)-(7.90) are canceled out, but the matter is still complicated. Indeed, the equation system closed, since the eleven unknown properties are given by the following introduced equations: (7.31) and (7.32) (mass balance), (7.31) (energy balance), (7.70) and (7.71) (thermodynamic laws), (7.66) (constitutive relation for the reaction kinetics) together with (7.33) (restriction), (7.42) and (7.43) (constitutive relations for the heat flux), and (7.74) and (7.75) (constitutive relations for the Helmholz free energy).

The two discussed models include the following material constants: C_1, C_2, K_1, K_2, L_{12}, and R_1 (or G_{12}). This can be compared to the number of material constants introduced in the Stefan's problem which does not include any constants related to the reaction kinetics.

The strategy discussed in this Section as a possible way to obtain equations describing the temperature field and the mass concentration field for the constituents at different times, can be extended, and cases where more than two constituents are considered can be studied. One example is the case of freezing pore water containing chlorides. In order to obtain equations for the temperature field and the mass concentration field of ice, liquid water and chlorides, a more detailed study of the reaction kinetics and the description of the Helmholz free energy for the individual constituents, must be done. Another important thermodynamic problem to be solved is cases, where phase changes occur and where

the constituents are also allowed to have a motion, i.e. when $\mathbf{x}'_a(\mathbf{x}, t) \neq \mathbf{0}$. In the presentation given in this Section, the motion was assumed to be restricted (i.e. $\mathbf{x}'_a(\mathbf{x}, t) = \mathbf{0}$). The (global) motion of liquid water during the freezing of pore water may, however, play an important rule when, for example, the damages of concrete at low temperatures are studied.

8. A few remarks on environmentally induced strains for brittle materials

In this Section, a stress-strain relation for the solid skeleton will be discussed. The properties dealt with in previous Sections will be introduced into the description of the stresses, e.g. liquid water concentration and temperature. The method used to calculate stresses and strains is the so-called smeared crack approach [55] which is a generalization of the fictitious crack model (FCM) [56]. Similar approaches can be studied in [57], [58] and [59]. The general concept of the mixture theory will not be used, since the system will be treated as one single constituent only. However, the possibilities of improving the description by introducing special properties of the individual constituents is recognized and will be discussed briefly.

The main approximation of the coupling between stress-strains and environmental effects such as temperature and moisture is that the mass and heat transfer equations can be used without considering the stresses and strains in the solid skeleton. That is, no coupling is introduced from the stress-strain calculations to the mass and heat transfer equations. Crack patterns caused by environmental and mechanical loads can, however, be predicted by the smeared crack approach. Therefore, an indirect coupling can be introduced by considering anisotropic flow properties caused by cracks for the liquid water and the dissolved matter present in the pore system.

It is noted that threshold values in terms of deformations, crack patterns and bearing capacity are important factors when trying to estimate the service life of concrete structures. This makes the description of the environmentally induced strains and stresses an important subject in durability considerations.

The smeared crack approach is believed to be a proper model when studying durability of brittle materials, since the important effect of softening is introduced. Furthermore, crack patterns and paths can be followed during loading and unloading directly, without introducing any assumption of the crack paths in advance. Stability and collapse situations of the global structure can also be studied with this approach.

It was seen from Figure 7.1 that ice growth in a pore system can be estimated by measuring deformations of a specimen. Stringent evaluations of such experiments can not, however, be performed without having a realistic description of deformations. This can be obtained by introducing the concept of stresses and strains. This Section focuses on the constitutive relation between the stress and strains for brittle materials.

In fact, the deformations induced by ice growth are also consequences of changes in temperature and liquid water concentration. These changes occur simultaneously. The material parameters such as the elastic moduli will surely also be effected in these situations. Here, such phenomena will be analyzed and it will be shown that they lead to an equation which is anisotropic and inhomogeneous in time.

A constitutive relation linking the small strain tensor $\mathbf{e}_s$, compare the definition (2.43), and the stress tensor $\mathbf{T}_s$ will be introduced. In general terms, the strains can be considered as a function of the stresses $\mathbf{T}_s$, the temperature and the liquid water concentration, etc., i.e.

$$\mathbf{e}_s = \mathbf{e}_s \left(\mathbf{T}_s, \Delta_{ref}\theta, \Delta_{ref}c_l, \Delta_{ref}c_{ice}\right) \tag{8.1}$$

where $\Delta_{ref}\theta$, $\Delta_{ref}c_l$, and $\Delta_{ref}c_{ice}$ are scalars representing the temperature difference, the difference of mass concentration of liquid water and the difference of mass concentration of ice from a reference state where no thermal or swelling expansion exists. It should be noted that the strain tensor can not be a function of the gradients of θ, c_l, and c_{ice}. Indeed, the momentum supply term $\hat{\mathbf{p}}_a$ can be constituted with gradients of θ, c_l, and c_{ice}, when the description of stresses for the individual constituents is considered.

The correctness of introducing the terms $\Delta_{ref}\theta$, $\Delta_{ref}c_l$, and $\Delta_{ref}c_{ice}$ can be studied by considering an isotropic tensor function $\mathbf{f}$ of a second order in a general case such as

$$\mathbf{M} = \mathbf{f}\left(\mathbf{N}, H_1, H_2, H_3\right) \tag{8.2}$$

where $\mathbf{M}$ and $\mathbf{N}$ are of a second order, and where H_1, H_2, and H_3 are scalars (so-called hidden or internal variables). The following must hold for the quantity $\mathbf{M}$:

$$\mathbf{M} = \alpha_1\mathbf{I} + \alpha_2\mathbf{N} + \alpha_3\mathbf{N}^2 \tag{8.3}$$

where the scalars α_1, α_2, and α_3 are material parameters, e.g. compare [60].

If $\mathbf{M} = \mathbf{e}_s$, $\mathbf{N} = \mathbf{T}_s$, $H_1 = \Delta_{ref}\theta$, $H_2 = \Delta_{ref}c_l$ and $H_3 = \Delta_{ref}c_{ice}$, are set the equation (8.3) gives

$$\mathbf{e}_s = \alpha_1\mathbf{I} + \alpha_2\mathbf{T}_s + \alpha_3\mathbf{T}_s^2 \tag{8.4}$$

where α_1, α_2, and α_3 may depend on the stress invariants $\mathrm{tr}\mathbf{T}_s$, $\mathrm{tr}\mathbf{T}_s^2$, and $\mathrm{tr}\mathbf{T}_s^3$ as well as on $\Delta_{ref}\theta$, $\Delta_{ref}c_l$, and $\Delta_{ref}c_{ice}$.

By putting

$$\alpha_1 = -\frac{v_s}{E_s} tr\mathbf{T}_s + \alpha_\theta \Delta_{ref}\theta\mathbf{I} + \alpha_l \Delta_{ref} c_l \mathbf{I} + \alpha_{ice}\Delta_{ref} c_{ice}\mathbf{I} \tag{8.5}$$

and

$$\alpha_2 = \frac{1+v_s}{E_s}; \qquad \alpha_3 = 0 \tag{8.6}$$

the following classic format of a stress-strain relation is obtained :

$$\mathbf{e}_s = \frac{1+v_s}{E_s}\mathbf{T}_s - \frac{v_s}{E_s}\left(\mathrm{tr}\mathbf{T}_s\right)\mathbf{I} + \alpha_\theta \Delta_{ref}\theta\mathbf{I} + \alpha_l \Delta_{ref} c_l \mathbf{I} + \alpha_{ice}\Delta_{ref} c_{ice}\mathbf{I} \tag{8.7}$$

That is, by insertion of (8.5) and (8.6) into (8.4). If the terms $\alpha_l \Delta c_l \mathbf{I}$ and $\alpha_{ice}\Delta c_{ice}\mathbf{I}$ are ignored the equation (8.7) represents the classical thermoelasticity problem, e.g. compare [60], [55].

The primary unknown quantities in this problem are the stress tensor $\mathbf{T}_s$ and the displacements $\mathbf{w}_s$. Hence, the equation (8.7) must be supplemented with a second equation, which is the balance of linear momentum (2.69) for the solid matrix s, i.e.

$$\mathbf{0} = \mathrm{div}\,\mathbf{T}_s + \rho\mathbf{b}_s + \hat{\mathbf{p}}_s \tag{8.8}$$

where it is assumed that the term $\rho_s \mathbf{x}_s''$ is small compared to the others, i.e. $\rho_s \mathbf{x}_s'' = \mathbf{0}$. Furthermore, the momentum supply $\hat{\mathbf{p}}_s$ will be set to zero, since the coupling is treated with the internal variables.

It should particularly be observed that the material constants α_l and α_{ice} denote the expansion of the solid as a consequence of a deviation from the reference state of mass concentrations of liquid water and ice.

In fact, using the equations (8.7) and (8.8) to calculate the stresses and strains due to mechanical and environmental loads is a method, which suffers from serious drawbacks when the formation of ice in the pore system is included. One important phenomenon is that the separate phases, i.e. the solid, liquid water and ice, exhibit different thermal contractions, which can not be explicitly modeled with the equation (8.7), since no special properties of the individual constituent are considered explicitly in the model.

To be able to somewhat capture this type of phenomena, and their effects on stresses and strains, the thermal expansion coefficient α_θ can be averaged by the mass concentration of the individual constituents. Likewise, the elasticity moduli E_s in (8.7) must be considered to be effected mainly by the mass concentration of ice. The equation (8.7) does, however, capture the behavior when a decrease in

temperature and liquid water concentration (from the reference state) contracts the material. This contraction can at the same time be canceled out due to the formation of ice. Moreover, the linear elastic description in (8.7) is not representative for brittle porous materials such as cement-based materials due to the localization of fracture. The effect of softening in fracture zones will be incorporated into the description later by introducing the concept of fracture energy G_F and slip modulus G_s.

Since the properties $\Delta_{ref}\theta$, $\Delta_{ref}c_l$, and $\Delta_{ref}c_{ice}$ can be interpreted as the rate of change of θ, c_l, and c_{ice}, i.e. $\partial\theta/\partial t$, $\partial c_l/\partial t$, and $\partial c_{ice}/\partial t$, from an initial stress free state, equation (8.7) could be written as

$$\frac{\partial \mathbf{e}_s}{\partial t} = \frac{1+v_s}{2E_s}\frac{\partial \mathbf{T}_s}{\partial t} - \frac{v_s}{E_s}\left(\mathrm{tr}\frac{\partial \mathbf{T}_s}{\partial t}\right)\mathbf{I} + \alpha_\theta \frac{\partial \theta}{\partial t}\mathbf{I} + \alpha_l \frac{\partial c_l}{\partial t}\mathbf{I} + \alpha_{ice}\frac{\partial c_{ice}}{\partial t}\mathbf{I} \tag{8.9}$$

where v_s, E_s, α_θ, α_l, and α_{ice} are material constants. Under these conditions, the equation becomes homogeneous in time. However, in order to model the important effects of changes in material parameters due to formation of ice, an inhomogeneous equation in time must be used. In other words, the elastic strains will be determined as a function of both the rate of change of stresses and the total stress state.

By identifying the first two terms on the right-hand side of (8.9) as the elastic strain components and the rest of the terms as the corresponding environmentally induced strains, can equation (8.9) simply be interpreted as the sum of strain rates, i.e.

$$\dot{\mathbf{e}}_s = \dot{\mathbf{e}}_s^e + \dot{\mathbf{e}}_s^\theta + \dot{\mathbf{e}}_s^{c_l} + \dot{\mathbf{e}}_s^{c_{ice}} \tag{8.10}$$

The tensor notation and the flexibility matrix function C^e_{ijkm} are used to link the stress and the *elastic* strain as

$$e^e_{ij} = C^e_{ijkm}T_{km} \tag{8.11}$$

According to equation (8.7), the flexibility tensor function C^e_{ijkm} can be expressed in the compact fashion

$$C^e_{ijkm} = \gamma_e \delta_{ij}\delta_{km} + \kappa_e\left(\delta_{ik}\delta_{jm} + \delta_{im}\delta_{jk}\right) \tag{8.12}$$

where

$$\gamma_e = -\frac{v_s}{E_s}; \qquad \kappa_e = \frac{1+v_s}{2E_s} \tag{8.13}$$

Allowing for the material parameters γ_e and κ_e to be changed due to ice formation in the pore system, the rate of change of the strain tensor can, according to (8.11), be obtained by differentiation as

$$\dot{e}^e_{ij} = C^e_{ijkm}\dot{T}_{km} + \dot{C}^e_{ijkm}T_{km} \tag{8.14}$$

The differentiation of γ_e yields

$$\dot{\gamma}_e = -\frac{1}{E_s}\dot{v}_s + \frac{v_s}{E_s^2}\dot{E}_s \tag{8.15}$$

and the differentiation of κ_e

$$\dot{\kappa}_e = \frac{1}{2E_s}\dot{v}_s - \frac{(1+v_s)}{2E_s^2}\dot{E}_s \tag{8.16}$$

where E_s and v_s are assumed to be functions of the mass concentration of ice in the pore system, i.e. $E_s = E_s(c_{ice}(\mathbf{x},t))$ and $v_s = v_s(c_{ice}(\mathbf{x},t))$, where v_s is the Poisson's ratio.

If (8.12), (8.15), and (8.16) are used, the rate of change of the flexibility tensor function C^e_{ijkm} can be written as

$$\dot{C}^e_{ijkm} = \dot{\gamma}_e\delta_{ij}\delta_{km} + \dot{\kappa}_e\left(\delta_{ik}\delta_{jm} + \delta_{im}\delta_{jk}\right) \tag{8.17}$$

In the same manner, the rate of change of the thermal strain contribution in (8.10) can be written as

$$\dot{e}^\theta_{ij} = \alpha_\theta\dot{\theta}\delta_{ij} + \dot{\alpha}_\theta\theta\delta_{ij} \tag{8.18}$$

where the thermal expansion coefficient α_θ for the solid as a whole is assumed to be a function of the mass concentration of ice in the pore system, i.e. $\alpha_\theta = \alpha_\theta(c_{ice}(\mathbf{x},t))$.

The expansion coefficient α_{c_l} due to changes in mass concentration of liquid water is assumed to be constant. Therefore, the rate of change of the strain tensor $e^{c_l}_{ij}$, simply becomes

$$\dot{e}^{c_l}_{ij} = \alpha_{c_l}\dot{c}_l\delta_{ij} \tag{8.19}$$

It is assumed that the strain rates induced by a variation of the mass concentration of ice from the reference stress-free state can be written as

$$\dot{e}^{c_{ice}}_{ij} = \alpha_{c_{ice}}\dot{c}_{ice}\left(\delta_{ij} + C^{c_{ice}}_{ijkm}T_{km}\right) \tag{8.20}$$

This is the format to constitute a stress-dependent environmentally induced strain proposed by e.g. [55] and [61]. The assumption (8.20) suggests that the strains due to deviation from the stress-free state in terms of mass concentration of ice are also dependent on the total stress state T_{km}. If only the effects on the strains of purely mechanical loads and changes of mass concentration of ice are considered, the constitutive relation (8.20) states that the sum of the simultaneously developed strains is not the same as the two separate strain contributions. In [55], an equation of the format (8.20) is used to simulate the well-known Pickett effect, i.e. the fact that the strains due to combined outer mechanical and moisture changes are bigger than the sum of the strains when these phenomena occur separately. In [61], an equation of the same format, i.e. (8.20), is used to model the stress-strain behavior of concrete at high temperatures.

The two material constants in the flexibility tensor $C_{ijkm}^{c_{ice}}$ which describe the stress dependency of ice-induced strains are given by the isotropic linear elastic format as

$$C_{ijkm}^{c_{ice}} = \gamma_{c_{ice}} \delta_{ij} \delta_{km} + \kappa_{c_{ice}} \left(\delta_{ik} \delta_{jm} + \delta_{im} \delta_{jk} \right) \tag{8.21}$$

As discussed in Section 7, the expansion of the solid skeleton due to transformation of water (or vapor) to ice can not totally be interpreted as the volume expansion during such transformations, since the water/ice transformation may occur in partly empty pore spaces. Furthermore, due to moisture transport during freeze/thaw, the effect of the spacing factor between the larger pores must be considered. Compare the discussion in Section 7.

The important effect of localization of fracture will be introduced in the stress-strain relation by an additional term describing the strain rate in the fracture zones, denoted $\dot{\mathbf{e}}_s^f$. Hence, the total strain rate is written as

$$\dot{\mathbf{e}}_s = \dot{\mathbf{e}}_s^e + \dot{\mathbf{e}}_s^\theta + \dot{\mathbf{e}}_s^{c_l} + \dot{\mathbf{e}}_s^{c_{ice}} + \dot{\mathbf{e}}_s^f \tag{8.22}$$

In order to evaluate $\dot{\mathbf{e}}_s^f$ in both loading and unloading situations, the so-called smeared crack approach suggested in [55] is used. This model is, however, extended to account for the material parameters describing the fracture zone dependent on the mass concentration of ice in the pore system.

In essence, the smeared crack approach in [55] suggests that a crack will be initiated if the tensile strength f_t in the principal direction of the stress is reached. The crack is assumed to be located normal to the principal direction of the stresses in a representative volume (REV).

Softening or loading and unloading is assumed to occur in this crack depending on the loading, i.e. the deformation in the crack is assumed to be partly recoverable. If the stress in the principal direction normal to the first developed crack in REV reaches the tensile strength f_t, a second crack will be assumed to develop perpendicular to the first created crack within the same domain. Furthermore, a third crack may develop in the same manner and perpendicular to the other two cracks.

To describe the method, a local coordinate system $\mathbf{x}^*$ is introduced, where x_1^*-axis is the direction normal to the first developed crack. If a second crack is initiated, the x_2^*-axis will be normal to that crack plane. That is, the coordinate system $\mathbf{x}^*$ will be orthogonal due to the assumptions of crack patterns within REV.

The smeared crack approach suggested in [55] is a generalization of the fictitious crack model according to [56] and [62]. This latter model is based on the fact that when a specimen is loaded in tension, fracture is localized in a thin zone only. The deformation caused by the fracture in this zone is modelled by a fictitious crack, the width w_α^* of which represents the total fracture deformation in the zone. The material outside the fracture zone is assumed to be unaffected by cracking, but in a global sense, the domain outside the fracture zone will be unloaded due to the consumption of strain energy in the crack.

If a global domain is considered it is possible to follow the development of a crack pattern in time using the smeared crack approach. This makes the method useful when considering environmentally induced loads, since they generally change with time.

The energy G_F necessary to create one unit area of an open traction-free crack is defined by the integral

$$G_F = \int_0^{w_c} T_{\alpha\alpha}^* dw_\alpha^* \tag{8.23}$$

where $T_{\alpha\alpha}^*$ is the stress component normal to the crack plane, and w_α^* is the total deformation in the cracked zone normal to the crack plane. The notations α and β are used for the crack numbers 1 and 2 in REV, and are also used for directions perpendicular to the cracks. In fact, α and β will be used as tensor indici, but the summation convention is not applied for repeated index. The value w_c represents the deformation in the crack zone when the normal stress has dropped to zero.

For simplicity, a linear function between $T^*_{\alpha\alpha}$ and w^*_α, is assumed as

$$T^*_{\alpha\alpha} = f_t + N w^*_\alpha \tag{8.24}$$

where f_t is the uniaxial tensile strength and N is the (negative) slope of the function $T^*_{\alpha\alpha}(w^*_\alpha)$. The function (8.24) describes the stress-deformation relation during softening in the developed fracture zone. The tensile strength can be interpreted as a local failure criterion.

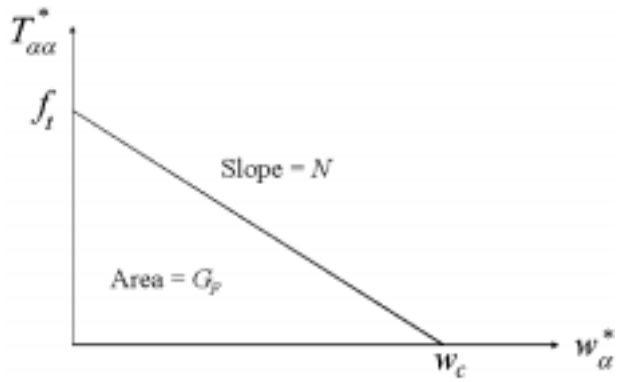

Figure 8.1: *Relation between the stress and crack width normal to the crack plane.*

In order to somewhat capture the effect of ice formation in the pore system on the stiffness in the developed crack, it is assumed that the initiation of fracture, i.e. when $T^*_{\alpha\alpha} = f_t$, is dependent on the concentration of ice in the material.

The initiation criterion $T^*_{\alpha\alpha} = f_t(c_{ice})$ is adopted. The fracture energy G_F, is assumed to be constant and hence independent of the concentration of ice. These assumptions mean that the softening behavior becomes somewhat more brittle. Therefore, the fracture zone will sustain a lower maximum strain if the initiation of a crack occurs at a high tensile stress compared to an initiation at a low tensile stress. It must be noted, however, that the total dissipated energy to create a traction-free fully opened crack is the same independently of the initiation criterion. Furthermore, it is assumed that the 'stiffness' defined by the negative slope of the softening stress-strain curve in the fracture zone N, is a constant determined solely by G_F and the initiation criterion $f_t(c_{ice})$, see Figure 8.1. Hence, N is assumed to be constant independently of changes of the concentration of ice after the crack has been initiated. The properties $E_s = E_s(c_{ice}(\mathbf{x}, t))$ and

$v_s = v_s(c_{ice}(\mathbf{x}, t))$, describing the material outside the fracture zone also contribute to a change in the global response as the ice concentration is changed.

According to (8.24), the value w_c can be expressed as

$$w_c = -\frac{f_t}{N} \tag{8.25}$$

If this relation is used together with (8.23) and (8.24), the slope N can be expressed as

$$N = -\frac{f_t^2}{2G_F} \tag{8.26}$$

which shows that the slope N in the fracture zone is high if the initiation of the crack occurs at a high tensile stress f_t, since the fracture energy G_F is assumed to be constant. Furthermore, the deformation w_c, which corresponds to a traction-free crack, will be affected in a similar way, compare (8.24).

In order to add the elastic and fracture deformations, it is convenient to introduce the concept of strains. A fracture (small) strain tensor $\mathbf{e}^f$ is introduced, which represents the mean strain in a region that includes a discrete crack. In the introduced local coordinate system, the fracture strain $e^{*f}_{\alpha\alpha}$, i.e. the strain normal to the crack plane, is defined as

$$e^{*f}_{\alpha\alpha} = \frac{w^*_\alpha}{L_\alpha} \tag{8.27}$$

where L_α is the equivalent length associated with the direction of the crack and the shape of the local domain (e.g. a local finite element), where the crack is formed.

The length L_α can, however, not be chosen arbitrarily. By considering the case of maximum elastic energy stored in a linear elastic material in a one-dimensional case given as

$$W^{*e}_{\alpha\alpha} = \frac{1}{2}\frac{f_t^2}{E} \tag{8.28}$$

where E is the elastic modulus, and where the maximum tensile stress is denoted f_t, and the total dissipation energy is

$$W^{*f}_{\alpha\alpha} = G_F \tag{8.29}$$

The ratio between the maximum elastic energy and the total dissipation energy is introduced as

$$\lambda^f = \frac{W^{*f}_{\alpha\alpha}}{W^{*e}_{\alpha\alpha}} = \frac{2G_F E}{f_t^2} \tag{8.30}$$

From (8.26) and (8.30), it follows that

$$N = -\frac{E}{\lambda^f} \tag{8.31}$$

where λ^f (m) is referred to as the characteristic length, which is a measure of the brittleness of the material.

By using (8.24) and (8.27), the stress-strain relation in the softening zone can be expressed as

$$T^*_{\alpha\alpha} = f_t + NL_\alpha e^{*f}_{\alpha\alpha} \tag{8.32}$$

If it is assumed for the moment that the parameters f_t, N and L_α are constant properties, the rate of change of stresses normal to the crack plane can be written as

$$\dot{T}^*_{\alpha\alpha} = NL_\alpha \dot{e}^{*f}_{\alpha\alpha}$$

If lateral deformations in the crack are ignored, the sum of the rate of change of the fracture and elastic strains becomes

$$\dot{e}^*_{\alpha\alpha} = \dot{e}^{*f}_{\alpha\alpha} + \dot{e}^{*e}_{\alpha\alpha} = \left(\frac{1}{NL_\alpha} + \frac{1}{E}\right)\dot{T}^*_{\alpha\alpha} \tag{8.33}$$

If (8.33) is written as

$$\dot{T}^*_{\alpha\alpha} = \frac{E}{1 + \frac{E}{NL_\alpha}}\dot{e}^*_{\alpha\alpha} = \frac{E}{1 - \frac{\lambda^f}{L_\alpha}}\dot{e}^*_{\alpha\alpha} \tag{8.34}$$

where (8.31) is used, it becomes clear that the restriction

$$L_\alpha < \lambda^f \tag{8.35}$$

must hold, since the slope of the stress-strain curve must be negative in the softening zone. In other words, an elongation in the softening zone must correspond to a decrease of the tensile stress normal to the crack plane. Furthermore, it is shown in [63] that a general three-dimensional case must fulfill the following safe restrictions:

$$L_1 < \frac{\lambda^f}{1+v}; \qquad L_2 < \frac{\lambda^f}{1+v}; \qquad L_3 < \frac{\lambda^f}{1+v}; \tag{8.36}$$

The characteristic length λ^f is measured to be λ^f = 10-30 (mm) for cement paste, 200-400 (mm) for cement mortar, and 400-800 (mm) for normal concrete [64]. That is, the element sizes (or the size of REV) L_α can be chosen with

considerable freedom. It should be noted, however, that λ^f is given by (8.31), hence the safe restriction must be checked for all possible initiations in terms of $T^*_{\alpha\alpha} = f_t(c_{ice})$, since this criterion together with a constant G_F determines the N-value. Furthermore, the elastic modulus E in the undamaged neighboring zones is assumed to be a function of the concentration of ice, i.e. $E(c_{ice})$, during fracturing also. The restriction (8.35) will therefore be changed into the more severe criterion

$$\lambda^f_{\min} = -\frac{E_{\min}}{N_{\max}}; \qquad L_\alpha < \lambda^f_{\min} \tag{8.37}$$

where $E_{\min}$ is the lowest possible elastic modulus (i.e. when the ice concentration is zero) and $N_{\max}$ is the highest possible negative slope in the softening zone (i.e. the initiation of fracture occurs when the concentration of ice in the pore system is at maximum). It should be noted that this is a local restriction. The global response might be subjected to so-called snap-back phenomena without violating the local safety restriction $L_\alpha < \lambda^f_{\min}$.

If (8.27) and (8.24) are combined, and also differentiated with respect to time, the rate of change of the strain $\dot{e}^{*f}_{\alpha\alpha}$ is given as

$$\dot{e}^{*f}_{\alpha\alpha} = J_\alpha \dot{T}^*_{\alpha\alpha} \tag{8.38}$$

where the compliance J_α becomes

$$J_\alpha = \frac{1}{(NL_\alpha)} \quad (\text{when: } \dot{w}^*_\alpha > 0 \text{ and } w^*_\alpha = w^*_{\alpha\max}) \tag{8.39}$$

and where $w^*_{\alpha\max}$ is the previously obtained maximum crack opening length. This is simply an indicator controlling whether the total stress-strain point is on the loading surface described by the material function $T^*_{\alpha\alpha} = T^*_{\alpha\alpha}(w^*_\alpha)$ or not. The rate of change of the deformation in the crack plane is denoted $\dot{w}^*_\alpha$.

Since the unloading in fracture zones is of importance due to outer climatic load variations, some realistic assumptions on the behavior of crack closing must be introduced. The following linear assumption is made for the relation between the tensile stress and the crack width normal to the crack plane, [55]:

$$w^*_\alpha = \left[\gamma_f + \left(1 - \gamma_f\right)\frac{T^*_{\alpha\alpha}}{f_\alpha}\right] w^*_{\alpha\max} \tag{8.40}$$

The parameter f_α, is according to (8.24) and Figure 8.2, written as

$$f_\alpha = f_t + N w^*_{\alpha\max} \tag{8.41}$$

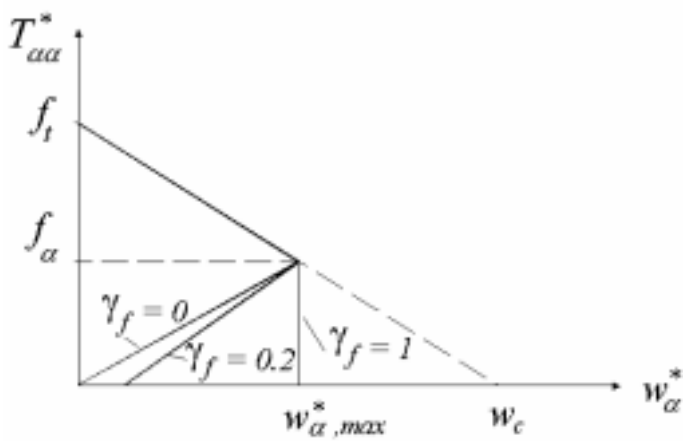

Figure 8.2: *Different assumed unloading paths, [55].*

$\gamma_f = 0$ represents a total recovery of the fracture when the stress normal to the crack plane reaches zero. $\gamma_f = 1$ represents the situation, when the fracture is totally irrecoverable, compare Figure 8.2. In [55], the value $\gamma_f = 0.2$ is suggested, since this value fairly well captures the effect of partially recoverable fractures found experimentally in [65].

Substitution of equation (8.27) into (8.40) gives

$$e^{*f}_{\alpha\alpha} = \left[\gamma_f + \left(1-\gamma_f\right)\frac{T^*_{\alpha\alpha}}{f_\alpha}\right]\frac{w^*_{\alpha\max}}{L_\alpha} \tag{8.42}$$

and differentiation gives

$$\dot{e}^{*f}_{\alpha\alpha} = \left(1-\gamma_f\right)\frac{w^*_{\alpha\max}}{L_\alpha\left(f_t + N w^*_{\alpha\max}\right)}\dot{T}^*_{\alpha\alpha} \tag{8.43}$$

where also (8.40) is used. When the actual crack deformation is smaller than $w^*_{\alpha\max}$, and when the stress normal to the crack is positive the compliance J_α can, according to (8.43), be identified as

$$J_\alpha = \left(1-\gamma_f\right)\frac{w^*_{\alpha\max}}{L_\alpha\left(f_t + N w^*_{\alpha\max}\right)} \text{ (when: } w^*_\alpha < w^*_{\alpha\max} \text{ and } T^*_{\alpha\alpha} > 0) \tag{8.44}$$

When γ_f is constant, the compliance J_α during elastic unloading and loading in the softening zone is different, depending on at which value of the tensile strength $f_t(c_{ice})$ the crack is initiated.

During situations with compressive loading in a previously developed fracture zone, the deformation is assumed to be given by the isotropic linear elasticity relation (8.14). Thus the fracture strain rate in compression is assumed to be zero.

$$J_\alpha = 0 \ \text{(compression; i.e. } T^*_{\alpha\alpha} < 0) \tag{8.45}$$

The shear displacement in the crack plane (in the direction of the β axis), denoted $w^{*s}_{\alpha\beta}$, is an important property when the stress-strain relations for general geometries and loadings are studied. In [66], it is proposed that the shear displacement can be approximated by

$$w^{*s}_{\alpha\beta} = \frac{w^*_\alpha}{G_s} T^*_{\alpha\beta}; \qquad (\alpha \neq \beta) \tag{8.46}$$

where, again, w^*_α is the crack width directed normal to the crack plane. The material parameter G_s can be referred to as the slip modulus in the fracture zone. The stress component $T^*_{\alpha\beta}$ denotes the shear stress in the crack plane.

It should be observed that the stress normal to the crack plane also affects the shear displacement $w^{*s}_{\alpha\beta}$, and that the fracture process zone is path-dependent when both normal and shear displacements in the fracture process zone are considered [67]. This effect will, however, not be included in the model.

By defining the shear strains in the same manner as in conventional kinematic and elastic theories and by, again, introducing the equivalent lengths L_α and L_β, [55],

$$e^{*f}_{\alpha\beta} = \frac{1}{2}\left(\frac{w^{*s}_{\alpha\beta}}{L_\alpha} + \frac{w^{*s}_{\beta\alpha}}{L_\beta}\right); \qquad (\alpha \neq \beta) \tag{8.47}$$

is obtained. The relations (8.27) and (8.46) give

$$w^{*s}_{\alpha\beta} = \frac{L_\alpha e^{*f}_{\alpha\alpha}}{G_s} T^*_{\alpha\beta} \quad \text{and} \quad w^{*s}_{\beta\alpha} = \frac{L_\beta e^{*f}_{\beta\beta}}{G_s} T^*_{\beta\alpha}; \qquad (\alpha \neq \beta) \tag{8.48}$$

If the symmetry of stresses in the crack plane, written as $T^*_{\alpha\beta} = T^*_{\beta\alpha}$ is considered, equations (8.47) and (8.48) give

$$e^{*f}_{\alpha\beta} = \frac{1}{2}\left(e^{*f}_{\alpha\alpha} + e^{*f}_{\beta\beta}\right)\frac{T^*_{\alpha\beta}}{G_s}; \qquad (\alpha \neq \beta) \tag{8.49}$$

where it should be noted that equivalent lengths L_α and L_β cancels.

Table 8.1: Introduced material constants and parameters.

Mat. param.	Remarks
$v_s(c_{ice})$	*Poisson's ratio*
$E_s(c_{ice})$	*Elastic moduli*
G_F	*Fracture energy, assumed constant*
$f_t(c_{ice})$	*Init. crit. for fracture, also determines the stiffn. in softening*
γ_f	*Unloading and reloading in the softening zone*
G_s	*Slip modulus in the fractured plane*
$\alpha_\theta(c_{ice})$	*Thermal expansion parameter*
α_{c_l}	*Moisture expansion parameter*
$\alpha_{c_{ice}}$	*Ice expansion parameter*
$\gamma_{c_{ice}}$ *and* $\kappa_{c_{ice}}$	*Stress dependent strains due to ice formation*

The rate of shear strain in the crack plane is obtained by differentiating (8.49). The material parameter G_s is considered to be constant. Then equation (8.49) becomes

$$\dot{e}^{*f}_{\alpha\beta} = \left(\dot{e}^{*f}_{\alpha\alpha} + \dot{e}^{*f}_{\beta\beta}\right)\frac{T^*_{\alpha\beta}}{2G_s} + \left(e^{*f}_{\alpha\alpha} + e^{*f}_{\beta\beta}\right)\frac{\dot{T}^*_{\alpha\beta}}{2G_s}; \qquad (\alpha \neq \beta) \tag{8.50}$$

The properties $\dot{e}^{*f}_{\alpha\alpha}$ and $\dot{e}^{*f}_{\beta\beta}$ are replaced with the relation (8.38), thus the equation (8.50) can be written as

$$\dot{e}^{*f}_{\alpha\beta} = B_{\alpha\beta}\dot{T}^*_{\alpha\alpha} + B_{\beta\alpha}\dot{T}^*_{\beta\beta} + A_{\alpha\beta}\dot{T}^*_{\alpha\beta}; \qquad (\alpha \neq \beta) \tag{8.51}$$

where

$$A_{\alpha\beta} = \frac{e^{*f}_{\alpha\alpha} + e^{*f}_{\beta\beta}}{2G_s}; \qquad (\alpha \neq \beta) \tag{8.52}$$

and

$$B_{\alpha\beta} = \frac{J^*_\alpha T^*_{\alpha\beta}}{2G_s}; \quad B_{\beta\alpha} = \frac{J^*_\beta T^*_{\alpha\beta}}{2G_s}; \quad (\alpha \neq \beta) \tag{8.53}$$

where the symmetry condition $T^*_{\alpha\beta} = T^*_{\beta\alpha}$ was used.

The general linear relation between the rate of change of the stress tensor $\dot{T}^*_{rs}$ and the rate of change of the fracture strain tensor $\dot{e}^{*f}_{pq}$ in the local Cartesian coordinate system (which orientation in relation to the global coordinate system depends on the orientation of the induced fracture) can be written in tensor format

as (e.g. compare [60])

$$\dot{e}^{*f}_{pq} = C^{*f}_{pqrs}\dot{T}^{*}_{rs} \tag{8.54}$$

where the fracture flexibility tensor C^{*f}_{pqrs} is assumed to be constant with respect to loading within the time increment considered. Moreover, in the general case, the symmetry of T^{*}_{rs} and e^{*f}_{pq} gives the following relation:

$$C^{*f}_{pqrs} = C^{*f}_{pqsr}; \quad C^{*f}_{pqrs} = C^{*f}_{qprs} \tag{8.55}$$

The symmetry property given by the restriction for hyper-elastic materials (e.g. compare [60]) gives

$$C^{*f}_{pqrs} = C^{*f}_{rspq} \tag{8.56}$$

where it should be noted that a somewhat inconsistent assumption is introduced, since hyper-elasticity requires that an additional condition is imposed on the material functions α_1, α_2, and α_3, compare (8.4). This restriction stems from the second axiom of thermodynamics, compare [60] for details. Here, it will be assumed, however, that it is sufficient to use the symmetry condition (8.38) both for loading and unloading in the softening zone. The complications involved in satisfying the dissipation conditions (i.e. the second axiom of thermodynamics) are the reason why no consideration is taken to changes of properties in the softening zone due to for example ice formation, once the crack propagation has been initiated.

By considering (8.38) and (8.50) together with the symmetry properties of the flexibility tensors (8.55) and (8.56), the following components can be identified [55]:

$$C^{*f}_{1111} = J_1; \quad C^{*f}_{2222} = J_2; \quad C^{*f}_{3333} = J_3 \tag{8.57}$$

$$C^{*f}_{1212} = C^{*f}_{1221} = C^{*f}_{2112} = C^{*f}_{2121} = \frac{A_{12}}{2} \tag{8.58}$$

$$C^{*f}_{2323} = C^{*f}_{2332} = C^{*f}_{3223} = C^{*f}_{3232} = \frac{A_{23}}{2} \tag{8.59}$$

$$C^{*f}_{1212} = C^{*f}_{1221} = C^{*f}_{2112} = C^{*f}_{2121} = \frac{A_{31}}{2} \tag{8.60}$$

$$C^{*f}_{1211} = C^{*f}_{2111} = B_{12} \tag{8.61}$$

$$C^{*f}_{1222} = C^{*f}_{2122} = B_{21} \tag{8.62}$$

$$C^{*f}_{2322} = C^{*f}_{3222} = B_{23} \tag{8.63}$$

$$C^{*f}_{2333} = C^{*f}_{3233} = B_{32} \tag{8.64}$$

$$C^{*f}_{3133} = C^{*f}_{1333} = B_{31} \tag{8.65}$$

$$C^{*f}_{3111} = C^{*f}_{1311} = B_{13} \tag{8.66}$$

All other components are zero. It should be noted that A_{12}, A_{23}, and A_{31} are divided by the factor two to compensate for the fact that the rate of change of T^*_{rs} appears as T^*_{rs} and T^*_{sr}, and for the fact that $T^*_{rs} = T^*_{sr}$ due to symmetry.

The stress and fracture strain rate tensors expressed in the local coordinate system (given by the directions of the crack planes) can be transformed to a global coordinate system by the standard transformation rules

$$\dot{T}^*_{rs} = a_{rk} a_{sm} \dot{T}_{km} \tag{8.67}$$

and

$$\dot{e}^f_{ij} = a_{pi} a_{qj} \dot{e}^{*f}_{pq} \tag{8.68}$$

The tensor property a_{rk} represents the $\cos\varphi_{rk}$ values, where φ_{rk} is the angle between the local x^*_r-axis and the global x_k-axis.

The relation between the fracture strain rate and stress rate in the global system can be formed by combining (8.54) and (8.68) as

$$\dot{e}^f_{ij} = a_{pi} a_{qj} C^{*f}_{pqrs} \dot{T}^*_{rs} \tag{8.69}$$

Then, by introducing (8.67) into (8.69),

$$\dot{e}^f_{ij} = a_{pi} a_{qj} C^{*f}_{pqrs} a_{rk} a_{sm} \dot{T}_{km} \tag{8.70}$$

is obtained. That is, the fracture behavior can be considered in the local orthogonal coordinate system x^*_r (determined by the direction of the first and the second induced crack in the same REV) and then be transformed to the global system by the transformation $a_{pi} a_{qj} C^{*f}_{pqrs} a_{rk} a_{sm}$.

Since the elastic part of the strains is isotropic, i.e. independent of any transformation of coordinates, the homogeneous part of the elastic flexibility tensor can be written as $C^e_{pqrs} = C^{*e}_{pqrs}$. Then, it follows that the elastic flexibility tensor and the fracture flexibility tensor in the local coordinate system relating the global strain rate and stress rate are additative. In principle, one can illustrate this by the relation

$$C^{*f+e}_{pqrs} = C^e_{pqrs} + C^{*f}_{pqrs} \tag{8.71}$$

The sum of the fracture and elastic strain rates can therefore be written as a function of the stress rates $\dot{T}_{km}$ and the total stress state T_{km} as

$$\dot{e}_{ij}^{e+f} = a_{pi}a_{qj}C_{pqrs}^{*f+e}a_{rk}a_{sm}\dot{T}_{km} + \dot{C}_{ijkm}^{e}T_{km} \tag{8.72}$$

where it should be noted that the constitutive relation for the elastic strain, i.e. (8.14), makes the equation inhomogeneous in time due to the modelling of the rate of change of E_s and v_s caused by ice formation in the pore system. Furthermore, the description of the material in the global coordinate system will be anisotropic due to cracking.

The total contribution of strains, including environmental effects, is

$$\dot{e}_{ij} = a_{pi}a_{qj}C_{pqrs}^{*f+e}a_{rk}a_{sm}\dot{T}_{km} + \dot{C}_{ijkm}^{e}T_{km} + \dot{e}_{ij}^{\theta} + \dot{e}_{ij}^{c_l} + \dot{e}_{ij}^{c_{ice}}$$

where the constitutive relations for $\dot{e}_{ij}^{\theta}$, $\dot{e}_{ij}^{c_l}$, and $\dot{e}_{ij}^{c_{ice}}$ are given by (8.18), (8.19), and (8.20) respectively. These relations include the changes of θ, c_l, and c_{ice} from a defined reference state. It is supposed that these quantities can be calculated using the equations discussed in previous Sections, i.e. without considering any coupling of stress and strains in the heat and mass transfer equations.

However, since crack patterns caused by environmental and mechanical loads can be predicted by the smeared crack approach, anisotropic flow properties can be introduced for the water, vapor, and dissolved matter in the pore solution, e.g. compare [68] and [69]. This means that an indirect coupling of deformations can be introduced into the mass transfer equations. This is realized to be an important effect, which can easily be introduced into the mass transport equations discussed in the previous Sections.

A numerical solution within the finite element concept has been established by the originators to the presented smeared crack approach and will therefore not be discussed, compare [55].

9. Numerical methods in transient problems

In this Section, a presentation of the *weak forms* of the mass balance and linear momentum equations in Cartesian coordinates will be discussed. The general frame-independent description will now be dropped in favor of a matrix presentation in Cartesian coordinates.

Indeed, the weak form of a differential equation does not arise from any approximations introduced and therefore it may be surprising that it is discussed in association with numerical methods. However, the finite element method (FEM) is based on this formulation.

The finite element method can be studied in, for example, [70], [71], [72], and [73].

9.1. Weak formulation of the mass balance equations

The mass balance equation appears, typically, in the following form, e.g. compare with (2.56) and (2.57):

$$\rho\frac{\partial c_a}{\partial t} + \rho\dot{\mathbf{x}}\cdot\operatorname{grad} c_a = -\operatorname{div}(\rho_a\mathbf{u}_a) + \hat{c}_a \tag{9.1}$$

which can be referred to as a *strong formulation*. This equation will now be reformulated using a Cartesian coordinate system. At the end of this section, the weak form of (9.1) will be reached.

When an uncoupled equation with only one unknown parameter is considered, e.g. a temperature or a mass concentration, there are no additional assumptions introduced when reaching the weak formulation. It should be clear, however, that the field equations to be discussed will be somewhat limited as they only hold in the Cartesian coordinate system.

Here, a set of coupled equations are to be solved. For the sake of simplicity, it is assumed that it is possible to find a suitable method to solve the individual equations separately by a *staggered solution procedure*. This means that it is assumed that a correct solution path can be followed by solving one equation for one parameter by having the other coupling terms, determined from other equations, constant during a short time-step. If equation (9.1) is used as an example, this means that the mass concentration c_a is solved, assumed that the properties ρ, $\dot{\mathbf{x}}$, and $\hat{c}_a$ can be considered constant during a short time-step. The justness of such an assumption could, simply speaking, be checked by gradually reducing the length of the time-step until the solution converges. This subject

will be discussed in more detail in association with stability and convergence requirements.

To distinguish the general operators div and grad, which hold in any frame, from the operators in the Cartesian frame, the following notation will be made:

$$\nabla\cdot \equiv \text{div}; \quad \nabla \equiv \text{grad} \tag{9.2}$$

For simplicity reasons, the following change of property denomination will be introduced: $\mathbf{j}_a = \rho_a \mathbf{u}_a$. Furthermore, c_a will be replaced by a potential ϕ_a, which can be interpreted as the mass concentration c_a, or the temperature θ. The potential ϕ_a is introduced due to the fact that, in a numerical sense, there is no distinction between the two balance equations as they appear in this work, e.g. compare (3.8) and (3.20).

The first step towards the weak formulation is to introduce an arbitrary function $v(\mathbf{x})$, which is a scalar function of spatial position only. There is no assumption involved in multiplying expression (9.1) with v and integrating over a representative volume V as

$$\int_V v\nabla\cdot\mathbf{j}_a\,dV + \int_V v\rho\frac{d\phi_a}{dt}\,dV + \int_V v\rho\dot{\mathbf{x}}^{\mathrm{T}}\nabla\phi_a\,dV - \int_V v\hat{c}_a\,dV = 0 \tag{9.3}$$

where the column vector properties are defined

$$\mathbf{j}_a = \begin{bmatrix} j_{1a} \\ j_{2a} \\ j_{3a} \end{bmatrix};\ \dot{\mathbf{x}} = \begin{bmatrix} \dot{x}_1 \\ \dot{x}_2 \\ \dot{x}_3 \end{bmatrix} \tag{9.4}$$

and the gradient operator on ϕ_a and the divergence operator on $\mathbf{j}_a$, are defined

$$\nabla\phi_a = \begin{bmatrix} \frac{d\phi_a}{dx_1} \\ \frac{d\phi_a}{dx_2} \\ \frac{d\phi_a}{dx_3} \end{bmatrix}; \quad \nabla\cdot\mathbf{j}_a = \frac{dj_{1a}}{dx_1} + \frac{dj_{2a}}{dx_2} + \frac{dj_{3a}}{dx_3} \tag{9.5}$$

The *Green-Gauss theorem* applied to the first term on the left-hand side of (9.3) gives

$$\int_V v\nabla\cdot\mathbf{j}_a dV = \oint_S v\mathbf{j}_a^{\mathrm{T}}\mathbf{n}\,dS - \int_V (\nabla v)^{\mathrm{T}}\mathbf{j}_a\,dV \tag{9.6}$$

where $\mathbf{n}$ is the unit vector, normal to the boundary S, and directed out of the region V and ∇v is the gradient operating on the arbitrary scalar function v. The

properties are defined by the following column vectors:

$$\nabla v = \begin{bmatrix} \frac{dv}{dx_1} \\ \frac{dv}{dx_2} \\ \frac{dv}{dx_3} \end{bmatrix}; \ \mathbf{n} = \begin{bmatrix} n_1 \\ n_2 \\ n_3 \end{bmatrix}; \ |\mathbf{n}| = 1 \tag{9.7}$$

If (9.6) is inserted into (9.3)

$$\begin{aligned} \int_V (\nabla v)^{\mathrm{T}} \, \mathbf{j}_a \, dV &= \oint_S v \mathbf{j}_a^{\mathrm{T}} \mathbf{n} \, dS + \int_V v\rho \frac{d\phi_a}{dt} \, dV \\ &\quad + \int_V v\rho \dot{\mathbf{x}}^{\mathrm{T}} \nabla \phi_a \, dV - \int_V v\hat{c}_a \, dV \end{aligned} \tag{9.8}$$

is yielded. To solve the differential equation (9.8), boundary conditions are required. These boundary conditions may, typically, be of the form

$$j_{an} = \mathbf{j}_a^{\mathrm{T}} \mathbf{n} = h_a \qquad \text{on } S_{\mathrm{h}} \tag{9.9}$$

$$\phi_a = g_a \qquad \text{on } S_{\mathrm{g}} \tag{9.10}$$

where h_a and g_a are known quantities. S_{h} is that part of the boundary S, on which the flow, or flux j_{an}, is known (*natural boundary condition*), whereas S_{g}, is the part of the boundary S on which the properties ϕ_a are known (*essential boundary condition*). The sum of the boundaries S_{h} and S_{g} constitute the entire boundary S. It should be noted, however, that it is possible to describe the known properties h_a and g_a in the same position. The boundary conditions (9.9) and (9.10) can also be described in terms of combinations of j_{an} and ϕ_a, which are often adopted when convection occurs along the boundary.

Insertion of the natural boundary condition (9.9) into (9.8) yields

$$\begin{aligned} \int_V (\nabla v)^{\mathrm{T}} \, \mathbf{j}_a \, dV &= \oint_{S_{\mathrm{h}}} v h_a \, dS + \oint_{S_{\mathrm{g}}} v j_{an} \, dS + \int_V v\rho \frac{d\phi_a}{dt} \, dV \\ &\quad + \int_V v\rho \dot{\mathbf{x}}^{\mathrm{T}} \nabla \phi_a \, dV - \int_V v\hat{c}_a \, dV \end{aligned} \tag{9.11}$$

$$\phi_a = g_a \qquad \text{on } S_{\mathrm{g}} \tag{9.12}$$

where h_a is a known quantity along S_{h}, whereas the flux j_{an} is unknown along the boundary S_{g}.

The two equations (9.11) and (9.12) are called the weak form, in which the constitutive relation for $\mathbf{j}_a$ has not yet been introduced.

The equation considered is not only a function of spatial coordinates $\mathbf{x}$, but also a function of time t, i.e. $\phi_a(\mathbf{x}, t)$. It should be noted that the introduced arbitrary scalar v is a function of $\mathbf{x}$ only. Therefore, an additional arbitrary scalar $W(t)$ must be introduced into (9.11) as

$$\begin{aligned}\int_{t_1}^{t_2} W \int_V (\nabla v)^{\mathrm{T}} \mathbf{j}_a \, dV dt \;=\; & \int_{t_1}^{t_2} W \oint_{S_{\mathrm{h}}} v h_a \, dS dt \\ & + \int_{t_1}^{t_2} W \oint_{S_{\mathrm{g}}} v j_{an} \, dS dt \\ & + \int_{t_1}^{t_2} W \int_V v \rho \frac{d\phi_a}{dt} \, dV dt \\ & + \int_{t_1}^{t_2} W \int_V v \rho \dot{\mathbf{x}}^{\mathrm{T}} \nabla \phi_a \, dV dt \\ & - \int_{t_1}^{t_2} W \int_V v \hat{c}_a \, dV dt\end{aligned} \tag{9.13}$$

where the whole expression is integrated over a period of time $\Delta t = t_2 - t_1$. In doing this, it is possible to obtain numerical solutions to transient differential equations of type (9.1) by making suitable choices for the functions $v(\mathbf{x})$ and $W(t)$ in (9.13). However, in the general case, the constitutive relation for $\mathbf{j}_a$ must be specified before solving the equation.

The robustness and accuracy of different choices of $v(\mathbf{x})$ and $W(t)$ will be discussed later.

The essential boundary condition can now be expressed as a function of time by

$$\phi_a = g_a \qquad \text{on } S_{\mathrm{g}} \;\; \text{at the time level, } t \tag{9.14}$$

Furthermore, the potential ϕ_a in V at time $t = 0$ can be expressed as

$$\phi_a = g_{ta=0} \qquad \text{in } V \;\; \text{at } (\mathbf{x}, 0) \tag{9.15}$$

which is called an *initial condition*.

9.2. Weak formulation of the linear momentum equations

In this Section, the weak form of the linear momentum equation will be derived. Contrary to the derivation of the weak form of the mass balance equation, the constitutive relation in question will be inserted before the weak form has been reached. This means that the generality will be lost, but on the other hand it will

be clear what kind of boundary conditions will be of interest in the problem dealt with.

The momentum balance equation used is: (compare (3.28))

$$\rho_a \frac{\partial \mathbf{x}'_a}{\partial t} = \operatorname{div} \mathbf{T}_a + \hat{\mathbf{p}}_a \tag{9.16}$$

where it is assumed that the term $\mathbf{x}'_a \cdot \operatorname{grad} \mathbf{x}'_a$ is small compared to the others. The assumption of a linear newtonian fluid without any volumetric viscosity, e.g. (3.34), gives

$$\mathbf{T}_a = \mu_a \left[\frac{\partial x'_{ia}}{\partial x_j} + \frac{\partial x'_{ja}}{\partial x_i} - \delta_{ij} \frac{2}{3} \frac{\partial x'_{ia}}{\partial x_i} \right] - \delta_{ij} \pi_a \tag{9.17}$$

where the hydrostatic pressures π_a have simply been separated from the deviatoric stresses caused by the motion of the fluid. Compare the discussion in Section 3.2.

As in the previous Section, the Cartesian coordinate system will be used, and the general frame-independent description will be exchanged since only matrixes will be defined, which hold in the Cartesian system. First, the stress tensor $\mathbf{T}_a$ will be formulated as

$$\mu_a \left[\frac{\partial x'_{ia}}{\partial x_j} + \frac{\partial x'_{ja}}{\partial x_i} - \delta_{ij} \frac{2}{3} \frac{\partial x'_{ia}}{\partial x_i} \right] = \mu_a \mathbf{D}_0 \tilde{\nabla} \mathbf{x}'_a \tag{9.18}$$

where the terms on the right-hand side of the identity sign are not yet defined. By using the summation convention for the properties in (9.17), the following components of the *deviatoric part* of the stress tensor $\mathbf{T}_a$ are obtained:

$$\tau_{11a} = \frac{4}{3} \frac{\partial x'_{1a}}{\partial x_1} - \frac{2}{3} \left(\frac{\partial x'_{2a}}{\partial x_2} + \frac{\partial x'_{3a}}{\partial x_3} \right) \tag{9.19}$$

$$\tau_{12a} = \frac{\partial x'_{1a}}{\partial x_2} + \frac{\partial x'_{2a}}{\partial x_1} \tag{9.20}$$

$$\tau_{13a} = \frac{\partial x'_{1a}}{\partial x_3} + \frac{\partial x'_{3a}}{\partial x_1} \tag{9.21}$$

$$\tau_{22a} = \frac{4}{3} \frac{\partial x'_{2a}}{\partial x_2} - \frac{2}{3} \left(\frac{\partial x'_{1a}}{\partial x_1} + \frac{\partial x'_{3a}}{\partial x_3} \right) \tag{9.22}$$

$$\tau_{23a} = \frac{\partial x'_{2a}}{\partial x_3} + \frac{\partial x'_{3a}}{\partial x_2} \tag{9.23}$$

$$\tau_{33a} = \frac{4}{3}\frac{\partial x'_{3a}}{\partial x_3} - \frac{2}{3}\left(\frac{\partial x'_{2a}}{\partial x_2} + \frac{\partial x'_{3a}}{\partial x_3}\right) \tag{9.24}$$

where the symmetry for $\mathbf{T}_a$ can be used to identify the remaining terms. The matrix operator $\tilde{\nabla}^{\mathrm{T}}$ and the vector $\mathbf{x}'_a$ are defined as

$$\tilde{\nabla}^{\mathrm{T}} = \begin{bmatrix} \frac{\partial}{\partial x_1} & 0 & 0 & \frac{\partial}{\partial x_2} & \frac{\partial}{\partial x_3} & 0 \\ 0 & \frac{\partial}{\partial x_2} & 0 & \frac{\partial}{\partial x_1} & 0 & \frac{\partial}{\partial x_3} \\ 0 & 0 & \frac{\partial}{\partial x_3} & 0 & \frac{\partial}{\partial x_1} & \frac{\partial}{\partial x_2} \end{bmatrix}; \quad \mathbf{x}'_a = \begin{bmatrix} x'_{1a} \\ x'_{2a} \\ x'_{3a} \end{bmatrix} \tag{9.25}$$

A column vector is used to represent all components in the deviatoric part of the stress tensor τ_a and the momentum supply term $\hat{\mathbf{p}}_a$ as

$$\bar{\tau}_a = \begin{bmatrix} \tau_{11a} \\ \tau_{22a} \\ \tau_{33a} \\ \tau_{12a} \\ \tau_{21a} \\ \tau_{32a} \end{bmatrix}; \quad \hat{\mathbf{p}}_a = \begin{bmatrix} \hat{p}_{1a} \\ \hat{p}_{2a} \\ \hat{p}_{3a} \end{bmatrix} \tag{9.26}$$

It is now clear that the constitutive matrix must take on the following form in order to represent the general notation (9.18) in the Cartesian coordinate system:

$$\mathbf{D}_0 = \begin{bmatrix} \frac{4}{3} & -\frac{2}{3} & -\frac{2}{3} & 0 & 0 & 0 \\ -\frac{2}{3} & \frac{4}{3} & -\frac{2}{3} & 0 & 0 & 0 \\ -\frac{2}{3} & -\frac{2}{3} & \frac{4}{3} & 0 & 0 & 0 \\ 0 & 0 & 0 & 1 & 0 & 0 \\ 0 & 0 & 0 & 0 & 1 & 0 \\ 0 & 0 & 0 & 0 & 0 & 1 \end{bmatrix} \tag{9.27}$$

Furthermore, the divergence operating on the stress tensor $\mathbf{T}_a$ must be expressed in terms of the Cartesian coordinate system. Again, if the defined matrix operator $\tilde{\nabla}$ is used the relation

$$\nabla \cdot \mathbf{T}_a \equiv \tilde{\nabla}^{\mathrm{T}} \mu_a \bar{\tau}_a - \nabla \pi_a \tag{9.28}$$

is found, where the identity $\mathrm{div}\pi_a \equiv \nabla \pi_a$ is used. $\nabla \pi_a$ is defined

$$\nabla \pi_a = \begin{bmatrix} d\pi_a/dx_1 & d\pi_a/dx_2 & d\pi_a/dx_2 \end{bmatrix}^{\mathrm{T}} \tag{9.29}$$

If (9.17) and (9.28) are used it becomes clear that the following identity holds:

$$\nabla \cdot \mathbf{T}_a \equiv \tilde{\nabla}^{\mathrm{T}} \mu_a \mathbf{D}_0 \tilde{\nabla} \mathbf{x}'_a - \nabla \pi_a \tag{9.30}$$

Equation (9.16) can now be represented in the Cartesian system by the following expression:

$$\rho_a \frac{d\mathbf{x}'_a}{dt} = \tilde{\nabla}^{\mathrm{T}} \mu_a \mathbf{D}_0 \tilde{\nabla} \mathbf{x}'_a - \nabla \pi_a + \hat{\mathbf{p}}_a \tag{9.31}$$

In order to reach the weak formulation of (9.16) or (9.31), the expression is multiplied by a vector weight function $\mathbf{v}(\mathbf{x})$ and integrated over a representative volume V. In contrast to the problem in Section 9.1, which contains the primary unknown scalar property $\phi_a(\mathbf{x}, t)$, this problem is of a vector type due to the unknown velocity field $\mathbf{x}'_a(\mathbf{x}, t)$. Hence, the weight function to be used must be a vector function. The weight function in the problem considered is defined

$$\mathbf{v} = \begin{bmatrix} v_1 \\ v_2 \\ v_3 \end{bmatrix} \tag{9.32}$$

If (9.31) is multiplied by the weight function $\mathbf{v}$, and integrated over the representative volume V gives

$$\begin{aligned} \int_V \rho_a \mathbf{v}^{\mathrm{T}} \frac{d\mathbf{x}'_a}{dt} dV \;\; = \;\; & \int_V \left(\tilde{\nabla}\mathbf{v}\right)^{\mathrm{T}} \mu_a \mathbf{D}_0 \tilde{\nabla} \mathbf{x}'_a dV \\ & - \int_V \mathbf{v}^{\mathrm{T}} \nabla \pi_a dV + \int_V \mathbf{v}^{\mathrm{T}} \hat{\mathbf{p}}_a dV \end{aligned} \tag{9.33}$$

It should be noted, again that $\operatorname{div} \pi_a \equiv \nabla \pi_a$. The Green-Gauss theorem can then be used to separate the hydrostatic pressures at the boundary surface from the *internal* hydrostatic pressures within the body V:

$$\int_V \mathbf{v}^{\mathrm{T}} \nabla \pi_a dV = \oint_S \mathbf{v}^{\mathrm{T}} \pi_a \mathbf{n} \, dS - \int_V \left(\nabla^{\mathrm{T}} \mathbf{v}\right) \pi_a dV \tag{9.34}$$

where

$$\nabla^{\mathrm{T}} = \begin{bmatrix} d/dx_1 & d/dx_2 & d/dx_2 \end{bmatrix} \tag{9.35}$$

In order to reduce the number of symbols and facilitate the numerical computation, the last term on the left-hand side of (9.34) is rewritten as

$$\int_V \left(\nabla^{\mathrm{T}} \mathbf{v}\right) \pi_a dV = \int_V \left(\tilde{\nabla}\mathbf{v}\right)^{\mathrm{T}} \pi_a \mathbf{m} dV \tag{9.36}$$

where

$$\mathbf{m}^{\mathrm{T}} = \begin{bmatrix} 1 & 1 & 1 & 0 & 0 & 0 \end{bmatrix}$$

and where the operator $\tilde{\nabla}$ is given by (9.25).

Now, the weak formulation of (9.31) can be written

$$\begin{aligned} \int_V \rho_a \mathbf{v}^{\mathrm{T}} \frac{d\mathbf{x}'_a}{dt} dV &= \int_V \left(\tilde{\nabla}\mathbf{v}\right)^{\mathrm{T}} \mu_a \mathbf{D}_0 \tilde{\nabla}\mathbf{x}'_a dV \\ &\quad - \oint_{S_g} \mathbf{v}^{\mathrm{T}} g_a \mathbf{n}\, dS + \int_V \left(\tilde{\nabla}\mathbf{v}\right)^{\mathrm{T}} \pi_a \mathbf{m} dV + \int_V \mathbf{v}^{\mathrm{T}} \hat{\mathbf{p}}_a dV \end{aligned} \tag{9.37}$$

and

$$\pi_a = g_a \qquad \text{on } S_{\mathrm{g}} \tag{9.38}$$

where g_a is a known value of the hydrostatic pressure at the part S_g of the boundary.

Based on the same arguments used in association with the weak formulation of the quasi-static problem, a scalar weight function W can be introduced, which is a function of time t only, i.e. $W(t)$.

If the whole expression (9.37) is multiplied by W and integrated over the time domain $\Delta t = t_2 - t_1$,

$$\begin{aligned} \int_{t_1}^{t_2} W \int_V \rho_a \mathbf{v}^{\mathrm{T}} \frac{d\mathbf{x}'_a}{dt} dV dt &= \int_{t_1}^{t_2} W \int_V \left(\tilde{\nabla}\mathbf{v}\right)^{\mathrm{T}} \mu_a \mathbf{D}_0 \tilde{\nabla}\mathbf{x}'_a dV dt \\ &\quad - \int_{t_1}^{t_2} W \oint_{S_g} \mathbf{v}^{\mathrm{T}} g_a \mathbf{n}\, dS dt \\ &\quad + \int_{t_1}^{t_2} W \int_V \left(\tilde{\nabla}\mathbf{v}\right)^{\mathrm{T}} \pi_a \mathbf{m} dV \\ &\quad + \int_{t_1}^{t_2} W \int_V \mathbf{v}^{\mathrm{T}} \hat{\mathbf{p}}_a dV dt \end{aligned} \tag{9.39}$$

$$\pi_a = g_a \qquad \text{on } S_{\mathrm{g}} \ \text{ at the time level}, t \tag{9.40}$$

$$\pi_a = g_{ta=0} \qquad \text{in } V \ \ at\,(\mathbf{x}, 0) \tag{9.41}$$

is obtained, where g_a is the known hydrostatic pressure at the boundary S_g at the time level t, and $g_{ta=0}$ is the initial hydrostatic pressure field in the domain V at the initial time $t = 0$.

9.3. Finite element formulation with the Galerkin method of the steady-state version of the quasi-static problem

In order to reach the finite element formulation, the weak formulation of the balance equation (9.11) will be supplemented with approximations for the arbitrary scalar function $v(\mathbf{x})$ and for the unknown property ϕ_a. The standard Galerkin type of weighting will be used. In Section 9.4, the accuracy of this approximation will be discussed, and it will be shown that the Galerkin method, applied to the weight function v, yields unsatisfactory results for equations containing significant first order derivatives. Therefore, another method is suggested. The discussion in Sections 9.4 and 9.5 will indirectly motivate the choice of approximations for $v(\mathbf{x})$ and ϕ_a respectively, and will therefore not be treated in this Section. It should be noted, however, that the approximations for the variation of ϕ_a in the time domain are not treated until Section 9.5 below.

The equation to be supplemented by approximations for v is, e.g. equation (9.11).

$$\begin{aligned}\int_V (\nabla v)^{\mathrm{T}}\ \mathbf{j}_a\, dV \;=\; & \oint_{S_{\mathrm{h}}} v h_a\, dS + \oint_{S_{\mathrm{g}}} v j_{an}\, dS + \int_V v\rho \frac{d\phi_a}{dt}\, dV \\ & + \int_V v\rho \dot{\mathbf{x}}^{\mathrm{T}} \nabla\phi_a\, dV - \int_V v\hat{c}_a\, dV\end{aligned} \tag{9.42}$$

It should also be noted that the essential boundary condition to this problem is

$$\phi_a = g_a \qquad \text{on } S_{\mathrm{g}} \tag{9.43}$$

The constitutive relations for the term $\mathbf{j}_a \equiv \rho_a \mathbf{u}_a$ in the quasi-static approach are typically of a gradient type of the unknown property ϕ_a with additional gradient dependencies of properties calculated with other equations than those discussed here. This general way of constituting $\mathbf{j}_a$ is illustrated as

$$\mathbf{j}_a = -\mathbf{D}_\phi \nabla\phi_a - (\mathbf{D}\nabla\vartheta + ...) \tag{9.44}$$

where ϕ_a is the property to be solved and ϑ is another property, the gradient of which also affects the mass flow of the ath constituent.

For example, ϕ_a may be the mass concentration of the ath constituent, and ϑ may be the temperature for the whole mixture: Compare for example, the constitutive relation (3.15). It should be noticed that the term $\mathbf{D}\nabla\vartheta$ in the general description of the constitutive relation (9.44) will appear as a source/sink term in the weak form of the balance equation (9.42), partly since the parameter

solved is ϕ_a and partly due to the fact that ϑ is assumed to be known from other equations than (9.42).

The description of how the additional term $\mathbf{D}\nabla\vartheta$ is added to the equation will not be taken any further, since it is trivial when treating the equation system in the proposed staggered way.

The property $\mathbf{D}_\phi$ is introduced as an orthotropic constitutive matrix as

$$\mathbf{D}_\phi = \begin{bmatrix} k_{1\phi} & 0 & 0 \\ 0 & k_{2\phi} & 0 \\ 0 & 0 & k_{3\phi} \end{bmatrix} \tag{9.45}$$

where $\mathbf{D}_\phi$ may be a function of the unknown property ϕ_a making the equation in question non-linear.

The concentration field of the unknown property ϕ_a is approximated by the element nodal values $\mathbf{a}_a^e$ and by the shape function $\mathbf{N}(\mathbf{x})$ as

$$\phi_a = \mathbf{N}\mathbf{a}_a^e \tag{9.46}$$

Simply speaking, the approximation suggests that the nodal values can be interpolated to obtain values *within* the elements. The most elementary choice is to interpolate linearly between the nodal points, that is, the components in $\mathbf{N}$ are *bilinear* functions of the position $\mathbf{x}$.

In the general three-dimensional case considered here, the components of an element containing eight nodal points may be arranged as

$$\mathbf{N} = \begin{bmatrix} N_1 & N_2 & N_3 & N_4 & N_5 & N_6 & N_7 & N_8 \end{bmatrix} \tag{9.47}$$

According to the Galerkin method the weight function is

$$v = \mathbf{N}\mathbf{c} \tag{9.48}$$

where $\mathbf{c}$ is an arbitrary matrix. This approximation will somewhat be explained in Section 9.4 through the use of an indirect method.

Since $v = v^{\mathrm{T}}$, the equation (9.48) can also be rewritten as

$$v = \mathbf{c}^{\mathrm{T}}\mathbf{N}^{\mathrm{T}} \tag{9.49}$$

It is apparent from the weak form (9.42) that the gradients of the function v and ϕ_a are necessary. Therefore, the gradient operating on the shape function $\mathbf{N}$

is introduced as $\nabla \mathbf{N}(\mathbf{x}) = \mathbf{B}(\mathbf{x})$ where $\mathbf{B}$ is defined as

$$\mathbf{B} = \begin{bmatrix} \frac{\partial N_1}{\partial x_1} & \frac{\partial N_2}{\partial x_1} & \frac{\partial N_3}{\partial x_1} & \frac{\partial N_4}{\partial x_1} & \frac{\partial N_5}{\partial x_1} & \frac{\partial N_6}{\partial x_1} & \frac{\partial N_7}{\partial x_1} & \frac{\partial N_8}{\partial x_1} \\ \frac{\partial N_1}{\partial x_2} & \frac{\partial N_2}{\partial x_2} & \frac{\partial N_3}{\partial x_2} & \frac{\partial N_4}{\partial x_2} & \frac{\partial N_5}{\partial x_2} & \frac{\partial N_6}{\partial x_2} & \frac{\partial N_7}{\partial x_2} & \frac{\partial N_8}{\partial x_2} \\ \frac{\partial N_1}{\partial x_3} & \frac{\partial N_2}{\partial x_3} & \frac{\partial N_3}{\partial x_3} & \frac{\partial N_4}{\partial x_3} & \frac{\partial N_5}{\partial x_3} & \frac{\partial N_6}{\partial x_3} & \frac{\partial N_7}{\partial x_3} & \frac{\partial N_8}{\partial x_3} \end{bmatrix} \tag{9.50}$$

The gradient of ϕ_a can now be expressed as

$$\nabla \phi_a = \mathbf{B}\mathbf{a}_a^e \tag{9.51}$$

The gradient of the weight function v is

$$\nabla v = \mathbf{c}^{\mathrm{T}}\mathbf{B}^{\mathrm{T}} \tag{9.52}$$

If the approximations for v and ϕ_a and their corresponding gradients, i.e. (9.46), (9.49), (9.51), and (9.52), are inserted into the weak form (9.42), and it is noted that the matrix $\mathbf{c}^{\mathrm{T}}$ cancels,

$$\begin{aligned} \int_V \mathbf{B}^{\mathrm{T}}\mathbf{D}_\phi\mathbf{B}\,dV\mathbf{a}_a^e + \int_V \underset{\sim}{\mathbf{N}}^{\mathrm{T}}\,\rho\,\underset{\sim}{\dot{\mathbf{x}}}\,\mathbf{B}\,dV\mathbf{a}_a^e \;=\; & -\oint_{S_{\mathrm{h}}} \mathbf{N}^{\mathrm{T}} h_a\,dS \\ & -\oint_{S_{\mathrm{g}}} \mathbf{N}^{\mathrm{T}} j_{an}\,dS \\ & -\int_V \mathbf{N}^{\mathrm{T}}\rho\mathbf{N}\frac{d\mathbf{a}_a^e}{dt}\,dV \\ & +\int_V \mathbf{N}^{\mathrm{T}}\hat{c}_a\,dV \end{aligned} \tag{9.53}$$

is obtained, with the essential boundary condition

$$\phi_a = g_a \qquad \text{on } S_{\mathrm{g}} \tag{9.54}$$

$\underset{\sim}{\mathbf{N}}$ and $\underset{\sim}{\dot{\mathbf{x}}}$ are introduced as

$$\underset{\sim}{\mathbf{N}} = \begin{bmatrix} \mathbf{N} \\ \mathbf{N} \\ \mathbf{N} \end{bmatrix}; \quad \underset{\sim}{\dot{\mathbf{x}}} = \begin{bmatrix} \dot{x}_1 & 0 & 0 \\ 0 & \dot{x}_2 & 0 \\ 0 & 0 & \dot{x}_3 \end{bmatrix} \tag{9.55}$$

The individual terms in (9.53) are often expressed in the compact *assembled* form

$$\mathbf{C}\dot{\mathbf{a}} + \left(\mathbf{K} + \tilde{\mathbf{K}}\right)\mathbf{a} + \mathbf{f} = 0 \tag{9.56}$$

where

$$\mathbf{C} = \int_V \mathbf{N}^{\mathrm{T}} \rho \mathbf{N} \, dV \tag{9.57}$$

This is called the *consistent damping matrix*. An alternative way of writing the damping term $\mathbf{C}$ is to use a '*lumped*' matrix, which is almost always applied when the finite difference method is used. The pros and cons of the two different damping terms are discussed in [71].

The time derivative is

$$\dot{\mathbf{a}} = \frac{d\mathbf{a}}{dt} \tag{9.58}$$

where it should be noted that no approximation for the time derivative is introduced. This is dealt with below in Section 9.5.

The matrix

$$\mathbf{K} = \int_V \mathbf{B}^{\mathrm{T}} \mathbf{D}_\phi \mathbf{B} \, dV \tag{9.59}$$

represents the *stiffness matrix*. In this case, a more illustrative name would be the *conductivity matrix*. The term $\tilde{\mathbf{K}}$ will be referred to as the *convection matrix*, defined as

$$\tilde{\mathbf{K}} = \int_V \underset{\sim}{\mathbf{N}}^{\mathrm{T}} \, \rho \, \underset{\sim}{\dot{\mathbf{x}}} \, \mathbf{B} \, dV \tag{9.60}$$

The last definition is the *load vector*

$$\mathbf{f} = \oint_{S_{\mathrm{h}}} \mathbf{N}^{\mathrm{T}} h_a \, dS + \oint_{S_{\mathrm{g}}} \mathbf{N}^{\mathrm{T}} j_{an} \, dS - \int_V \mathbf{N}^{\mathrm{T}} \hat{c}_a \, dV \tag{9.61}$$

which carries information about both the natural boundary conditions and the source/sink terms of the problem.

The finite element formulation (9.53-9.54) must be supplemented with approximations for ϕ_a in the time domain. This will be discussed in Section 9.5.

9.4. Accuracy of different weight functions in problems with significant first order derivatives

It is possible to argue for certain choices of the weight function $v(\mathbf{x})$ by considering a simple *test problem* consisting of a one-dimensional steady-state version of an equation of the type (9.1) without any natural boundary conditions or source/sink terms. Thus, the differential equation in the problem considered is

$$\rho \dot{x}_1 \frac{d\phi_a}{dx_1} = \frac{d\phi_a}{dx_1}\left(k_{1\phi} \frac{d\phi_a}{dx_1}\right) \tag{9.62}$$

where a constitutive relation of gradient type is used, compare (9.44). According to (9.53), the discretisized local finite element formulation of (9.62) is given as

$$\int_0^h \mathbf{B}^{\mathrm{T}} k_{1\phi} \mathbf{B}\, dx_1 \mathbf{a}_a^e + \int_0^h \mathbf{N}^{\mathrm{T}} \rho \dot{x}_1 \mathbf{B}\, dx_1 \mathbf{a}_a^e = \mathbf{0} \tag{9.63}$$

where the domain of the problem is $0 \leq x_1 \leq L$. The following elementary linear shape function $\mathbf{N}(x_1) = [1 - x_1/L \quad x_1/L]$ is used. The derivative of $\mathbf{N}(x_1)$ becomes $d\mathbf{N}(x_1)/dx_1 = \mathbf{B}(x_1) = [-1/L \quad 1/L]$, and the nodal parameter is $\mathbf{a}_a^{e\mathrm{T}} = \begin{bmatrix} \tilde{\phi}_1^e & \tilde{\phi}_2^e \end{bmatrix}$. The two terms in (9.63) are given explicitly as

$$\int_0^h \mathbf{B}^{\mathrm{T}} k_{1\phi} \mathbf{B}\, dx_1 = \frac{k_{1\phi}}{h} \begin{bmatrix} 1 & -1 \\ -1 & 1 \end{bmatrix} \tag{9.64}$$

and

$$\int_0^h \mathbf{N}^{\mathrm{T}} \rho \dot{x}_1 \mathbf{B}\, dx_1 = \frac{\rho \dot{x}_1}{2} \begin{bmatrix} -1 & 1 \\ -1 & 1 \end{bmatrix} \tag{9.65}$$

If the standard procedure for assembling a local element for a typical *internal* node i is used as well as equal elements with size h, the following matrix relation

$$\frac{k_{1\phi}}{h} \begin{bmatrix} 1 & -1 & 0 \\ -1 & 2 & -1 \\ 0 & -1 & 1 \end{bmatrix} \begin{bmatrix} \tilde{\phi}_{i-1} \\ \tilde{\phi}_i \\ \tilde{\phi}_{i+1} \end{bmatrix} + \frac{\rho \dot{x}_1}{2} \begin{bmatrix} -1 & 1 & 0 \\ -1 & 0 & 1 \\ 0 & -1 & 1 \end{bmatrix} \begin{bmatrix} \tilde{\phi}_{i-1} \\ \tilde{\phi}_i \\ \tilde{\phi}_{i+1} \end{bmatrix} = \mathbf{0} \tag{9.66}$$

is obtained. The assembled equation for node i is obtained by considering the middle row in (9.66) as

$$\frac{k_{1\phi}}{h} \left(-\tilde{\phi}_{i-1} + 2\tilde{\phi}_i - \tilde{\phi}_{i+1} \right) + \frac{\rho \dot{x}_1}{2} \left(-\tilde{\phi}_{i-1} + \tilde{\phi}_{i+1} \right) = 0 \tag{9.67}$$

which is a typical way of writing equations with the finite difference method (FDM).

Out of convenience only, the parameter Pe^e is introduced as

$$Pe^e = \frac{\rho \dot{x}_1 h}{2 k_{1\phi}} \tag{9.68}$$

This is known as the *element Peclet number*. If the definition of the element Peclet number is used, the equation (9.67) can be written as

$$(-Pe^e - 1)\, \tilde{\phi}_{i-1} + 2\tilde{\phi}_i + (Pe^e - 1)\, \tilde{\phi}_{i+1} = 0 \tag{9.69}$$

An alternative way to reach (9.67) or alternatively (9.69) is to make a *Taylor expansion* around the middle point node i, as is done in finite difference methods. Thus, the direct approximations for the derivatives of the unknown parameter ϕ are

$$\frac{d\phi}{dx} \mid_i = \frac{\tilde{\phi}_{i+1} - \tilde{\phi}_{i-1}}{2h} \tag{9.70}$$

and

$$\frac{d^2\phi}{dx^2} \mid_i = \frac{\tilde{\phi}_{i+1} - 2\tilde{\phi}_i + \tilde{\phi}_{i-1}}{h^2} \tag{9.71}$$

where the lowest possible linear expansion is used. By inserting these approximations directly into the governing differential equation (9.62) a nodal equation identical to that obtained by simple linear shape functions using the Galerkin type of weighting is obtained.

The standard Galerkin weighting (9.48), or the finite difference approximations (9.70) and (9.71) are, however, unfavorable approximations when dealing with equations containing first order derivatives. This can easily be shown by considering a steady-state, one-dimensional test example, e.g. the assembled nodal equation (9.69). If, for example, $\tilde{\phi}_{i-1} = 0$ and $\tilde{\phi}_{i+1} = 100$, the nodal equation (9.69) gives $\tilde{\phi}_i = 50(1 - Pe^e)$, which yields a negative value if $Pe^e > 1$ for any considered values of $\tilde{\phi}_{i-1}$ and $\tilde{\phi}_{i+1}$, e.g. compare [72]. This is, of course, a physically unrealistic result which may, however, be overcome.

One way to remove the drawback of negative values is to use the so-called *full upwinding approach*, that is to use the following assumptions for the first order derivatives:

$$\frac{d\phi}{dx} \mid_i = \frac{\tilde{\phi}_i - \tilde{\phi}_{i-1}}{h} \qquad \text{if } \dot{x}_1 > 0 \tag{9.72}$$

$$\frac{d\phi}{dx} \mid_i = \frac{\tilde{\phi}_{i+1} - \tilde{\phi}_i}{h} \qquad \text{if } \dot{x}_1 < 0 \tag{9.73}$$

A direct insertion of the approximations (9.72) and (9.71) into the governing differential equation gives the nodal equation for positive values of the mean velocity $\dot{x}_1$ as

$$(-2Pe^e - 1)\,\tilde{\phi}_{i-1} + (2Pe^e + 2)\,\tilde{\phi}_i - \tilde{\phi}_{i+1} = 0 \tag{9.74}$$

This upwinding scheme only gives accurate results if the element Peclet number is very high, compare Figures 9.2-9.4. The problem of inaccurate negative values is, however, removed.

In order to justify the choice of another weight function v than the one used in the standard Galerkin method (or any other method than the standard finite

difference approximation and the full upwinding approach), the exact solution to the test problem (9.62) is considered. The test problem is

$$\rho \dot{x}_1 \frac{d\phi}{dx_1} - \frac{d\phi}{dx_1}(k_{1\phi}\frac{d\phi}{dx_1}) = 0 \tag{9.75}$$

with the essential boundary conditions

$$\phi = \phi_L \qquad \text{at } x_1 = 0 \tag{9.76}$$

$$\phi = \phi_R \qquad \text{at } x_1 = L \tag{9.77}$$

in the considered domain $0 \leq x \leq L$. The analytical solution to this problem is (e.g. compare [74]):

$$\phi_a = \frac{\left(e^{(Pex/L)} - 1\right)(\phi_R - \phi_L)}{e^{(Pe)} - 1} + \phi_L \tag{9.78}$$

where the *Peclet number* Pe is defined

$$Pe = \frac{\rho \dot{x}_1 L}{k_{1\phi}} \tag{9.79}$$

Note that the *Peclet number* Pe is defined slightly different than the *element* Peclet number Pe^e.

The analytical solution to equation (9.75), i.e., equation (9.78), is illustrated in Figure 9.1 for different *Peclet numbers,* only positive values of $\dot{x}_1$ are considered. The essential boundary conditions $\phi_L = 0$ and $\phi_R = 1$ are used in the domain $0 \leq x \leq L$. It is observed that high Peclet numbers result in a so-called *boundary layer* near the right-hand side boundary.

In order to motivate a numerical method which yields satisfactory results for equations containing significant first-order derivatives, the test problem (9.75) will be considered further.

In a numerical approach, one can express the equation (9.75) as

$$\frac{\partial J}{\partial x} = 0 \tag{9.80}$$

where

$$J = \dot{x}_1 \phi - k_{1\phi}\frac{\partial \phi}{\partial x_1} \tag{9.81}$$

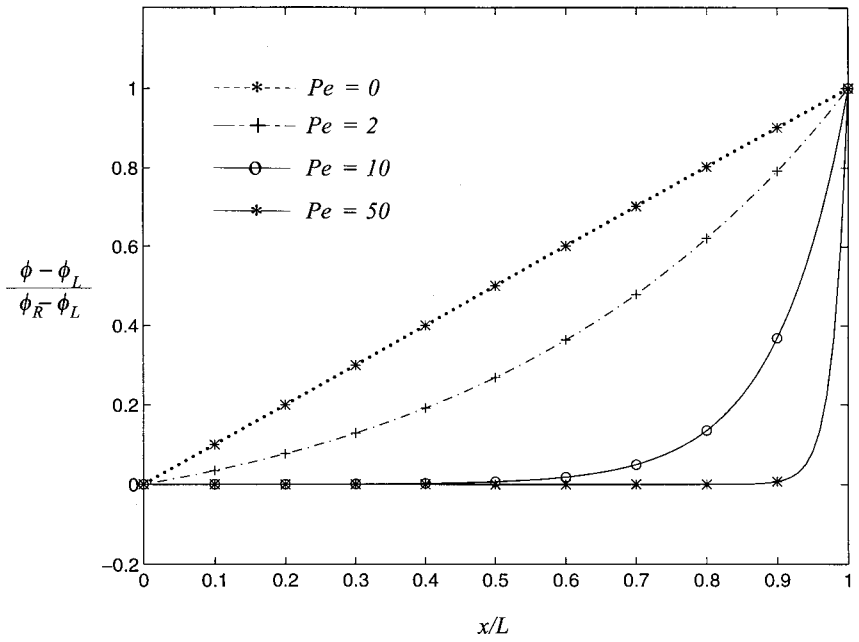

Figure 9.1: *Analytical solutions to the problem given by equation (9.74-9.76) for different Peclet numbers.*

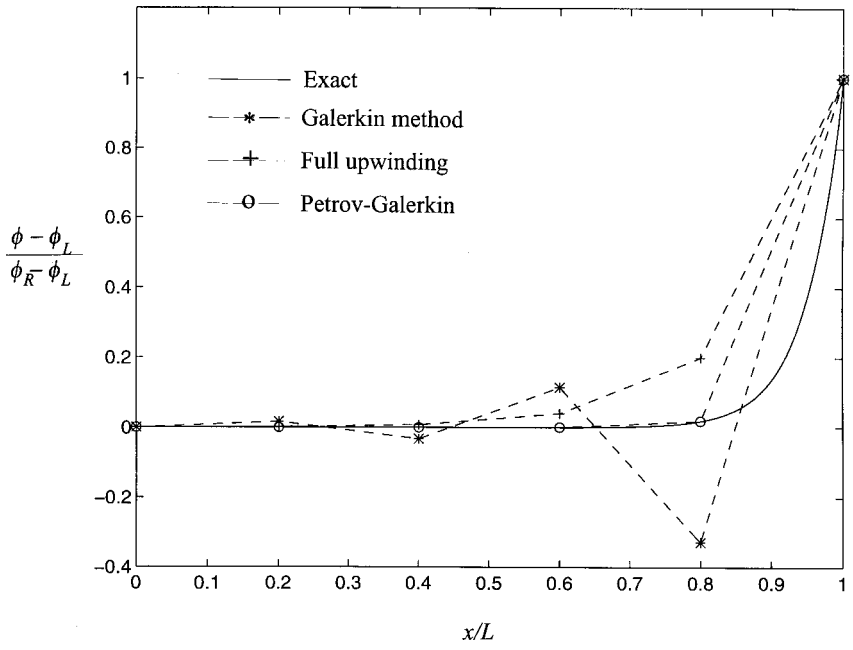

Figure 9.2: *The test problem defined by equation (9.74-9.76). Different solutions based on the case with five elements.*

In this context, one may interpret J as a flux passing through a stationary unit area. As a result of this, the following balance criteria must be fulfilled:

$$J\mid_{i+1/2} - J\mid_{i-1/2} = 0 \tag{9.82}$$

where the points $i+1/2$ and $i+1/2$ are located in the center of the two elements considered.

If the value of ϕ and the gradient of ϕ at the center of the right-hand element with the origin of x located at the middle node i is considered, the analytical expression to the problem gives the following two relations:

$$\phi\mid_{x=h/2} = \frac{\left(e^{(Pe/2)} - 1\right)(\phi_R - \phi_L)}{e^{(Pe)} - 1} + \phi_L \tag{9.83}$$

$$\frac{d\phi}{dx}\mid_{x=h/2} = \frac{e^{(Pe/2)} Pe\,(\phi_R - \phi_L)}{h\,(e^{(Pe)} - 1)} \tag{9.84}$$

By inserting these relations directly into (9.81), in order to get an expression for $J\mid_{i+1/2}$,

$$J\mid_{i+1/2} = \dot{x}_1\tilde{\phi}_i + \dot{x}_1\frac{\left(\tilde{\phi}_i - \tilde{\phi}_{i+1}\right)}{(e^{(Pe)} - 1)} \tag{9.85}$$

is obtained. If the same procedure is performed for the left-hand element, in order to get an expression for $J\mid_{i-1/2}$,

$$J\mid_{i-1/2} = \dot{x}_1\tilde{\phi}_{i-1} + \dot{x}_1\frac{\left(\tilde{\phi}_{i-1} - \tilde{\phi}_i\right)}{(e^{(Pe)} - 1)} \tag{9.86}$$

is yielded. Now, the balance criteria (9.82) together with (9.85) and (9.86) give the nodal equation for the internal node i as

$$(-1-c)\,\tilde{\phi}_{i-1} + (2+c)\,\tilde{\phi}_i - \tilde{\phi}_{i+1} = 0 \tag{9.87}$$

where

$$c = e^{(2Pe^e)} - 1 \tag{9.88}$$

in which the identity $Pe \equiv 2Pe^e$ is used. This scheme gives exact values of ϕ at the nodes, since it is based on the analytical solution to the differential equation in question. The presented method is called the *exponential method,* and was first used by practitioners of finite volume techniques, e.g. compare [71] and

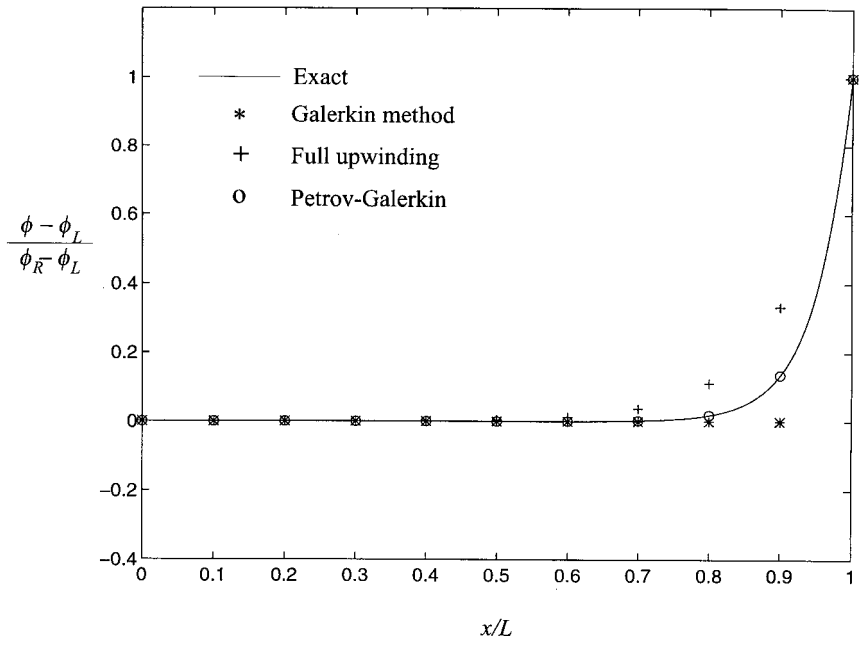

Figure 9.3: *The test problem defined by equation (9.74-9.76). Different solutions based on the case with ten elements.*

[72]. Note that for $Pe^e = 0$, the scheme (9.87) is identical with the Galerkin method corresponding to the diffusive term only; i.e. when no convective terms are present.

One important thing about equations containing significant first derivatives, such as equation (9.75), is that oscillatory solutions may occur also to steady-state problems. The exponential method discussed above has the benefit of always giving oscillation-free solutions to steady-state problems. The Galerkin method, or the finite difference method, will, however, give an oscillatory result if the element Peclet number Pe^e exceeds unity [75]. This drawback can be overcome by using small elements, but such a procedure is in most applications very uneconomical.

Figures 9.2-9.4 show the performance of the different schemes presented. The full upwinding approach overestimates the values near the boundary layer. For element Peclet numbers greater than unity, the Galerkin method or the finite difference method gives oscillatory results even in the steady-state problem considered here. Exact values are obtained through the exponential method or the

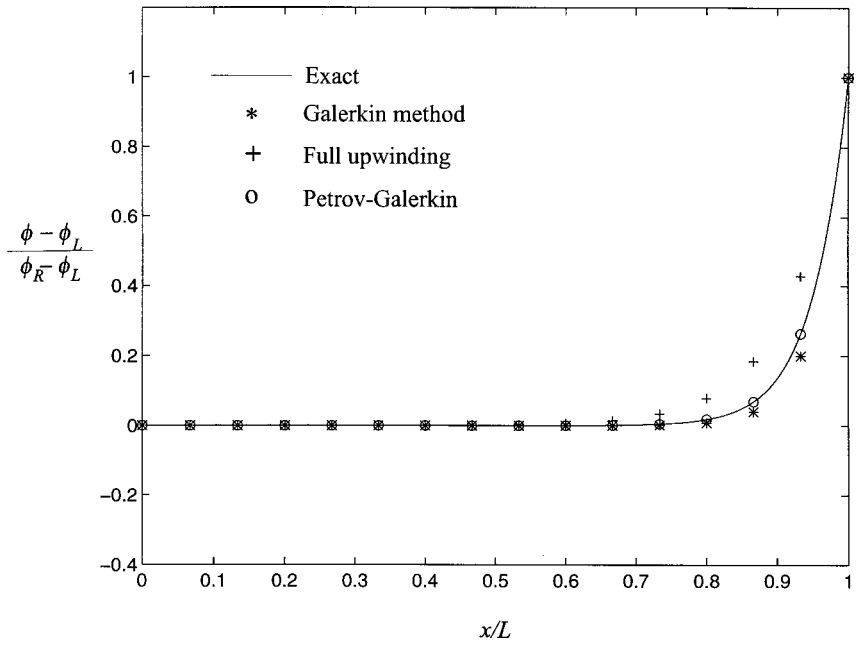

Figure 9.4: *The test problem defined by equation (9.74-9.76). Different solutions based on the case with fifteen elements.*

optimal Petrov-Galerkin method, which will be discussed below. Both methods are based on the analytical solution to the test problem considered.

In the context of finite elements, the exponential method in one-dimension corresponds to the following choice of the weight function:

$$v = \mathbf{c}^{\mathrm{T}} \left(\mathbf{N}^{\mathrm{T}} + \alpha_{opt} \frac{h}{2} \frac{\dot{x}_1}{|\dot{x}_1|} \mathbf{B}^{\mathrm{T}} \right) \tag{9.89}$$

where

$$\alpha_{opt} = \coth Pe^e - \frac{1}{Pe^e} \tag{9.90}$$

The proof of the optimality of this type of weight function, called the *Petrov-Galerkin method* or *optimal upwinding method*, is given in [75]. The optimality can, alternatively, be confirmed by making an assembly for an internal node i using the weight function (9.89) and noting that

$$\coth Pe^e = \left(e^{Pe^e} + e^{(-Pe^e)} \right) / \left(e^{Pe^e} - e^{(-Pe^e)} \right)$$

E.g. compare (9.66) and (9.67). It should be observed, however, that the unknown parameter ϕ is approximated in the standard manner — compare (9.46). The result obtained is identical to the nodal equation (9.87), thus the Petrov-Galerkin method yields exact values at the nodes when equations of the type (9.75) are considered. This means that the exponential method and the optimal Petrov-Galerkin method are identical.

The Petrov-Galerkin method is reduced to the standard Galerkin method (or the standard finite difference method) if the parameter α_{opt} is set to zero. Furthermore, if the parameter α_{opt} is set to unity, the full upwinding approximation is obtained. Compare the equations (9.87) and (9.74). The exponential method, or equally the Petrov-Galerkin method, will, however, be used due to its generality and its small computational expense compared to other methods, and also due to the fact that it is based on the analytical solution. Hence, it gives exact values at the nodes.

In [75] it is shown that if

$$|\alpha| > \alpha_{crit} = 1 - \frac{1}{Pe^e} \tag{9.91}$$

oscillatory solutions will never arise (considering steady-state situations only).

The results presented in Figures 9.2-9.4 show indeed that with $\alpha = 0$, i.e. the Galerkin procedure, oscillations will occur when $Pe^e > 1$. Figure 9.5 shows the variation of α_{opt} and α_{crit} with the element Peclet number Pe^e.

It is very important to note that *all* terms in a differential equation to be reformulated to the weak form should be multiplied by the actual weight function used, e.g. compare equation (9.42). Otherwise, the motivation of including an arbitrary function, which operates on the whole equation, fails. When the Petrov-Galerkin method is used, this means that the time derivatives and the source/sink terms must be affected by the choice of spatial weighting of the unknown parameter. In fact, it has been shown that incorrect solutions are obtained if the proper Petrov-Galerkin weighting on all terms present in the considered equation is not included, compare [71]. This important fact is indeed not obvious when a simple direct finite difference approximation applied to equations is used, containing significant first order spatial derivatives.

The matrixes which appear in the one-dimensional version of equation (9.56) are given explicitly below as

$$\mathbf{C} = \int_0^h \left(\mathbf{N}^{\mathrm{T}} + \alpha_{opt} \frac{h}{2} \frac{\dot{x}_1}{|\dot{x}_1|} \mathbf{B}^{\mathrm{T}} \right) \rho \mathbf{N} \, dx_1 = \tag{9.92}$$

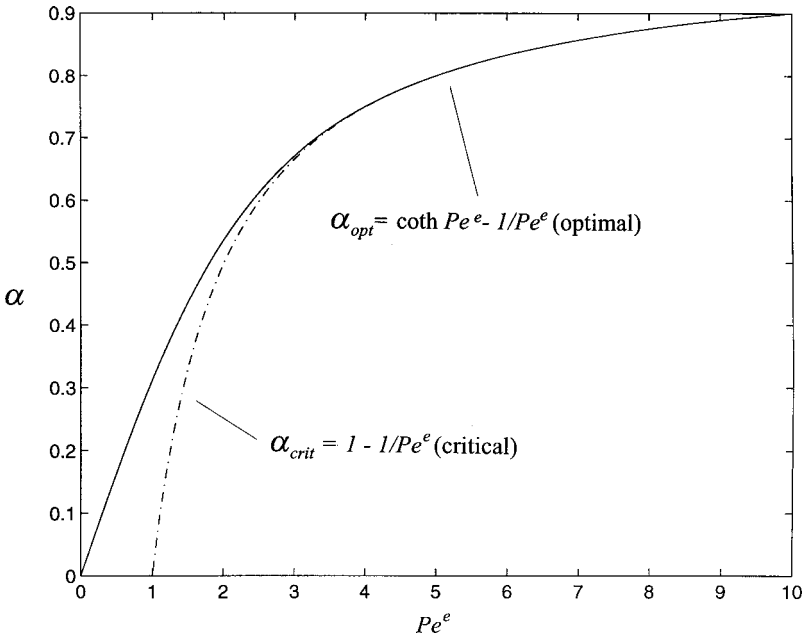

Figure 9.5: *Critical (stable) and optimal values of* α *as a function of the element Peclet number* Pe^e*, [71].*

$$\frac{\rho h}{6}\begin{bmatrix} 2 & 1 \\ 1 & 2 \end{bmatrix} + \alpha_{opt}\frac{\rho h}{4}\begin{bmatrix} -1 & -1 \\ 1 & 1 \end{bmatrix}\frac{\dot{x}_1}{|\dot{x}_1|}$$

where $\mathbf{C}$ is the local consistent damping matrix.

The local conductivity matrix $\mathbf{K}$ appears in its normal form as

$$\mathbf{K} = \int_0^h \mathbf{B}^{\mathrm{T}} k_{1\phi} \mathbf{B}\, dx_1 = \frac{k}{h}\begin{bmatrix} 1 & -1 \\ -1 & 1 \end{bmatrix} \tag{9.93}$$

The local convection matrix $\tilde{\mathbf{K}}$ becomes

$$\begin{aligned} \tilde{\mathbf{K}} &= \int_0^h \left(\mathbf{N}^{\mathrm{T}} + \alpha_{opt}\frac{h}{2}\frac{\dot{x}_1}{|\dot{x}_1|}\mathbf{B}^{\mathrm{T}}\right)\mathbf{B}\, dx_1 = \\ &\frac{\dot{x}_1}{2}\begin{bmatrix} -1 & 1 \\ -1 & 1 \end{bmatrix} + \alpha_{opt}\frac{\dot{x}_1}{2}\begin{bmatrix} 1 & -1 \\ -1 & 1 \end{bmatrix}\frac{\dot{x}_1}{|\dot{x}_1|} \end{aligned} \tag{9.94}$$

The boundary vector is

$$\mathbf{f}_b = \left[\mathbf{N}^{\mathrm{T}} + \alpha_{opt}\frac{h}{2}\frac{\dot{x}_1}{|\dot{x}_1|}\mathbf{B}^{\mathrm{T}}\right]_0^h \tag{9.95}$$

and the load vector carrying information about source/sink terms becomes

$$\begin{aligned} \mathbf{f}_l &= -\int_0^h \left(\mathbf{N}^{\mathrm{T}} + \alpha_{opt}\frac{h}{2}\frac{\dot{x}_1}{|\dot{x}_1|}\mathbf{B}^{\mathrm{T}}\right)\hat{c}_a\, dx_1 = \\ &-\frac{\hat{c}_a h}{2}\begin{bmatrix} 1 \\ 1 \end{bmatrix} - \alpha_{opt}\frac{\hat{c}_a h}{2}\begin{bmatrix} -1 \\ 1 \end{bmatrix}\frac{\dot{x}_1}{|\dot{x}_1|} \end{aligned} \tag{9.96}$$

It can be seen that all terms except the local conductivity matrix $\mathbf{K}$ are affected by the optimal Petrov-Galerkin weighting.

The exponential schemes or the Petrov-Galerkin schemes have been applied with great success to general one-dimensional problems including convective terms. These approaches therefore appear attractive to the development of general two- and three-dimensional flow conditions. However, effective and accurate schemes for two- and three-dimensional problems have been difficult to reach. One method which will be discussed here is the *streamline optimal Petrov-Galerkin method,* which in essence works with the one-dimensional schemes along the streamlines *within* each element. The crux is that a characteristic element length in the direction of the velocity resultant along the streamlines must be introduced. This

means that the optimality of α has to be sought in a rather arbitrary manner. However, by using rectangular bilinear elements, the characteristic element length along the streamlines can be reasonably defined and accurate results obtained, compare Figures 9.7 - 9.10.

It can be observed that the element Peclet number now must be a 'vector' quantity, for example

$$\mathbf{P}e^e = \frac{h}{2k}\dot{\mathbf{x}}; \qquad \dot{\mathbf{x}} = \begin{bmatrix} \dot{x}_1 \\ \dot{x}_2 \\ \dot{x}_3 \end{bmatrix} \tag{9.97}$$

Hence, the upwinding approach needs to be 'directional'. In order to obtain an element Peclet number that is directional, the following assumption has been proposed:

$$Pe^e = \frac{|\dot{\mathbf{x}}|\, h_{ch}}{2k} \tag{9.98}$$

where

$$|\dot{\mathbf{x}}| = \left(\dot{x}_1^2 + \dot{x}_2^2 + \dot{x}_3^2\right)^{\frac{1}{2}} \tag{9.99}$$

and h_{ch} is some characteristic element length along the streamlines, i.e. along the direction of $\dot{\mathbf{x}}$ within the element: E.g. compare different definitions for h_{ch} given in [71]. It is observed that additional methods must be found in situations when the conductivity is not isotropic.

Now, the optimality of α, in a certain element can again be expressed as

$$\alpha_{opt} = \coth Pe^e - \frac{1}{Pe^e} \tag{9.100}$$

If the element Peclet number is defined as a scalar property as is done in (9.98) when dealing with two- and three-dimensional problems, it is possible to obtain the following weight function [76]:

$$v = \mathbf{c}^{\mathrm{T}}\left(\mathbf{N}^{\mathrm{T}} + \alpha_{opt}\frac{h_{ch}}{2}\left(\frac{\dot{x}_1\partial\mathbf{N}^{\mathrm{T}}/\partial x_1 + \dot{x}_2\partial\mathbf{N}^{\mathrm{T}}/\partial x_2 + \dot{x}_3\partial\mathbf{N}^{\mathrm{T}}/\partial x_3}{|\dot{\mathbf{x}}|}\right)\right) \tag{9.101}$$

This is based on the fact that convection is only active in the direction of the resultant mean velocity $\dot{\mathbf{x}}$. The weight function (9.101) is of course reduced to the one-dimensional case when the velocity components $\dot{x}_2$ and $\dot{x}_3$ are set to zero. Compare with (9.89). As of yet, there is no formal evidence which confirms the optimality of the streamline Petrov-Galerkin method in two- and three-dimensions.

Test examples performed indicate, however, that the method gives accurate solutions even for high element Peclet number flows.

It is interesting to observe that a characteristic element length is used also in other two- and three-dimensional applications than the one studied here, such as the smeared crack approach used within fracture mechanics.

9.5. Discrete approximation in time

The finite element method provides a useful generalization unifying many existing algorithms for solving transient problems. Some of the most famous will be described in the following Section. A discretization process applicable directly to the time domain will be discussed.

A finite time increment Δt will be considered, which is related to the time t_n and t_{n+1} as $t_{n+1} = t_n + \Delta t$, in order to obtain so-called *recurrence relations*. The main steps taken to obtain quite general recurrence relations are the introduction of approximations for the variation of $\mathbf{a}(t)$ and $\dot{\mathbf{a}}(t)$ in the time domain and also the selection of a significant weight function $W(t)$ in the time domain. In doing so, within the area of finite element method, a wide family of frequently used algorithms or schemes are provided.

The starting point will be the following equation, discretizated in the spatial domain only, e.g. compare (9.56)

$$\mathbf{C}\dot{\mathbf{a}}(\tau) + \left[\mathbf{K} + \tilde{\mathbf{K}}\right] \mathbf{a}(\tau) + \mathbf{f}(\tau) = 0 \tag{9.102}$$

where τ is a normalized time which is set to zero at time $t = t_n$, and which gives the value Δt at the time level $t = t_{n+1}$. The normalized time can therefore be defined as

$$\tau = t - t_n \tag{9.103}$$

The *linear* approximation for $\mathbf{a}(\tau)$ in the finite time domain t_n to t_{n+1} is given by

$$\mathbf{a}(\tau) \approx \hat{\mathbf{a}}(\tau) = \hat{N}_n \mathbf{a}_n + \hat{N}_{n+1} \mathbf{a}_{n+1} \tag{9.104}$$

where the time domain shape functions $\hat{N}_n$ and $\hat{N}_{n+1}$ are given by

$$\hat{N}_n = 1 - \frac{\tau}{\Delta t}; \qquad \hat{N}_{n+1} = \frac{\tau}{\Delta t} \tag{9.105}$$

By using the already defined linear shape functions $\hat{N}_n$ and $\hat{N}_{n+1}$, it is possible to express the approximation for the time derivatives $\dot{\mathbf{a}}(\tau)$ as

$$\dot{\mathbf{a}}(\tau) \approx \frac{d\hat{\mathbf{a}}(\tau)}{dt} = \frac{d\hat{N}_n}{dt}\mathbf{a}_n + \frac{d\hat{N}_{n+1}}{dt}\mathbf{a}_{n+1} \tag{9.106}$$

where the time derivatives of the shape functions are given directly from (9.105) as

$$\frac{d\hat{N}_n}{dt} = -\frac{1}{\Delta t}; \qquad \frac{d\hat{N}_{n+1}}{dt} = \frac{1}{\Delta t} \tag{9.107}$$

The spatial- and time-domain discretizated problem can now be expressed

$$\mathbf{C}\frac{d\hat{\mathbf{a}}(\tau)}{dt} + \left[\mathbf{K} + \tilde{\mathbf{K}}\right]\hat{\mathbf{a}}(\tau) + \hat{\mathbf{f}}(\tau) = 0 \tag{9.108}$$

where the transient load vector $\mathbf{f}$ is approximated in the same manner as $\mathbf{a}(\tau)$, i.e.,

$$\mathbf{f}(\tau) \approx \hat{\mathbf{f}}(\tau) = \hat{N}_n\mathbf{f}_n + \hat{N}_{n+1}\mathbf{f}_{n+1} \tag{9.109}$$

If the approximations (9.104), (9.106), and (9.109) are inserted into (9.108), and the whole expression (9.108) is multiplied with the weight function W and integrated over the time domain $\Delta t = t_{n+1} - t_n$, e.g. compare with (9.13),

$$\begin{aligned} \mathbf{0} \;=\; & \int_0^{\Delta t} W\left(\mathbf{C}\left(-\frac{1}{\Delta t}\mathbf{a}_n + \frac{1}{\Delta t}\mathbf{a}_{n+1}\right)\right) d\tau \\ & + \int_0^{\Delta t} W\left(\left(\mathbf{K} + \tilde{\mathbf{K}}\right)\left(\left(1 - \frac{\tau}{\Delta t}\right)\mathbf{a}_n + \frac{\tau}{\Delta t}\mathbf{a}_{n+1}\right)\right) d\tau \\ & + \int_0^{\Delta t} W\left(\left(1 - \frac{\tau}{\Delta t}\right)\mathbf{f}_n + \frac{\tau}{\Delta t}\mathbf{f}_{n+1}\right) d\tau \end{aligned} \tag{9.110}$$

is obtained. By dividing the whole expression with $\int_0^{\Delta t} W d\tau$, the following expression is obtained:

$$\begin{aligned} \mathbf{0} \;=\; & \frac{\mathbf{C}\left[\mathbf{a}_{n+1} - \mathbf{a}_n\right]}{\Delta t} + \left[\mathbf{K} + \tilde{\mathbf{K}}\right]\left[\mathbf{a}_n + \Theta\left(\mathbf{a}_{n+1} - \mathbf{a}_n\right)\right] \\ & + \mathbf{f}_n + \Theta\left(\mathbf{f}_{n+1} - \mathbf{f}_n\right) \end{aligned} \tag{9.111}$$

where

$$\Theta = \frac{1}{\Delta t}\frac{\int_0^{\Delta t} W\tau d\tau}{\int_0^{\Delta t} W d\tau} \tag{9.112}$$

Table 9.1: Some single time-step algorithms, [71].

Scheme	Weight function $W(\tau)$	Θ	Stability condition
truly explicit	$\delta(\tau-\tau_i)\,;\ \tau_i=0$	0	*conditional*
Crank-Nicolson	1	0.5	*unconditional*
Galerkin type 2	$\tau/\Delta t$	0.666	*unconditional*
Liniger	$\delta(\tau-\tau_i)\,;\ \tau_i=0.878\Delta t$	0.878	*unconditional*
truly implicit	$\delta(\tau-\tau_i)\,;\ \tau_i=\Delta t$	1	*unconditional*

The parameter Θ is a number between 0 and 1. Different choices of W yields different values of Θ. Some examples are given in Table 9.1. Equation (9.111) can now be solved with properly introduced natural and/or essential boundary conditions.

The unknown vector values $\mathbf{a}_{n+1}$, given the value of the vector $\mathbf{a}_n$, may for example be solved with the standard Gauss elimination techniques.

Some different schemes are summarized in Table 9.1, where δ represents a *dirac function* at the position τ_i in the normalized time domain $0 \leq \tau \leq \Delta t$.

A truly *explicit* (or *Euler*) scheme is obtained if the parameter Θ is set to zero. Such an approximation only yields a *conditional stability* condition, which means that a time step smaller than a critical time step Δt_{crit} must be searched for to avoid small initial errors increasing without limit. Different criteria for critical time-step values can be found in, e.g. [71] and [72]. A short discussion on this subject will be presented in the following paragraphs.

Values of Θ greater than or equal to 0.5 are shown to be *unconditionally stable* for equation systems, which are *symmetric* and *positive definite*. This can be shown by considering an eigenvalue problem of the actual equation [71].

The value $\Theta = 0.5$ corresponds to the well-known *Crank-Nicholson scheme*, and the value $\Theta = 1$ is a *backward difference scheme*. The value $\Theta = 0.878$ is known as the *Liniger algorithm,* in which Θ is chosen to minimize the whole domain error.

Figure 9.6 illustrates a comparison of the exact solution to a one degree of freedom problem of the equation (9.111) without any convective terms or source/sink terms present, i.e. $\tilde{\mathbf{K}} = \mathbf{0}$ and $\mathbf{f} = \mathbf{0}$. This makes the equation homogeneous and symmetric, with various choices of the parameter Θ. In this case, the amplification A is identical to the eigenvalue μ of the problem. The amplification in this example can be interpreted as the amplification of the nodal value at time n to the time $n+1$.

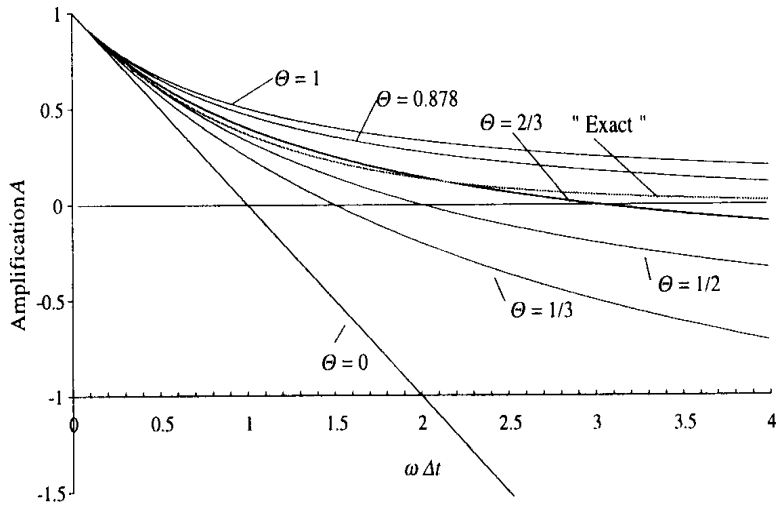

Figure 9.6: *Performance of different* Θ *algorithms.*

In Figure 9.6, w represents the ratio of the damping and stiffness terms, which in a *standard heat equation* correspond to the conductivity and the capacitance respectively. If the amplification μ, or equally A, is such that $|\mu| > 1$, all initial small errors will increase without limit. This means that if the parameter $w\Delta t$ exceeds 2, the solution of an explicit scheme, $\Theta = 0$, will be unstable and all initial values will grow without limit. Furthermore, *oscillations* will occur if the amplitude A becomes negative.

Apparently, the famous Crank-Nicholson scheme, $\Theta = 0.5$, will give oscillatory results if the parameter $w\Delta t$ exceeds 2. In this sense, the more implicit schemes are preferable, since they always give unconditional stable schemes without any oscillations which may pollute the solution.

However, when dealing with equations of the type (9.111), more elaborate procedures for assessment of stability and performance are needed, since the problem is not symmetric (due to the present of the term $\tilde{\mathbf{K}}$). One way is to determine the so-called *amplitude* and *relative celerity ratios*, e.g. [71].

In general, realistic critical time-steps can not be reached within the family of explicit schemes due to the fact that element Peclet numbers approach infinity when high *convective* flows are considered, i.e. when the mean velocity $\dot{x}_1$ is large compared with the material constant $k_{1\phi}$. Compare the definition of the element Peclet number, equation (9.79). If a time-step smaller than the critical can be

found using an explicit scheme, one advantage is obtained however: The equation system can be scaled row by row and the computational expense can become smaller.

It has been shown by amplitude and by the relative celerity ratios techniques that the Petrov-Galerkin weighting in spatial coordinates together with time domain weighting with $\Theta \geq 0.5$, yields unconditionally stable algorithms [71], i.e. no critical time steps have to be considered. The superior characteristics of the Petrov-Galerkin weighting together with unconditional stable choices of time integration compared to the other methods presented here, will be utilized in order to receive reliable solutions to the equations to be solved. It should be clear, however, that many different methods, with excellent performance, have been developed during the past few years, for instance the *mesh updating and interpolation method*, i.e. *characteristic-based methods*, and the *least square methods*, compare [72] and [71].

For example, the performance of a single time-step scheme, together with an optimal Petrov-Galerkin weighting in the spatial domain in two different problems where only convection is considered, are discussed. Only the convection is studied, since this phenomenon represents the main problem associated with numerical solutions.

The unconditional stable single time-step scheme used is a Liniger algorithm, i.e. $\Theta = 0.878$, since Pe^e tends to infinity in the test problems presented. Explicit schemes become very uneconomical, since extremely small elements have to be used to avoid unstable and oscillatory results.

Two test examples are treated by the calculation method described. The *first test example*, Figures 9.7 and 9.8, illustrate pure convection, i.e. there is no mass diffusion. Numerical integration and equally sized bilinear elements with 3x3 integration points are used to solve the diffusion-convection equation (9.111). The maximum value of the initial concentration field, Figure 9.7, is decreased by approximately 2% when 120 time-steps are used to calculate the new 'convected' concentration field, compare Figure 9.8. This is a measure of the calculation error since the shape of the initial concentration field should be the same throughout the process when no diffusion is active. The mean velocity field $\dot{\mathbf{x}}(\mathbf{x},t)$ is assumed to be constant in direction and magnitude throughout the whole space-time domain considered. The characteristic length in the direction of the mean velocity is assumed to be $h_{ch} = \sqrt{2}h$, where h is the length of the sides of the, equally sized, bilinear elements.

The *second test example*, Figures 9.7, 9.9, and 9.10, illustrate pure convection

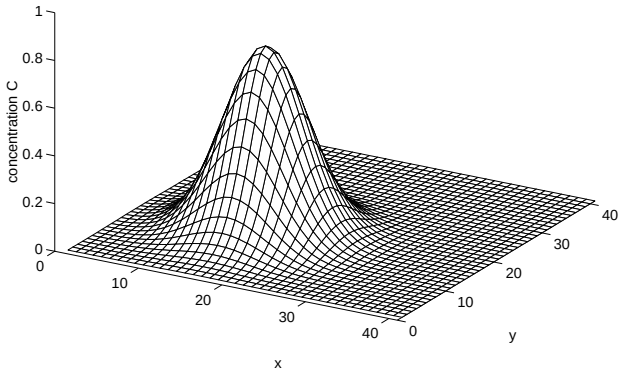

Figure 9.7: *Initial concentration field of C.*

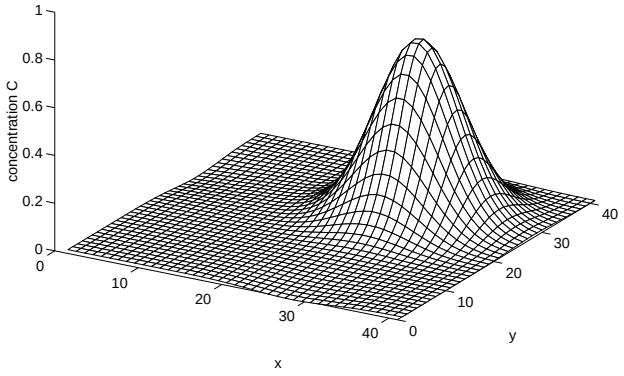

Figure 9.8: *Concentration field C after 120 computation steps. The initial concentration field in Figure 9.7 is convected throughout the domain. No diffusion takes place.*

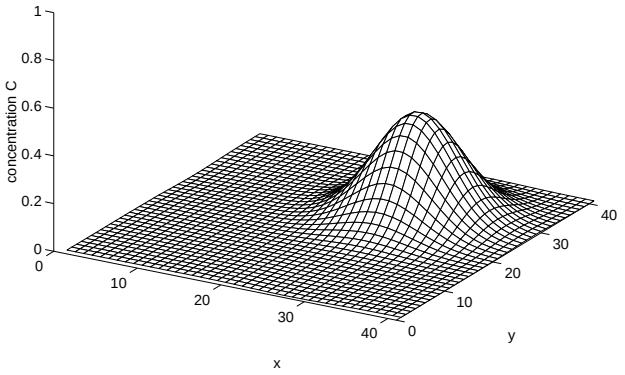

Figure 9.9: *The initial concentration field shown in Figure 9.7 is convected throughout the domain, simultaneosly mass is adsorbed onto the solid parts of the porous medium with a rate proportional to the concentration.*

with adsorption of mass onto the pore walls. The same magnitude and direction of the mean velocity $\dot{\mathbf{x}}(\mathbf{x},t)$ as in the previous example are used. The adsorption rate is assumed to be a linear function of the concentration C. The initial concentration field, Figure 9.7, is convected throughout the domain. Simultaneously, mass is adsorbed onto the pore walls. Compare Figure 9.9, where the free concentration field after 120 time-steps is illustrated, and Figure 9.10, where the motionless adsorbed mass after 120 time-steps is shown.

The transient sink term $\mathbf{f}$, i.e. the term describing the adsorption, is integrated into the time domain using the value $\Theta = 0.878$. Furthermore, the considered sink term $\mathbf{f}$ must be weighted with the same weight function v as is used for the other terms in the equation. In this case, the weight function v is thus given from the optimal streamline Petrov-Galerkin method, e.g. compare (9.96). If this is not done correctly, considerable errors will be introduced.

No oscillations are observed in the two test examples. Therefore the Liniger one time-step scheme and the optimal streamline Petrov-Galerkin method used in the examples represent the expected behavior fairly well, even in the two-dimensional case considered here.

A short discussion of the so-called *Newmark algorithm* will be performed in

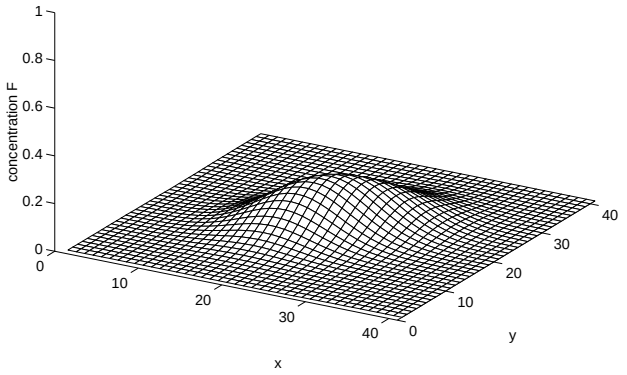

Figure 9.10: *Concentration field of motionless adsorbed mass after 120 computation steps.*

the following paragraphs. The Newmark scheme is a two time-step algorithm. It therefore makes equations, including second-order time derivatives, possible to solve, since a polynomial of second order is introduced to approximate the variations of $\mathbf{a}(\tau)$.

However, the primary purpose is not to present a solution strategy to problems like the full 'quasi'-harmonic equation, which includes second order time derivatives, but to find a better approximation to the first order time derivatives by the use of quadratic approximations in the time domain.

In highly non-linear problems, such as phase change problems, in which both matrices $\mathbf{C}$ and $\mathbf{K}$ are generally functions of the unknown parameter $\mathbf{a}$ itself, the Newmark family of schemes is quite popular. One of them is the Lees two time-step algorithm, which make it possible to evaluate all non-linear parameters at the current time level, and thus make equilibrium iterations unnecessary. In some problem of mass transport in porous materials considered, the phase change problem is important. A typical example is damages cased by ice formation of pore water in the material. This fact, among others, motivates the use of a more powerful scheme than the single time-step algorithms.

No special attention will be paid to the derivation of the Newmark algorithm since this follows the same methodology as was used to motivate the single time-

Table 9.2: Some Newmark algorithms, [71].

Scheme	γ Value	β Value	Stability condition
Central difference	0.5	0	*conditional*
Lees algorithm	0.5	1/3	*unconditional*
Zlamal	5/6	1	*unconditional*

step algorithm. The approximation for the unknown parameter $\mathbf{a}(\tau)$ is performed using shape functions in the time domain as

$$\mathbf{a}(\tau) \approx \hat{\mathbf{a}}(\tau) = \hat{N}_{n-1}\mathbf{a}_{n-1} + \hat{N}_n\mathbf{a}_n + \hat{N}_{n+1}\mathbf{a}_{n+1} \tag{9.113}$$

where $\mathbf{a}_n$ is the current known quantity at the normalized time level $\tau = 0$, $\mathbf{a}_{n-1}$ is the previously known quantity, and $\mathbf{a}_{n+1}$ is the unknown quantity searched for. It should be observed that the normalized time has its origin at time-level n and that $\tau = t/\Delta t$, which means that $\tau = -1$ at time level $n-1$ and $\tau = 1$ at time level $n+1$.

The quadratic type of approximation is expressed using the time domain shape functions as

$$\hat{N}_{n-1} = -\frac{\tau}{2}(1-\tau)\,; \quad \hat{N}_n = (1-\tau)(1+\tau)\,; \quad \hat{N}_{n+1} = \frac{\tau}{2}(1+\tau) \tag{9.114}$$

By following the methodology of the derivation of the single time-step algorithm, the following Newmark scheme

$$\begin{aligned} \mathbf{0} \;=\; & \left[\gamma\Delta t\mathbf{C} + \beta(\Delta t)^2\left(\mathbf{K}+\tilde{\mathbf{K}}\right)\right]\mathbf{a}_{n+1} + \\ & \left[(1-2\gamma)\Delta t\mathbf{C} + \left(\tfrac{1}{2}-2\beta+\gamma\right)(\Delta t)^2\left(\mathbf{K}+\tilde{\mathbf{K}}\right)\right]\mathbf{a}_n + \\ & \left[(-1+\gamma)\Delta t\mathbf{C} + \left(\tfrac{1}{2}+\beta-\gamma\right)(\Delta t)^2\left(\mathbf{K}+\tilde{\mathbf{K}}\right)\right]\mathbf{a}_{n-1} + \\ & \beta\mathbf{f}_{n+1} + \left(\tfrac{1}{2}-2\beta+\gamma\right)\mathbf{f}_n + \left(\frac{1}{2}+\beta-\gamma\right)\mathbf{f}_{n-1} \end{aligned} \tag{9.115}$$

is obtained, where the parameters

$$\gamma = \frac{1}{\Delta t}\frac{\int_{-1}^{+1} W\left(\tau+\frac{1}{2}\right)\tau d\tau}{\int_{-1}^{+1} W d\tau} \tag{9.116}$$

and

$$\beta = \frac{1}{\Delta t}\frac{\int_{-1}^{+1} \frac{1}{2}W(\tau(\tau+1))\,\tau d\tau}{\int_{-1}^{+1} W d\tau} \tag{9.117}$$

are obtained by dividing the whole weak formulation with $\int_{-1}^{+1} W d\tau$ in the same manner as is done to identify the parameter Θ.

Some famous Newmark schemes are shown in Table 9.2. The derivation of stability criteria for the Newmark family of schemes becomes more complicated than for the one time-step schemes and will not be discussed further. The subject can, however, be studied in [71] and [73].

10. A brief discussion of numerical methods and coupled systems

In this Section, the basic way of treating coupled equations numerically will be briefly discussed. It will be noticed that more approximations than those introduced in previous Sections must be considered in order to take the coupling terms into account.

10.1. General remarks

The equations for the constituents in Section 4 are coupled both at the governing differential equation level and at the boundaries. The coupling is mainly caused by the dependency of the mass concentration of liquid water on the diffusion parameters for the different constituents, and is also an effect of the reaction kinetics. Introduced assumptions concerning the reaction kinetics and the mass diffusion flows can also give rise to non-linear coupled equations.

At the boundary surfaces, the prescription of the mass concentration of vapor or liquid water is assumed to affect the flow behavior of all considered constituents through the same boundary surfaces. Hence, the coupling in terms of description of boundary conditions becomes important.

The mass diffusion flow behavior of the gaseous phases water-vapor, oxygen, and carbon dioxide is assumed to be coupled with the temperature field (i.e. a temperature gradient induced flow). Therefore, information from the equation describing the temperature gradients is necessary in order to create the equations describing the action of water-vapor, oxygen and carbon dioxide. Furthermore, the heat transfer equation and all equations describing diffusing matter will be affected by the mean velocity of the mixture. This convective flow contribution can not be solved numerically without treating the problem as a coupled equation system.

A truly coupled numerical discretization of the equations discussed in Section 4 becomes very complex. Therefore, the simplest possible way of solving the equation system will be discussed. This solution procedure is the so-called staggered solution process.

10.2. Some simple solution strategies for coupled equations

The staggered solution process is a method, by which each governing equation is solved separately. At every time step, however, information needed for the cou-

pling terms is taken from the other solved equations. Since the separate equations are not calculated simultaneously with a truly coupled equation-system, errors will be introduced. These errors may, however, be small when small time-steps are used.

Indeed the problem of describing the action of the diffusing matter in pore solution or in air-filled space requires a knowledge of mass concentration of liquid water and of the velocity field of liquid water in the pores. The mass concentration of liquid can, however, in general be determined by a solution independent of concentration fields of dissolved ions. Thus, the problem decouples in one direction. The same strategy can be used in the stress analysis discussed in Section 8. That is, the problem only couples, for example, in the temperature-stress direction, and thus, the temperature field can be calculated as a decoupled problem.

This simplified method of solving a coupled problem could, however, be somewhat improved for the case, where the mass diffusion flow of a constituent is described not only by its own gradient but also, for example, by the temperature gradient. In this very special case, it is possible to solve the mass concentration field of the constituent simultaneously with the temperature field. One advantage of this approach is that the same mesh and interpolation functions in the spatial and time domain for the two unknown quantities can be used.

The approach can be illustrated by considering a reduced version of equation (4.30) as

$$\rho\frac{\partial c_v}{\partial t} = D_v\frac{\partial^2 c_v}{\partial x^2} + D_{v\theta}\frac{\partial^2 \theta}{\partial x^2};\ \text{in } V \tag{10.1}$$

where the mass diffusion flow for the quantity c_v is constituted as functions of both the gradients of c_v and θ. The temperature θ is calculated using the standard transient heat conduction equation, i.e.

$$\rho C\frac{\partial \theta}{\partial t} = \lambda\frac{\partial^2 \theta}{\partial x^2};\ \text{in } V \tag{10.2}$$

The discretization of equation (10.1) takes the following form:

$$\mathbf{C}_v\dot{\mathbf{a}}_v + \mathbf{K}_v\mathbf{a}_v + \mathbf{K}_{v\theta}\mathbf{a}_\theta + \mathbf{f}_v = \mathbf{0} \tag{10.3}$$

Equation (10.2) is of a standard format, that is

$$\mathbf{C}_\theta\dot{\mathbf{a}}_\theta + \mathbf{K}_\theta\mathbf{a}_\theta + \mathbf{f}_\theta = \mathbf{0} \tag{10.4}$$

By forming block matrixes of the damping and stiffness matrixes as

$$\begin{bmatrix} \mathbf{C}_v & \bar{\mathbf{0}} \\ \bar{\mathbf{0}} & \mathbf{C}_\theta \end{bmatrix} \begin{Bmatrix} \dot{\mathbf{a}}_v \\ \dot{\mathbf{a}}_\theta \end{Bmatrix} + \begin{bmatrix} \mathbf{K}_v & \mathbf{K}_{v\theta} \\ \bar{\mathbf{0}} & \mathbf{K}_\theta \end{bmatrix} \begin{Bmatrix} \mathbf{a}_v \\ \mathbf{a}_\theta \end{Bmatrix} + \begin{Bmatrix} \mathbf{f}_v \\ \mathbf{f}_\theta \end{Bmatrix} = \mathbf{0} \tag{10.5}$$

it becomes clear that the two coupled equations (10.1) and (10.2) can be solved simultaneously in one step only, for each and every increment.

11. Discussion

11.1. Concluding remarks

A durability model based on continuum mechanics and a profound understanding of the destruction processes going on provides an idealized description of degradation phenomena in brittle porous materials. All material parameters introduced have a clear, stringent, physical meaning, and the proposed model may therefore be used to identify the relevance of the same parameters by experiments.

The course taken to obtain the governing equations for the diffusion of matter in the pore system was to assume that the diffusion constants for ions in water or gases in air could be scaled with a labyrinth factor which is a function of the porosity and the mass concentration of water in the pore system.

The exchange of mass among the constituents due to adsorption-desorption and chemical reactions was dealt with by constituting the reaction kinetics as modified second order reactions. The reason not to assume instantaneous reactions is that experiments indicate that the considered mass exchange processes taking place are diffusion controlled, on the micro-scopic level. The specific surface area, the temperature and the mass concentration of liquid water were assumed to be important properties affecting the reaction kinetics.

It was concluded that the description of the liquid water behavior in terms of mass concentration and velocity fields is very important as this affects nearly all degradation processes involved in inorganic porous materials. In order to obtain a realistic prediction of the behavior of liquid water in the pore system, a viscous newtonian fluid assumption was introduced. A thermodynamic force accounting for the interaction between the capillary sucked water and the pore walls was also included in this description.

It was argued that the water vapor and liquid water present in the pore system should be treated as two separate constituents. The main benefits of this approach are that temperature effects on the mass diffusion flow and the adsorption-desorption behavior of vapor may be introduced in a stringently explicit manner. Furthermore, it was shown that the velocity field of the liquid water plays an important role when it comes to describing the behavior of the dissolved ions in the pore solution. Reasonable predictions of the velocity field of liquid water can not be found when treating the vapor and liquid constituents by one governing differential equation only, since the diffusion and fixation of vapor are responsible for the distribution of liquid water within the pore system in a wide range of outer relative humidities. The main reason for development of significant velocity fields

of liquid water is, however, capillary suction. Under certain conditions, outer water pressure could also cause considerable convective velocity fields.

All constituents introduced in Section 4 are of interest in the reinforcement corrosion problem. The equation system describing such a multi-component diffusion must, however, be supplemented by more assumptions, taking into account the effect of corrosion currents which follows when the corrosion process has been initiated. This very important phenomenon will complicate the picture concerning the movement of the ions in the pore solution as they will be attracted or repelled from different corrosion zones by the electrical field. A brief discussion of how the diffusion velocities could be constituted when present in an electrical field was presented in Section 6. It was also noted that the constitutive behavior describing the binding of ions, e.g. the reaction kinetics describing adsorption-desorption of chloride ions, must be assigned with special assumptions when a significant electrical force drags ions in the streamline direction of the electric field. That is, ions will get stucked in cavities (in the pore system) which direction coincides with the electrical stream line direction. This phenomenon is not active when considering diffusion and binding of ions without the presence of electrical fields.

The formation of ice crystals in the pore system involves several complex physical mechanisms. The most obvious phenomenon to account for is the latent heat effect involved in the transformation of liquid water to ice and vice versa. In Stefan's problem, a material changes phase at a distinct temperature followed by adsorption or emission of the latent heat at a front propagating through the material. Some remarks on how to generalize Stefan's problem were discussed in Section 7. Such a generalization must account for propagation of ice through a material with a wide range of pore sizes. Serious problems must be overcome, such as the problem of describing the cryo-suction phenomenon where ice affects water from sources containing unfrozen water, such as water in very narrow pores. Furthermore, it seems reasonable to introduce a distribution function accounting for the degree of saturation of different pore sizes when the mass concentration in a representative volume, in which all pore sizes are represented, is known. When ice starts to form in the pore system such a distribution function will, however, be significantly changed during the freezing process. This fact indicates that the problem should be described at a lower level where the geometry of the pores is considered in an explicit manner. Assumptions introduced at a microscopic level are however, difficult to confirm by experiments. Another problem associated with ice growth in the pore system of porous materials is that ice may be formed by both fusion and sublimation. The shape of the formed crystals is very much

a question of the temperature at which the vapor is sublimated. The differently formed ice crystals will therefore affect the solid skeleton differently. It is noted also that calorimeter measurements can not reveal the amount of ice formed in the pore system directly without making assumptions of the latent heat of fusion and sublimation involved at different temperatures and at different mass concentrations of water in the pore system. One problem to be considered is, for example, that the latent heat of fusion of capillary water is different from the latent heat of fusion of adsorbed and capillary condensed water at a certain temperature.

Damage of solid porous materials due to freezing and thawing of pore water, changes of temperature or changes of moisture condition involves several complex physical phenomena. A brief discussion of how to constitute the stresses in the solid is presented in Section 8. Using the smeared crack approach model, outlined in Section 8, deformations and cracks in the solid may be predicted by introducing coupling terms and using information from the equations for the different constituents presented in Sections 4 to 7. When studying the mechanical behavior due to freezing and thawing of pore water, special considerations must be dealt with as the assumed material parameters describing the elastic-fracturing material of interest will be significantly changed under such conditions. The loading and unloading paths in the softening zone are discussed in detail. In service life predictions such cyclic environmentally induced loads are of major importance. Problems of involving changes of material properties in the softening zones, were, however, realized. These problems stem from the fact that the second axiom of thermodynamics must always be fulfilled. A simple way of introducing the effect on the material properties in the softening zone of the presence of ice in the pore system is proposed.

A rigid method of solving diffusion-convection problems numerically is outlined in Section 9. Several examples showed that the Petrov-Galerkin scheme, together with an unconditional time step method, yields good accuracy. This type of method could be used to solve the governing equations presented in Sections 4 to 7 for the diffusing and chemically reacting constituents. It is suspected, however, that the present internal transient source terms modelling the mass exchange among the constituents will present some difficulties. That is, the time scale for these reactions may be in conflict with the time scale for the diffusion process. This may introduce extremely expensive computations as very small time steps must be used in order to follow the correct solution path.

A staggered solution process is suggested for the coupled equations in Sections 4 to 7. This will demand the use of a powerful computer as information of the

current state of the different constituents must be stored in every time step. Indeed small time steps must also be used to capture the response due to a given environmental variation in terms of, for example, temperature, mass concentration of vapor, exposure to liquid water and chloride ions. A typical case to be modelled is the response due to cyclic deicing salt and rain water exposure for treating the reinforcement corrosion problem. Here consideration must be taken to (*i*) ingress of chlorides, (*ii*) moisture conditions and liquid water flow in the pore system, (*iii*) carbonation and leaching of hydroxides within the material, (*iv*) temperature effects.

11.2. Possible future developments

A natural extension of the presented work is to arrange specially designed experimental setups. Such experiments should be performed under controlled conditions which make possible the identification of the introduced material constants and parameters. In fact, the proposed constitutive relations give the necessary information of how these experiments may be performed in a systematic manner.

There is, however, much that can be done to improve the hypothesis on which the experimental work should be based. It is realized that the complex mechanisms underlying the constitutive behavior of diffusing matter in the pore system are a consequence of the complicated microstructure of the porous material. Due to the extremely high specific surface area of the cement paste, and the charged character of the solid matrix, matter that diffuses in air filled space or matter dissolved in the pore water will be highly affected. Indeed, the mechanisms on the micro-scale were modelled by introducing labyrinth factors for the diffusion parameters and by considering the mass diffusion controlled exchange of mass among the constituents with source/sink terms. Without any further attention these equations were assumed to be valid also at the macroscopic level (i.e. in terms of millimeters).

However, it seems more realistic to introduce the constitutive equations at the microscopic level as all mechanisms involved in the diffusion-chemical reaction process stem from thermodynamic forces at the same level. The geometry of different porous materials is unfortunately not very well documented on the microscale. Some indications of specific surface area and pore size distribution can, however, be obtained by sorption tests. Micro-scopic geometries may theoretically be used explicitly in models dealing with mass and heat transfer, in which the constitutive relations are introduced on the same scale. Homogenization theories

for upscaling of information between different scales exist. In these methods information is propagated to the macroscale by, for example, averaging the microscale balance laws. Such an averaging procedure may be performed by running different finite element simulations with a given geometry on the microscale level.

It should be noted, however, that the important capillary suction phenomenon is extremely difficult to model with constitutive relations on the microscale level with a given geometry. This is due to liquid water forming discontinuous curved surfaces caused by the hydrophilic character of the solid matrix. The surface energy of such a curved liquid water surface may contribute to a creeping flow of liquid islands or larger continuous liquid domains within the pore structure. The description of the behavior or the boundary surfaces between liquid water and the solid is realized to be complex. Furthermore, the mass concentration of liquid water at the microlevel is either one or zero, i.e. a serious discontinuity must be dealt with.

Several improvements in the description of the reinforcement corrosion phenomenon may be considered. The most important subject is perhaps to find the correct chemical stoichiometric relation involved in the corrosion process. The idealized proposed reactions presented in Section 6 might be much too simplified to capture the significant action involved in the production of rust. One possibility is to account for all complex reactions involved in such chemical reactions taking place in the pore solution. Furthermore, the polarization phenomena, occurring at the anode and cathode surfaces, are factors that need to be examined further. Some problems of specifying the boundary conditions in the equation describing the electrical potential field are realized. Further studies concerning this matter are needed. Two very important mechanisms were discussed at the end of Section 6. That is, (i) the initiation criteria and the identification of the location of the anode and cathode surfaces and (ii) the constitutive relation for the reaction rate of the production of rust when corrosion has been initiated. It should be noted, however, that such an initiation criterion is not supposed to be used as a threshold for the service life of a structure as it is suspected that the initiation occurs at an early stage. The production rate of rust might be slowed down after it has been initiated if the mechanisms involved are not favorable. That is, a threshold value in terms of, for example, the amount of rust (formed at a certain location) might be searched for.

The problems experienced when trying to establish a model for ice growth are, again, believed to be a consequence of not having significant available information of the mechanisms occurring at the microlevel. In order to obtain a macroscopic

continuum, describing ice growth in a pore system, a distributing function was introduced. The distribution function is supposed to give the saturation degree of different pore sizes at a given known mass concentration of liquid water, defined on a macrolevel. The cryo-suction mechanism will, however, change the distributing function during the freezing process. This calls for a more detailed study of the transient redistribution process of liquid water among the different pore sizes due to ice formation. Such considerations can not be successfully studied without considering the actual pore geometry on the microlevel. The introduction of constitutive relations on the microscopic level followed with a homogenization seems to be a fruitful way of improving the model outlined in Section 7.

A more detailed study of the consequences of introducing constitutive relations for the Helmholz free energy and the entropy for the individual constituents can be performed. By successfully constituting these properties the effect of, for example, dissolved ions (in the pore solution) on the ice growth can be modelled by using only one single energy equation for the mixture together with constitutive relations for the reaction kinetics.

Another interesting approach to be analyzed in this context is assigning each individual constituent a temperature. That is, each constituent participating in the freezing and thawing of pore water, e.g. liquid bulk water, vicinal water, vapor, ice, dissolved chloride ions and the solid matrix, is allowed to have different temperatures at the same spatial position. In such a consideration an energy balance equation for each constituent must be introduced. The approach is, however, realized to be very complex as not only the Helmholz free energies, the stress tensors and the entropies for all constituents must be properly constituted, but also the rate and extent of local interaction of energy among the constituents.

The description of the stresses, and hence the deformations, induced by external and environmentally induced strains was obtained using coupling terms when constituting the stress tensor for the solid matrix. The so-called smeared crack approach was used to obtain this description. Indeed, the important softening behavior, valid for brittle materials, may be modeled with this approach. It is realized, however, that some of the material parameters introduced for modeling the induced stresses caused by ice formation are somewhat weak. An improvement may, in fact, be obtained by considering the solid matrix and the ice in the pore system as a composite material. Advanced theories do exist in this area, based on approximations to the general mixture theories. It is believed that interesting conclusions concerning the mechanical behavior may be drawn from a model where the solid matrix and the ice are treated as a composite material.

Some basic methods for solving diffusion-convection problems involving chemical reactions, and modified newtonian fluid problems, were outlined in Section 9. These methods may be used to implement a computer program solving coupled equations dealing with diffusion-convection problems with several interacting constituents. Test simulations using different values of the introduced material parameters, using such a general program, are assumed to be a powerful tool when comparing global responses from measurements with different constitutive assumptions.

References

[1] Bowen, R.M. (1976). *Theory of Mixtures*, Part 1, In Continuum Physics, Edited by A. Cemal Erigen, Princeton University of Technology.

[2] Truesdell, C. (1985). *Rational Thermodynamics, Second Edition.* Springer-Verlag, New York.

[3] Svendsen, B. (1997). *On the Constituent Structure of a Classical Mixture*, Mecccanica Vol. 10**.** pp. 13-32**.**

[4] Bennethum, L.S. and Cushman J.S. (1996). *Multiscale, Hybride Mixture Theory for Swelling Systems-I: Balance Laws.* Int. J. Engng. Sci. Vol. 34. No. 2, pp. 125-145.

[5] Bennethum, L.S. and Cushman J.S. (1996). *Multiscale, Hybride Mixture Theory for Swelling Systems-II: Constitutive Theory.* Int. J. Engng. Sci. Vol. 34. No. 2, pp. 147-169.

[6] Bažant, Z.P. (1979). *Physical Model for Steel Corrosion in Concrete Sea Structures*, Journal of the Structural Division, Proc. ASCM, Vol. 105, No. ST6, pp. 1137-1166.

[7] Gérard, B. (1996). *Contribution des Couplages Mécanique-chimie-Transfert dans la Tenue a Long Terme des Ouvrages de Stockage de Déchets Radioactifs,* Ph.D. thesis, Laboratoire de Mécanique et Technologie, Paris, France.

[8] Adamson, A.W. (1990). *Physical Chemistry of Surfaces*, Fifth Edition, Wiley-interscience publication, New York.

[9] Powers, T.C. (1968). *The Thermodynamics of Volume Change and Creep.* Materials and structures, 6.

[10] Everett, D.H. (1958). *Some Problems in the Investigation of Porosity by Adsorption Methods.* The Structure and Properties of Porous Materials, London.

[11] Zsigmondy, R.Z. (1911). *Über die Struktur des Gels des Keiselsäure, Teorie der Entwässerung*, Z. Anorg. Chem., 356.

[12] Bear, J. (1979). *Hydraulics of Groundwater*, McGraw-Hill, Inc. New York.

[13] Christenson, H.K. (1985). J. Colloid Interfaces Sci., Vol. 104, pp. 234.

[14] Ahlgren, L. (1972). *Moisture Fixation in Porous Building Materials*, Division of Building Materials, Lund Institute of Technology.

[15] Janz, M. (1997). *Methods of Measuring the Moisture Diffusivity at High Moisture Levels*. Division of Building Materials, Lund Institute of Technology.

[16] Arvidsson, J. (1996). *Isoterma Fuktförlopp i Porösa Material* (in Swedish), Division of Building Physics, Lund Institute of Technology.

[17] Daïan, J.F. (1989). *Condensation and Isothermal Water Transfer in Cement Mortar: Part II -Transient Condensation of Water Vapor*, Transport in Porous Media Vol. 4. pp. 1-16, Kluwer Academic Publishers.

[18] De Boer, J.H. (1968). *The Dynamics Character of Adsorption*, Clarendon Press, Oxford.

[19] Luikov, A. V. (1966). *Heat and Mass Transfer in Capillary-porous Bodies.* Pergamon Press, Oxford.

[20] Pel, L. (1995). *Moisture Transport in Porous Building Materials*, Ph.D. thesis, Eindhoven University of Technology, Netherlands.

[21] Krus, M. (1996). *Moisture Transport and Storage Coefficients of Porous Mineral Building Materials, Theoretical Principles and New Test Methods.* Ph.D. thesis, Fraunhofer-Institute für Bauphysik, IRB Verlag, Fraunhofer-Informationszenrum Raum und Bau.

[22] Kuntzel, H.M. (1995). *Simultaneous Heat and Moisture Transport in Building Components, One- and Two-Dimensional Calculation Using Simple Parameters.* Ph.D. thesis, Fraunhofer-Institute für Bauphysik, IRB Verlag, Fraunhofer-Informationszenrum Raum und Bau.

[23] Fagerlund, G. (1993). *The Long Time Water Absorption in the Air-Pore Structure of Concrete,* Division of Building Materials, Lund Institute of Technology.

[24] Weast, R.C., Lide, D.R. Astle, M.J. and Beyer, W.H. (1989). *Handbook of Chemistry and Physics*, 70^{TH} Edition, CRC press, Inc. Boca Raton, Florida.

[25] Tuutti, K. (1982). *Corrosion of Steel in Concrete*, Report, Swedish Cement and Concrete Institute (CBI), Royal Institute of Technology, Stockholm, Sweden.

[26] Sandberg, P. (1995). *Critical Evaluation of Factors Affecting Chloride Initiated Reinforcement Corrosion in Concrete*. Division of Building Technology, Lund Institute of Technology.

[27] Tritthart, J. (1992). *Changes in Pore Water Composition and in Total Chloride Content at Different Levels of Cement Paste Plates Under Different Storage Conditions*, Cement and Concrete Research. Vol. 22, pp. 129-138.

[28] Sergi, G., Yu, S.W. and Page, C.L. (1992). *Diffusion of Chloride and Hydroxyl Ions in Cementitious Materials Exposed to a Saline Environment*, Magazine of Concrete Research. 1992, Vol. 44, No. 158, Mar., pp. 63-69.

[29] Atkins, P.W. (1994). *Physical Chemistry*, Fifth Edition, Oxford University press, Oxford.

[30] Crank, J. (1975). *The Mathematics of Diffusion*, Clarendon Press, Oxford.

[31] Wirje, A. and Offrell, P. (1996). *Kartering av Miljölast-kloridpenetratrion vid RV40* (in Swedish), Division of Building Technology, Lund Institute of Technology.

[32] Page, C.L., Lambert, P. and Vassie, P.R.W. (1991). *Investigations of Reinforcement Corrosion. 1. The Pore Electrolyte Phase in Chloride-Contaminated Concrete.* Materials and Structures, Vol. 24, No. 139, pp. 234-252.

[33] Glass, G.K. and Buenfeld, N.R. (1995). *The Determination of Chloride Binding Relationships*, Chloride Penetration into Concrete, Proceedings of the International Rilem Workshop, St-Rémy-lès-Chevreuse, France.

[34] Midglay, H.G. and Illston, J.M. (1984). *The Penetration of Chlorides into Hardened Cement Pastes,* Cement and Concrete Research. Vol. 14, pp. 546-558.

[35] Sandberg, P. (1996). *Durability of Concrete in Saline Environment*, Cementa AB, Sweden.

[36] Volkwein, A. (1991). *Untersuchungen über das Eindringen von Wasser und Chlorid in Beton*, Institute of Building Materials, Technical University of Munich.

[37] Taylor, H.F.W. (1990). *Cement Chemistry*, Academic Press.

[38] Ho, D.W.S. and Lewis, R.K. (1987). *Carbonation of Concrete and its Predictions*, Cement and Concrete Research, Vol. 17, pp. 489-504.

[39] Glasser, F.P., Lachowski, E.E. and Macphee, D.E. (1987). *Compositional Model for Calcium Silicate Hydrate (C-S-H) Gels: Their Solubilities, and Free Energies of Formation*, Journal of the American Ceramic Society, Vol. 70, No. 7, pp. 481-485.

[40] Saetta, A.V., Schrefler, B.A and Vitaliani, R.V. (1993). *The Carbonation of Concrete and the Mechanism of Moisture, Heat and Carbon Dioxide Flow Through Porous Materials*, Cement and Concrete Research. Vol. 23, pp. 761-772.

[41] Brieger, L. and Wittmann, F.H. (1986). *Numerical Simulation of Carbonation of Concrete*, Material and Science Restoration, Tech. Akad. Ess., Ostfildern.

[42] Tritthart, J. (1989). *The Influence of the Hydroxide Concentration in the Pore Solution of Hardened Cement Pastes on Chloride Binding.* Cement and Concrete Research. Vol. 19, pp. 683-691.

[43] Bentz, D.P. and Garboczi, E.J. (1992). *Modelling the Leaching of Calcium Hydroxide from Cement Paste: Effects on Pore Space Percolation and Diffusivity.* Materials and Structures, Vol. 25, pp. 523-533.

[44] Gjørv, O.E., Vennesland, Ø. and El-Busaidy, A.H.S. (1976). *Diffusion of Dissolved Oxygen Through Concrete*, Paper No. 17, National Association of Corrosion Engineers Meeting, Houston, Tex.

[45] Gjørv, O.E. and Vennesland, Ø. (1977). *Electrical Resistivity of Concrete in the Oceans*, Paper OTC 2803, Ninth Annual Offshore Technology Conference, Houston, Tex. May, 1977, pp. 581-588.

[46] Luping, T. (1996). *Chloride Transport in Concrete, Measurement and Prediction*, Ph.D. thesis, Chalmers University of Technology, Department of Building Materials, Göteborg, Sweden.

[47] Hauggaard, A.B., Damkilde, L. and Krenk, S. (1996). *An Energy Based Numerical Approach to Phase Change Problems*, Danish Center for Applied Mathematics and Mechanics, Department of Structural Engineering and Materials, Technical University of Denmark.

[48] Hobbs, P.V. (1974). *Ice Physics*, Clarendon Press, Oxford.

[49] Ozawa, H. and Kinosita, S. (1989). *Segregated Ice Growth on a Microporous Filter.* Journal of Colloid and Interface Science, Vol. 132, No. 1, pp. 113-124.

[50] Powers, T.C. (1953). *Theory of Volume Changes in Hardened Portland-Cement Paste During Freezing.* Highway Research Board, Vol. 32.

[51] Matsumoto, M. (1995). *On Prediction of Dynamic Behaviors of Moisture and Temperature in Buildings and Building Elements.* Mass-energy Transfer and Deterioration of Building Components, Models and Characterization of Transfer Properties, Proceeding of International Workshop, 9-11 January 1995, Paris-CSTB.

[52] Coussy, O. (1995). *Constitutive Modelling of Civil Engineering Materials Subjected to Therm-Hygro-Mechanical Couplings.* Mass-energy Transfer and Deterioration of Building Components, Models and Characterization of Transfer Properties, Proceeding of International Workshop, 9-11 January 1995, Paris-CSTB.

[53] Frémond, M. and Mikkola, M. (1991). *Thermomechanical Modelling of Freezing of Soil.* Ground Freezing 91, Yu and Wang (eds), Balkerna, Rotterdam.

[54] Lemaitre, J. and Chaboche, J.L. (1990). *Mechanics of Solid Materials*, Cambridge University Press.

[55] Dahlblom, O. (1987). *Constitutive Modelling and Finite Element Analysis of Concrete Structures with Regard to Environmental Influence.* Division of Structural Mechanics, Lund Institute of Technology.

[56] Hillerborg, A. (1978). *A Model for Fracture Analysis.* Lund Institute of Technology, Division of Building Materials, Lund, Sweden.

[57] Feenstra, P.H. and de Borst, R. (1993). *Aspects of Robust Computational Modeling for Plain and Reinforced Concrete.* Heron, Vol. 38, No. 4.

[58] Rots, J.G. and Blaauwendraad, J. (1989). *Crack Models for Concrete: Discrete or Smeared? Fixed, Multi-directional or Rotating?* Heron, Vol. 34, No. 1.

[59] van Mier, J.G.M. (1995). *Fracture Mechanics of Concrete: Will Applications Start to Emerge?* Heron, Vol. 40, No. 2, pp. 147-162.

[60] Ottosen, N.S. and Ristinmaa, M. (1995). *The Mechanics of Constitutive Modelling.* Department of Solid Mechanics, Lund Institute of Technology.

[61] Thelandersson, S. (1983). *On the Multiaxial Behavior of Concrete Exposed to High Temperature.* Nuclear Engineering and Design, Vol. 75, No. 2, pp. 271-282.

[62] Hillerborg, A., Modéer, M. and Petersson, P-E. (1976). *Analysis of Crack Formation and Crack Growth in Concrete by Means of Fracture Mechanics and Finite Elements.* Cement and Concrete Research, Vol. 6, pp. 773-782.

[63] Dahlblom, O. and Ottosen, N.S. (1990). *Smeared Crack Analysis Using Generalized Fictitious Model.* Journal of Engineering Mechanics, Vol. 116, No. 1, pp. 55-76.

[64] Hillerborg, A. (1985). *Numerical Methods to Simulate Softening and Fracture of Concrete.* Fracture Mechanics of Concrete: Structural Application and Numerical Calculations, G.C. Sih and A. DiTommaso, eds., Martinus Nijhoff Publ., Dordrecht, Netherlands, pp. 141-170.

[65] Reinhardt, H.W. (1984). *Fracture Mechanics of an Elastic Softening Material like Concrete.* Heron, Vol. 29, No. 2, Delft.

[66] Ottosen, N.S. and Dahlblom, O. (1986). *Smeared Crack Analysis Using a Nonlinear Fracture Model for Concrete.* Numerical Methods for Non-Linear Problems, Vol. 3, Edited by C. Taylor, D.R.J. Owen, E. Hinton and F.B. Damjanic. Pineridge Press, pp. 363-376.

[67] Hassanzadeh, M. (1991). *Behavior of Fracture Process Zones in Concrete Influenced by Simultaneously Applied Normal and Shear Displacements.* Division of Building Materials, Lund Institute of Technology.

[68] Snow, D.T. (1969). *Anisotropic Permeability of Fractured Media.* Water Resources Research, Vol. 5, No. 6, pp. 1273-1289.

[69] Chirlin, G.R. (1985). *Flow Through a Porous Medium with Periodic Barriers or Fractures.* Soc. of Petroleum Engineers Journal, pp. 358-362.

[70] Ottosen, N.S. and Petersson, H. (1992). *Introduction to the Finite Element Method.* Prentice Hall, London.

[71] Zienkiewicz, O.C. and Taylor, R.L. (1989). *The Finite Element Method, Fourth Edition, Vol. 2.* McGraw-Hill, London.

[72] Bathe, K.J. (1996). *The Finite Element Procedures*, Prentice Hall, Englewood Cliffs, New Jersey.

[73] Hughes, T.J.R. (1987). *The Finite Element Method, Linear Static and Dynamic Finite Element Analysis.* Prentice-Hall International Editions.

[74] Claesson, J. (1996). *Partial Differential Equations, Technical Applications.* Lecture Notes, Lund Institute of Technology, Departments of Mathematical Physics and Building Physics, Lund, Sweden.

[75] Christie, I. et al. (1976). *The Finite Element Methods for Second Order Differential Equations with Significant First Derivatives*, Int. J. Num. Meth. Eng., Vol. 10.

[76] Hughes, T.J.R. and Brooks, A.N. (1979). *Multi-dimensional Upwind Scheme with No Cross Wind Diffusion, Finite Elements for Convection Dominated Flows*, (Ed.. Hughes, T.J.R.), AMD 34, ASME.

Index